

KNOTS AND CHAOS IN THE RÖSSLER SYSTEM

ERAN IGRA

ABSTRACT. The Rössler System is one of the best known chaotic dynamical systems, exhibiting a plethora of complex phenomena - and yet, only a few studies tackled its complexity analytically. In this paper we find sufficient conditions for the existence of chaotic dynamics for the Rössler System at some specific parameter values at which the flow satisfies a certain heteroclinic condition. This will allow us to prove the existence of infinitely many periodic trajectories for the flow, and study their bifurcations in the parameter space of the Rössler system.

Keywords - The Rössler Attractor, Chaos Theory, Heteroclinic bifurcations, Topological Dynamics

1. INTRODUCTION

In 1976, Otto E. Rössler introduced the following system of Ordinary Differential Equations, depending on parameters $A, B, C \in \mathbf{R}^3$ [6]:

$$\begin{cases} \dot{X} = -Y - Z \\ \dot{Y} = X + AY \\ \dot{Z} = B + Z(X - C) \end{cases} \quad (1)$$

Inspired by the Lorenz attractor (see [2]), Otto E. Rössler attempted to find the simplest non-linear flow exhibiting chaotic dynamics. This is realized by the vector field above, as it has precisely one non-linearity, XZ in the \dot{Z} component, and its behavior models that of a taffy machine (see [9]) - and as observed by Rössler, the vector field appears to generate a chaotic attractor for $(A, B, C) = (0.2, 0.2, 5.7)$. In more detail, at these parameter values Rössler observed the first return map of the flow has the shape of a horseshoe (i.e., numerically), which is known to be chaotic (see [4]).

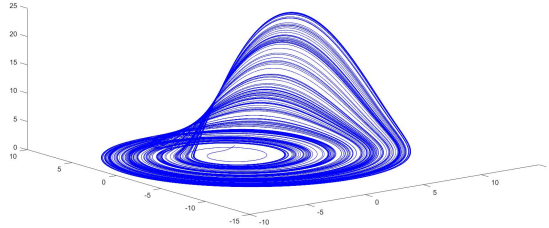


FIGURE 1. The Rössler attractor at $(A, B, C) = (0.2, 0.2, 5.7)$

Since its introduction in 1976, the Rössler system was the focus of many numerical studies - despite the simplicity of the vector field, the flow gives rise to many non-linear phenomena (see, for example: [29], [23], [21], [25], [24]). One particular feature is that varying the parameters A, B, C often leads to a change in the complexity of the system: that is, as the parameters are varied, more and more symbols appear in the first-return map of the flow (for more details, see [29], [23], [13], [27]). In a topological context, several numerical studies noted this variation of parameters changes the topology of the attractor - see, for example, [13], [27].

In contrast to the vast corpus of numerical studies, analytical results on the Rössler system are sparse. For example, in [16], the existence of periodic trajectories at some parameters was established; in [28] the existence of an invariant Torus (and its breakdown) at some parameters was proven; and in [22] the dynamics of the flow at ∞ were analyzed. As far as chaotic dynamics go, their existence at $(A, B, C) = (0.2, 0.2, 5.7)$ was proven with rigorous numerical methods - see [14], [19]. To our knowledge, no studies on the Rössler system attempted to prove its nonlinear phenomena (and in particular, its chaotic dynamics) by analytical tools. It is precisely this gap that this paper aims to address. In this paper we prove analytically, for the first time, sufficient conditions for the existence of complex dynamics in the Rössler system.

The key idea in everything that is to follow is that the existence of a certain heteroclinic knot at some parameters (A, B, C) forces the creation of complex dynamics for the first-return map (see Def.1.1 and Th.3.1 for the precise formulation). We denote such parameters as **trefoil parameters** (for a precise definition, see Def.2.4). In [30] it was proven the existence of a similar heteroclinic knot for the Lorenz system implies similar results - as such, this study and [30] lend further credence to the role of heteroclinic knots in the onset of complex dynamics. As must be stated, these heteroclinic knots and their connection to the onset of chaotic dynamics play a similar role to that of the homoclinic trajectories in Shilnikov's Theorem (see [3] for more details).

To state our main results, given parameter values $p = (A, B, C)$, denote by F_p the corresponding vector field. As we will see later on, there exists an open set of parameters $P \subseteq \mathbf{R}^3$, s.t. $\forall p \in P$, F_p generates a cross-section U_p which varies smoothly in p . Now, denote by $f_p : \overline{U_p} \rightarrow \overline{U_p}$ the first return map of F_p (wherever defined), and denote by $\sigma : \{1, 2\}^{\mathbf{N}} \rightarrow \{1, 2\}^{\mathbf{N}}$ the one sided-shift. We first prove the following result, about the global dynamics of F_p (see the discussion before Lemma 2.2 and Th.2.1):

Theorem 1. *There exists an open set of parameters $O \subseteq \mathbf{R}^3$ s.t. F_p can be extended to a vector field on S^3 with precisely three fixed points - two saddle-foci P_{In}, P_{Out} (of opposing indices) and a degenerate fixed point at ∞ . Moreover, both P_{In}, P_{Out} admit heteroclinic trajectories connecting them to ∞ .*

Th.1 would be proven in Section 2.1 - as we will discover, Th.1 and its corollaries serve as the backbone of almost all the results which come next. In particular, Th.1 will allow us to find a cross-section, $H_p \subseteq U_p$ on which the first-return map $f_p : \overline{H_p} \rightarrow \overline{H_p}$ is well-defined at every initial condition $x \in \overline{H_p}$ (see Lemma 3.0.1 and Prop.3.1). These results (as well as the other corollaries of Th.1) would allow us to state and prove the following criterion for the existence of complex dynamics for the Rössler system at trefoil parameters (see Th.3.1):

Theorem 2. *Let $p = (A, B, C) \in P$ be a trefoil parameter as given in Def.2.4. Then, there exists an f_p -invariant $Q \subseteq \overline{U_p}$ and a continuous $\pi : Q \rightarrow \{1, 2\}^{\mathbf{N}}$ such that:*

- $\pi \circ f_p = \sigma \circ \pi$.
- f_p is continuous on Q .
- $\pi(Q)$ includes every periodic symbol $s \in \{1, 2\}^{\mathbf{N}}$.
- Given any periodic $s \in \{1, 2\}^{\mathbf{N}}$ of minimal period $k > 0$, $\pi^{-1}(s)$ includes at least one periodic point for f_p of minimal period k .

The proof of Th.2 would take up most of Section 3, and will be carried by directly analyzing the vector field using (mostly) elementary methods. Despite the relative complexity and the many details and technicalities involved, the idea behind the proof of Th.2 is fairly simple - inspired by [19] and [17], we prove the existence of the heteroclinic trefoil knot forces the first-return map to have dynamics similar (though not the same) to those of a topological horseshoe (see [17] for a precise definition). Once Th.2 is proven, we apply it to analyze the dynamical complexity of the flow in and around trefoil parameters. Inspired by [14] and using both Th.2 and a Fixed-Point Index argument (see Ch.VII.5 in [5]), we prove the following Theorem in Section 4 (see Th.4.1):

Theorem 3. *Let $p \in P$ be a trefoil parameter, and let $v \in P$ s.t. $v \neq p$, and choose some $k > 0$. Then, provided v is sufficiently close to p , $f_v : \overline{U_v} \rightarrow \overline{U_v}$ has at least one periodic orbit of minimal period k .*

Or, in other words, Theorem 3 has the following meaning - the closer a parameter $v \in P$ is to a trefoil parameter p , the more complex its dynamics become. With these ideas in mind, we must remark that when the parameter space of the Rössler system was analyzed numerically, spiral bifurcation structures were observed (see, for example [29], [23], [21], [25]). In all these studies, these spiral structures always accumulated at some point p_0 , often referred to as a **periodicity hub**, which lies on the Shilnikov homoclinic curve (see [3]). As was observed in [24] (see pg. 430), the dynamics around some periodicity hubs may, in fact, be heteroclinic. This suggests Th.2 and 3 possibly have a part in explaining the emergence of such complex phenomena.

Finally, we must also stress that even though the results in this study all relate to the Rössler system, in practice most of our arguments in Section 3 and 4 are purely topological. As such, they can be generalized and applied to study nonlinear phenomena in a much wider class of smooth flows on \mathbf{R}^3 . In particular, they exemplify the potential of topological methods for explaining the emergence of nonlinear phenomena - and moreover, they attest to the importance of bounded heteroclinic trajectories to the emergence of chaotic and complex dynamics in three-dimensional flows. As such, our results (and in particular Th.2, Th.3 and Prop.4.2) should be compared with those of [15], where the bifurcations scenario around heteroclinic connections was studied in a two-parameter family of vector fields.

PRELIMINARIES

Let X be a metric space, with a metric d . For any $A \subseteq X$, we will denote by \overline{A} the closure of A , and by ∂A the boundary of A . Given any $x \in X, r > 0$, we denote the ball of radius r around x by $B_r(x)$. Also, given

$A, B, C, D \subseteq X$, we say that C **connects** A, B if C is connected and $A \cap C, B \cap C \neq \emptyset$. We say that D **separates** A, B if given any connected C which connects A, B , we also have $D \cap C \neq \emptyset$ - see the illustration in Fig.2. Moreover, we say a curve $\gamma : [0, 1] \rightarrow \mathbf{R}^3$ is **simple** or **not self intersecting** if for every $x, y \in [0, 1]$, $x \neq y$, $\gamma(x) \neq \gamma(y)$. Given a topological disc $D \subseteq \mathbf{R}^2$, we say D is a **Jordan domain** if its boundary ∂D can be parameterized by some $\gamma : [0, 1] \rightarrow \mathbf{R}^2$ s.t. $\gamma(0) = \gamma(1)$ and for every other $x, y \in (0, 1)$, $\gamma(x) \neq \gamma(y)$.

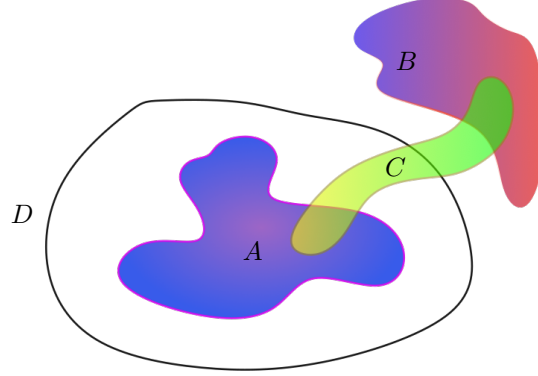


FIGURE 2. The set C connects A and B , while D separates them.

From now on given $(a, b, c) \in \mathbf{R}^3$, we switch to the more convenient form of the Rössler system, given by the following system of ODEs:

$$\begin{cases} \dot{x} = -y - z \\ \dot{y} = x + ay \\ \dot{z} = bx + z(x - c) \end{cases} \quad (2)$$

Denote this vector field corresponding to $(a, b, c) \in \mathbf{R}^3$ by $F_{a,b,c}$. This definition is slightly different from the one presented in Eq.1 - however, setting $p_1 = \frac{-C + \sqrt{C^2 - 4AB}}{2A}$, it is easy to see that whenever $C^2 - 4AB > 0$, $(X, Y, Z) = (x - ap_1, y + p_1, z - p_1)$ defines a change of coordinates between the vector fields in Eq.1 and Eq.2.

Before we continue, we must introduce a definition for chaotic dynamics:

Definition 1.1. Chaotic Dynamics Let Y be some topological space, and let $g : Y \rightarrow Y$ be continuous. We say g is **properly chaotic** provided the periodic orbits of g in Y are dense, and $\exists y \in Y$ s.t. $\overline{\{g^n(y)\}_{n>0}} = Y$. We say a first-return map $f : S \rightarrow S$ for a smooth flow on \mathbf{R}^3 is **chaotic** on some bounded invariant set $X \subseteq S$, if f is continuous on X and there exists a topological space Y , a properly chaotic $g : Y \rightarrow Y$ and a continuous, surjective, $\pi : X \rightarrow Y$ s.t. $\pi \circ f = g \circ \pi$.

For example, the Smale Horseshoe map (see [4]) is a properly chaotic map, while the first-return map of the Geometric Lorenz Attractor (see, for example, Ch.3 in [20]) is chaotic. As must be remarked, this definition is inspired (though not the same) from the one originally given in [12] - however, as we will see, it is the one necessary for the proof of existence of complex dynamics in Th.3.1.

To conclude this section, since the vector field in Eq.2 depends on three parameters, (a, b, c) , we must specify the region in the parameter space in which we prove our results. As observed in several numerical studies (see, for example, [23],[29],[21] and [24]), many interesting bifurcation phenomena occur at a very specific **open region** in the parameter space. In that parameter space the a, b, c parameters **always** satisfy $a, b \in (0, 1)$, $c > 1$ - and moreover, the vector field F_p always generates precisely two fixed points, P_{In}, P_{Out} , s.t. **both** are saddle-foci. Additionally, in these studies the eigenvalues of the linearization at P_{In} satisfy a resonance condition known as the **Shilnikov condition** (see [3] or below for a definition) - and moreover, this resonance condition is stable in the parameter space. Therefore, to make everything clear, let us write down the assumptions we impose on our parameter space P :

- **Assumption 1** - $\forall p \in P, p = (a, b, c)$ the parameters satisfy $a, b \in (0, 1)$ and $c > 1$. As can be seen, for every choice of such p , the vector field F_p generates precisely two fixed points - $P_{In} = (0, 0, 0)$ and $P_{Out} = (c - ab, b - \frac{c}{a}, \frac{c}{a} - b)$.
- **Assumption 2** - We assume that for every $p \in P$ the fixed points P_{In}, P_{Out} are both saddle-foci of opposing indices. In more detail, we always assume that P_{In} has a one-dimensional stable manifold,

W_{In}^s , and a two-dimensional unstable manifold, W_{In}^u . Conversely, we assume P_{Out} has a one-dimensional unstable manifold, W_{Out}^u , and a two-dimensional stable manifold, W_{Out}^s .

- **Assumption 3** - For every $p \in P$, let $\gamma_{In} < 0$ and $\rho_{In} \pm i\omega_{In}$, $\rho_{In} > 0$ denote the eigenvalues of $J_p(P_{In})$, the linearization of P_{In} , and set $\nu_{In} = |\frac{\rho_{In}}{\gamma_{In}}|$. Conversely, let $\gamma_{Out} > 0$, $\rho_{Out} \pm i\omega_{Out}$ s.t. $\rho_{Out} < 0$ denote the eigenvalues of $J_p(P_{Out})$ and define $\nu_{Out} = |\frac{\rho_{Out}}{\gamma_{Out}}|$. We will refer to ν_{In}, ν_{Out} as the respective saddle indices at P_{In}, P_{Out} , and we will always assume $(\nu_{In} < 1) \vee (\nu_{Out} < 1)$ - that is, for every $p \in P$ **at least** one of the fixed points satisfies the Shilnikov condition (see [3] for more details).

As must be remarked, the parameter space P we are considering is not only open in the parameter space, but in fact also **includes** the region considered in the numerical studies cited above.

2. THE GLOBAL DYNAMICS OF THE VECTOR FIELD F_p , $p \in P$.

A central theme in this paper is that parameters in P at which there exist certain heteroclinic connections force the creation of chaotic dynamics in the Rössler System. Generically, one cannot expect heteroclinic trajectories for the vector field in Eq.2 to be stable in the parameter space P - however, as we will prove in this section, in a sense this is **almost** the case. More precisely, in this section we will prove that given any $p = (a, b, c) \in P$, the vector field F_p **always** generates two unbounded, invariant one-dimensional separatrices in the parameter space, connecting each fixed point to ∞ (in S^3) - see Th.2.1. As Th.2.1 gives us information on the global dynamics of the flow, later on in Sections 3 and 4 Th.2.1 and its corollaries will form a major element in many of our results.

This section is organized as follows - we begin Section 2 with a quick analysis of the vector field. Following that, we first prove the existence of a cross-section U_p , a half-plane which intersects transversely every periodic trajectory generated by F_p (see Lemma 2.1). Having done so, we turn to analyze the behavior of F_p on its unbounded trajectories - i.e., we analyze the global dynamics of F_p , which will be done in Th.2.1. The proof of Th.2.1 will be relatively long, forming the bulk of Section 2. Once Th.2.1 is proven, we define the notion of a Trefoil Parameter (see Def.2.4) - and then apply it with Th.2.1 to prove Cor.2.1.6, where we study the dynamical complexity of F_p around ∞ (see Cor.2.1.6). Later in this paper, we will apply Th.2.1 (and the Lemmas and Propositions used in its proof) to prove a criterion for chaotic dynamics for the Rössler system.

To begin, fix some parameter $p = (a, b, c) \in P$ and consider the plane $Y_p = \{(x, -\frac{x}{a}, z) | x, z \in \mathbf{R}\} = \{\dot{y} = 0\}$ (with \dot{y} taken w.r.t. F_p - see Eq.2). Let $N_p = (1, a, 0)$ denote the normal vector to Y_p , - by computation F_p is tangent to Y_p **precisely** at the straight line $l_p = \{(t, -\frac{t}{a}, \frac{x}{a}) | t \in \mathbf{R}\}$. Hence, $Y_p \setminus l_p$ consists of two components, both half-planes - let $U_p = \{(x, -\frac{x}{a}, z) | x, z \in \mathbf{R}, -z + \frac{x}{a} < 0\}$ denote the upper half of $Y_p \setminus l_p$, and denote by $L_p = \{(x, -\frac{x}{a}, z) | x, z \in \mathbf{R}, -z + \frac{x}{a} > 0\}$ the lower half. As l_p is a straight line, we immediately conclude the following, useful fact:

Lemma 2.1. *Let $s \in \mathbf{R}^3$ be an initial condition that is not a fixed point, whose forward trajectory γ_s is bounded, and does not limit to a fixed point - then, γ_s intersects U_p transversely infinitely many times. In particular, any bounded invariant set (which is not a fixed point) intersects U_p transversely at least once.*

Now, denote by $f_p : \overline{U_p} \rightarrow \overline{U_p}$ the first-return map, wherever defined - by Lemma 2.1, it is defined at least around every periodic trajectory for F_p . We are thus led to the following question - on which initial conditions in $\overline{U_p}$ the first-return map g_p is defined? If we could answer this question, we could analyze the flow dynamics generated by F_p . By Lemma 2.1, the only initial conditions $x \in \overline{U_p}$ on which f_p is possibly undefined are those whose trajectories either limit to fixed points, or blow up to ∞ . This implies that in order to analyze the first-return map, we must study the unbounded dynamics of F_p - and in particular, its dynamics around ∞ - that is, its global dynamics.

To make this discussion more precise, let us consider the flow generated by the extension of F_p to the one-point compactification of \mathbf{R}^3 , S^3 . We first recall Th.1 in [22], where the dynamics of F_p around ∞ were analyzed by the means of the Poincaré sphere. In that paper it was proven the behaviour of F_p on $\{(x, y, z) | x^2 + y^2 + z^2 > r\}$ is independent of $r > 0$ (for any sufficiently large r) - which proves we can extend F_p to S^3 by adding ∞ as a fixed point for the flow. Therefore, from now on, **unless said otherwise**, we always consider F_p to be a vector field on S^3 with precisely three fixed points - P_{In}, P_{Out} and ∞ . This leads us to ask - just how well behaved is F_p around ∞ ? To answer this question, we now quickly prove:

Lemma 2.2. *For any $p \in P$, F_p is not C^1 at ∞ .*

Proof. For any $(x, y, z) = v \in \mathbf{R}^3$ consider the linearized vector field $J_p(v)$ at v - namely, the Jacobian matrix of F_p at $v \in \mathbf{R}^3$ (see Eq.2.) Now, choose some $\lambda \in \mathbf{R}$ and note the equation $\det(J_p(v)) = \lambda$ can be rewritten as $z = \frac{\lambda + c - x - ab}{a}$. This proves the set $S_\lambda = \{\det(J_p(v)) = \lambda\}$ is a plane in \mathbf{R}^3 - which implies that when we extend \mathbf{R}^3 to S^3 we have $\infty \in \partial S_\lambda$ (with ∂S_λ taken in S^3). We conclude that for any $\lambda_1 \neq \lambda_2$, we have $\{\infty\} = \partial S_{\lambda_1} \cap \partial S_{\lambda_2}$

- which proves $\det(J_p(v))$ takes infinitely many values at any neighborhood of ∞ . As such F_p cannot be C^1 at ∞ and the Lemma follows. \square

Lemma 2.2 teaches us we **cannot** analyze F_p as a smooth vector field on S^3 . However, even though F_p is not C^1 at ∞ , it still is C^1 in \mathbf{R}^3 , i.e. on $S^3 \setminus \{\infty\}$. This motivates us to prove Th.2.1 - as we will see in the remainder of Section 2 (as well as Sections 3 and 4), Th.2.1 allows us to bypass the obstacle posed by Lemma 2.2 by reducing the dynamics of F_p by those of a R_p : a smooth vector field on S^3 , which can be chosen to coincide with F_p on an arbitrarily large set in \mathbf{R}^3 . To state it, recall W_{In}^s is the stable, one-dimensional invariant manifold of the saddle focus P_{In} - and that W_{Out}^u is the unstable, one dimensional manifold of the saddle focus P_{Out} . We now prove:

Theorem 2.1. *For every $p \in P$, F_p generates two heteroclinic trajectories:*

- $\Gamma_{In} \subseteq W_{In}^s$, which connects P_{In}, ∞ in S^3 .
- $\Gamma_{Out} \subseteq W_{Out}^u$, which connects P_{Out}, ∞ in S^3 .

As a consequence, for every sufficiently large $r > 0$, there exists a smooth vector field on S^3 , R_p , s.t.:

- R_p coincides with F_p on the open ball $B_r(P_{In})$.
- R_p has precisely three fixed points in S^3 - namely, P_{In} and P_{Out} .
- R_p generates a heteroclinic trajectory which connects P_{In}, P_{Out} and passes through ∞ .

Proof. Let $(a, b, c) = p \in P$ be a parameter, and recall we denote by F_p the corresponding vector field (see Eq.2). Due to the length of the argument and the amount of details involved, we will split the proof into several stages - however, despite the length of the argument, the idea behind the proof of Th.2.1 is relatively straightforward. The sketch of the proof is as follows:

- In Stage *I* we analyze the local dynamics of F_p on two cross-sections: $\{\dot{x} = 0\}$ and $\{\dot{y} = 0\}$.
- In Stage *II* we use the results from Stage *I* and the interplay between the two cross-sections $\{\dot{x} = 0\}$ and $\{\dot{y} = 0\}$ to construct a three-dimensional body, C_{In} which traps Γ_{In} , a component of W_{In}^s . As we will prove, $C_{In} \subseteq \{\dot{y} \leq 0\}$, from which it would follow that Γ_{In} is a heteroclinic connection between P_{In}, ∞ .
- In Stage *III* we do the same for the outer fixed-point, P_{Out} - that is, we prove, using an almost symmetrical argument to Stage *II*, the existence of a three-dimensional body $C_{Out} \subseteq \{\dot{y} \leq 0\}$, trapping Γ_{Out} , a component of W_{Out}^u which is also a heteroclinic connection between P_{Out}, ∞ .
- In Stage *IV* we conclude the proof of Th.2.1 by constructing the vector field R_p . We do so by using the Poincare-Hopf Theorem to smoothen F_p around ∞ , thus constructing the vector field R_p . As we will prove, R_p can be constructed s.t. it coincides with F_p on an arbitrarily large set in \mathbf{R}^3 . Furthermore, by the existence of $\Gamma_{In}, \Gamma_{Out}$, we will construct R_p s.t. it has precisely two fixed points in S^3 , P_{In} and P_{Out} - connected by an unbounded heteroclinic trajectory.

2.0.1. Stage I - a tale of two cross-sections. We begin with the cross-section $\{\dot{x} = 0\}$, given by the parameterization $\{(x, y, -y) | x, y \in \mathbf{R}\}$ (see Eq.2). From this parameterization $\{\dot{x} = 0\}$ is a plane, which proves $\mathbf{R}^3 \setminus \{\dot{x} = 0\}$ is composed of two open regions. The first is $\{\dot{x} > 0\}$, defined by $\{(x, y, -z) | x, y, z \in \mathbf{R}, y < -z\}$ and lying **below** $\{\dot{x} = 0\}$ - the second is $\{\dot{x} < 0\}$, given by the parameterization $\{(x, y, -z) | x, y, z \in \mathbf{R}, y > -z\}$ and lying **above** $\{\dot{x} = 0\}$ (see Fig.5 for an illustration). Now, recall we denote by W_{In}^s the one-dimensional stable invariant manifold of P_{In} , and by W_{In}^u the two-dimensional unstable invariant manifold of P_{In} . Similarly, we denote by W_{Out}^u the unstable one-dimensional invariant manifold of P_{Out} , and by W_{Out}^s the stable two-dimensional, invariant manifold of P_{Out} . We first prove:

Lemma 2.3. *The two-dimensional W_{Out}^s, W_{In}^u and the one dimensional W_{Out}^u, W_{In}^s are non-tangent to $\{\dot{x} = 0\}$ at P_{In}, P_{Out} , respectively. In particular, W_{Out}^s, W_{In}^u are transverse to $\{\dot{x} = 0\}$ at P_{Out}, P_{In} , respectively.*

Proof. The normal vector to $\{\dot{x} = 0\}$ is $(0, 1, 1)$ - therefore, for every point $v \in \{\dot{x} = 0\}$, the dot-product is $F_p(v) \bullet (0, 1, 1) = x + ay + bx - xy + cy$ - as such, $F_p(v) \bullet (0, 1, 1) \neq 0$ precisely when $y \neq \frac{-x(b+1)}{a+c-x}$. This proves the set $\{\dot{x} = 0\} \setminus \{(x, y, -y) | y = \frac{-x(b+1)}{a+c-x}\}$ is composed of three components, A_1, A_2, A_3 , defined thus:

- For $v \in A_1 \cup A_2$ we have $F_p(v) \bullet (0, 1, 1) < 0$.
- For $v \in A_3$ we have $F_p(v) \bullet (0, 1, 1) > 0$.

See Fig.3 for an illustration. That is, on A_1, A_2 the vector field F_p points inside $\{\dot{x} > 0\}$, while on A_3 it points inside $\{\dot{x} < 0\}$. The sets A_1, A_2, A_3 are separated from one another by the curve $\sigma(x) = (x, -\frac{x(b+1)}{a+c-x}, \frac{x(b+1)}{a+c-x})$, $x \neq c + a$, on which F_p is tangent to $\{\dot{x} = 0\}$ (see Fig.3 for a illustration). By computation, the tangent vectors to $\sigma(x)$ are given by $\sigma'(x) = (1, \frac{-(b+1)(a+c)}{(a+c-x)^2}, \frac{(b+1)(a+c)}{(a+c-x)^2})$.

Now, consider the linearization of F_p at P_{In} , denoted by $J_p(P_{In})$ - by direct computation, $\sigma'(x)$ is not an eigenvector for $J_p(P_{In})$ (for every $x \neq c + a$). Hence, since $P_{In} = \sigma(0)$, W_{In}^u must be transverse to $\{\dot{x} = 0\}$ at P_{In} - a similar argument now proves W_{In}^s cannot be tangent to σ at P_{In} . Finally, by considering $J_p(P_{Out})$ - the

linearization of F_p at P_{Out} - the same arguments prove W_{Out}^s is transverse to $\{\dot{x} = 0\}$ at P_{Out} , and that W_{Out}^u is non-tangent to σ at P_{Out} . \square

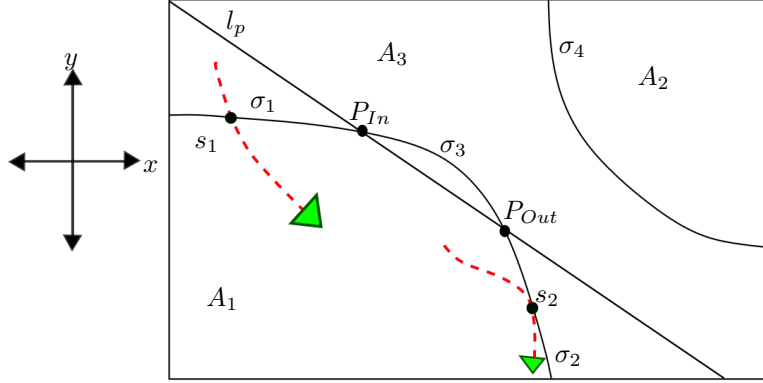


FIGURE 3. the geography of $\{\dot{x} = 0\}$. Observe the flow lines arriving from below $\{\dot{x} = 0\}$.

Having proven Lemma 2.3, we now proceed by characterizing the local behaviour of F_p on initial conditions lying in σ , the tangency curve of F_p to $\{\dot{x} = 0\}$ (see the proof of Lemma 2.3 for the definition, and Fig.3 for an illustration). As computed in the proof of Lemma 2.3, σ is parameterized by $\sigma(x) = (x, -\frac{x(b+1)}{a+c-x}, \frac{x(b+1)}{a+c-x})$, $x \neq c+a$, and it separates the regions A_1, A_2, A_3 on $\{\dot{x} = 0\}$ (see the definition in the proof of Lemma 2.3, and the illustration in Fig.3). Now, recall $P_{Out} = (c-ab, b-\frac{c}{a}, \frac{c}{a}-b)$ - since $c+a > c-ab$, from $P_{In} = (0, 0, 0)$ we conclude P_{Out}, P_{In} lie on the same component in σ . Set A_1 as the component of $\{v \in \{\dot{x} = 0\} | F_p(v) \bullet (0, 1, 1) < 0\}$ s.t. $P_{In}, P_{Out} \in \partial A_1$ - by this discussion, ∂A_1 is a component of σ .

From now on, given any $s \in \mathbf{R}^3$ denote by γ_s its trajectory, $\gamma_s(0) = s$. By computation, $\sigma \setminus \{P_{In}, P_{Out}\}$ is composed of four components, $\sigma_1, \sigma_2, \sigma_3, \sigma_4$ s.t. σ_1 connects P_{In}, ∞ , and σ_2 connects P_{Out}, ∞ , and σ_3 connects P_{In}, P_{Out} (see the illustration in Fig.3). We now prove the following fact about the local dynamics of F_p on σ , thus concluding our analysis of $\{\dot{x} = 0\}$:

Lemma 2.4. *For every initial condition $s \in \sigma_1, \sigma_2$, there exists $\epsilon > 0$ s.t. for every time $t \in (-\epsilon, \epsilon), t \neq 0$, we have $\gamma_s(t) \in \{\dot{x} > 0\} \cap \{\dot{y} < 0\} \cap \{\dot{z} > 0\}$. Additionally, $\sigma_3, \sigma_4 \subseteq \{\dot{y} > 0\}$.*

Proof. We first prove that for every $s \in \sigma_1, \sigma_2$, there exists $\epsilon > 0$ s.t. given $t \in (-\epsilon, \epsilon), t \neq 0$ we have $\gamma_s(t) \in \{\dot{x} > 0\} \cap \{\dot{y} < 0\} \cap \{\dot{z} > 0\}$. To this end, recall Eq.2. By the discussion above, ∂A_1 is parameterized by $\sigma(x) = (x, -\frac{x(b+1)}{a+c-x}, \frac{x(b+1)}{a+c-x})$, $x < c+a$. By computation, $F_p(x, -\frac{x(b+1)}{a+c-x}, \frac{x(b+1)}{a+c-x}) = (0, \frac{-x^2+cx-abx}{a+c-x}, \frac{x^2-cx+abx}{a+c-x})$ - therefore, for $x < 0$ or $c-ab < x < c+a$ we have $\frac{-x^2+cx-abx}{a+c-x} < 0$. Hence, for $x < 0$ or $c-ab < x < c+a$, $F_p(\sigma(x))$, the tangent to the orbit of $\sigma(x)$, points into A_1 while the vector field points downwards into $\{\dot{x} > 0\}$ - which proves the trajectory of an initial condition $\sigma(x)$ with $x < 0$ or $c-ab < x < c+a$ leaves ∂A_1 and enters the region $\{\dot{x} > 0\} \cap \{\dot{y} < 0\} \cap \{\dot{z} > 0\}$ (see Fig.3 for an illustration). Since points on σ_1, σ_2 correspond to initial conditions $\sigma(x)$ s.t. $x < 0$ and $c-ab < x < c+a$ (respectively), we conclude the flow lines arrive at σ_1, σ_2 from $\{\dot{x} > 0\} \cap \{\dot{y} < 0\} \cap \{\dot{z} > 0\}$ - that is, writing $s = \sigma(x)$, $\exists \epsilon_1 > 0$ s.t. $\forall t \in (-\epsilon_1, 0), \gamma_s(t) \in \{\dot{x} > 0\} \cap \{\dot{y} < 0\} \cap \{\dot{z} > 0\}$.

A similar argument applied to $-F_p$ (i.e. to the inverse flow) proves that $\forall s \in \sigma_1 \cup \sigma_2$ there exists some $\epsilon_2 > 0$ s.t. $\gamma_s(t) \in \{\dot{x} > 0\} \cap \{\dot{y} < 0\} \cap \{\dot{z} > 0\}$ whenever $t \in (0, \epsilon_2)$ (see Fig.3 for an illustration). Hence, we conclude that given any $s \in \sigma_1, \sigma_2$, there exists $\epsilon > 0$ s.t. given $t \in (-\epsilon, \epsilon), t \neq 0$ we have $\gamma_s(t) \in \{\dot{x} > 0\} \cap \{\dot{y} < 0\} \cap \{\dot{z} > 0\}$. To conclude the proof of Lemma 2.4 we need now prove that $\sigma_3, \sigma_4 \subseteq \{\dot{y} > 0\}$. To do so, recall we have $F_p(x, -\frac{x(b+1)}{a+c-x}, \frac{x(b+1)}{a+c-x}) = (0, \frac{-x^2+cx-abx}{a+c-x}, \frac{x^2-cx+abx}{a+c-x})$, which proves that for $x \in (0, c-ab)$ or $x > a+c$ we have $\frac{-x^2+cx-abx}{a+c-x} > 0$ - since σ_3, σ_4 correspond to points $\sigma(x)$ where $x \in (0, c-ab)$ or $x > a+c$ respectively, we're done. \square

We now turn our attention to the local dynamics of F_p on the cross section $\{\dot{y} = 0\}$. To do so, first recall the cross-sections $Y_p = \{\dot{y} = 0\}$, U_p, L_p , analyzed in the discussion preceding Lemma 2.1 - in particular, recall $(1, a, 0)$ is the normal vector to Y_p , and that for $v \in U_p$, $F_p(v) \bullet (1, a, 0) < 0$, while for $v \in L_p$, $F_p(v) \bullet (1, a, 0) > 0$. We will now quickly replicate the arguments of Lemmas 2.3 and 2.4 to describe the local dynamics of F_p on Y_p . First, let us make some general remarks - since $\{\dot{y} = 0\}$ is a plane, $\mathbf{R}^3 \setminus \{\dot{y} = 0\}$ is composed of two components - $\{\dot{y} > 0\}$ parameterized by $\{(x, y, z) | x, y, z \in \mathbf{R}^3, x > -ay\}$ and $\{\dot{y} < 0\}$, given by $\{(x, y, z) | x, y, z \in \mathbf{R}^3, x < -ay\}$ - both

are open, connected regions in \mathbf{R}^3 (see the illustration in Fig.5). By this discussion we conclude that on U_p , F_p points inside $\{\dot{y} < 0\}$, while on L_p it points inside $\{\dot{y} > 0\}$. In fact, we can say more - by direct computation it also follows that $U_p = \{\dot{y} = 0\} \cap \{\dot{x} < 0\}$ and $L_p = \{\dot{y} = 0\} \cap \{\dot{x} > 0\}$. In addition, it also follows that on U_p the vector field F_p points inside the quadrant $\{\dot{x} < 0\} \cap \{\dot{y} < 0\}$ and on L_p inside the quadrant $\{\dot{x} > 0\} \cap \{\dot{y} > 0\}$.

As proven in the discussion preceding Lemma 2.1, the tangency set of F_p to Y_p is a curve parameterized by $l_p(x) = (x, -\frac{x}{a}, \frac{x}{a}), x \in \mathbf{R}$. By computation, the tangent vector to $l_p(x)$ is $l'_p(x) = (1, -\frac{1}{a}, \frac{1}{a})$. Therefore, using the Jacobian matrix precisely like we did in Lemma 2.3 we conclude (see the illustration in Fig.4):

Corollary 2.1.1. *The two dimensional, invariant manifolds W_{In}^u, W_{Out}^s are transverse to U_p, L_p at both P_{In}, P_{Out} .*

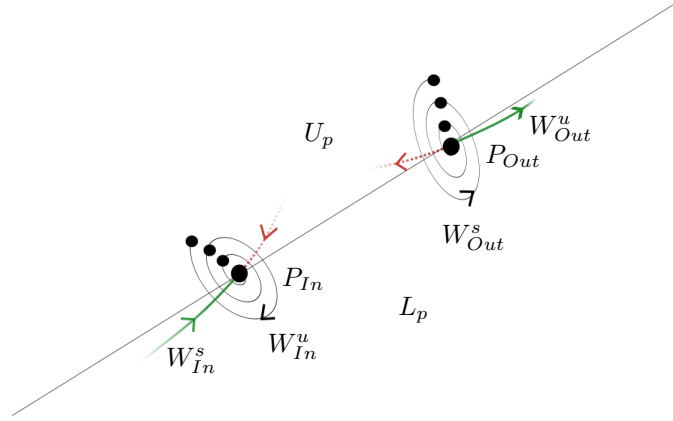


FIGURE 4. The local dynamics around the fixed points. The green and red flow lines are the one-dimensional separatrices in W_{In}^s, W_{Out}^u .

Similarly to Lemma 2.4, we now characterize the local behavior of F_p on l_p . Recall that given any $s \in \mathbf{R}^3$, we denote by γ_s its trajectory, $\gamma_s(0) = s$. We now prove:

Lemma 2.5. $l_p = \{\dot{x} = 0\} \cap \{\dot{y} = 0\}$. Additionally, given $s \in l_p, s = (x, -\frac{x}{a}, \frac{x}{a}), x \in \mathbf{R}$, then for $x < 0$ or $x > c - ab$, there exists some $\epsilon > 0$ s.t. $\gamma_s(t) \in \{\dot{y} < 0\} \cap \{\dot{z} > 0\}$ for all $t \neq 0, t \in (-\epsilon, \epsilon)$. Conversely, when $x \in (0, c - ab)$ we have $s \in \{\dot{z} < 0\}$, and there exists an $\epsilon > 0$ s.t. for $t \in (-\epsilon, \epsilon), t \neq 0$ we have $\gamma_s(t) \in \{\dot{y} > 0\} \cap \{\dot{z} < 0\}$.

Proof. From $F_p(l_p(x)) = (0, 0, bx + \frac{x^2}{a} - \frac{cx}{a})$ we conclude $l_p = \{\dot{y} = 0\} \cap \{\dot{x} = 0\}$ (see Fig.5 for an illustration). Now, $bx + \frac{x^2}{a} - \frac{cx}{a}$ is a quadratic polynomial vanishing precisely at P_{In}, P_{Out} - therefore $F_p(l_p(x))$ points in the positive z -direction precisely when $x < 0$ or $x > c - ab$ - in particular, at such x , the vector $F_p(l_p(x))$ is tangent to H_p . Now, recall the normal vector to U_p is $(1, a, 0)$, and that by computation, for all $v \in U_p$ we have $F_p(v) \bullet (1, a, 0) < 0$ (see the discussion preceding Lemma 2.1). We therefore conclude the vector field F_p points on U_p inside $\{\dot{y} < 0\}$. As such, by previous discussion we conclude that for $x < 0$ or $x > c - ab$ the trajectory of $l_p(x)$ arrives at $l_p(x)$ from $\{\dot{y} < 0\} \cap \{\dot{z} > 0\}$ (the region in the front of Fig.5) and flows back straight back inside $\{\dot{y} < 0\} \cap \{\dot{z} > 0\}$ (see Fig.5 for an illustration). Hence, all in all, given $s = l_p(x), x < 0$ or $x > c - ab$, there exists an $\epsilon > 0$ s.t. $\gamma_s(t) \in \{\dot{y} < 0\} \cap \{\dot{z} > 0\}$ for all $t \neq 0, t \in (-\epsilon, \epsilon)$.

Finally, from $F_p(l_p(x)) = (0, 0, bx + \frac{x^2}{a} - \frac{cx}{a})$ we conclude that for $x < 0, x > c - ab$ we have $l_p(x) \in \{\dot{z} > 0\}$ - and for $x \in (0, c - ab), l_p(x) \in \{\dot{z} < 0\}$. A similar argument to the one used in the previous paragraph now proves that for $s = l_p(x), 0 < x < c - ab$ there exists some $\epsilon > 0$ s.t. for $t \neq 0, t \in (-\epsilon, \epsilon)$ we have $\gamma_s(t) \in \{\dot{y} > 0\} \cap \{\dot{z} < 0\}$ and Lemma 2.5 now follows. \square

Having completed the analysis of $\{\dot{x} = 0\}$ and $\{\dot{y} = 0\}$, we are now ready to prove the existence of Γ_{In} , a separatrix in the one-dimensional, stable manifold W_{In}^s which connects P_{In}, ∞ .

2.0.2. Stage II - the existence of Γ_{In} , an unbounded component of the one-dimensional invariant manifold of P_{In} . To begin, recall we denote by W_{In}^s the one-dimensional, invariant manifold of P_{In} . In this section we use the results proven in Stage I to prove the existence of $\Gamma_{In} \subseteq W_{In}^s$ - and we do so by constructing a three-dimensional body $C_{In} \subseteq \{\dot{y} \geq 0\} \cap \{\dot{x} \geq 0\}$ s.t. no trajectories can enter C_{In} in forward time (see Prop.2.1). As we will see, this would imply C_{In} traps Γ_{In} , a component of W_{In}^s . Thus, reversing the flow, we will conclude the trajectory of every initial condition on Γ_{In} blows up to ∞ under the **inverse** flow (see Cor.2.1.3) - from which

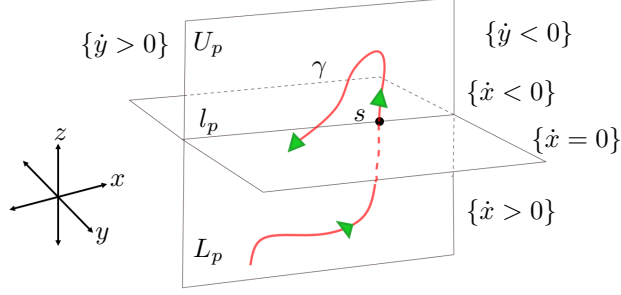


FIGURE 5. The trajectory of an initial condition $s = l_p(x)$, $x < 0$ or $x > c - ab$.

it would follow that P_{In}, ∞ are connected by a heteroclinic trajectory in W_{In}^s .

To begin, first consider the plane $\{x = 0\} = \{(0, y, z) | y, z \in \mathbf{R}\}$. Its normal vector is $(1, 0, 0)$, which, by computation (and Eq.2), proves $F_p(0, y, z) \bullet (1, 0, 0) = -y - z = \dot{x}$. Therefore, since $(1, 0, 0)$ points inside the region $\{(x, y, z) | x > 0\} = \{x > 0\}$ we immediately conclude:

Lemma 2.6. *For every $v \in \{x = 0\}$, $F_p(v) \bullet (1, 0, 0) \geq 0$ if and only if $v \in \{\dot{x} \geq 0\} \cap \{x = 0\}$. In particular, on $\{x = 0\} \cap \{\dot{x} > 0\}$ the vector field F_p points inside $\{x > 0\}$ - and on $\{x = 0\} \cap \{\dot{x} < 0\}$, F_p points inside $\{x < 0\}$ (see the illustration in Fig.6).*

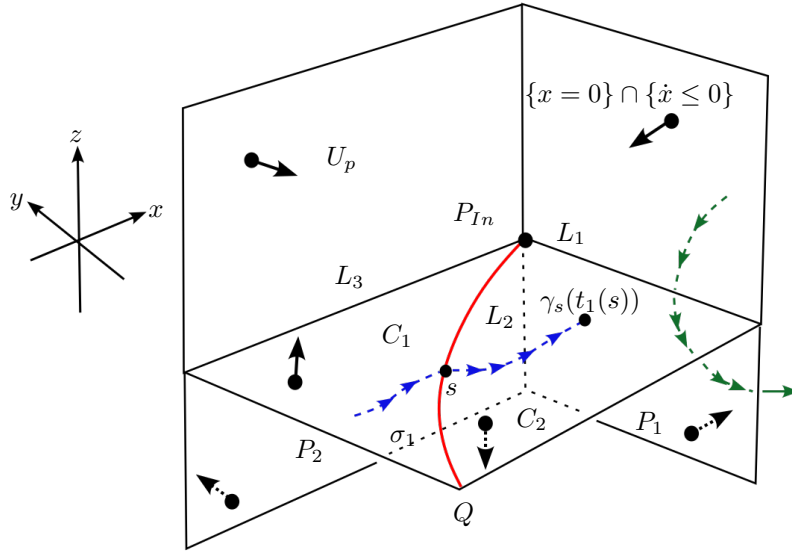


FIGURE 6. The set Q , along with the directions of F_p on P_1, P_2 , and $P_3 = C_1 \cup C_2$. The blue line is the trajectory of an initial condition $s \in \sigma_1$, while the green is a trajectory of some initial condition in L_1 . Q is the quadrant trapped between P_1, P_2 and P_3 .

We are now ready to state and prove Prop.2.1. To begin, first recall we proved in Stage I that both $\{\dot{x} = 0\}, \{\dot{y} = 0\}$ are planes transverse to one another (see Lemma 2.5 and the illustration in Fig.5). As we proved in Stage I, $\mathbf{R}^3 \setminus \{\dot{x} = 0\}$ is composed of two connected regions - $\{\dot{x} > 0\}$ and $\{\dot{x} < 0\}$ - and similarly, $\mathbf{R}^3 \setminus \{\dot{y} = 0\}$ is also composed of two regions, $\{\dot{y} > 0\}$ and $\{\dot{y} < 0\}$. Since $\{\dot{x} = 0\} \cap \{\dot{y} = 0\}$ is a transverse intersection, $\mathbf{R}^3 \setminus (\{\dot{x} = 0\} \cup \{\dot{y} = 0\})$ is made up of four connected regions (see the illustration in Fig.5). Now, consider the quadrant $Q = \{\dot{x} \geq 0\} \cap \{\dot{y} \leq 0\} \cap \{x \leq 0\}$, trapped between the three planes $\{\dot{x} = 0\}, \{\dot{y} = 0\}$ and $\{x = 0\}$ (see the illustration in Fig.6). We now prove:

Proposition 2.1. *There exists a three-dimensional, connected set C_{In} , s.t.:*

- $P_{In} \in \partial C_{In}$, $P_{Out} \notin \partial C_{In}$.
- $C_{In} \subseteq \{\dot{y} \leq 0\} \cap \{\dot{x} \geq 0\}$.
- For every $v \in \partial C_{In}$, $F_p(v)$ is either tangent or points into $\mathbf{R}^3 \setminus C_{In}$ - that is, given any initial condition $s \notin C_{In}$, its forward trajectory never enters C_{In} .

Proof. We prove Prop.2.1 as a sequence of interconnected short, technical Lemmas and their Corollaries. The idea behind the proof is as follows - recall the curve σ_1 introduced at Stage I (see the discussion after Lemma 2.3, and Fig.3 for an illustration). By studying the behaviour of F_p on ∂Q we will infer that given any $s \in \sigma_1$, the forward trajectory of s eventually hits ∂Q transversely (see Lemma 2.9). This will allow us to define the region C_{In} , trapped between the said flow lines and ∂Q - as we will prove, given any $v \in \partial C_{In}$, $F_p(v)$ is either tangent to ∂C_{In} at v or points outside of C_{In} (see Lemma 2.10), from which Prop.2.1 will follow.

Therefore, per this sketch of proof, we begin by studying the behaviour of F_p on ∂Q . By its definition above, the set Q is a quadrant trapped by three planes, given by the following parameterizations:

- $\{\dot{x} = 0\} = \{(x, y, -y) | x, y \in \mathbf{R}\}.$
- $\{\dot{y} = 0\} = \{(x, -\frac{x}{a}, z) | x, z \in \mathbf{N}\}.$
- $\{x = 0\} = \{(0, y, z) | y, z \in \mathbf{R}\}.$

In order to study the behaviour of F_p on ∂Q , we now define the following three curves, all of which lie in ∂Q and consist of transverse intersections (see the illustration in Fig.6):

- $L_1 = \{x = 0\} \cap \{\dot{x} = 0\} \cap \{\dot{y} \leq 0\}$, which is parameterized by $\{(0, y, -y) | y \leq 0\}.$
- $L_2 = \{x = 0\} \cap \{\dot{y} = 0\} \cap \{\dot{x} \geq 0\}$, which is parameterized by $\{(0, 0, z) | z \leq 0\}.$
- $L_3 = \{\dot{y} = 0\} \cap \{\dot{x} = 0\} \cap \{x \leq 0\}$, parameterized by $\{(x, -\frac{x}{a}, \frac{x}{a}) | x \leq 0\}.$ In particular, recalling the curve l_p from Stage I and its parameterization (the tangency curve to $\{\dot{y} = 0\}$ - see Lemma 2.5), we conclude $L_3 = \{l_p(x) | x \leq 0\}.$

By definition, the curves L_1, L_2, L_3 all connect the fixed point $P_{In} = (0, 0, 0)$ to ∞ - moreover, since $P_{Out} = (c - ab, \frac{ab-c}{a}, \frac{c-ab}{a})$, by $c - ab > 0$ (see the discussion in page 3), we conclude $P_{Out} \notin L_1 \cup L_2 \cup L_3$ (see Fig.6 for an illustration). Additionally, $\partial Q \setminus (L_1 \cup L_2 \cup L_3)$ is composed of three disjoint planar sets, P_1, P_2, P_3 , defined as follows (see the illustration in Fig.6):

- P_1 is the interior of the convex hull of L_1 and L_2 - by definition, P_1 is a subset of $\{x = 0\} \cap \{\dot{x} \geq 0\}$. By Cor.2.6, F_p points inside $\{x > 0\}$ on P_1 .
- P_2 is the interior of convex hull of L_2 and L_3 - as such, it is a subset of the cross-section $L_p = \{\dot{y} = 0\} \cap \{\dot{x} > 0\}$ (see the discussion before Lemma 2.1). By the discussion preceding Cor.2.1.1, on P_2 the vector field F_p points into $\{\dot{y} > 0\}$.
- P_3 is the convex hull of L_1 and L_3 - as such, it is a subset of $\{\dot{x} = 0\}$.

As a consequence from the definitions of P_1, P_2, P_3 above, we now prove:

Lemma 2.7. *Assume $v \in \partial Q \setminus (P_3 \cup L_1)$ is **not** a fixed-point for F_p . Then, $F_p(v)$ points outside of Q (see the illustration in Fig.6).*

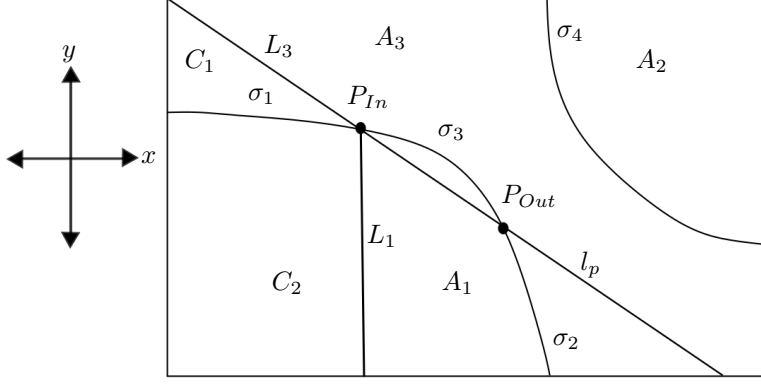
Proof. First, recall we defined Q as the quadrant $Q = \{\dot{x} \geq 0\} \cap \{\dot{y} \leq 0\} \cap \{x \leq 0\}$. By the discussion above, if $v \in \partial Q \setminus (P_3 \cup L_1)$, there are precisely three possibilities:

- $v \in P_1.$
- $v \in P_2.$
- $v \in L_2 \cup L_3.$

By the discussion and definition of P_1, P_2 and P_3 above, if $v \in P_1$, $F_p(v)$ points inside $\{x > 0\}$ - and if $v \in P_2$, $F_p(v)$ points inside $\{\dot{y} > 0\}$. By the definition of Q as the intersection $\{\dot{x} \geq 0\} \cap \{\dot{y} \leq 0\} \cap \{x \leq 0\}$ we conclude that if $v \in P_1 \cup P_2$, $F_p(v)$ points outside of Q . Therefore, to conclude the proof of the Lemma 2.7, it would suffice to prove that on $v \in L_2 \cup L_3$, $F_p(v)$ points outside of Q .

We first prove it for L_3 . To this end, recall we parameterize L_3 by $L_2(x) = (x, -\frac{x}{a}, \frac{x}{a}), x \leq 0$, and that $P_{In} = (0, 0, 0) = L_3(0)$ - in particular, since the fixed point $P_{Out} \notin Q$, we have $P_{Out} \notin Q$. Therefore, by this discussion, it would suffice to prove that for any $x < 0$, $F_p(L_3(x))$ points outside Q . To do so, recall that by the definition of L_3 , we have $L_2 \subseteq \{\dot{x} = 0\}$. Further recall the normal vector to $\{\dot{x} = 0\}$ is $(0, 1, 1)$ - which, by direct computation, implies $F_p(x, -\frac{x}{a}, \frac{x}{a}) \bullet (0, 1, 1) = \frac{x^2 - cx + abx}{a}$. The polynomial $\frac{x^2 - cx + abx}{a}$ vanishes precisely for $x = 0, c - ab$ - therefore recalling we assume w.r.t. $p = (a, b, c)$ that $a, b \in (0, 1)$ and $c > 1$ (see the discussion in page 3), we conclude $c - ab > 0$. Therefore, $\frac{x^2 - cx + abx}{a}$ is positive for $x < 0$, and it follows that whenever $x < 0$, $F_p(x, -\frac{x}{a}, \frac{x}{a}) \bullet (0, 1, 1) > 0$. Additionally, recalling the set A_3 (see the proof of Lemma 2.3 for a definition), this entire discussion proves that for every $x < 0$, $(x, -\frac{x}{a}, \frac{x}{a}) \in A_3$. Since on A_3 the vector field F_p points into $\{\dot{x} < 0\}$, by $Q \subseteq \{\dot{x} \leq 0\}$ we finally conclude that given $x < 0$, $F_p(L_3(x))$ points outside of Q .

Recalling $L_2 \subseteq \{\dot{y} = 0\} \cap \{\dot{x} > 0\}$ and that the normal vector to $\{\dot{y} = 0\}$ is $(1, a, 0)$, a similar argument establishes that given $x \in L_3$, we have $x \in L_p$ - hence, by the results of Stage I, for $v \in L_3 \setminus \{P_{In}\}$, $F_p(v)$ points inside $\{\dot{y} > 0\}$, that is, outside of Q . The proof of Lemma 2.7 is now complete. \square

FIGURE 7. The lines L_1, L_3 and the regions C_1, C_2 on $\{\dot{x} = 0\}$.

Having proven Lemma 2.7, we now study the dynamics of F_p on P_3 - as we will discover, it is the only subset of ∂Q through which trajectories can enter Q . To this end, let us recall the curve σ , parameterized by $\sigma(x) = (x, -\frac{x(b+1)}{a+c-x}, \frac{x(b+1)}{a+c-x})$, (defined for $x \neq c+a$), is the tangency curve of F_p to $\{\dot{x} = 0\}$ - moreover, recall we denote by $\sigma_1 = \{\sigma(x) | x \leq 0\}$ the a component of $\sigma \setminus \{P_{In}, P_{Out}\}$ which connects P_{In}, ∞ in S^3 (see the discussion in Lemma 2.3 and Lemma 2.4, and the illustration in Fig.3). By Lemma 2.4 we conclude $\sigma_1 = Q \cap \sigma$ (see the illustration in Fig.6). Since σ_1 , by definition, is a curve on $\{\dot{x} = 0\}$ and since $Q \subseteq \{\dot{x} \geq 0\}$, it follows $\sigma_1 \subseteq \partial Q \cap \{\dot{x} = 0\}$ - which implies $\sigma_1 \subseteq \overline{P_3}$ (see the illustration in Fig.7). We now prove:

Lemma 2.8. $P_3 \setminus \sigma_1$ consists of two components, C_1, C_2 s.t. given $s \in \mathbf{R}^3$, its trajectory can enter Q **only** by hitting C_2 transversely.

Proof. To begin, recall that by its definition σ is the tangency curve of F_p to the cross-section $\{\dot{x} = 0\}$. Therefore, since $\sigma_1 = Q \cap \sigma$, given $v \in P_3$ we have $F_p(v) \bullet (0, 1, 1) = 0$ precisely when $v \in \sigma_1$ - and as a consequence, the sign of $F_p(v) \bullet (0, 1, 1)$ is constant on both C_1, C_2 . Now, choose some $v \in L_3$ - as shown during the proof of Lemma 2.7, for $v \in L_3$, $F_p(v) \bullet (0, 1, 1) > 0$, which proves that for $v \in C_1$, $F_p(v) \bullet (0, 1, 1) > 0$. Therefore, F_p points inside $\{\dot{x} < 0\}$ on C_1 - that is, on C_1 the vector field F_p points outside of Q (see the illustration in Fig.6). A similar argument applied to L_1 and C_2 proves that for $v \in C_2$, $F_p(v) \bullet (0, 1, 1) < 0$ - hence F_p points on C_2 inside Q .

Therefore, given any $s \in \mathbf{R}^3$ whose trajectory eventually enters Q , by Lemma 2.7 and the paragraph above it **cannot** enter Q by hitting transversely $\partial Q \setminus (C_2 \cup \sigma_1)$ - i.e., it can only enter Q by hitting $C_2 \cup L_1$. However, by the discussion preceding Cor.2.6, $L_1 = \{\dot{x} = 0\} \cup \{x = 0\}$ is the tangency curve of F_p to the plane $\{x = 0\}$, parameterized by $\{(0, y, -y) | y \leq 0\}$. Recalling the normal vector to $\{\dot{x}\}$ is $(0, 1, 1)$, we conclude $F_p(v) \bullet (0, 1, 1) < 0$ on any $v \in L_1$ - and recalling the discussion in the proof of Lemma 2.3, we conclude $F_p(v)$ points inside $\{\dot{x} \geq 0\}$ at every $v \in L_1$. Therefore, since on L_1 the vector field F_p is tangent to $\{x = 0\}$, given $v \in L_1$, its trajectory arrives at v from $\{x > 0\}$, hits v , then bounces back to $\{x > 0\}$ - see the illustration in Fig.6. As such, the trajectories of initial conditions $s \in Q$ cannot escape Q by hitting L_1 , and Lemma 2.8 follows. \square

Having completed the proof of Lemma 2.8 we can almost begin constructing C_{In} , which would conclude the proof of Prop.2.1. As stated earlier, we will construct C_{In} out of flow lines which connect regions in ∂Q - and to do so we need more information about how trajectories for the flow can escape Q . To this end, consider the curve σ_1 , and choose some initial conditions $s \in \sigma_1$. Recall $\sigma_1 \subseteq Q$ and that we denote the trajectory of $s \in \sigma_1$ by $\gamma_s(t), t \in \mathbf{R}, \gamma_s(0) = s$. Further recall we denote by W_{In}^s the stable, one-dimensional manifold of P_{In} - we now prove:

Lemma 2.9. For every $s \in \sigma_1 \setminus W_{In}^s$, there exists some **minimal** $t > 0$ s.t. $\gamma_s(t) \notin Q$ - that is, the forward-trajectory of every initial condition in $\sigma_1 \setminus W_{In}^s$ eventually escapes Q .

Proof. Recall $Q = \{\dot{x} \geq 0\} \cap \{\dot{y} \leq 0\} \cap \{x \leq 0\}$, and that we parameterize σ_1 by $\{(x, -\frac{x(b+1)}{a+c-x}, \frac{x(b+1)}{a+c-x}) | x < 0\}$. Therefore, given any $s \in \sigma_1$, its x -coordinate is strictly lesser than 0 - hence, by Lemma 2.4, given every $s \in \sigma_1$, there exists some ϵ s.t. for every $r \in [0, \epsilon)$, $\gamma_s(r) \in Q$ - in particular, by Lemma 2.4, for every $r \in (0, \epsilon)$, $\gamma_s(r) \in \{\dot{x} \geq 0\}$. Since by its definition that are no fixed-points in σ_1 (see the discussion before Lemma 2.4), given $s \in \sigma_1 \setminus W_{In}^s$ there are precisely two possibilities to consider:

- There exists some $t_0 > 0$ s.t. $\gamma_s(t_0) \in \{\dot{x} < 0\}$.
- For every $t > 0$, $\gamma_s(t) \in \{\dot{x} \geq 0\}$.

In the first possibility, there is little to prove - since $Q \subseteq \{\dot{x} \geq 0\}$, by $\gamma_s(t_0) \in \{\dot{x} < 0\}$ we immediately conclude $\gamma_s(t_0) \notin Q$. Therefore, to conclude the proof we must show that even if for every $t > 0$, $\gamma_s(t) \in \{\dot{x} \geq 0\}$, the trajectory of s eventually escapes Q . To do so, recall that given $s \in \sigma_1 \setminus W_{In}^s$, its x -coordinate is strictly lesser than 0, i.e., $s \in \{x < 0\}$. Therefore, if for every $t > 0$ we have $\gamma_s(t) \in \{\dot{x} \geq 0\}$, provided $s \notin W_{In}^s$ (i.e. not attracted to $P_{In} = (0, 0, 0)$), the x -coordinate along γ_s must grow monotonically - which implies the existence of some t_0 s.t. $\gamma_s(t_0) \in \{x > 0\}$. Since by its definition $Q \subseteq \{x \leq 0\}$, this proves $\gamma_s(t_0) \notin Q$ and Lemma 2.9 follows. \square

Now, recall Lemmas 2.7 and 2.8. Together they imply that given $s \in \sigma_1$, its forward trajectory can escape Q **only** by hitting $\partial Q \setminus (C_2 \cup \sigma_1)$ transversely (see the illustration in Fig.6). Therefore, recalling that given an initial condition $s \in \mathbf{R}^3$ we denote its trajectory by γ_s , $\gamma_s(0) = 0$, Lemma 2.9 motivates us to define the following (see Fig.6 for an illustration):

Definition 2.1. Let $s \in \sigma_1$ be an initial condition, $s \neq P_{In}$. Then, denote by $0 < t_1(s) \leq \infty$ the first **positive** time s.t. $\gamma_s(t_1(s)) \in P_1 \cup P_2 \cup C_1 \cup L_1 \cup L_2 \cup L_3$. We say $t_1(s) = \infty$ if and only if **both** of the following to conditions apply to s :

- $s \in W_{In}^s \cap \sigma_1$.
- For every $t > 0$, $\gamma_s(t) \in Q$ - that is, the trajectory of s tends to P_{In} **from within** Q .

If $t_1(s) = \infty$, we write $\gamma_s(t_1(s)) = P_{In}$.

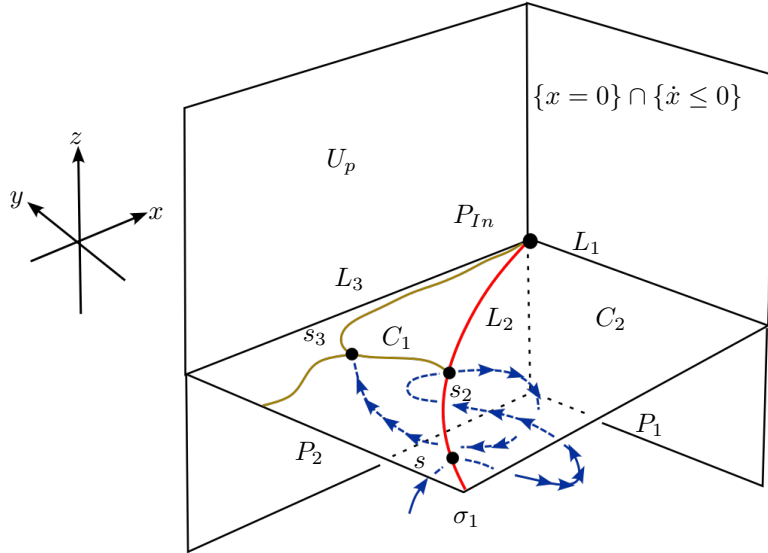


FIGURE 8. The curve γ is the brown line. The trajectory of s_1 hits σ_1 at s_2 before flowing to $\gamma_{s_1}(t_1(s)) = s_3$, which forces a branching in γ .

By Lemma 2.9, $t_1(s)$ is finite for every $s \in \sigma_1 \setminus W_{In}^s$. And provided $s \in W_{In}^s \cap \sigma_1$ does not tend to P_{In} through Q , $t_1(s)$ is also finite - otherwise, $t_1(s) = \infty$. Using the definition of t_1 , we can now finally construct the body C_{In} , thus concluding the proof of Prop.2.1. To begin, denote by $T = P_1 \cup P_2 \cup C_1 \cup L_1 \cup L_2 \cup L_3$, and consider the set $\gamma = \cup_{s \in \sigma_1} \gamma_s(t_1(s))$ - by the discussion above, we immediately conclude $\gamma \subseteq T$. Now, let Γ denote the collection of flow-lines connecting σ_1, γ (see the illustration in fig.8) - by definition, $\Gamma \subseteq Q$. Since by Lemma 2.8 $\gamma_s(t_1(s)) \notin C_2$ for every $s \in \sigma_1$, we conclude $\Gamma \cap C_2 = \emptyset$. Now, consider $Q \setminus \Gamma$ - by this discussion $Q \setminus \Gamma$ includes precisely two components - we therefore define C_{In} as the component of $Q \setminus \Gamma$ s.t. $C_{In} \cap C_2 = \emptyset$. Since $P_{In} \in \sigma_1$ and since $P_{Out} \notin Q$, by the definition of C_{In} we immediately conclude:

Corollary 2.1.2. $P_{In} \in \partial C_{In}$, and $P_{Out} \notin \overline{C_{In}}$. Moreover, $C_{In} \subseteq \{\dot{y} \geq 0\} \cap \{\dot{x} \geq 0\}$.

Proof. First, by definition, $P_{In} \in \overline{\sigma_1}$ - which, by the definition of Γ , implies $P_{In} \in \partial C_{In}$. Moreover, recall $P_{Out} = (c - ab, \frac{ab-c}{a}, \frac{c-ab}{a})$, and that per our assumptions on the constants a, b, c , we have $a, b \in (0, 1)$, $c > 1$ (see the discussion at page 3). This proves $c - ab > 0$ - and since $Q = \{\dot{x} \geq 0\} \cap \{\dot{y} \leq 0\} \cap \{x \leq 0\}$, we conclude both $P_{Out} \notin \overline{Q}$, $Q \subseteq \{\dot{x} \geq 0\} \cap \{\dot{y} = 0\}$. Therefore, since by definition $C_{In} \subseteq Q$, this discussion proves both $P_{Out} \notin \overline{C_{In}}$ and $C_{In} \subseteq \{\dot{x} \geq 0\} \cap \{\dot{y} \leq 0\}$, and Cor.2.1.2 follows. \square

Therefore, having proven Cor.2.1.2, in order to conclude the proof of Prop.2.1 it remains to prove that given every $s \in \mathbf{R}^3$, its forward trajectory under F_p can never enter C_{In} . We do so in the following Lemma:

Lemma 2.10. *At every $v \in \partial C_{In}$, either $F_p(v)$ is tangent to ∂C_{In} , or F_p points outside of C_{In} - that is, given any $s \in \mathbf{R}^3 \setminus C_{In}$, its forward trajectory never enters C_{In} under the flow.*

Proof. By definition, ∂C_{In} is composed of flow-lines in Γ and regions on T . Recalling $T = P_1 \cup P_2 \cup C_1 \cup L_1 \cup L_2 \cup L_3$, by Lemmas 2.8 and 2.9 we know F_p points outside of Q throughout $T \cap \partial C_{In}$ - since $C_{In} \subseteq Q$, we conclude F_p also points outside C_{In} throughout $T \cap \partial C_{In}$. As such, because by definition F_p is tangent to Γ , Lemma 2.10 now follows. \square

Having proven Cor.2.1.2 and Lemma 2.10, we can summarize our findings as follows. We have proven the existence of a three-dimensional body C_{In} s.t.:

- $P_{In} \in \partial C_{In}$, and $P_{Out} \notin \overline{C_{In}}$.
- $C_{In} \subseteq \{\dot{x} \geq 0\} \cap \{\dot{y} \leq 0\}$.
- Given any $s \in \partial C_{In}$, $F_p(s)$ is either tangent to ∂C_{In} or points outside of C_{In} .

In other words, we have completed the proof of Prop.2.1. \square

Having proven Prop.2.1, we can now conclude Stage II - namely, we are now ready to prove the existence of an invariant, unbounded, one dimensional manifold $\Gamma_{In} \subseteq C_{In}$. To this end, given $t \in \mathbf{R}$, we denote the flow generated by F_p at time t by ϕ_t^p . Furthermore, denote by ψ_t^p the flow generated by the vector field $J_p(P_{In})$ - i.e., the linearization of F_p at P_{In} . By the Hartman-Grobman Theorem there exists some $r > 0$ s.t the flow ϕ_t^p in $B_r(P_{In})$ is orbitally equivalent to ψ_t^p in $B_d(P_{In})$, $d > 0$. Namely, there exists a homeomorphism $H : B_r(P_{In}) \rightarrow B_d(P_{In})$ s.t. $H(\phi_t^p(x)) = \psi_t^p(H(x))$.

Now, since F_p is either tangent or points outside C_{In} on ∂C_{In} , we conclude that given $v \in \partial C_{In}$, $-F_p(v)$ is either tangent or points **inside** C_{In} - in other words, no trajectories escape C_{In} under the inverse flow. As such, it immediately follows that given an initial condition in $C_{In} \cap B_r(P_{In})$, its backwards trajectory **cannot** hit $\partial C_{In} \cap \overline{B_r(P_{In})}$ - that is, the component C of $C_{In} \cap B_r(P_{In})$ s.t. $P_{In} \in \partial C$ is a topological cone. Setting $K = H(C)$, by this discussion we conclude no trajectories for the linearization of $-F_p$ at P_{In} (i.e., the vector field $-J_p(P_{In})$) can escape K through $\partial K \setminus B_d(P_{In})$. Therefore, there exists some eigenvector for $J_p(P_{In})$ in K - which, in turn, proves the existence of Γ_{In} , an invariant manifold for P_{In} , s.t. $\Gamma_{In} \cap C_{In} \cap B_r(P_{In}) \neq \emptyset$. Therefore, since no trajectories can escape C_{In} under the inverse flow, given any $x \in \Gamma_{In} \cap C_{In} \cap B_r(P_{In})$, for every $t < 0$ we have $\phi_t^p(x) \in C_{In}$ - which proves $\Gamma_{In} \subseteq C_{In}$.

Now, recall P_{In} is a saddle-focus with a 2-dimensional unstable manifold, W_{In}^u , transverse to P_{In} at $\{\dot{x} = 0\}$ (see Lemma 2.3 and the illustration in Fig.4). As such, the backwards trajectory of initial conditions in W_{In}^u must intersect **both** $\{\dot{x} > 0\}$ and $\{\dot{x} < 0\}$ infinitely many times. By the construction of C_{In} in Prop.2.1, $C_{In} \cap \{\dot{x} < 0\} = \emptyset$ - therefore, since no trajectories can escape C_{In} under the inverse flow this implies Γ_{In} **cannot** intersect $\{\dot{x} < 0\}$ - hence Γ_{In} is **not** a flow line in W_{In}^u . This proves Γ_{In} is a component of W_{In}^s , the unstable, one-dimensional manifold of P_{In} - and since $\Gamma_{In} \cap W_{In}^u = \emptyset$, it cannot be a homoclinic trajectory to P_{In} . Additionally, since $P_{Out} \notin \overline{C_{In}}$ (see Prop.2.1), because $\Gamma_{In} \subseteq C_{In}$ we also conclude $P_{Out} \notin \overline{\Gamma_{In}}$.

As such, all that remains is to conclude Stage II is to prove Γ_{In} is unbounded. However, since $C_{In} \subseteq \{\dot{x} \geq 0\} \cap \{\dot{y} \leq 0\}$ we conclude **both** $-\dot{x}$, $-\dot{y}$ never change their sign on Γ_{In} . Since by previous paragraph Γ_{In} is **not** a homoclinic trajectory to P_{In} or a heteroclinic trajectory to P_{Out} , we conclude that given any $x \in \Gamma_{In}$, $\lim_{t \rightarrow -\infty} \phi_t^p(x) = \infty$. Therefore, we have proven:

Corollary 2.1.3. *There exists a component $\Gamma_{In} \subseteq W_{In}^s$, s.t. Γ_{In} is a heteroclinic trajectory for F_p in S^3 , connecting the fixed-points P_{In} and ∞ .*

2.0.3. Stage III - the existence of Γ_{Out} , an unbounded component of the one-dimensional invariant manifold of P_{Out} . Having proven the existence of Γ_{In} , we will prove the analogous result for P_{Out} - namely, we will now prove the existence of a heteroclinic connection Γ_{Out} , a subset of the one-dimensional W_{Out}^u , which connects P_{Out}, ∞ . Similarly to Stage II, we will do so by constructing C_{Out} , a trapping set for Γ_{Out} . Despite some slight differences, in practice the proof will be almost symmetric to the one in Stage II. This section is organized as follows - similarly to Stage II, we begin by studying the local dynamics of F_p on some plane, which passes through the saddle-focus P_{Out} . After that, we prove Prop.2.2, in which we construct the three-dimensional body C_{Out} by hand - as we will see, again we have $C_{Out} \subseteq \{\dot{x} \geq 0\} \cap \{\dot{y} \geq 0\}$. Following that, similar arguments to those used in Stage II will imply C_{Out} contains Γ_{Out} , a component of W_{Out}^u which connects P_{Out}, ∞ (see Cor.2.1.4).

To begin, recall $P_{Out} = (c - ab, \frac{ab-c}{a}, \frac{c-ab}{a})$, and consider the plane $\{x = c - ab\} = \{(c - ab, y, z) | y, z \in \mathbf{R}\}$ - further recall that by the discussion in page 3, $c - ab > 0$. A similar argument to that used to prove Lemma 2.6 now implies:

Lemma 2.11. *For every $v \in \{x = c - ab\}$, $F_p(v) \bullet (1, 0, 0) \geq 0$ if and only if $v \in \{\dot{x} \geq 0\} \cap \{x = c - ab\}$. In particular, on $\{x = c - ab\} \cap \{\dot{x} > 0\}$ the vector field F_p points inside $\{x > c - ab\}$ - and on $\{x = c - ab\} \cap \{\dot{x} < 0\}$, F_p points inside $\{x < c - ab\}$ (see the illustration in Fig.10).*

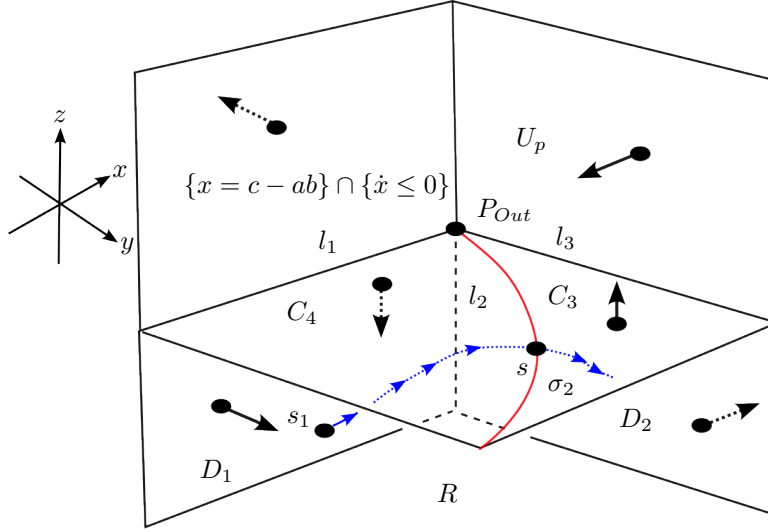


FIGURE 9. The region R , trapped between D_1, D_2 and $D_3 = C_3 \cup C_4$, along with the directions of F_p on ∂R . The blue curve denotes the forward-trajectory of $s_1 = \gamma_s(t_2(s))$ to $s \in \sigma_2$.

Now, similarly to the definition of Q in Stage II, consider the quadrant $R = \{\dot{x} \geq 0\} \cap \{\dot{y} \leq 0\} \cap \{x \geq c - ab\}$, trapped between the three planes $\{\dot{x} = 0\}$, $\{\dot{y} = 0\}$ and $\{x = c - ab\}$ (see the illustration in Fig.9). Analogously to Prop.2.1, we now prove:

Proposition 2.2. *There exists a three-dimensional, connected set C_{Out} , s.t.:*

- $P_{Out} \in \partial C_{Out}$, $P_{In} \notin \partial C_{Out}$.
- $C_{Out} \subseteq \{\dot{y} \leq 0\} \cap \{\dot{x} \geq 0\}$.
- For every $v \in \partial C_{Out}$, $F_p(v)$ is either tangent or points inside C_{Out} - that is, given any initial condition $s \in C_{Out}$, its forward trajectory never escapes C_{Out} .

Proof. Similarly to the proof of Prop.2.1, we will prove Prop.2.2 as a sequence of interconnected Lemmas and their Corollaries. The idea behind the proof is also similar - recall the curve σ_2 introduced at Stage I (see the discussion after Lemma 2.3, and Fig.3 for an illustration). By studying the behaviour of F_p on ∂R we will infer that given any $s \in \sigma_2$, the **backwards** trajectory of s eventually hits ∂R transversely (see Lemma 2.13). This will allow us to define the region C_{Out} , trapped between the said flow lines and ∂R - then, similarly to the proof in Stage II, it would follow that given any $v \in \partial C_{Out}$, $F_p(v)$ is either tangent to ∂C_{Out} at v or points inside of C_{Out} , thus completing the proof.

Therefore, similarly to the proof of Prop.2.1, we begin by studying the behaviour of F_p on ∂R . By its definition above, let us recall R is a quadrant trapped by three planes, given by the following parameterizations:

- $\{\dot{x} = 0\} = \{(x, y, -y) | x, y \in \mathbf{R}\}$.
- $\{\dot{y} = 0\} = \{(x, -\frac{x}{a}, z) | x, z \in \mathbf{R}\}$.
- $\{x = c - ab\} = \{(c - ab, y, z) | y, z \in \mathbf{R}\}$.

In order to study the behaviour of F_p on ∂R , we again define three curves, all of which lie in ∂R (see the illustration in Fig.10):

- $l_1 = \{x = c - ab\} \cap \{\dot{x} = 0\} \cap \{\dot{y} \leq 0\}$, which is parameterized by $\{(c - ab, y, -y) | y \leq \frac{ab-c}{a}\}$.
- $l_2 = \{x = c - ab\} \cap \{\dot{y} = 0\} \cap \{\dot{x} \geq 0\}$, which is parameterized by $\{(c - ab, 0, z) | z \leq \frac{c-ab}{a}\}$.
- $l_3 = \{\dot{y} = 0\} \cap \{\dot{x} = 0\} \cap \{x \geq c - ab\}$, parameterized by $\{(x, -\frac{x}{a}, \frac{x}{a}) | x \leq 0\}$. In particular, recalling the curve l_p from Stage I and its parameterization (see Lemma 2.5), we conclude $l_3 = \{l_p(x) | x \geq c - ab\}$.

By definition, the curves l_1, l_2, l_3 all connect the fixed point $P_{Out} = (c - ab, \frac{ab-c}{a}, \frac{c-ab}{a})$ to ∞ . Moreover, $\partial R \setminus (l_1 \cup l_2 \cup l_3)$ is composed of three disjoint planar sets, D_1, D_2, D_3 , defined as follows (see the illustration in Fig.6):

- D_1 is the interior of the convex hull of l_1 and l_2 - by definition, P_1 is a subset of $\{x = c - ab\} \cap \{\dot{x} \geq 0\}$. By Cor.2.6, F_p points inside $\{x > c - ab\}$ on D_1 - that is, that is, by the definition of R , on D_2 F_p points **inside** R .
- D_2 is the interior of convex hull of l_2 and l_3 - as such, it is a subset of $L_p = \{\dot{y} = 0\} \cap \{\dot{x} > 0\}$ (see the discussion before Lemma 2.1). By the discussion preceding Cor.2.1.1, on D_2 the vector field F_p points into $\{\dot{y} > 0\}$ - that is, on D_2 F_p points **outside** R .
- D_3 is the convex hull of l_1 and l_3 - as such, it is a subset of $\{\dot{x} = 0\}$.

To continue, similarly to what we did in Stage II, we now study the dynamics of F_p on D_3 . To this end, let us recall the curve σ , parameterized by $\sigma(x) = (x, -\frac{x(b+1)}{a+c-x}, \frac{x(b+1)}{a+c-x})$ (for $x \neq c + a$), is the tangency curve of F_p to $\{\dot{x} = 0\}$ - moreover, recall we denote by $\sigma_2 = \{\sigma(x) | c - ab < x < a + c\}$, the component of $\sigma \setminus \{P_{In}, P_{Out}\}$ which connects P_{Out}, ∞ in S^3 (see the discussion in Lemma 2.3 and Lemma 2.4, and the illustration in Fig.3). By Lemma 2.4 we conclude $\sigma_2 = R \cap \sigma$ (see the illustration in Fig.10). Since σ_2 is a curve on $\{\dot{x} = 0\}$, and because $R \subseteq \{\dot{x} \geq 0\}$, we again conclude $\sigma_2 \subseteq \partial R \cap \{\dot{x} = 0\}$ - that is, $\sigma_2 \subseteq \bar{D}_3$ (see the illustration in Fig.7). Therefore, similar arguments to those used to prove Lemma 2.8 now imply:

Lemma 2.12. $D_3 \setminus \sigma_2$ consists of two components, C_3, C_4 s.t. given $s \in \mathbf{R}^3$, its forwards-trajectory can enter R **only** by hitting $B = C_4 \cup D_1 \cup l_1$ transversely.

To continue, much like we did in Stage II, we will construct C_{Out} out of flow lines which begin at σ_2 - however, this time we will do so using the inverse flow. To this end, recall the curve σ_2 , and choose some initial conditions $s \in \sigma_2$. Recall $\sigma_2 \subseteq R$ and that we denote the trajectory of $s \in \sigma_2$ by $\gamma_s(t), t \in \mathbf{R}, \gamma_s(0) = s$. Further recall we denote by W_{Out}^u the unstable, one-dimensional manifold of P_{Out} - we now prove an analogue of Lemma 2.9:

Lemma 2.13. For every $s \in \sigma_2 \setminus W_{Out}^u$, there exists some **maximal** $t < 0$ s.t. $\gamma_s(t) \notin R$ - that is, every initial condition in $\sigma_2 \setminus W_{Out}^u$ eventually escapes R under the inverse flow.

Proof. Recall $R = \{\dot{x} \geq 0\} \cap \{\dot{y} \leq 0\} \cap \{x \geq c - ab\}$, and that we parameterize σ_2 by $\{(x, -\frac{x(b+1)}{a+c-x}, \frac{x(b+1)}{a+c-x}) | a + c < x < c - ab\}$. Therefore, given any $s \in \sigma_2$, its x -coordinate is strictly greater than $c - ab$ - therefore, by Lemma 2.4, given $s \in \sigma_2$, there exists some ϵ s.t. for every $r \in (-\epsilon, 0], \gamma_s(r) \in R$. In particular, by Lemma 2.4, for every $r \in (-\epsilon, 0), \gamma_s(r) \in \{\dot{x} \geq 0\}$. Therefore, similarly to the proof of Lemma 2.9, given $s \in \sigma_2 \setminus W_{Out}^u$ there are, again, precisely two possibilities to consider:

- There exists some $-\infty < t_0 < 0$ s.t. $\gamma_s(t_0) \in \{\dot{x} < 0\}$.
- For every $t < 0, \gamma_s(t) \in \{\dot{x} \leq 0\}$.

In the first possibility, there is little to prove - since $R \subseteq \{\dot{x} \geq 0\}$, by $\gamma_s(t_0) \in \{\dot{x} < 0\}$ we immediately conclude $\gamma_s(t_0) \notin R$. Therefore, to conclude the proof we must show that even in the second possibility the trajectory of s eventually escapes R (at some negative time). To do so, recall we proved that given $s \in \sigma_2$ its x -coordinate is strictly greater than $c - ab$ - i.e., $s \in \{x > c - ab\}$. Therefore, if for every $t < 0$ we have $\gamma_s(t) \in \{\dot{x} \geq 0\}$, provided $s \notin W_{Out}^u$ (that is, the trajectory of s is **not** attracted to $P_{Out} = (c - ab, \frac{ab-c}{a}, \frac{c-ab}{a})$ under the inverse flow), the x -coordinate along γ_s must decrease - and since by assumption $\lim_{t \rightarrow -\infty} \gamma_s(t) \neq P_{Out}$, there exists some $t_0 < 0$ s.t. $\gamma_s(t_0) \in \{x < c - ab\}$. Since by its definition $R \subseteq \{x \geq c - ab\}$, this proves $\gamma_s(t_0) \notin R$ and Lemma 2.13 follows. \square

Now, combining Lemma 2.12 and Lemma 2.13 we conclude that given $s \in \sigma_2$, its backwards trajectory can escape R **only** by hitting $B = C_4 \cup l_1 \cup D_1$ (see the illustration in Fig.9). Therefore, similarly to Def.2.1, we now define:

Definition 2.2. Let $s \in \sigma_2$ be an initial condition, $s \neq P_{Out}$. Then, denote by $0 > t_2(s) \geq -\infty$ the first **negative** time s.t. $\gamma_s(t_2(s)) \in B$. We say $t_2(s) = -\infty$ **if and only if** the following two conditions are both satisfied:

- $s \in W_{Out}^u \cap \sigma_2$.
- For every $t < 0, \gamma_s(t) \in R$ - that is, the trajectory of s tends to P_{Out} **from inside** R .

If $t_2(s) = -\infty$, we write $\gamma_s(t_2(s)) = P_{Out}$.

See Fig.9 for an illustration. By Lemma 2.13, we conclude that for every $s \in \sigma_2 \setminus W_{Out}^u$, $t_2(s)$ is defined and finite. And provided $s \in W_{Out}^u \cap \sigma_2$ does not tend to P_{Out} through R , $t_2(s)$ is also defined and finite - otherwise, $t_2(s) = -\infty$.

Again, similarly to how we utilized t_1 , we now define C_{Out} as follows - consider the set $\delta = \cup_{s \in \sigma_2} \gamma_s(t_2(s))$ (see the illustration in Fig.10) - by Lemma 2.12, we immediately conclude $\delta \subseteq B = D_1 \cup C_4 \cup l_1$. Now, let Δ denote the set of flow-lines connecting σ_2, δ (see the illustration in fig.10) - by the definition of t_2 , the curve $\gamma_s(t_2(s), 0) \subseteq R$, which proves $\Delta \subseteq R$. Since by Lemma 2.12 $\gamma_s(t_2(s)) \notin (C_3 \cup D_2 \cup l_3)$ for every $s \in \sigma_2$, we conclude $\Delta \cap (C_3 \cup D_2 \cup l_3) = \emptyset$ (see the illustration in Fig.10). Again, the same arguments used in Stage II now

prove $R \setminus \Delta$ includes precisely two components - and again, similarly to the proof of Prop.2.1, we define C_{Out} as the component of $R \setminus \Delta$ s.t. $C_{Out} \cap (C_3 \cup D_3 \cup l_3) = \emptyset$.

Now, recall we have $P_{Out} \in \overline{\sigma_2}$, and that $P_{In} = (0, 0, 0)$, $R \subseteq \{x \geq c - ab\}$, $c - ab > 0$ - which implies $P_{In} \notin R$. Additionally, by the construction above, it is also clear ∂C_{Out} is composed of flow lines in Δ and regions in B . Therefore, since by Lemma 2.13 F_p points inside R on B , similar arguments to the proofs of Cor.2.1.2 and Lemma 2.10 now imply:

- $P_{Out} \in \partial C_{Out}$, and $P_{In} \notin \overline{C_{Out}}$.
- $C_{Out} \subseteq \{\dot{y} \geq 0\} \cap \{\dot{x} \geq 0\}$.
- At every $v \in \partial C_{Out}$, either $F_p(v)$ is tangent to ∂C_{Out} , or $F_p(v)$ points inside of C_{Out} - that is, given any initial condition $s \in C_{Out}$, its forward trajectory never escapes C_{Out} .

In other words, the proof of Prop.2.2 is now complete. \square

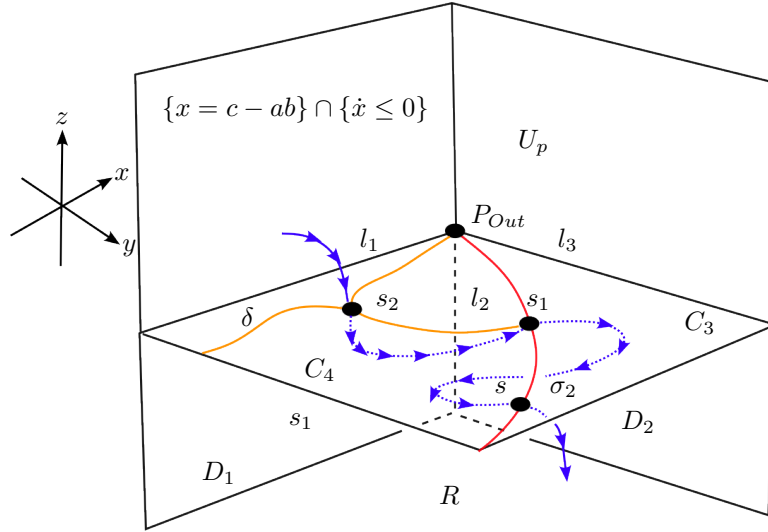


FIGURE 10. The forward-trajectory of $s_2 = \gamma_s(t_2(s))$ which connects it with $s_1, s \in \sigma_2$. This forces δ , the orange line, to be branched.

Having proven Prop.2.2, we can now conclude Stage III of the proof of Th.2.1 - namely, we are now ready to prove the existence of an unbounded heteroclinic connection $\Gamma_{Out} \subseteq W_{Out}^u$, connecting P_{Out}, ∞ :

Corollary 2.1.4. *There exists a components Γ_{Out} of W_{Out}^u in C_{Out} , connecting P_{Out}, ∞ .*

Proof. Recall that P_{Out} is a saddle-focus with a two-dimensional stable manifold W_{Out}^s and a one-dimensional unstable manifold W_{Out}^u . Moreover, recall that given $t \in \mathbf{R}$ we denote the flow generated by F_p at time t by ϕ_t^p . Additionally, similarly to Stage II, denote by ψ_t^p the flow generated by the vector field $J_p(P_{Out})$ - i.e., the linearization of F_p at P_{Out} . By the Hartman-Grobman Theorem there exists some $r > 0$ s.t the flow ϕ_t^p in $B_r(P_{Out})$ is orbitally equivalent to ψ_t^p in $B_d(P_{Out}), d > 0$. Namely, there exists a homeomorphism $H : B_r(P_{Out}) \rightarrow B_d(P_{Out})$ s.t. $H(\phi_t^p(x)) = \psi_t^p(H(x))$.

By our construction of C_{Out} , $\forall s \in C_{Out}$ the trajectory of s under the flow is trapped in C_{Out} - as such, the trajectories of initial conditions in $C_{Out} \cap B_r(P_{Out})$ cannot hit the topological cone $\partial C_{Out} \cap B_r(P_{Out})$. Therefore, similarly to the argument used to prove Cor.2.1.3, we conclude there exists some eigenvector for $J_p(P_{Out})$ in $K = H(C_{Out} \cap B_r(P_{Out}))$ - which, again, implies the existence of some invariant manifold for P_{Out}, Γ_{Out} , in C_{Out} . Now, recall Cor.2.1.1 proves the two-dimensional stable manifold for P_{Out}, W_{Out}^s , is transverse to $\{\dot{y} = 0\}$ at P_{Out} - that is, given $x \in W_{Out}^s$, its forwards-trajectory intersects **both** components of $\{\dot{y} \neq 0\}$ infinitely many times. As a consequence, from $C_{Out} \subseteq \{\dot{y} \leq 0\}$ we conclude Γ_{Out} is not a flow line in W_{Out}^s - which proves Γ_{Out} is a component of W_{Out}^u , and in particular, that Γ_{Out} is not a homoclinic trajectory to P_{Out} . Moreover, since by construction $P_{In} \notin \overline{C_{Out}}$, from $\Gamma_{Out} \subseteq \overline{C_{Out}}$ we conclude that Γ_{Out} cannot be a heteroclinic trajectory which connects P_{In}, P_{Out} .

Now, by $\Gamma_{Out} \cap C_{Out} \subseteq \{\dot{y} \leq 0\} \cap \{\dot{x} \geq 0\}$ we conclude both \dot{y}, \dot{x} do not change their sign along Γ_{Out} . Since by previous paragraph Γ_{Out} is not a homoclinic trajectory or a bounded heteroclinic trajectory, we conclude that given any $x \in \Gamma_{Out}$, $\lim_{n \rightarrow \infty} \phi_t^p(x) = \infty$. In other words, we have just proven Γ_{Out} is an unbounded heteroclinic trajectory in W_{Out}^u which connects P_{Out} and ∞ - hence Cor.2.1.4 follows. \square

2.0.4. Stage IV - constructing the vector field R_p and concluding the proof of Th.2.1. Having proven the existence of $\Gamma_{In}, \Gamma_{Out}$, invariant, unbounded one-dimensional manifolds in W_{In}^s, W_{Out}^u , respectively, we can now conclude the proof of Th.2.1. Namely, we will now use the fact $\overline{\Gamma_{Out}}, \overline{\Gamma_{In}}$ connect at ∞ to prove the existence of a smooth vector field on S^3 , R_p , s.t. the following conditions are satisfied:

- For every sufficiently large $r > 0$, we can construct R_p s.t. it coincides on $\{(x, y, z) | x^2 + y^2 + z^2 < r\}$ with F_p , the original vector field given by Eq.2.
- R_p has precisely two fixed points in S^3 - P_{In}, P_{Out} .
- R_p generates an unbounded heteroclinic trajectory, connecting P_{In}, P_{Out} .

To begin, recall $l_p = \{\dot{x} = 0\} \cap \{\dot{y} = 0\}$ (see Lemma 2.5). Now, given $r > 0$ consider $S_r = \{|w| = r, w \in \mathbf{R}^3\}$ - F_p can point on S_r at the $(0, 0, -d), d > 0$ direction **only** at $S_r \cap l_p$. Further recall we earlier parameterized l_p by $\{(x, -\frac{x}{a}, \frac{x}{a}), x \in \mathbf{R}\}$, and that $F_p(l_p(x)) = (0, 0, bx + \frac{x^2 - xc}{a})$ (see Lemma 2.5). For any sufficiently large $|x|$, the polynomial $bx + \frac{x^2 - xc}{a}$ is positive - therefore, for any sufficiently large $r > 0$, F_p **cannot** point at the $(0, 0, -d), d > 0$ direction on S_r . This proves the index of F_p at the fixed point at ∞ is 0 - that is, the fixed point at ∞ can **only** be some degenerate fixed point for F_p .

Hence, by Hopf's Theorem (see pg. 51 in [18]), for every sufficiently large r , F_p is homotopic on the set $D_r = \{w \in \mathbf{R}^3 | |w| \geq r\}$ to a vector field which generates a tubular flow. Hence, applying Hopf's Theorem, we conclude that for a sufficiently large r we can smoothly deform F_p at D_r by some smooth homotopy which removes the fixed point at ∞ . As the index is 0, we do so s.t. no new fixed points are generated in D_r - in particular, we do so s.t. ∞ becomes a regular initial condition for the flow, with non-zero \dot{y} velocity (in other words, we take ∞ out of the cross-section $\{\dot{y} = 0\}$ - see the discussion preceding Lemma 2.1). More importantly, because $\infty \in \overline{\Gamma_{In}} \cup \overline{\Gamma_{Out}}$, we construct this perturbation s.t. $\Gamma_{In}, \Gamma_{Out}$ connect to a heteroclinic connection passing through ∞ - the curve Γ .

Now, denote the vector field constructed above by R_p - by construction it is a smooth vector S^3 - and by the process described above, given a sufficiently large $r > 0$ we can construct R_p s.t. it coincides with F_p on $\{(x, y, z) | x^2 + y^2 + z^2 > r\}$. As a consequence, the construction above also proves R_p has precisely two fixed points in S^3 - P_{In}, P_{Out} , connected by an unbounded heteroclinic trajectory, Γ . Theorem 2.1 is now proven. \square

Remark 2.1. In [29] it was observed a component of W_{Out}^u always tends to infinity. As such, Th.2.1 (and in particular, Cor.2.1.4) is an analytic proof of this numerical observation.

Having proven Th.2.1, it is time to introduce the definition of a trefoil parameter for the Rössler system. As stated at the introduction, in this paper we are interested at the dynamics of the Rössler System where the vector field satisfies a very specific heteroclinic condition - we will refer to such parameters as "trefoil parameters". To make everything more precise, let us begin with the following definition:

Definition 2.3. Let $p \in P$ be s.t. there exists a **bounded** heteroclinic trajectory for F_p in $W_{In}^s \cap W_{Out}^u$, connecting P_{In}, P_{Out} . In that case we say p is a **heteroclinic parameter** - see the illustration at Fig.11.

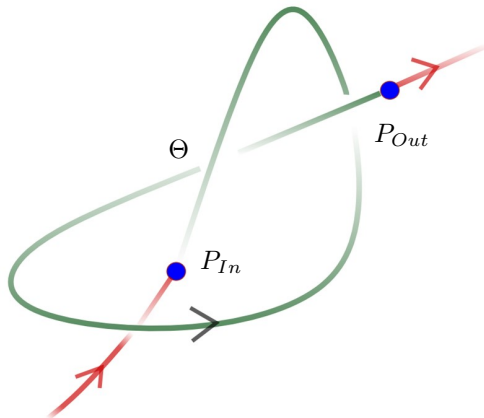


FIGURE 11. a heteroclinic trefoil knot (see Def.2.4). Θ denotes the bounded heteroclinic connection.

Having defined heteroclinic parameters for the Rössler system, we can now introduce the definition of a trefoil parameter. However, before doing so, let us first motivate it. To begin, recall that one recurring observation in the numerical studies of the Rössler System is that at many parameters, trajectories which are repelled from P_{In} are

shielded from escaping to ∞ by the two-dimensional W_{Out}^s (see, for example, Section V in [29]). Additionally, as observed numerically in [29], there exist regions in the parameter space P where the dynamics vary from bounded to unbounded. Namely, there exists a partition of P to three subsets - S_1, S_2 , separated by a set S_3 , s.t. the following occurs:

- For parameters $p \in S_1$, the vector field F_p generates an attractor (not necessarily chaotic). In particular, for $p \in S_1$, the two-dimensional W_{Out}^s appears to shield trajectories from escaping to ∞ , while a bounded component of the one-dimensional W_{Out}^u repels them towards the attractor. As must be remarked, the numerical evidence also points that for $p \notin P$, there may yet exist an attractor - however, in that case its basin of attraction may be bounded (see [26]).
- For parameters $p \in S_2$, the dominant behavior is unbounded - that is, the two-dimensional W_{Out}^u no longer shields trajectories from blowing up to ∞ .
- For parameters $p \in S_3$, the attractor coincides with W_{Out}^s .

As observed numerically in [29], there exists a parameter $p \in P$, at $p = (a, b, c) \approx (0.468, 0.3, 4.615)$, lying close to ∂A_1 s.t. F_p generates a bounded heteroclinic trajectory Θ as in Fig.11 - and moreover, the corresponding attractor is both inseparable from both fixed-points P_{In}, P_{Out} , **and** appears to be wrapped around the heteroclinic trajectory Θ (see Fig.5.B1 in [29]). Now, recall the separatrices $\Gamma_{In}, \Gamma_{Out}$ from Th.2.1 - provided $\Gamma_{In}, \Gamma_{Out}$ and Θ are **not** asymptotically linked, the union $\Lambda = \Gamma_{In} \cup \Gamma_{Out} \cup \Theta \cup \{P_{In}, P_{Out}, \infty\}$ forms a trefoil knot in S^3 (in fact, we will soon prove this is the case - see Cor.13). Therefore, motivated by the discussion above and Fig.5.B1 from [29], we now define the following type of a parameter:

Definition 2.4. Let $p \in P$ be a heteroclinic parameter and Λ be as above. Let Θ denote the bounded heteroclinic connection - that is, the bounded component of $\Lambda \setminus \{P_{Out}, P_{In}\}$. We say p is a **trefoil parameter** provided the following three conditions are satisfied:

- Θ is as in Fig.11.
- We have $W_{In}^u = W_{Out}^s$ (w.r.t. F_p)- that is, the two-dimensional manifolds coincide for F_p .
- $\Theta \cap \overline{U_p} = \{P_0\}$ is a point of transverse intersection.

See Fig.11 and Fig.12 for illustrations.

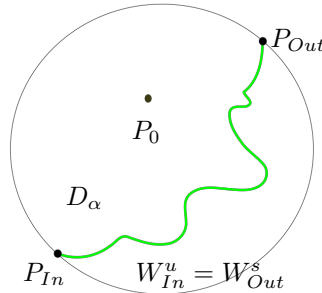


FIGURE 12. The geography of the cross-section U_p for a trefoil parameter $p \in P$, sketched as a disc for simplicity. The green arc denotes $W_{In}^u \cap \overline{U_p} = W_{Out}^s \cap \overline{U_p}$. The set D_α corresponds to $B_\alpha \cap \overline{U_p}$.

The discussion above motivates us to consider trefoil parameters as an idealized form of the dynamics observed at Fig.5.B1 from [29] - which we will analyze for the remainder of this paper. By its definition, we aim to capture the numerical properties listed above. In particular, we formalize the numerically-observed shielding of the Rössler attractor from ∞ by W_{Out}^s **and** its inseparability from both fixed-points by imposing the assumption that at trefoil parameters we have $W_{Out}^s = W_{In}^u$. As such, for trefoil parameters, the set $W_{In}^s = W_{Out}^u$ forms the boundary of a bounded topological ball $B_\alpha \subseteq \mathbf{R}^3$, $P_{In}, P_{Out} \in \partial B_\alpha$. As must be stated, B_α is generically unstable - that is, a generic C^1 perturbation of F_p would destroy **both** B_α and the heteroclinic connection Θ (see also Remark 3.3).

At this stage it must be remarked that in Def.2.4 we **do not** assume the set Λ indeed forms a trefoil knot in S^3 . However, as we will now see, Def.2.4 does imply this is the case. Namely, we prove:

Corollary 2.1.5. Let $p \in P$ be a trefoil parameter, and let $\Gamma_{In}, \Gamma_{Out}$ be as in Th.2.1 and let Θ be as in Def.2.4. Then, $\Lambda = \Gamma_{In} \cup \Gamma_{Out} \cup \Theta \cup \{P_{In}, P_{Out}, \infty\}$ forms a trefoil knot in S^3 .

Proof. To begin, recall that by Stages II and III of the proof of Th.2.1, both $\Gamma_{In}, \Gamma_{Out}$ are trapped inside three-dimensional bodies, C_{In}, C_{Out} , respectively, s.t. $C_{In} \subseteq \{(x, y, z) | x \leq 0\}$, and $C_{Out} \subseteq \{(x, y, z) | x \geq c - ab\}$. Since by our assumptions on the parameter space P we always have $c - ab > 0$ (see the discussion at 3), C_{In}, C_{Out}

are separated by the open set $C = \{(x, y, z) | x \in (0, c - ab)\}$ - hence it follows $\Gamma_{In}, \Gamma_{Out}$ cannot be knotted with one another (see Fig.13 for an illustration). Recalling we denote by B_α the bounded (topological) ball in \mathbf{R}^3 bounded by $W_{In}^u = W_{Out}^s$, since both $\Gamma_{In}, \Gamma_{Out}$ are unbounded by the invariance of B_α under F_p it follows $(\Gamma_{In} \cup \Gamma_{Out}) \cap B_\alpha = \emptyset$. Now, since the one-dimensional W_{Out}^u is transverse to $\partial B_\alpha = W_{Out}^s$, because Γ_{Out}, Θ are both components of W_{Out}^u , by $\Gamma_{Out} \cap \overline{B_\alpha} = \emptyset$ we conclude $\Theta \subseteq B_\alpha$. As a consequence, because $\Theta \subseteq B_\alpha$ and because B_α can be contracted to a point, it now follows $\Lambda = \Gamma_{In} \cup \Gamma_{Out} \cup \Theta \cup \{P_{In}, P_{Out}, \infty\}$ is a trefoil knot in S^3 and Prop.2.1.5 now follows. \square

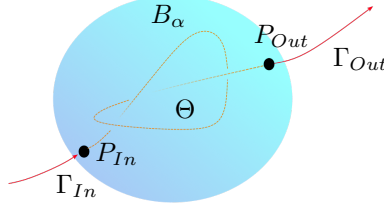


FIGURE 13. The separatrix Θ trapped inside B_α , sketched as a the blue sphere.

As we will see later in Section 3, the existence of a trefoil parameter $p \in P$ guarantees the existence of complex, chaotic dynamics for the Rössler system both at trefoil parameters - and around them (see Th.3.1 and 4.1, respectively). In the meanwhile, we conclude Section 2 with one final result, which is also a Corollary of both Th.2.1 and Def.2.4:

Corollary 2.1.6. *Let $p \in P$ be a trefoil parameter. Then, given an arbitrarily large compact $K \subseteq \mathbf{R}^3$, F_p can be approximated by smooth vector fields K_p on S^3 s.t.:*

- $K_p \rightarrow F_p$ on K (in the C^∞ metric).
- K_p always satisfies Shilnikov's chaotic homoclinic scenario.

Proof. Let $p \in P$ be a trefoil parameter. By Th.2.1, we can always perturb F_p into a smooth vector field on S^3 , R_p - and per Th.2.1, R_p generates a heteroclinic connection Γ through ∞ , which flows from P_{Out} towards P_{In} (in infinite time). Additionally, since $p \in P$, recall we always have $(\nu_{Out} < 1) \vee (\nu_{In} < 1)$ (see the discussion at page 3).

Now, to prove Cor.2.1.6 assume first that $\nu_{Out} < 1$. Since R_p is a smooth vector field on S^3 , we can perturb R_p around the fixed point P_{In} by connecting Γ and some trajectory on $W_{In}^u = W_{Out}^s$ to ζ , a homoclinic trajectory to P_{Out} . Denote by K_p the resulting vector field - as must be remarked, K_p is a smooth vector field on S^3 . Moreover, given any compact $K \subseteq \mathbf{R}^3$, since R_p can be chosen to coincide with F_p on K , we can choose the vector field K_p to be arbitrarily close to F_p on K (in the C^∞ metric). As $\nu_{Out} < 1$, from Shilnikov's Theorem (see [3]) the dynamics of K_p around the homoclinic trajectory are chaotic - in particular, they include infinitely many suspended Smale Horseshoe maps. When $\nu_{In} < 1$, similar arguments (when applied to $-F_p$) allow us to infer the same result. \square

As must be remarked, in light of the numerical evidence Corollary 2.1.6 may appear surprising - especially so, since most numerical studies observed the existence of open regions in the parameter space, intersecting with the chaotic Shilnikov homoclinic curves, **at which no chaotic dynamics were detected** (see, for example, [23],[21],[29]). Even though such numerical evidence appears to contradict Cor.2.1.6, in practice it is not so: for even if $\forall p \in P$ the vector field F_p generates some suspended Smale Horseshoes around ∞ (that is, similarly to Shilnikov's Theorem), those dynamics may well be restricted to meagre or null sets - as such, they may be hard to observe, no matter how stable they are in the parameter space. However, as must also be stated, Cor.2.1.6 does, in fact, correlates with the results of some numerical studies. To see how, let us assume $p \in P$ is a parameter at which F_p generates a stable, attracting periodic trajectory T , which attracts an open, unbounded set of initial conditions in \mathbf{R}^3 . As observed numerically in [23], for such parameters, given a generic initial condition $s \in \mathbf{R}^3$ its trajectory behaves a-periodically for a long duration of time - at least until it gets sufficiently close to T , after which it settles down and tends to T relatively orderly. This strange numerical behavior was termed **Transient Chaos** in [23] - as such, Cor.2.1.6 is a possible analytic explanation for the existence of these transient chaotic dynamics

3. CHAOTIC DYNAMICS AND TREFOIL KNOTS

From now given $(a, b, c) = p \in P$, let F_p denote its corresponding vector field (see Eq.2) - that is, F_p is the vector field generating the Rössler system corresponding to p . To continue, recall our definition of chaotic dynamics in Def.1.1 - our main objective in this section is to prove the chaoticity of the dynamics generated by the Rössler

system at trefoil parameters $p \in P$ (see Def.2.4). Namely, in Th.3.1 we prove the existence of a trefoil parameter $p \in P$ implies F_p generates chaotic dynamics - which includes infinitely many periodic trajectories. In order to do so, by Def.1.1, it follows that in order to prove Th.3.1 we must first reduce the dynamics of the vector field F_p to a first-return map, whose dynamics we shall analyze. Therefore, this Section is organized as follows -

- First, we define a cross-section $\overline{D_\alpha} \subseteq U_p$ (with U_p as in Lemma 2.1), on which the first-return map is well-defined - as we will prove, D_α is a topological disc on U_p , s.t. $P_{In}, P_{Out} \in \partial D_\alpha$ (see Prop.3.1).
- Second, we will analyze the discontinuities of the first-return map in D_α , which will motivate the proof of Th.3.1 - see Prop.3.5.
- Finally, using these tools (as well as several results from Section 2), we prove Th.3.1 by direct, qualitative analysis of the vector field F_p .

As must be remarked, Th.3.1 has several implications and corollaries, some of which are Theorems in their own right (see, for example, Prop.4.1 and Th.4.1) - however, due to the length of the proof of Th.3.1, we will defer the discussion of these results to Section 4.

To begin, let $p \in P$ be a trefoil parameter. Per Def.2.4 this implies the two-dimensional manifolds W_{Out}^s, W_{In}^u coincide - hence $W_{In}^u = W_{Out}^s$ forms the boundary of a three-dimensional topological ball, the set B_α described at the end of Section 2 - in particular, it follows, $\overline{B_\alpha}$ is **bounded**. Now, recall the cross-section U_p is a plane - see the discussion before Lemma 2.1 (for simplicity, in what follows we will occasionally consider U_p as a topological disc rather than a plane). Let us begin by setting $D_\alpha = B_\alpha \cap U_p$. We now claim:

Lemma 3.1. *Let $p \in P$ be a trefoil parameter - then, the set D_α is non-empty, and satisfies $P_{In}, P_{Out} \in \partial D_\alpha$.*

Proof. Recall Cor.2.1.1 in Section 2, where we proved W_{In}^u, W_{Out}^s are transverse to U_p at P_{In}, P_{Out} (respectively). Since $p \in P$ is a trefoil parameter, by $\partial B_\alpha = W_{In}^u = W_{Out}^s$ and because B_α is a topological ball it follows $U_p \setminus W_{In}^u$ intersects both components of $\mathbf{R}^3 \setminus \partial B_\alpha$ - which, by definition, implies $U_p \cap B_\alpha \neq \emptyset$. Therefore, since by definition $P_{In}, P_{Out} \in \partial B_\alpha \cap \partial U_p$ by $D_\alpha = B_\alpha \cap U_p$ it follows $P_{In}, P_{Out} \in \partial D_\alpha$ and the assertion follows. See the illustration in Fig.12. \square

Now, recall that at the end of Section 2 we showed, by definition, that B_α is bounded (see the discussion before Cor.2.1.6). We will now prove first-return map $f_p : \overline{D_\alpha} \rightarrow \overline{D_\alpha}$ is well defined. To motivate why this is so, recall that by definition, since ∂B_α is invariant under **both** $F_p, -F_p$ it follows $\overline{B_\alpha}$ is also invariant under the flow generated by F_p . Therefore, since B_α is also bounded, we conclude that given any $s \in \overline{B_\alpha}$, its trajectory is bounded as well. Therefore, from Lemma 2.1 it **heuristically** follows the first-return map $f_p : \overline{D_\alpha} \rightarrow \overline{D_\alpha}$ is well defined - however, there is one caveat in this argument: by Lemma 2.1, the first-return map in undefined for initial conditions $s \in U_p$ whose trajectory tends to a fixed point (or to ∞). Therefore, before we can conclude the first-return map is well-defined, we need to ask what is the possible behavior for the trajectories of initial conditions $s \in \overline{B_\alpha}$. Since $\overline{B_\alpha}$ is bounded, given $s \in \overline{B_\alpha}$ its trajectory cannot blow up to ∞ - **however**, it can still limit to a fixed point, which occurs precisely for $s \in W_{In}^s \cup W_{Out}^s$. Since p is a trefoil parameter, we already know $\partial B_\alpha = W_{Out}^s \cup \{P_{In}, P_{Out}\}$ - as such, in order to study the first-return map rigorously, we must first analyze $D_\alpha \cap W_{In}^s, B_\alpha \cap W_{In}^s$.

To do so, recall that by Def.2.4 $P_0 \in W_{In}^s$ is the unique intersection point of the bounded heteroclinic connection Θ with U_p - and that it is a point of transverse intersection. Therefore, we now prove:

Lemma 3.2. *Let $p \in P$ be a trefoil parameter. Then, with the notations above, $W_{In}^s \cap \overline{D_\alpha} = \{P_0\}$, and moreover, P_0 is interior to D_α .*

Proof. To begin, recall we showed in the proof of Cor.2.1.5 that $\Theta \subseteq B_\alpha$, and that $\Gamma_{In} \cap \overline{B_\alpha} = \emptyset$ (with $\Gamma_{In} \subseteq W_{In}^s$ as in Th.2.1 - see the illustration in Fig.13). Therefore, by $W_{In}^s = \Gamma_{In} \cup \Theta$ and the definition of both P_0 (see Def.2.4) and $D_\alpha = B_\alpha \cap U_p$ it follows that $\{P_0\} = \Theta \cap \overline{U_p} \subseteq \overline{D_\alpha}$. Now, since $D_\alpha = B_\alpha \cap U_p$ it follows $\partial D_\alpha \subseteq \partial U_p \cup \partial B_\alpha$ - and since $p \in P$ is a trefoil parameter, by Def.2.4 P_0 is an interior point for U_p , which implies $P_0 \notin \partial D_\alpha \cap \partial U_p$ (see the illustration in Fig.12). Additionally, let us recall Θ is a heteroclinic trajectory from P_{Out} to P_{In} (see the illustration in Fig.11) - which implies $\Theta \cap W_{Out}^s = \emptyset$. However, by definition $\partial B_\alpha = W_{Out}^s \cup \{P_{In}, P_{Out}\}$, therefore $P_0 \notin \partial D_\alpha \cap \partial B_\alpha$. All in all, by the discussion above we conclude $P_0 \notin \partial D_\alpha$ - and since $\{P_0\} = \Theta \cap \overline{U_p} \subseteq \overline{D_\alpha}$ we conclude P_0 is interior to D_α and Lemma 3.2 now follows. \square

As an immediate consequence we now conclude:

Corollary 3.0.1. *Let $p = (a, b, c) \in P$ be a trefoil parameter - then, the first-return map $f_p : \overline{D_\alpha} \setminus \{P_0\} \rightarrow \overline{D_\alpha} \setminus \{P_0\}$ for F_p is well-defined (and conversely, so is its inverse $f_p^{-1} : \overline{D_\alpha} \setminus \{P_0\} \rightarrow \overline{D_\alpha} \setminus \{P_0\}$).*

Proof. To begin, consider $s \in W_{Out}^s$, the two-dimensional, stable invariant manifold of the saddle focus P_{Out} . By Cor.2.1.1, the two-dimensional stable manifold W_{Out}^s is transverse to U_p at P_{Out} - which implies the trajectory

of s hits U_p transversely infinitely many times. Therefore, since $\partial B_\alpha = W_{Out}^s \cup \{P_{In}, P_{Out}\}$ it follows that given $s \in \partial B_\alpha$ which is **not** a fixed-point, the forward trajectory of s hits U_p transversely infinitely many times.

Now, consider an initial condition $s \in B_\alpha$, $s \notin \Theta$ - since B_α is an open (topological) ball in \mathbf{R}^3 it follows $s \notin \partial B_\alpha$ - hence, the forward trajectory of s does not limit to P_{Out} . Moreover, because $s \notin \Theta$ by $\Theta = W_{In}^s \cap B_\alpha$ it follows $s \notin W_{In}^s$ - which implies the forward trajectory of s does not limit to P_{In} . Overall, we conclude the forward trajectory of s **does not** limit to a fixed point. Additionally, because B_α is bounded, by the invariance of B_α under both $F_p, -F_p$, it follows the forward trajectory of s is trapped in a bounded set. Therefore, by Lemma 2.1 the forward trajectory of s eventually hits U_p transversely. Combined with previous paragraph, all in all we conclude that given **any** initial condition $s \in \overline{B_\alpha} \setminus (\Theta \cup \{P_{In}, P_{Out}\})$, the forward-trajectory of s eventually hits the cross-section U_p transversely. A similar argument applied to the inverse flow proves that given an initial condition $s \in \overline{B_\alpha} \setminus \Theta \cup \{P_{In}, P_{Out}\}$, its backwards trajectory also eventually hits U_p transversely.

Now, recall we defined $D_\alpha = B_\alpha \cap U_p$. Because B_α is invariant under both $F_p, -F_p$, by previous paragraphs it follows that given $s \in \overline{D_\alpha} \setminus \Theta$ **both** its backwards **and** forward trajectories return to $\overline{U_p}$ precisely at $\overline{B_\alpha} \cap \overline{U_p} = \overline{D_\alpha}$. Additionally, since $s \notin \Theta$ by $\Theta \cap \overline{D_\alpha} = \{P_0\}$ (see Lemma 3.2), it follows the forward trajectory of s under F_p never hits P_0 . As such, by $\overline{D_\alpha} \setminus \Theta = \overline{D_\alpha} \setminus \{P_0\}$ we conclude the first-return map $f_p : \overline{D_\alpha} \setminus \{P_0\} \rightarrow \overline{D_\alpha} \setminus \{P_0\}$ is well-defined (with $f_p(P_{In}) = P_{In}$, $f_p(P_{Out}) = P_{Out}$). A similar argument proves $f_p^{-1} : \overline{D_\alpha} \setminus \{P_0\} \rightarrow \overline{D_\alpha} \setminus \{P_0\}$ is also well-defined, and Cor.3.0.1 now follows. \square

Remark 3.1. *In fact, using the invariance of B_α under the flow, the argument used to prove Cor.3.0.1 trivially implies both $f_p(\overline{D_\alpha} \setminus \{P_0\}) = \overline{D_\alpha} \setminus \{P_0\}$, $f_p^{-1}(\overline{D_\alpha} \setminus \{P_0\}) = \overline{D_\alpha} \setminus \{P_0\}$.*

Having proven the first-return map is well-defined on $\overline{D_\alpha} \setminus \{P_0\}$, we now study the topology of D_α - as we will prove in Prop.3.1 below, D_α is a two-dimensional topological disc on U_p , a fact which will be used many times in the proof of Th.3.1. To begin, however, we must first recall several notions and technical details proven in Section 2 (and in particular, in Stage I of the proof of Th.2.1).

To begin, first recall the cross-section $\{\dot{x} = 0\} = \{(x, y, -y) | x, y \in \mathbf{R}\}$ analyzed in Stage I of the proof of Th.2.1 - as shown in the proof of Lemma 2.3, the tangency curve of F_p to the cross-section $\{\dot{x} = 0\}$, denoted by σ , is parameterized by $\sigma(x) = (x, -\frac{x(b+1)}{a+c-x}, \frac{x(b+1)}{a+c-x})$ - and recall the curves $\sigma_1 = \{\sigma(x) | x < 0\}$, $\sigma_2 = \{\sigma(x) | x \in (c-ab, a+c)\}$ and $\sigma_3 = \{\sigma(x) | x \in (0, c-ab)\}$ (in particular, $\sigma(0) = P_{In}$, $\sigma(c-ab) = P_{Out}$ - see the proof of Lemma 2.3 and the illustration in Fig.3). Additionally, recall that given $s \in \mathbf{R}^3$ we denote its trajectory by $\gamma_s(t)$, $\gamma_s(0) = s$ - therefore, using a similar argument to the proof of Lemma 2.4, we conclude:

Lemma 3.3. *Given $s \in \sigma_3$, there exists an $\epsilon > 0$ s.t. $\forall t \neq 0, |t| < \epsilon, \gamma_s(t) \in \{\dot{x} < 0\} \cap \{\dot{y} > 0\}$ (see the illustration in Fig.17).*

Moreover, recall we also proved $\mathbf{R}^3 \setminus \{\dot{x} = 0\}$ consists of two components - $\{\dot{x} < 0\}$ which lies **above** $\{\dot{x} = 0\}$, and $\{\dot{x} > 0\}$ which lies **below** it (see the illustration in Fig.5). As proven in Lemma 2.3, $\{\dot{x} = 0\} \setminus \sigma$ consists of three-regions: A_1, A_2, A_3 (see Fig.3) s.t. F_p points into $\{\dot{x} > 0\}$ on A_1, A_2 and into $\{\dot{x} < 0\}$ on A_3 (see the illustration in Fig.14). In particular, recall:

- $A_1 = \{(x, -y, y) | x < a+c, y < -\frac{x(b+1)}{a+c-x}\}$. On A_1 the vector field F_p points into $\{\dot{x} > 0\}$ - that is, below $\{\dot{x} = 0\}$ (see the illustration in Fig.14). In particular, $\partial A_1 = \sigma_1 \cup \sigma_2 \cup \sigma_3 \cup \{P_{In}, P_{Out}\}$.
- $A_2 = \{(x, -y, y) | x > a+c, y < -\frac{x(b+1)}{a+c-x}\}$ - on A_2 the vector field F_p also points into $\{\dot{x} > 0\}$. Also, $\partial A_2 = \{\sigma(x) | x > a+c\}$.
- $A_3 = \{(x, -y, y) | x \neq a+c, y > -\frac{x(b+1)}{a+c-x}\}$ - on A_3 the vector field F_p points into $\{\dot{x} < 0\}$, that is, above $\{\dot{x} = 0\}$ (see the illustration in Fig.14) - and moreover, $\partial A_3 = \sigma$ (see the illustration in Fig.3).

Additionally, recall we proved in Stage I of the proof of Th.2.1 that the cross-section $\{\dot{y} = 0\}$ is transverse to $\{\dot{x} = 0\}$ - and that the intersection $\{\dot{y} = 0\} \cap \{\dot{x} = 0\}$ is a curve, l_p , parameterized by $l_p(x) = (x, -\frac{x}{a}, \frac{x}{a})$, $x \in \mathbf{R}$ (see the illustration in Fig.5 and Fig.14). In particular, recall l_p is the tangency curve of F_p to $\{\dot{y} = 0\}$ and that $\{\dot{y} = 0\} \setminus l_p$ is composed of two components - $U_p = \{\dot{y} = 0\} \cap \{\dot{x} < 0\}$, and $L_p = \{\dot{y} = 0\} \cap \{\dot{x} > 0\}$ (see the illustration in Fig.5 and Fig.14). As shown before the proof of Cor.2.1.1, on U_p the vector field F_p points into $\{\dot{y} < 0\}$ (the region in front of $\{\dot{y} = 0\}$), while on L_p , F_p points into $\{\dot{y} > 0\}$ (the region below $\{\dot{y} = 0\}$) - see the illustration in Fig.14). As a consequence from this discussion, by $P_{In} = (0, 0, 0)$, $P_{Out} = (c-ab, \frac{ab-c}{a}, \frac{c-ab}{a})$ we conclude $l_p \cap \sigma = \{P_{In}, P_{Out}\}$ (see the illustration in Fig.14).

To continue, from now on, denote by $l = \{l_p(x) | x \in (0, c-ab)\}$ (that is, l is the sub-arc on l_p connecting P_{In}, P_{Out} - see Fig.14 and Fig.15). Also, from now on, set $L = \partial B_\alpha \cap \overline{U_p}$. We can now state and prove Prop.3.1:

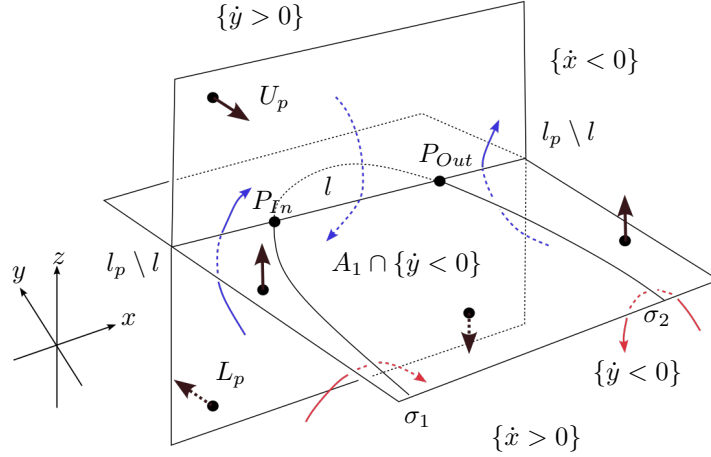


FIGURE 14. The directions of F_p on A_1 , σ_1 , σ_2 and A_1 , along with a sketch of some flow lines on σ_1 , σ_2 and $l, l_p \setminus l$.

Proposition 3.1. *Let $p = (a, b, c) \in P$ be a trefoil parameter as in Def.2.4, and let F_p denote the corresponding vector field, given by Eq.2. Then, with previous notations:*

- $D_\alpha = B_\alpha \cap \overline{U_p}$ is a Jordan domain on $\overline{U_p}$ s.t. $\partial D_\alpha = l \cup L \cup \{P_{In}, P_{Out}\}$ (see the illustration in Fig.23). In particular, L is a Jordan arc in U_p with endpoints P_{In}, P_{Out} - i.e., $\overline{L} \cap l_p = \{P_{In}, P_{Out}\}$.
- $B_\alpha \cap \overline{A_3} = V_\alpha$ is also a Jordan domain, bounded by $\sigma_3 \cup \rho \cup \{P_{In}, P_{Out}\}$, with $\rho = \partial B_\alpha \cap A_3$. Moreover, $V_\alpha \subseteq \{y > 0\}$ (see the illustration in Fig.23).

Proof. To begin, recall we assume $p \in P$ is a trefoil parameter - hence, by definition we have $W_{In}^u = W_{Out}^s$, and therefore also $\partial B_\alpha = W_{Out}^s \cup \{P_{In}, P_{Out}\} = W_{In}^u \cup \{P_{In}, P_{Out}\}$. The proof of Prop.3.1 is highly technical and based on directly analyzing the dynamics of F_p - therefore, we will split it into four Lemmas. A sketch of proof is as follows -

- As a first step, we begin by proving two facts: the first is that $\overline{B_\alpha} \cap (\sigma_1 \cup \sigma_2) = \emptyset$. The second is that $\overline{B_\alpha} \cap \overline{A_2} = \emptyset$ - as we will see, both follow from the boundedness of B_α (see Lemmas 3.4 and 3.5).
- Secondly, we prove $\partial B_\alpha \cap l = \emptyset$, which, combined with previous results, implies both $\partial B_\alpha \cap A_1$, $\partial B_\alpha \cap A_3$ are curves connecting P_{In}, P_{Out} . In particular, it would then immediately follow V_α is a Jordan domain (see Lemma 3.6).
- Finally, we prove $V_\alpha \subseteq \{y > 0\}$, which, as a corollary, implies D_α is a topological disc (see Lemma 3.7 and the discussion following it) - which would conclude the proof of Prop.3.1.

To begin, let us first recall $\sigma_1 = \{\sigma(x) | x < 0\}$, $\sigma_2 = \{\sigma(x) | x \in (c - ab, a + c)\}$ (see the discussion after Lemma 2.3). Using the results of Stages II and III in the proof of Th.2.1, we first prove the following Lemma:

Lemma 3.4. *Let $p \in P$ be a trefoil parameter. Then, $\overline{B_\alpha} \cap (\sigma_1 \cup \sigma_2) = \emptyset$.*

Proof. Recall the 3-dimensional body C_{In} introduced in the proof of Th.2.1 - see Stage II in the proof of Th.2.1. By Prop.2.1 (and its proof), we already know no backwards trajectory can escape C_{In} under the inverse flow - and that $C_{In} \subseteq \{y \leq 0\}$. Additionally, by its construction, it follows $\sigma_1 \subseteq \partial C_{In}$ - which, by the invariance of C_{In} under the **inverse** flow, implies the **backwards** trajectories of σ_1 never escape $\overline{C_{In}}$ - hence, given any $s \in \sigma_1$, its backwards trajectory diverges to ∞ . As a consequence, because $\overline{B_\alpha}$ is both bounded and invariant under F_p , we conclude $\overline{B_\alpha} \cap \sigma_1 = \emptyset$.

Similarly, by its construction in Prop.2.2, the three-dimensional body C_{Out} is invariant under the flow, lies in $\{y \leq 0\}$, and satisfies $\sigma_2 \subseteq \partial C_{Out}$ - that is, as shown in Prop.2.2, given an initial condition $s \in C_{Out}$, its forward-trajectory never escapes C_{Out} . Therefore, a similar argument now proves that given any $s \in \sigma_2$, its forward-trajectory is trapped in $\overline{C_{Out}}$, hence diverges to ∞ - and as a consequence, it similarly follows $\sigma_2 \cap \overline{B_\alpha} = \emptyset$. All in all, we have proven $\overline{B_\alpha} \cap (\sigma_1 \cup \sigma_2) = \emptyset$ and Lemma 3.4 follows. \square

Having proven $\overline{B_\alpha} \cap (\sigma_1 \cup \sigma_2) = \emptyset$, we now prove a similar result for A_2 , the region of $\{x = 0\}$ described above:

Lemma 3.5. *Let $p \in P$ be a parameter (not necessarily trefoil) - then, $\overline{B_\alpha} \cap \overline{A_2} = \emptyset$.*

Proof. We first prove that given an initial condition $s \in \overline{A_2}$, its forward trajectory diverges to ∞ - then, using an argument similar to the one used to prove Lemma 3.4, we will conclude $\overline{A_2} \cap \overline{B_\alpha} = \emptyset$.

To begin, recall that given any $s \in \mathbf{R}^3$, we parameterize its trajectory by $\gamma_s(t)$, $t \in \mathbf{R}$, $\gamma_s(0) = s$. We first prove that given any $s \in \overline{A_2} \subseteq \{\dot{x} = 0\}$, $\lim_{t \rightarrow \infty} \gamma_s(t) = \infty$. To do so, choose some $s \in \overline{A_2}$, $s = (x_0, y_0, z_0)$, and consider the half-planes $H_0 = \{\dot{x} > 0\} \cap \{(x, y, z) | x = x_0, y \geq y_0\}$, $H_1 = \{\dot{x} > 0\} \cap \{(x, y, z) | y = y_0, x \geq x_0\}$. These planes intersect at the line $l_0 = \{(x_0, y_0, z) | z < z_0\}$ (see the illustration in Fig.16). In particular, H_0, H_1 and the region $H_3 = \{(x, y, -y) \in A_2 | x \geq x_0, y_0 \geq y_0\}$ together form the boundary of a closed quadrant Q , which lies strictly inside $\{\dot{x} \geq 0\}$ - with $H_3 = Q \cap \{\dot{x} = 0\}$ (see the illustration in Fig.16 and 15). Now, recall we parameterize ∂A_2 by $\sigma(x) = (x, -\frac{x(b+1)}{a+c-x}, \frac{x(b+1)}{a+c-x})$, $x > c + a$ - therefore, by the concavity of ∂A_2 in $\{\dot{x} = 0\}$ we conclude $H_3 \subseteq \overline{A_2}$ (see the illustration in Fig.16 and 15).

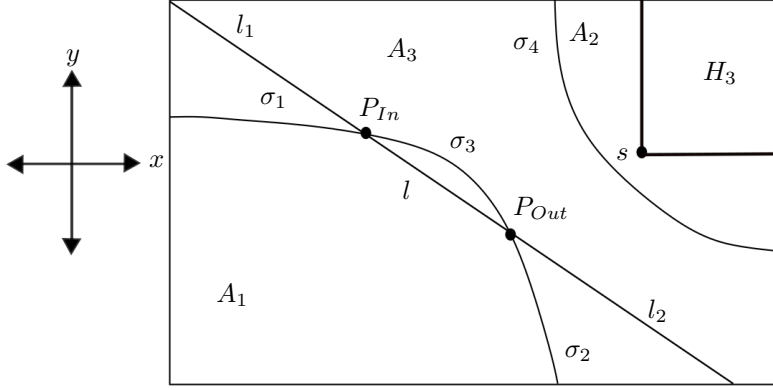


FIGURE 15. H_3 , the upper edge of Q and a sub-region of $\overline{A_2}$.

Now, as proven in Lemma 2.3, on A_2 the vector field F_p points into $\{\dot{x} > 0\}$, i.e., **below** the cross-section $\{\dot{x} = 0\}$ - hence, on H_3 the vector field F_p must point into the quadrant Q . Additionally, because the normal vectors to H_0, H_1 are $(1, 0, 0)$, $(0, 1, 0)$ (respectively), by calculation it follows F_p points into Q on both H_1, H_0 - therefore, all in all, we conclude F_p points into Q throughout ∂Q (see the illustration in Fig.16). As a consequence, given **any** $\omega \in Q$ and every $t > 0$, $\gamma_\omega(t) \in Q$ - i.e., no forward trajectory can escape Q . Hence, because we constructed Q s.t. $s = (x_0, y_0, z_0) \in \overline{Q}$, by this discussion we conclude that given any $t > 0$, $\gamma_s(t) \in Q$ - i.e., the forward trajectory of s is trapped in Q . Therefore, by $Q \subseteq \{\dot{x} \geq 0\}$ it follows the x -component in γ_s blows up when $t \rightarrow \infty$, which implies $\lim_{t \rightarrow \infty} \gamma_s(t) = \infty$. Since we chose an arbitrary $s \in \overline{A_2}$ it follows that given any $s \in \overline{A_2}$, $\lim_{t \rightarrow \infty} \gamma_s(t) = \infty$.

Having proven the trajectories of initial conditions $s \in \overline{A_2}$ explode to ∞ , we can now conclude Lemma 3.5. To so so, recall that $\overline{B_\alpha}$ is both bounded and invariant under the flow - therefore, by the argument above we immediately conclude $\overline{B_\alpha} \cap \overline{A_2} = \emptyset$, and Lemma 3.5 now follows. \square

Remark 3.2. As must be remarked, the argument above actually proves that given any $p \in P$ - not necessarily a trefoil parameter - the trajectories of initial conditions in $\overline{A_2}$ **always** diverges to ∞ .

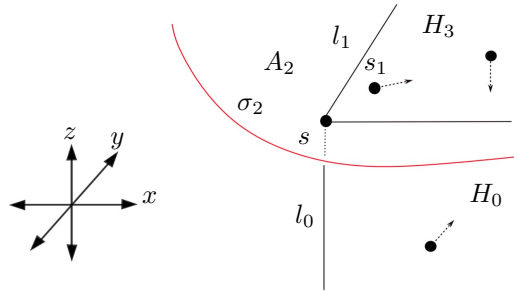


FIGURE 16. The directions of F_p on the body Q s.t. $s \in \partial Q$ (with $l_1 = H_1 \cap A_2$, and $s_1 \in H_1$). Since F_p points inside Q throughout ∂Q , no trajectory can escape Q in positive time.

We now use Lemma 3.4 and 3.5 to prove V_α, D_α are both Jordan domains in A_3, U_p (respectively). We do so in two stages - first we prove Lemmas 3.6 which implies this result for V_α , after which we prove 3.7 which

proves the same for D_α . To begin, recall we parameterize l_p by $l_p(x) = (x, -\frac{x}{a}, \frac{x}{a})$, $x \in \mathbf{R}$, and that we defined $l = \{l_p(x) | x \in (0, c - ab)\}$ as the sub-arc of l_p connecting P_{In}, P_{Out} (see Fig.14). By direct computation, we have $l \subseteq A_1$ (see Fig.15). Moreover, recall $l_p(0) = P_{In}$, $l_p(c - ab) = P_{Out}$, and denote the two components of $l_p \setminus l$ by $l_1 = \{l_p(x) | x \leq 0\}$, and $l_2 = \{l_p(x) | x \geq c - ab\}$ (see the illustration in Fig.15).

Now, recall $p \in P$ is a trefoil parameter, which implies $W_{Out}^s = W_{In}^u$ (see Def.2.4). Now, set ρ_{Out} as the component of $W_{Out}^s \cap \overline{A_3}$ which begins at P_{Out} (see the illustration in Fig.17) - by Lemma 2.3, ρ_{Out} is well-defined. Similarly, consider the set $\mu = \partial B_\alpha \cap \overline{A_1}$ - by Lemma 3.4, $\mu \cap (\sigma_1 \cup \sigma_2) = \emptyset$, and by Cor.2.1.1 there exists μ_{Out} , a component of μ , beginning at P_{Out} . We now prove:

Lemma 3.6. *Let $p \in P$ be a trefoil parameter - then, μ is an arc in $A_1 \cap \{\dot{y} < 0\}$ connecting P_{In}, P_{Out} . In particular, $\mu \cap l = \emptyset$.*

Proof. To begin, recall W_{Out}^s is transverse to **both** $\{\dot{x} = 0\}$, $\{\dot{y} = 0\}$ at P_{Out} (see Lemma 2.3 and Cor.2.1.1) - therefore, it follows that locally around P_{Out} , μ_{Out} is an arc which begins at P_{Out} and enters $A_1 \cap \{\dot{y} < 0\}$ **immediately** upon leaving P_{Out} (see the illustration in Fig.17). We will prove Lemma 3.6 by showing μ_{Out} cannot intersect l - and we do so by contradiction. That is, assume $\mu_{Out} \cap l \neq \emptyset$, and set α_{Out} as the sub-arc of μ_{Out} which connects P_{Out} and p_1 , the first point of intersection between μ_{Out} , l - see the illustration in Fig.17. By the discussion above, α_{Out} connects P_{Out}, p_1 through $A_1 \cap \{\dot{y} < 0\}$. Because p_1 is the first point of intersection of α_{Out}, l it follows $P_{In} \notin \alpha_{Out}$.

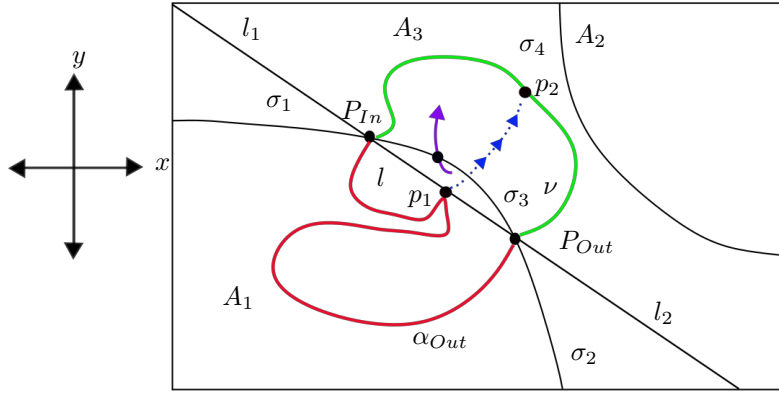


FIGURE 17. An eagle's view of $\{\dot{x} = 0\}$ - in this scenario, for simplicity, the red curve denotes $\mu = \mu_{Out}$, while the green denotes $\rho_{Out} = \rho$. The purple arc denotes a local flow line for an initial condition on σ_3 , while the blue line is the trajectory connecting p_1 to $p_2 = \gamma_{p_1}(t(p_1))$. We prove in Lemma 3.6 this scenario is impossible.

To continue, consider the forward-trajectories of α_{Out} - by the definition of $A_1 \subseteq \{\dot{x} = 0\}$ (see the discussion before Prop.3.1 or after Lemma 2.3), it follows that once the trajectory of $s \in \alpha_{Out}$ leaves α_{Out} it **immediately** enters $\{\dot{x} > 0\}$ below $\{\dot{x} = 0\}$ (see the discussion after Lemma 2.3 and the illustration in Fig.17). Now, recall $\overline{B_\alpha}$ is bounded, and that by definition $\alpha_{Out} \subseteq \mu \subseteq \partial B_\alpha$ - moreover, recall we denote by $\gamma_s, \gamma_s(0) = s$ the trajectory of a given $s \in \mathbf{R}^3$. As proven above, for $s \in \alpha_{Out}$ there exists some positive $t(s)$ s.t. for $r \in (0, t)$, $\gamma_s(r) \in \{\dot{x} > 0\}$ - and because ∂B_α is bounded, $t(s)$ must be finite, i.e., $\gamma_s(t(s)) \in \{\dot{x} = 0\}$ and for $r > t(s)$ sufficiently close to t we have $\gamma_s(r) \in \{\dot{x} < 0\}$. In other words, γ_s escapes $\{\dot{x} > 0\}$ at $\gamma_s(t(s))$ (see the illustration in Fig.17) - which can only occur by hitting A_3 transversely, i.e. $\gamma_s(t(s)) \in A_3$ (see the illustration in Fig.18).

Now, let us analyze the set $\nu = \cup_{s \in \alpha_{Out}} \gamma_s(t(s)) \subseteq \overline{A_3}$. Since $\alpha_{Out} \subseteq \partial B_\alpha$, by the invariance of ∂B_α under the flow it follows $\nu \subseteq \partial B_\alpha$ - which, by Lemmas 3.4 and 3.5 implies $\nu \cap (\partial A_2 \cup \sigma_1 \cup \sigma_2) = \emptyset$. However, by Lemma 3.3, we know the **backwards** trajectories of initial conditions in σ_3 arrive from $\{\dot{x} < 0\}$ (see the illustration in Fig.17) - therefore, because the flow line connecting $s \in \alpha_{Out}$ with $\gamma_s(t(s))$ runs through $\{\dot{x} > 0\}$ we conclude $\gamma_s(t(s)) \notin \sigma_3$. Therefore, recalling $\partial A_3 = \partial A_2 \cup \sigma_1 \cup \sigma_2 \cup \sigma_3 \cup \{P_{In}, P_{Out}\} = \sigma$, we conclude $\nu \cap \partial A_3 = \emptyset$ - which implies ν is a curve in A_3 , with one endpoint at P_{Out} . Moreover, by the definition of ρ_{Out} above we immediately conclude $\nu \subseteq \rho_{Out}$ (see the illustration in Fig.17).

We now proceed to generate a contradiction. To do so, recall we assume $p_1 = (x_1, y_1, z_1)$ is the first intersection point of μ_{Out} and l - by the discussion above, p_1 flows to a point $(x_2, y_2, z_2) = \gamma_{p_1}(t(p_1)) = p_2 \in \nu$ (see the illustration in Fig.17). Since $p_1 \in l = \{l_p(x) | x \in (0, c - ab)\}$, by Lemma 2.5 it follows the flow line connecting $p_1, \gamma_{p_1}(t(p_1))$ runs through $\{\dot{y} > 0\} \cap \{\dot{x} > 0\}$ - as a consequence, $y_2 > y_1$, $x_2 > x_1$ (see the illustration in Fig.17). Conversely,

a similar argument applied to the **inverse** flow implies there exists a point $(x_0, y_0, z_0) = p_0 \in \overline{A_3} \cap \{\dot{y} > 0\}$ and a negative r s.t. $\gamma_{p_1}(r) = p_0$ - moreover, the flow-line connecting p_0, p_1 lies in $\{\dot{y} > 0\}$, which implies $y_0 < y_1$ (see the illustration in Fig.18). Trivially, we have $y_2 > y_1 > y_0$, which implies $p_2 \neq p_0$.

Now, let $h : \overline{A_1} \rightarrow \overline{A_1}$ denote the first-return map for $\overline{A_1}$ (wherever defined). Since α_{Out} is a curve in $A_1 \cap W_{Out}^s$ with one endpoint interior to A_1 (that is p_1) and the other P_{Out} , it immediately follows $h(\alpha_{Out}) \subset \alpha_{Out}$ - that is, for every $s \in \alpha_{Out}$ there exists a finite, positive time $r(s) > t(s) > 0$ s.t. $\gamma_s(r(s))$ is strictly interior to α_{Out} (see the illustration in Fig.18). Now, recall trajectories in $\{\dot{y} > 0\}$ can escape $\{\dot{y} \geq 0\}$ only by hitting transversely the half-plane $\overline{U_p} = \{\dot{y} = 0\} \cap \{\dot{x} < 0\}$, which, given $s \in \alpha_{Out}$, implies there exists an $r(s) > k(s) > t(s) > 0$ s.t. the flow line leaving $\gamma_s(t(s))$ hits some $\gamma_s(k(s)) = \omega \in \overline{U_p}$ **before** hitting $\gamma_s(r(s))$ (see the illustration in Fig.18). Additionally, since p_1 is the **first** intersection between μ_{Out}, l and because $h(\alpha_{Out}) \subset \alpha_{Out}$ it follows $\cup_{s \in \alpha_{Out}} \gamma_s(k(s))$ is a subset of a curve β_{Out} in U_p , with one endpoint at p_1 - and moreover, we have $\beta_{Out} \cap l = \{p_1\}$ and for every $\omega \in \beta_{Out}, \omega \neq p_1$ there exists some positive $j(\omega) > 0$ s.t. $\gamma_\omega(j(\omega)) \in \alpha_{Out}$ (by definition, because $p_1 \in \alpha_{Out}, j(p_1) = 0$). Now, let us recall the flow line connecting $\gamma_s(t(s)), \gamma_s(k(s))$ lies in $\{\dot{y} > 0\}$. Therefore, for $s = p_1$, we conclude the same is true for the flow line connecting $p_2, p_3 = \gamma_{p_1}(k(p_1)) = (x_3, y_3, z_3)$, which implies $y_3 > y_2 > y_1 > y_0$ - in particular, p_1 **does not** maximize the y -coordinate on β_{Out} (see the illustration in Fig.18).

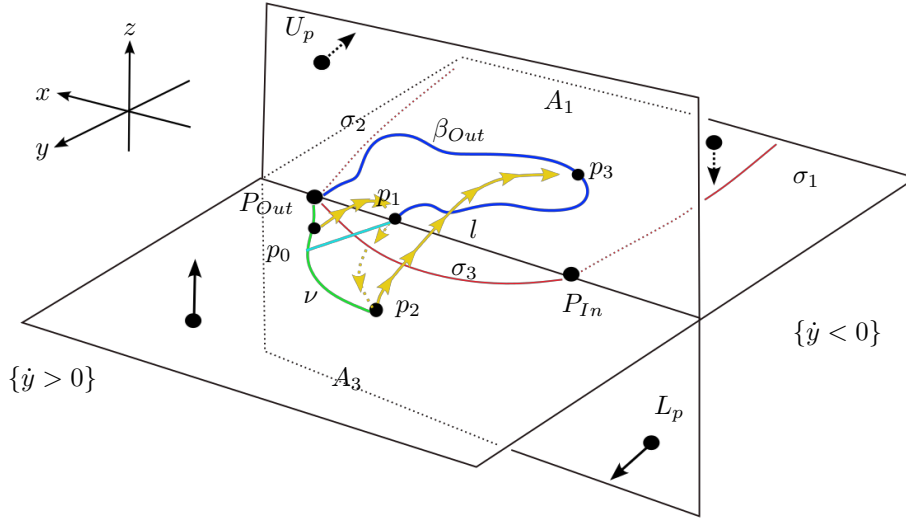


FIGURE 18. The trajectory connecting p_0 to p_3 through p_1, p_2 is sketched in yellow, while the cyan line denotes $H \cap \{\dot{x} = 0\} \cap \partial C$ (in particular, $\gamma_{p_3}(i(p_3)) = p_2, p_3 = \gamma_{p_1}(k(p_1))$). Moreover, the directions of F_p on U_p, L_p, A_1 and A_2 are sketched, and the y -coordinate increases along the flow line connecting p_0, p_3 . We prove this scenario cannot exist.

Now, consider the backwards trajectories of β_{Out} . Since β_{Out} flows to α_{Out} it follows $\beta_{Out} \subseteq W_{Out}^s$ - which, since p is a trefoil parameter implies that given $\omega \in \beta_{Out}$ there exists a maximal $-\infty < i(\omega) < 0$ s.t. $\gamma_\omega(i(\omega)) \in \overline{A_3} \cap \{\dot{y} > 0\}$ (see the illustration in Fig.18). Additionally, recall $p_2 = (x_2, y_2, z_2), p_1 = (x_1, y_1, z_1)$, and that we proved $y_1 < y_2$. Now, set $H = \{(x, y_1, z) | x, z \in \mathbf{R}\} \cap \{\dot{y} > 0\}$ (see the illustration in Fig.18), and denote by S the collection of flow lines connecting α_{Out}, ν and Ω as the collection of flow lines connecting $\beta_{Out}, \zeta = \cup_{\omega \in \beta_{Out}} \gamma_\omega(i(\omega))$ (by this discussion, $\nu \subseteq \zeta$). In particular, $\Omega \cup S$ includes a flow line γ connecting p_1 to p_3 through p_2 , and moreover, the y coordinate strictly increases along γ when we flow from p_1 to $p_2 = \gamma_{p_3}(i(p_3))$ (see the illustration in Fig.18). Therefore, it follows $H \cap (S \cup \Omega)$ includes a Jordan curve J , enclosing a Jordan domain D s.t. $p_1 \in J$. Therefore, there exists a three-dimensional body C trapped between S, Ω and H (see the illustrations in Fig.18 and Fig.19) - moreover, C is a topological cone, s.t. P_{Out} is its vertex and D is its base. Moreover, by its construction, we have $C \subseteq \{(x, y, z) | y < y_1\}$ - and given any $s \in W_{Out}^s$ sufficiently close to $P_{Out}, s \in \partial C$.

Since $P_{In} = (0, 0, 0), y_1 \neq 0$, by $P_{In} \notin \alpha_{Out}$ it follows $P_{In} \notin \overline{C}$. Furthermore, because the normal vector to H is $(0, 1, 0)$ we conclude F_p points into $\{(x, y, z) | y > y_1\}$ on D - therefore, by definition, the vector field F_p points outside C on D , and on $\partial C \setminus D$ it is tangent to ∂C (see the illustration in Fig.19). Therefore, trajectories can only escape \overline{C} under the flow - and as such, no trajectory escapes \overline{C} under the inverse flow. As stated in previous paragraph, ∂C includes every $s \in W_{out}^s$ sufficiently close to P_{Out} , which implies the backwards trajectories of such s are trapped in \overline{C} . However, since $p \in P$ is a trefoil parameter we have $W_{In}^u = W_{Out}^s$ - which implies the backwards trajectory of any $s \in W_{Out}^s$ must tend to P_{In} (in infinite time). Since by construction $P_{In} \notin \overline{C}$ we have

is a contradiction - hence, we conclude p_1 cannot exist, i.e., α_{Out} cannot exist which immediately implies $\mu_{Out} \cap l = \emptyset$.

Therefore, once μ_{out} leaves P_{Out} and enters $A_1 \cap \{\dot{y} > 0\}$ it cannot intersect l , hence $\mu_{Out} \subseteq \{\dot{y} > 0\} \cap \overline{A_1}$ (see the illustration in Fig.23)- hence, l separates σ_3 from $\{\dot{y} > 0\} \cap \overline{A_1}$ it follows $\mu_{Out} \cap \sigma_3 = \emptyset$ (see the illustration in Fig.23). Additionally, by $\partial(\overline{A_1} \cap \{\dot{y} > 0\}) = \sigma_1 \cup \sigma_2 \cup \{P_{In}, P_{Out}\}$ and because μ_{Out} is a component of $\mu = W_{Out}^s \cap \overline{A_1}$, by Lemma 3.4 we conclude $\mu_{Out} \cap (\sigma_1 \cup \sigma_2) = \emptyset$. As such, by the boundedness of W_{Out}^s it follows μ_{Out} is a curve which begins at P_{Out} and terminates at either P_{In} or P_{Out} - and since $p \in P$ is a trefoil parameter, by $W_{Out}^s = W_{In}^u$ we conclude μ_{Out} terminates at P_{In} . That is, all in all we have proven μ_{Out} is a component of $\mu = W_{Out}^s \cap \overline{A_1}$ which is a curve in $A_1 \cap \{\dot{y} > 0\}$ which begins at P_{Out} and terminates at P_{In} , satisfying $l \cap \mu_{Out} = \emptyset$. As such, by $W_{Out}^s = W_{In}^u$ we conclude $\mu_{Out} = \mu$ and Lemma 3.6 follows (see the illustration in Fig.23). \square

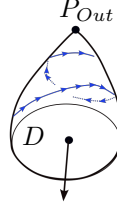


FIGURE 19. The cone C , along with the directions of F_p on the base D and a flow line on $C \setminus D$ which spirals to P_{Out} . The existence of such a cone is impossible for trefoil parameters $p \in P$.

Now, consider the forward-trajectories of μ . By Lemma 3.6, μ is a curve in $A_3 \cap \{\dot{y} > 0\}$ - therefore, given $s \in \mu$, a similar argument to the one used at the beginning of the proof of Lemma 3.6 implies there exists a minimal, positive time $\infty > t(s) > 0$ s.t. $\gamma_s(t(s)) \in A_3 \setminus \partial A_3$. Therefore, let us denote by $\rho = \cup_{s \in \mu} \gamma_s(t(s))$ - it immediately follows ρ is a Jordan arc in $A_3 \setminus \{\dot{y} > 0\}$, s.t. $\rho \cup \sigma_3 \cup \{P_{In}, P_{Out}\}$ enclose a Jordan domain $V_\alpha \subseteq A_3$ (see the illustrations in Fig. and 23). Additionally, since $A_3 \setminus \partial V_\alpha$ is divided to a bounded and unbounded component, by the boundedness of $\partial B_\alpha = \overline{W_{Out}^s}$ it follows $V_\alpha = B_\alpha \cap A_3$. Using a similar construction to the proof of Lemma 3.6, we now prove the following Lemma - which implies the second assertion of Prop.3.1:

Lemma 3.7. *Let $p \in P$ be a trefoil parameter - then, $\rho \subseteq \{\dot{y} > 0\} \cap A_3$. As a consequence, $V_\alpha \subseteq \{\dot{y} > 0\}$.*

Proof. To begin, recall that since $p \in P$ is a trefoil parameter, by Def.2.4 we have $W_{In}^u = W_{Out}^s$ - hence, since $\partial B_\alpha = W_{In}^u \cup \{P_{In}, P_{Out}\} = W_{Out}^s \cup \{P_{In}, P_{Out}\}$, it follows $\rho = W_{In}^u \cap A_3 = W_{Out}^s \cap A_3$. Therefore, a similar argument to the one used at the beginning of Lemma 3.6 implies that for a sufficiently small $r > 0$, $B_r(P_{In}) \cap \rho, B_r(P_{Out}) \cap \rho$ are both subsets of $A_3 \cap \{\dot{y} > 0\}$ (see the illustration in Fig.20). Therefore, similarly to the proof of Lemma 3.6, it would therefore suffice to prove that once ρ leaves P_{In} or P_{Out} , it does not intersect l_p - from which it would follow ρ lies strictly in $\{\dot{y} > 0\}$, thus implying Lemma 3.7. To this end, recall $l \subseteq A_1$ (see the illustration in Fig.17) - therefore, since $\rho \subseteq A_3$, it would suffice to prove $\rho \cap l_p \setminus l = \emptyset$. Recalling we denote by l_1, l_2 the components of $l_p \setminus l$ (see the discussion before Lemma 3.6 and the illustration in Fig.20), it would suffice to show $\rho \cap l_i = \emptyset$, $i = 1, 2$. We will prove this is the case by contradiction, by considering the cases $\rho \cap l_1 \neq \emptyset$, $\rho \cap l_2 \neq \emptyset$ separately - in both cases, we will construct a cone, similarly to what we did in Lemma 3.6, from which a contradiction would issue.

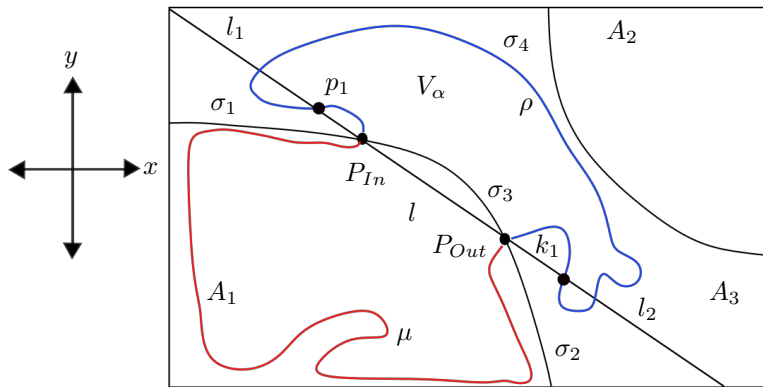


FIGURE 20. An eagle's view of $\{\dot{x} = 0\}$ - in this scenario, ρ intersects both l_1, l_2 . We prove this scenario is impossible.

We begin by showing $\rho \cap l_1 = \emptyset$, and as stated above, we do so by contradiction. Therefore, assume $\rho \cap l_1 \neq \emptyset$, and similarly to the proof of Lemma 3.6, let $p_1 \in \rho \cap l_1$, $p_1 = (x_1, y_1, z_1)$ denote the **first** point of intersection in $\rho \cap l_1$ (see Fig.20). Now, consider the backwards trajectory of p_1 - by the boundedness of $\overline{B_\alpha}$ and by $p_1 \in \partial B_\alpha$, similarly to the proof in Lemma 3.6 there exists a maximal $-\infty < t_1 < 0$ s.t. the following are satisfied:

- $p_2 = \gamma_{p_1}(t_1) \in \overline{U_p}$.
- For every $t \in (t_1, 0)$, $\gamma_{p_1}(t) \in \{\dot{y} < 0\}$.

That is, if $\gamma_{p_1}(t_1, 0)$ is the flow-line connecting p_2 to p_1 , then $\gamma_{p_1}(t_1, 0) \subseteq \{\dot{y} < 0\}$. As such, since $p_2 = (x_2, y_2, z_2)$ lies on the **backwards** trajectory of p_1 , writing $\gamma_{p_1}(t) = (x(t), y(t), z(t))$, $t \in [t_1, 0]$ we conclude y_1 minimizes the y -coordinate on $y(t), t \in [t_1, 0]$, while y_2 maximizes it (see the illustration in Fig.21). Now, set $H_{In} = \{(x, y_1, z) | x, z \in \mathbf{R}\} \cap \{\dot{y} \leq 0\}$ - similarly to the proof of Lemme 3.6 we conclude H_{In} and ∂B_α trap a three-dimensional body D_{In} (see the illustration in Fig.21). In particular, D_{In} is a topological cone with a base H_{In} and a vertex at P_{In} , satisfying $P_{Out} \notin \overline{D_{In}}$ (see the illustration in Fig.22). Moreover, since the normal vector to H_{In} is $(0, 1, 0)$, by direct computation we conclude that on $H_{In} \cap \partial D_{In} = T_{In}$, F_p points into D_{In} - and since $\partial D_{In} \setminus T_{In} \subseteq \partial B_\alpha$, F_p is tangent to $\partial D_{In} \setminus T_{In}$. As a consequence, no trajectories can escape $\overline{D_{In}}$.

Now, recall we assume $p \in P$ is a trefoil parameter (see Def.2.4) - which, as we saw earlier, implies by $W_{Out}^s = W_{In}^u = \partial B_\alpha \setminus \{P_{In}, P_{Out}\}$. Therefore we conclude that given $x \in \partial D_{In} \setminus T_{In}$, $x \neq P_{In}$ and $t > 0$, $\gamma_x(t) \in \overline{D_{In}}$. However, any such x satisfies $x \in W_{Out}^s$, yet, by $P_{Out} \notin \overline{D_{In}}$ we have $\lim_{t \rightarrow \infty} \gamma_x(t) \neq P_{Out}$ - a contradiction. As a consequence, $\rho \cap l_1 = \emptyset$.

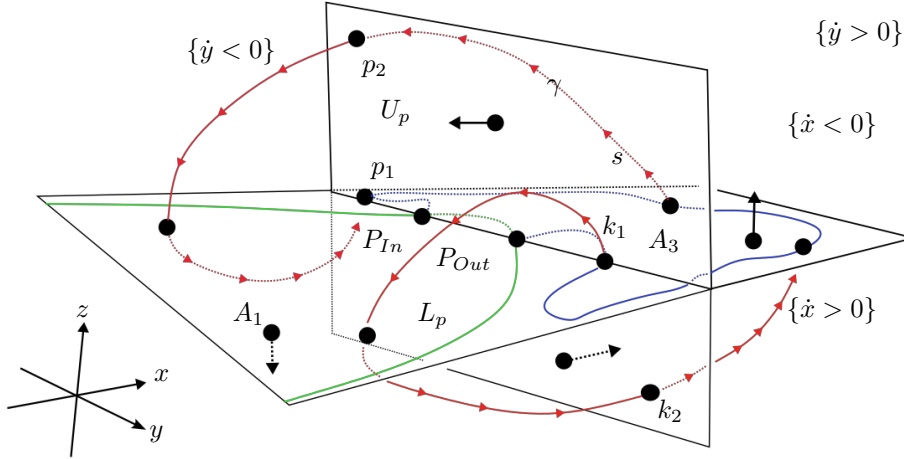


FIGURE 21. The scenario where $p_1 \in l_1$, $k_1 \in l_2$, sketched along with their flow lines and the directions of F_p on L_p, U_p, A_1 and A_3 - we prove this scenario is impossible. The green and blue lines denote σ and ρ , respectively.

We now use a symmetric argument to prove $\rho \cap l_2 = \emptyset$, and again, we do so by contradiction. That is, assume $\rho \cap l_2 \neq \emptyset$, and let $k_1 \in \rho \cap l_2$, $p_1 = (x_1, y_1, z_1)$ denote the **first** point of intersection in $\rho \cap l_2$ (see Fig.20). Now, consider the forward trajectory of k_1 - by the boundedness of $\overline{B_\alpha}$ and by $k_1 \in \partial B_\alpha$, similarly to the proof in Lemma 3.6 there exists a maximal $0 < t_2 < \infty$ s.t. the following are satisfied:

- $k_2 = \gamma_{k_1}(t_2) \in \overline{L_p}$ (see the illustration in Fig.21).
- For every $t \in (0, t_2)$, $\gamma_{k_1}(t) \in \{\dot{y} < 0\}$.

That is, if $\gamma_{k_1}(0, t_2)$ is the flow-line connecting k_1 to k_2 , then $\gamma_{k_1}(0, t_2) \subseteq \{\dot{y} < 0\}$. As such, since $k_2 = (x_2, y_2, z_2)$ lies on the **forwards** trajectory of k_1 , writing $\gamma_{k_1}(t) = (x(t), y(t), z(t))$, $t \in [0, t_2]$ we conclude symmetrically y_1 maximizes the y -coordinate on $y(t), t \in [0, t_2]$, while y_2 minimizes it (see the illustration in Fig.21). Now, similarly, set $H_{Out} = \{(x, y_1, z) | x, z \in \mathbf{R}\} \cap \{\dot{y} \leq 0\}$ - similarly to the proof of Lemme 3.6 we conclude H_{Out} and ∂B_α trap a three-dimensional body D_{Out} (see the illustration in Fig.21). Again, D_{Out} is a topological cone with a base H_{Out} and a vertex at P_{Out} , satisfying $P_{In} \notin \overline{D_{Out}}$. Moreover, since the normal vector to H_{Out} is $(0, 1, 0)$, similarly we conclude that on $H_{Out} \cap \partial D_{Out} = T_{Out}$, F_p points **outside** of D_{Out} - and since F_p is tangent to $\partial D_{Out} \setminus T_{Out} \subseteq \partial B_\alpha$, (see the illustration in Fig.22), no trajectories can enter $\overline{D_{Out}}$ under the flow - and none can escape under the **inverse** flow.

Again, because $p \in P$ is a trefoil parameter, by $W_{Out}^s = W_{In}^u = \partial B_\alpha \setminus \{P_{In}, P_{Out}\}$ we conclude that given $x \in \partial D_{Out} \setminus T_{Out}$, $x \neq P_{Out}$ and $t < 0$, $\gamma_x(t) \in \overline{D_{Out}}$. However, any such x satisfies $x \in W_{Out}^u$, and yet, by

the author plans to study the connection between the boundedness of the two-dimensional manifolds W_{Out}^s, W_{In}^u and the existence of the Rössler attractor.

To continue, given a trefoil parameter $p \in P$, let us first recall that by Cor.3.0.1, the first-return map $f_p : \overline{D_\alpha} \setminus \{P_0\} \rightarrow \overline{D_\alpha} \setminus \{P_0\}$ is well defined - and by Prop.3.1, $\overline{D_\alpha} \setminus \{P_0\}$ is homeomorphic to the closed unit disc in \mathbf{R}^2 , punctured at the origin (with P_0 as in Def.2.4 - see Fig.12 for an illustration). As described in the beginning of this section, we now proceed to study the continuity properties of f_p on $\overline{D_\alpha} \setminus \{P_0\}$ - following which we state and prove Th.3.1.

To begin, from now on unless stated otherwise, $(a, b, c) = p \in P$ would always denote a trefoil parameter as in Def.2.4, while Θ would always denote the bounded component of W_{In}^s, W_{Out}^u which flows from P_{Out} to P_{In} - in other words, Θ is the bounded heteroclinic connection for the vector field F_p , given by Def.2.4. Moreover, from now on l would always denote the arc $\{l_p(x) | x \in (0, c - ab)\}$ in $l_p(x) = (x, -\frac{x}{a}, \frac{x}{a}), x \in \mathbf{R}$, the tangency curve of F_p to the cross-section $\{\dot{y} = 0\}$ (see the discussion preceding Lemma 2.1). To motivate our results, let us first recall P_0 is the **unique** point of intersection between Θ and the cross-section U_p (see Def.2.4), and that P_0 is interior to the cross-section $D_\alpha \subseteq \overline{U_p}$ (see Cor.3.2) - which, by previous paragraph, implies $D_\alpha \setminus \{P_0\}$ contains a topological annulus centered at P_0 . Since P_0 flows to P_{In} (in infinite time), as P_0 is interior to U_p and because $P_{In} \in \partial U_p$, we would expect f_p to be discontinuous at P_0 - if only because the said annulus has to be torn by f_p . This motivates us to prove the following Proposition, characterizing the discontinuities of f_p in the topological disc D_α :

Proposition 3.2. *Let $p \in P$ be a trefoil parameter. Then, the discontinuities of f_p in D_α are given by $f_p^{-1}(l) \cap D_\alpha$ (with l as in Prop.3.1). In addition, there exists an arc of discontinuity points for f_p , $\delta \subseteq \overline{D_\alpha}$ s.t.:*

- δ connects $P_0 \in D_\alpha$ and a point $\delta_0 \in \partial D_\alpha \setminus \{P_{In}, P_{Out}\}$.
- $f_p(\delta) \subseteq l$.
- δ is the **only** curve of discontinuity points for f_p with an endpoint strictly interior to D_α .

Proof. We first characterize the discontinuities of f_p in D_α by proving they correspond to $f_p^{-1}(l) \cap D_\alpha$. To this end, first, recall D_α is a topological disc bounded by $l \cup L \cup \{P_{In}, P_{Out}\}$, with $L = \partial B_\alpha \cap U_p$ (see Prop.3.1) - as such, by the invariance of ∂B_α under the flow we have $f_p(L) = L$. Now, since f_p is a first-return map generated by a smooth flow, for f_p to be discontinuous at some interior $s \in D_\alpha, s \neq P_0$, the flow line connecting $s, f_p(s)$ must be **tangent** to $\overline{D_\alpha}$ at $f_p(s)$ - that is, for an interior point $s \in D_\alpha$ to be a discontinuity for f_p , $f_p(s)$ must lie in l_p , the tangency set of F_p to $\overline{U_p}$ (see the illustrations in Fig.24 and Fig.14). Since D_α is a topological disc inside $\overline{U_p}$, by the invariance of $\overline{D_\alpha}$ under f_p this occurs **precisely** when $f_p(s) \in \overline{D_\alpha} \cap l_p$. By Prop.3.1 we have $L \cap l_p = \emptyset$, hence by Prop.3.1 $\overline{D_\alpha} \cap l_p$ is simply the curve $l \cup \{P_{In}, P_{Out}\}$ (see the illustration in Fig.24).

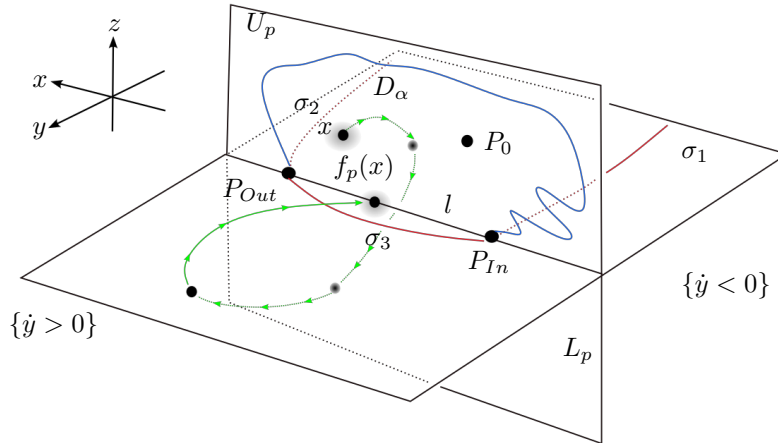


FIGURE 24. The trajectory of an interior point $x \in D_\alpha$ s.t. $f_p(x) \in l$. The shaded neighborhood is torn at l due to the tangency of F_p at l , thus generating a discontinuity.

Now, let us recall P_{In}, P_{Out} are both saddle foci. By Cor.2.1.1, W_{Out}^s , the two-dimensional stable manifold of P_{Out} is transverse to U_p at P_{Out} - therefore, given any initial condition $s \in \overline{U_p}, s \neq P_{Out}$, it follows $f_p(s) \neq P_{Out}$. Conversely, the one-dimensional invariant manifold of P_{In}, W_{In}^s , intersects D_α at P_0 (see Cor.4.2), and at P_0 f_p is undefined - which again implies that given $s \in \overline{D_\alpha} \setminus \{P_0\}, s \neq P_{In}$, we have $f_p(s) \neq P_{In}$. All in all, it follows the discontinuity set of f_p in D_α is **precisely** the set $f_p^{-1}(l) \cap D_\alpha$ - moreover, every component of $f_p^{-1}(l) \cap D_\alpha$ is an

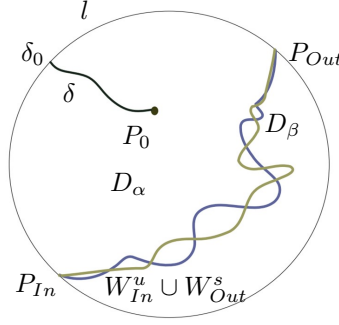


FIGURE 25. the curve δ , with endpoints P_0, δ_0 . l is the arc on ∂D_α connecting $P_{In}, P_{Out}, \delta_0$.

arc in $\overline{D_\alpha}$ (see the illustration in Fig.24).

Having characterized the discontinuities of f_p in D_α , we now proceed to define and analyze the curve δ . To do so, we first prove f_p is continuous around P_{In} (in $\overline{D_\alpha}$) - to do so, recall that by Cor.2.1.1 the two-dimensional unstable manifold of P_{In} , W_{In}^u , is transverse to ∂U_p at P_{In} . Since P_{In} is a saddle-focus, initial conditions on the arc l_p sufficiently close to P_{In} must be mapped inside U_p by f_p (see the illustration in Fig.24) - which, by the orientation-preserving properties of the flow, proves f_p is continuous on some neighborhood of P_{In} in $\overline{U_p}$. Therefore, by $\overline{D_\alpha} \subseteq \overline{U_p}$ (see the illustration in Fig.24), we conclude f_p is continuous on some neighborhood of P_{In} in $\overline{D_\alpha}$ as well.

We can now prove the existence of the discontinuity curve δ as posited above. To do so, consider some closed loop ζ in D_α , surrounding P_0 . Since p is a trefoil parameter, the trajectory of P_0 flows to P_{In} in infinite time, without ever hitting $\overline{D_\alpha}$ along the way (see Def.2.4) - hence, f_p cannot be continuous on ζ : for if it was continuous on ζ , $f_p(\zeta)$ would be a closed curve in D_α surrounding P_{In} . Because this is impossible, by the discussion above there must exist a discontinuity on $\zeta_0 \in \zeta$, $f_p(\zeta_0) \in l$. Varying the loop ζ continuously in D_α we construct a curve δ of discontinuity points, connecting P_0 and some point δ_0 in ∂D_α , s.t. $\delta \setminus \{\delta_0\} \subseteq D_\alpha$ (see the illustration in Fig.25).

Having proven the existence of δ , our next objective is to prove the following two facts:

- $\delta_0 \neq P_{In}$.
- $\delta_0 \neq P_{Out}$.

The proof of $\delta_0 \neq P_{In}$ is immediate - to see why this is so, recall we already proved f_p is continuous around P_{In} , i.e., f_p maps points in $\overline{D_\alpha}$ sufficiently close to P_{In} away from l . Hence, since $f_p(\delta) \subseteq l$, we must have $\delta_0 \neq P_{In}$. The proof $\delta_0 \neq P_{Out}$ would require a different approach. To this end, we first make several observations. First recall that D_α is an invariant subset (w.r.t. f_p) on the cross-section U_p , and that by Remark 3.1, $f_p(\overline{D_\alpha} \setminus \{P_0\}) = \overline{D_\alpha} \setminus \{P_0\}$. Having made these remarks, we can prove $\delta_0 \neq P_{Out}$. To do so, assume otherwise - if $\delta_0 = P_{Out}$, by $f_p(P_{Out}) = P_{Out}$ we conclude $f_p(\delta)$ is an arc on l whose closure connects P_{Out} and P_{In} - hence we must have $l = f_p(\delta)$. Since the discontinuities of f_p are given by $f_p^{-1}(l) \cap D_\alpha$, this would imply f_p is continuous on $D_\alpha \setminus \delta$ - and by the continuity and injectivity of f_p (i.e. it is a homeomorphism of the topological disc $D_\alpha \setminus \delta$), it would follow $f_p(D_\alpha \setminus \delta)$ is homeomorphic to $D_\alpha \setminus \delta$. Since $f_p(\delta) = l$, $f_p(L) = L$, it now follows $f_p(D_\alpha \setminus \delta)$ must fill D_α , i.e., $f_p(D_\alpha \setminus \delta) = D_\alpha$. This implies there exists a point $y \in \overline{D_\alpha} \setminus \delta$ s.t. $f_p(y) = P_0$ - because $P_0 \in \delta$ by definition, it follows there exists some $y \in D_\alpha \setminus \{P_0\}$ s.t. $f_p(y) = P_0$. Since by Remark 3.1 we have $f_p(\overline{D_\alpha} \setminus \{P_0\}) = \overline{D_\alpha} \setminus \{P_0\}$, this is a contradiction - hence, we conclude $\delta_0 \neq P_{Out}$.

Therefore, having proven $P_{Out}, P_{In} \notin \delta$, in order to conclude the proof of Lemma 3.2 it remains to show that given **any** discontinuity curve for f_p $\rho \subseteq D_\alpha$ s.t. ρ has an endpoint strictly **interior** to D_α , then $\rho = \delta$. To this end, let us denote by $Dis(f_p) = f_p^{-1}(l) \cap D_\alpha$, the set of all the discontinuity points of f_p in D_α . We immediately conclude interior points in D_α which are **not** P_0 **cannot** form components in $Dis(f_p)$ - since given an interior point $x \in D_\alpha \setminus \{P_0\}$ s.t. $f_p(x) \in l$, because l is an open Jordan arc by the continuity of the flow there exists an arc $\gamma \subseteq D_\alpha$, $x \in \gamma$, s.t. $f_p(\gamma)$ is an arc on l . This proves all the components of $Dis(f_p)$ are arcs in D_α . The exact same argument also proves **any** component of $Dis(f_p)$ which is an arc must have at least one endpoint on the arc l .

We can now prove that given a component $\rho \subseteq Dis(f_p)$ with an endpoint interior to D_α , then $\rho = \delta$. We first prove that given such a component ρ , one of its endpoints has to be P_0 . To do so, let us recall we have proven earlier that given $x \in D_\alpha \setminus \{P_{In}, P_{Out}, P_0\}$ we have $f_p(x) \neq P_{Out}, P_{In}, P_0$. Now, assume by contradiction $\rho \subseteq Dis(f_p)$ is a component with an endpoint strictly interior to D_α , and parameterize ρ by $[0, 1]$ s.t. $\rho(0) \in l$,

$\rho(1) \in D_\alpha$. If $\rho(1) \neq P_0$, since l is an open Jordan arc and because by previous paragraph $f_p(\rho(1)) \neq P_{In}, P_{Out}$, by the continuity of the flow f_p^{-1} must be continuous on a neighborhood of $f_p(\rho(1))$ inside the arc l (see Fig.24). Because this contradicts the maximality of ρ as a component of $Dis(f_p)$, we conclude the **only** possibility is that the trajectory of $\rho(1)$ tends to P_{In} , i.e. $\rho(1) = P_0$ - that is, we have just proven that if ρ is a component of $Dis(f_p)$ with an endpoint $\rho(1)$ strictly interior to D_α , that endpoint must be P_0 .

We now prove $\rho = \delta$, thus concluding the proof of Prop.3.2. By definition, we have $f_p(\rho), f_p(\delta) \subseteq l$. However, l is an arc on ∂D_α whose endpoints are P_{In}, P_{Out} - as such, since P_0 lies in both ρ, δ and because P_0 tends to P_{In} in infinite time, $P_{In} \in \overline{f_p(\delta)} \cap \overline{f_p(\rho)}$. Since both $f_p(\delta), f_p(\rho)$ are arcs on l with an endpoint at P_{In} , it follows $f_p(\rho \setminus \{P_0\}) \cap f_p(\delta \setminus \{P_0\}) \neq \emptyset$ - therefore, by the Existence and Uniqueness Theorem $\rho \cap \delta \neq \emptyset$. Since ρ, δ are both components of $Dis(f_p)$, it follows that $\rho = \delta$, and Prop.3.2 follows. See Fig.26 for an illustration. \square

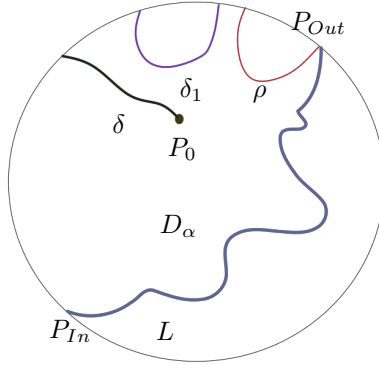


FIGURE 26. The discontinuity curves for f_p in D_α - δ, ρ , and δ_1 , another possible discontinuity curve. In this sketch, U_p is drawn for simplicity as a disc.

In fact, we can say more. Extending the results of Prop.3.2 to the fixed point P_{Out} we now conclude:

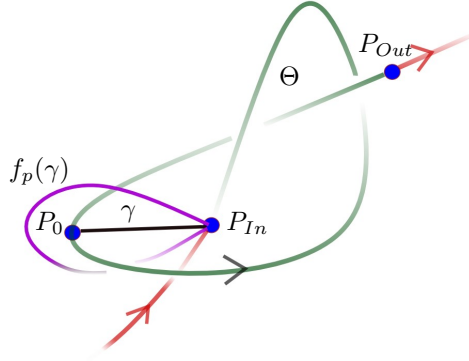
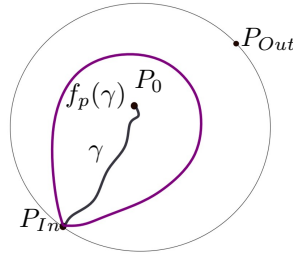
Corollary 3.0.2. *Let $p \in P$ be a trefoil parameter. Then, there exists a component $\rho \subseteq Dis(f_p)$ s.t. $P_{Out} \in \bar{\rho}$ and $\delta \neq \rho$ (see Fig.26 for an illustration).*

Proof. Let us recall the two-dimensional stable manifold for P_{Out} , W_{Out}^s , is transverse to the cross-section U_p at P_{Out} (see Cor.2.1.1). This implies that the **backwards** trajectories of initial conditions on the arc l sufficiently close to P_{Out} all hit U_p transversely - or, in other words, there exists a curve $\rho \subseteq Dis(f_p)$, $P_{Out} \in \bar{\rho}$, s.t. $f_p(\rho)$ is an arc on l with an endpoint at P_{Out} . Since by Cor.3.1 $l \subseteq \overline{D_\alpha}$, by the forward and backwards invariance of $\overline{D_\alpha}$ under f_p (see Cor.3.0.1) we conclude $\rho \subseteq \overline{D_\alpha}$ - and since $P_{Out} \in \bar{\rho}$, from $P_{Out} \notin \delta$ (see Prop.3.2) we immediately have $\rho \neq \delta$ and Cor.3.0.2 now follows (see the illustration in Fig.26). \square

We are now ready to state and prove Th.3.1 - that is, we are now ready to prove that given a trefoil parameter $p \in P$, the first-return map $f_p : \overline{D_\alpha} \rightarrow \overline{D_\alpha}$ is chaotic on some invariant set $Q \subseteq \overline{D_\alpha}$ (in the sense of Def.1.1). To motivate the proof, let us first introduce a heuristic which explains why we expect the dynamics of F_p to be chaotic - as will be made clear, this heuristic argument will later be made rigorous, forming the backbone of the proof. To begin, consider a scenario as in Fig.27. That is, given a trefoil parameter $p \in P$ and the corresponding bounded heteroclinic trajectory Θ (see Def.2.4), choose some curve $\gamma \subseteq \overline{D_\alpha}$ s.t. γ connects the fixed point P_{In} and P_0 in $\overline{D_\alpha}$ (with P_0 as in Def.2.4 - see the illustration in Fig.27).

Now, let us suspend the curve γ along Θ , the bounded component of the heteroclinic trefoil knot (see the illustration in Fig.27). By the topology of Θ , we conclude it constrains γ to return to D_α as in Fig.27 - that is, $f_p(\gamma)$ is a closed loop in the topological disc D_α , which begins and terminates at the fixed point P_{In} . Therefore, we can impose $f_p(\gamma)$ on the topological disc D_α roughly as in Fig.28 - which, heuristically, implies the existence of a Smale Horseshoe map for f_p in the cross-section D_α .

In practice, due to Prop.3.2 and Cor.3.0.2 the heuristic described above is hard to justify rigorously - that is, the claim $f_p(\gamma)$ is a closed loop is far from immediate, since given an arbitrary curve $\gamma \subseteq \overline{D_\alpha}$ by Prop.3.2 and Cor.3.0.2 there is no reason to assume $f_p(\gamma)$ is even connected. However, as we will now prove, provided we work carefully enough and restrict ourselves to another cross-section $H_p \subseteq D_\alpha$, this heuristic becomes a rigorous proof. Therefore, we finally prove:

FIGURE 27. Flowing γ along the trefoil. Θ is the green separatrix.FIGURE 28. imposing $f_p(\gamma)$ on H_p .

Theorem 3.1. Let $(a, b, c) = p \in P$ be a trefoil parameter, and let F_p denote the vector field generating the corresponding Rössler system. Also, denote by $\sigma : \{1, 2\}^{\mathbb{N}} \rightarrow \{1, 2\}^{\mathbb{N}}$ the one sided shift - then, there exists a cross-section $H_p \subseteq D_\alpha$ and an f_p -invariant $Q \subseteq \overline{H_p}$ s.t. the following holds:

- $\overline{H_p}$ is a closed topological disc.
- f_p is continuous on Q .
- There exists a neighborhood N of P_{In}, P_{Out} s.t. for any periodic trajectory T in Q , $T \cap N = \emptyset$ - that is, the periodic trajectories in Q all lie uniformly away from the fixed points P_{In}, P_{Out} .
- There exists a continuous $\pi : Q \rightarrow \{1, 2\}^{\mathbb{N}}$ s.t. $\pi \circ f_p = \sigma \circ \pi$.
- Given any $s \in \{1, 2\}^{\mathbb{N}}$ which is **not** the constant $\{1, 1, 1, \dots\}$ nor pre-periodic to it, $s \in \pi(Q)$.
- Let $s \in \{1, 2\}^{\mathbb{N}}$ be periodic of minimal period k . Then, $\pi^{-1}(s)$ contains a periodic point x_s for f_p of minimal period k .

In particular, f_p is chaotic on Q w.r.t. Def.1.1.

Proof. To begin, recall that by Prop.3.2 the discontinuities of f_p in the (open) topological disc D_α are given by $f_p^{-1}(l) \cap D_\alpha$. Now, before sketching the proof of Th.3.1, let us first recall that Prop.3.2 and Cor.3.0.2 together imply that even though f_p is discontinuous at some curves in the cross-section D_α , these discontinuities are mild, in a sense - namely, they occur when the trajectory of some interior point $x \in D_\alpha$ flows to the arc $l \subseteq \partial D_\alpha$. As such, both Prop.3.2 and Cor.3.0.2 motivate us to construct the cross-section H_p and the set Q by analyzing the invariant set of f_p in $\overline{D_\alpha} \setminus l$ - in fact, these two constructions would form the core of the proof of Th.3.1.

Due to the length of the argument and the large amount of technical details involved, we divide the proof of Th.3.1 into three consecutive stages:

- In Stage *I* we construct the cross-section H_p . As remarked above, we do so by studying the discontinuities of f_p in D_α , or more precisely, the topology of the set $f_p^{-1}(l)$. As we will prove, there exists a component H_p of $D_\alpha \setminus f_p^{-1}(l)$, a topological disc, s.t. both fixed points P_{In}, P_{Out} and the curve δ from Prop.3.2 lie in ∂H_p .
- In Stage *II* we analyze the topology of $f_p(H_p)$ and $f_p^{-1}(l)$ inside $\overline{D_\alpha}$. We will prove, the set $f_p^{-1}(l)$ is a connected curve in $\overline{D_\alpha}$, from which it would follow that for every $n \geq 0$, $f_p^{-n}(\delta_0) \in \overline{H_p}$ (with δ_0 as in Prop.3.2).
- Finally, in Stage *III* we tie these results together and construct the set Q , thus concluding the proof of Th.3.1.

As must be stated, the results in Stages *I* and *II* are strongly dependent on the results and analysis performed in Section 2 - in particular, they are dependent on the analysis of the two cross-sections $\{\dot{x} = 0\}$ and $\{\dot{y} = 0\}$ performed during the proof of Th.2.1 (see Lemmas 2.3, 2.4, 2.5 and Cor.2.1.1).

3.1. Stage I - constructing the cross-section H_p . Per the description above, we begin by constructing and defining the cross-section $H_p \subseteq D_\alpha$. To this end, recall the curve σ introduced in Stage *I* of the proof of Th.2.1 - that is, recall the cross-section $\{\dot{x} = 0\}$ analyzed in Lemmas 2.3 and 2.4, and that the curve $\sigma \subseteq \{\dot{x} = 0\}$ corresponds to the set where the vector field F_p is tangent to $\{\dot{x} = 0\}$. Further recall $\sigma \setminus \{P_{In}, P_{Out}\}$ is composed of four components, $\sigma_1, \sigma_2, \sigma_3$ and σ_4 (see the discussion after the proof of Lemma 2.3 and the illustrations in both Fig.3 and Fig.29).

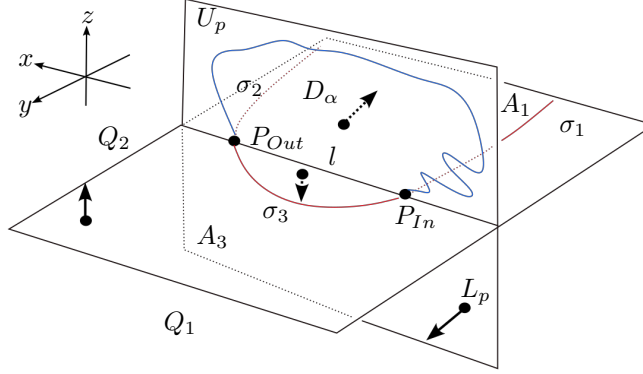


FIGURE 29. The configuration of $\{\dot{y} = 0\}$, $\{\dot{x} = 0\}$ along with the directions of F_p on their respective components. The blue curve denotes L - see Prop.3.1.

Now, recall the cross-section U_p (see the discussion before Lemma 2.1), and recall ∂U_p is the curve l_p (see the illustrations in Fig.3 and Fig.5) parameterized by $l_p(x) = (x, -\frac{x}{a}, \frac{x}{a})$, $x \in \mathbf{R}$ - in particular, recall the arc l corresponds to $\{l_p(x) | x \in (0, c - ab)\}$ (by $P_{In} = l_p(0)$, $P_{Out} = l_p(c - ab)$ we immediately have $P_{In}, P_{Out} \in \bar{l}$). As proven in Lemma 2.5, given $s \in l$, there exists some $\epsilon > 0$ s.t. for $|t| < \epsilon$, $t \neq 0$, $\gamma_s(t) \in \{\dot{y} > 0\}$. Now, recall $l_p = \{\dot{x} = 0\} \cap \{\dot{y} = 0\}$ and that $\{\dot{x} > 0\}$ lies **below** the plane $\{\dot{x} = 0\}$ (see Lemma 2.5 and the illustration in Fig.5). Additionally, recall that for $s \in l$ we have $F_p(s)$ points in the negative z -direction (see the proof of Lemma 2.5) - therefore, it follows there exists some maximal $0 < \epsilon_1 \leq \epsilon$ s.t. for $t \in (0, \epsilon_1)$ we have $\gamma_s(t) \in \{\dot{x} > 0\}$ (see the illustration in Fig.29 or Fig.14). Recalling $\{\dot{x} > 0\}$ is the region **below** the plane $\{\dot{x} = 0\}$ (see the illustration in Fig.5 and Fig.29), by this discussion it follows that for $t \in (0, \epsilon_1)$, $\gamma_s(t)$ lies **below** $\{\dot{x} = 0\}$.

To continue, let σ be as above, and recall $\{\dot{x} = 0\} \setminus \sigma$ is composed of three components: A_1, A_2, A_3 s.t. $\sigma_3 \subseteq \partial A_1 \cap \partial A_3$. As shown in the course of proof of Lemma 2.3 and the following discussion in Stage *I* of the proof of Th.2.1, on A_1 the vector field F_p points inside $\{\dot{x} > 0\}$ - that is, F_p points below $\{\dot{x} = 0\}$. Conversely, on A_3 the vector field F_p points inside $\{\dot{x} < 0\}$, i.e. above $\{\dot{x} = 0\}$ (see the illustrations in both Fig.14 and Fig.29). With these ideas in mind, we now prove the following technical Lemma, which, nonetheless, forms an important element in the proof of Th.3.1:

Lemma 3.8. *Let $p \in P$ be a trefoil parameter and let D_α be as in Prop.3.1 - then, there exists a first-hit map $h : \overline{D_\alpha} \rightarrow A_3 \cap \{\dot{y} > 0\}$, s.t. the following holds:*

- *h is continuous and injective. Moreover, given $s \in \overline{D_\alpha}$, $h(s)$ lies on the interior of the forward trajectory connecting $s, f_p(s)$ - i.e., γ_s must pass through $h(s)$ **before** hitting $f_p(s) \in \overline{D_\alpha}$.*
- *$h(l) = l'$ is a Jordan arc in $A_3 \cap \{\dot{y} > 0\}$ connecting the fixed-points P_{In}, P_{Out} .*
- *$\overline{D_\alpha}$ is homeomorphic to the topological disc $\overline{T_\alpha} = h(\overline{D_\alpha})$.*

Proof. We prove Lemma 3.8 by analyzing the forward-trajectories of initial conditions $s \in \overline{D_\alpha}$ - namely, given $s \in \overline{D_\alpha}$, define $t_1(s) > 0$ as the first positive time s.t. $\gamma_s(t_1(s)) \in \overline{A_3}$ (where defined). As we will now see, Lemma 3.8 will follow provided we prove the function $h : \overline{D_\alpha} \rightarrow \overline{A_3} \cap \{\dot{y} \geq 0\}$ defined by $h(s) = \gamma_s(t_1(s))$ is continuous - and we will do so by proving that given $s \in \overline{D_\alpha}$, $\gamma_s(t_1(s))$ is a transverse intersection point between γ_s and A_3 , i.e., we will prove $\gamma_s(t_1(s)) \notin \partial A_3$.

Let us begin by proving the assertion above for $s \in l$ - by the proof of Lemma 2.5 we already know that given $s \in l$, $F_p(s)$ points in the negative z -direction. Therefore, by the transverse intersection of $\{\dot{x} = 0\}$ and $\{\dot{y} = 0\}$ and because $\{\dot{x} > 0\}$ is the region **below** $\{\dot{x} = 0\}$ (see the proof of Lemma 2.5 and the illustration in Fig.29) we conclude that given $s \in l$, its forward-trajectory γ_s enters $\{\dot{y} > 0\} \cap \{\dot{x} > 0\}$ immediately upon leaving s - see the

illustration in Fig.30). As such, since by definition $\overline{D_\alpha} \subseteq \overline{U_p}$, from $U_p = \{\dot{x} < 0\} \cap \{\dot{y} = 0\}$ it follows that since γ_s , the trajectory of s , must return to $\overline{D_\alpha}$ at $f_p(s)$, γ_s must first exit the open quadrant $Q_1 = \{\dot{x} > 0\} \cap \{\dot{y} > 0\}$ (see the illustration in Fig.29). As shown before the proof of Cor.2.1.1, on $L_p = \{\dot{y} = 0\} \cap \{\dot{x} > 0\}$ the vector field F_p points inside $\{\dot{y} > 0\}$ (see the illustration in Fig.30), hence γ_s can escape Q_1 **only** through hitting $\{\dot{x} = 0\} \cap \{\dot{y} > 0\}$ - after which it enters $Q_2 = \{\dot{x} < 0\} \cap \{\dot{y} > 0\}$ (in particular, the sign of \dot{y} along the flow-line connecting $s, f_p(s)$ is non-negative, and vanishes precisely at $s, f_p(s)$ - see the illustration in Fig.29). As discussed after the proof of Lemma 2.3, this can occur **only** at the region $\overline{A_3} \subseteq \{\dot{x} = 0\}$ - which implies that given $s \in l$, $t_1(s)$ is well-defined, and $\gamma_s(t_1(s)) \in A_3 \cap \{\dot{y} > 0\}$ (see the illustration in Fig.30).

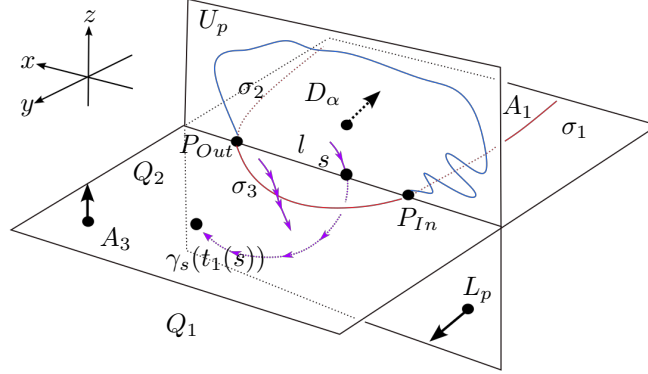


FIGURE 30. The flow line connecting $s, \gamma_s(t_1(s))$ and the local dynamics of F_p on σ_3 .

By this discussion we also conclude $\gamma_s(t_1(s))$ lies strictly in $\overline{A_3} \cap \{\dot{y} > 0\}$. Moreover, because γ_s flows from s to $\gamma_s(t_1(s))$ through the quadrant Q_1 , using Lemma 2.5 and Lemma 2.4 a similar argument to the one used in the proof of Prop.3.1 implies $\gamma_s(t_1(s))$ is a **transverse** intersection point between $A_3 \cap \{\dot{y} > 0\}$ and the flow-line γ_s - i.e. $\gamma_s(t_1(s))$ is strictly interior to the region $A_3 \cap \{\dot{y} > 0\}$ (see the illustration in Fig.31). In particular, it follows $l' = \cup_{s \in l} \gamma_s(t_1(s))$ is a curve in $A_3 \cap \{\dot{y} > 0\}$ whose closure connects the fixed-points P_{In}, P_{Out} (see the illustration in Fig.31). Moreover, the collection of flow-lines connecting l, l' form a canoe-shaped surface C which lies wholly inside $\{\dot{x} \geq 0\} \cap \{\dot{y} \geq 0\}$ (see the illustration in Fig.32).

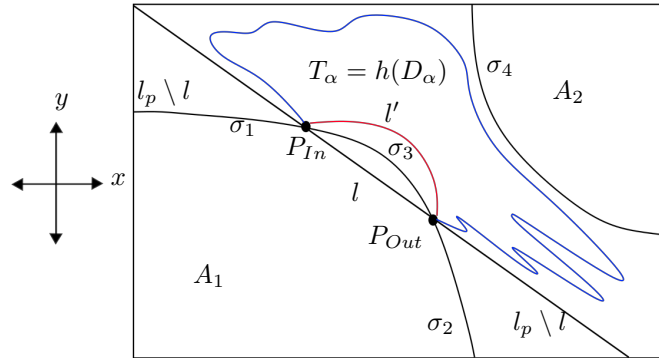
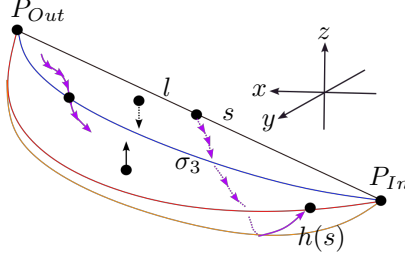


FIGURE 31. The curves l and l' . The blue line represents $L' = \cup_{s \in L} \gamma_s(t_1(s))$.

We now use these observations to conclude the proof. To do so, consider an initial condition $s \in L$ - as shown in the proof of Prop.3.1, $\partial B_\alpha \cap A_3 \subseteq A_3 \cap \{\dot{y} > 0\}$ - which, by the invariance of B_α and by $L = \partial B_\alpha \cap U_p$ (see Prop.3.1) implies that given an initial condition $s \in L$, it arrives at $\gamma_s(t_1(s))$ from Q_1 , or in other words, given any $s \in L$, $\gamma_s(t_1(s)) \in A_3 \cap \{\dot{y} > 0\}$. As such, similarly to the argument above we conclude that for $s \in L$, $\gamma_s(t_1(s))$ is a transverse intersection point between $\gamma_s, A_3 \cap \{\dot{y} > 0\}$. Therefore, $L' = \cup_{s \in L} \gamma_s(t_1(s))$ is a curve in $A_3 \cap \{\dot{y} > 0\}$ connecting P_{In}, P_{Out} (see the illustration in Fig.31) - and by the orientation preserving of the flow, we conclude $h(D_\alpha) = T_\alpha$ is the **closed** Jordan domain in $A_3 \cap \{\dot{y} > 0\}$ trapped between L' and l' (see the illustration in Fig.31) - in particular, it follows that for $s \in \overline{D_\alpha} \setminus \{P_0\}$, $h(s)$ is interior to the forward trajectory connecting $s, f_p(s)$, i.e., γ_s must pass through $h(s)$ **before** hitting $f_p(s) \in \overline{D_\alpha}$. Finally, by the Existence and Uniqueness Theorem h is automatically injective - hence it is a homeomorphism, and Lemma 3.8 now follows. \square

FIGURE 32. The body C , and the directions of F_p on it.

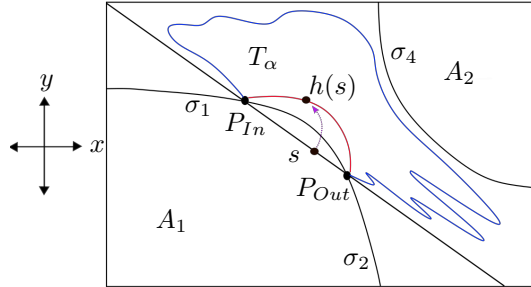
Despite its technical nature, Lemma 3.8 has the following geometric meaning - by Lemma 3.8, given any $s \in \overline{D_\alpha}$, its forward trajectory must first hit the disc $\overline{T_\alpha}$ **before** hitting $f_p(s) \in \overline{D_\alpha}$. Additionally, by Remark 3.1, we have $f_p(\overline{D_\alpha} \setminus \{P_0\}) = \overline{D_\alpha} \setminus \{P_0\}$ - as such, by $l \subseteq \partial D_\alpha$ we immediately conclude:

Corollary 3.1.1. *Given an initial condition $s \in l$, $f_p^{-1}(s)$ is well defined - and moreover, the **backwards** trajectory of s must hit $\overline{T_\alpha}$ **before** hitting $f_p^{-1}(s)$.*

Now, recall we parameterize l by $l_p(x) = (x, -\frac{x}{a}, \frac{x}{a})$, $x \in (0, c - ab)$. As such, since $l' = h(l)$, it follows we can parameterize l' by $l'(x) = (v(x), y(x), z(x))$, $x \in (0, c - ab)$. We now prove the following fact, which will be useful later on:

Corollary 3.1.2. *The function $v : (0, c - ab) \rightarrow \mathbf{R}$ is non-decreasing.*

Proof. To begin, let $\Pi(x, y, z) = x$ denote the projection to the x -axis, and $v(x) = \Pi \circ h \circ l_p(x)$, $x \in (0, c - ab)$. By definition, l is a curve whose closure connects the fixed-points P_{In}, P_{Out} - as such, by Lemma 3.8 $l' = h(l)$ is a smooth curve in $A_3 \cap \{\dot{y} > 0\}$, satisfying $\lim_{x \rightarrow 0} l'(x) = P_{In}$, $\lim_{x \rightarrow c - ab} l'(x) = P_{Out}$ (see the illustration in Fig.33) - which implies $h \circ l_p : (0, c - ab) \rightarrow l'$ is also a smooth map. Therefore it follows $v : (0, c - ab) \rightarrow \mathbf{R}$ is also smooth, and satisfies $\lim_{x \rightarrow 0} v(x) = 0$, $\lim_{x \rightarrow c - ab} v(x) = c - ab$ - therefore, by this discussion it follows Cor.3.1.2 would follow provided we show $\frac{dv}{dx}(x) \geq 0$ for all $x \in (0, c - ab)$.

FIGURE 33. An initial condition $s \in l$ flowing through $\{\dot{x} > 0\} \cap \{\dot{y} > 0\}$ (that is, below $\{\dot{x} = 0\}$ to $h(s) \in l' \subseteq A_3$. In particular, l' lies away from σ_3 , the curve separating l, l' .

We first prove there exists some $x_0 \in (0, c - ab]$ s.t. for $x \in (0, x_0)$ we have $\frac{dv}{dx}(x) \geq 0$. To do so, first recall that given $s \in l$, as shown in the proof of Lemma 3.8 the trajectory connecting $s, h(s)$ flows through $\{\dot{x} > 0\}$ (see the illustration in Fig.33). Now, recall l is parameterized by $l_p(x) = (x, -\frac{x}{a}, \frac{x}{a})$, $x \in (0, c - ab)$ - therefore, given $x_1 \in (0, c - ab)$ and setting $s_1 = (x_1, -\frac{x_1}{a}, \frac{x_1}{a})$, $h(s_1) = (v(x_1), y(x_1), z(x_1))$ it follows $v(x_1) \geq x_1 > 0$ - which implies that for $x \in (0, c - ab)$, $v(x)$ is always positive. Therefore, by $\lim_{x \rightarrow 0} v(x) = 0$, $\lim_{x \rightarrow c - ab} v(x) = c - ab > 0$ it follows there exists some maximal $x_0 \in (0, c - ab]$ s.t. for $x \in (0, x_0)$ we have $\frac{dv}{dx}(x) \geq 0$. Consequentially, by previous discussion, Lemma 3.1.2 would immediately follow if we prove $x_0 = c - ab$, i.e., that $l_p(x_0) = P_{Out}$.

In order to do so, we must first quickly study the level sets of \dot{x}, \dot{y} . By computation, for every $r < 0$, the set $\{\dot{x} = r\}$ is given by the plane $\{(x, -y, y - r) | x, y \in \mathbf{R}\}$ (in particular, $\{\dot{x} = r\}$ lies **above** $\{\dot{x} = 0\}$). Conversely, for $R > 0$, the set $\{\dot{y} = R\}$ is given by the plane $\{(x, -\frac{x}{a} + \frac{R}{a}, z) | x, z \in \mathbf{R}\}$ (see the illustration in Fig.35). Since the normal vector to $\{\dot{y} = R\}$ is $N = (1, a, 0)$ it follows that given $v \in \{\dot{y} = R\}$, $F_p(v) \cdot N \geq 0$ precisely on the half-plane $\{\dot{y} = R\} \cap \{\dot{x} \geq -R\}$ - and moreover, $F_p(v) \cdot N = 0$ precisely on the straight line $l_R = \{\dot{y} = R\} \cap \{\dot{x} = -R\}$ (see the illustration in Fig.35). In particular, let us remark that with previous notations, since $a > 0$ it follows $l_R \subseteq Q_2$, i.e., it lies **above** the plane $\{\dot{x} = 0\}$ and **below** the plane $\{\dot{y} = 0\}$ - see the illustration in Fig.41 and Fig.35).

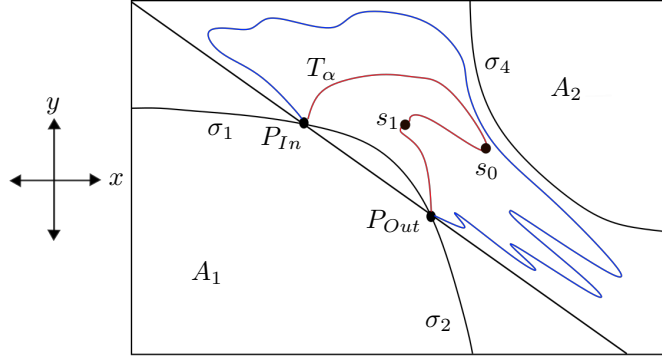


FIGURE 34. The red curve denotes l' - in this scenario, the x -coordinate for s_1 is strictly lesser than the x coordinate for s_0 . We prove this scenario is impossible.

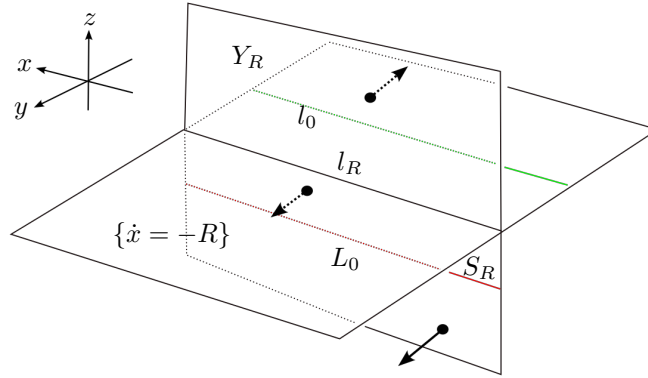


FIGURE 35. The plane $Y_R = \{y = R\}$ and $\{x = -R\} = X_R$ along with the directions of F_p on Y_R . The red line L_R denotes $\{x = 0\} \cap Y_R$, the green line l_0 denotes $\{y = 0\} \cap X_R$ while $l_R = Y_R \cap X_R$. S_R is the strip on Y_R trapped between L_0, l_0 .

We are now ready to prove $x_0 = c - ab$, and we do so by contradiction. That is, assume x_0 is in fact interior to $(0, c - ab)$. Since x_0 was defined as the maximal point in $(0, c - ab)$ s.t. $\frac{dv}{dx}(x) \geq 0$ for $x \in (0, x_0)$, it follows x_0 is a local maximum for v - which implies there exists some $x_1 > x_0$ s.t. on (x_0, x_1) , v is decreasing, i.e., $\frac{dv}{dx}(x) < 0$ (see the illustration in Fig.34). As such, it follows v is maximized on $[0, x_1]$ at x_0 - conversely, v is minimized on $(x_0, x_1]$ at x_1 . Now, write $s_0 = h \circ l_p(x_0) = (v(x_0), y(x_0), z(x_0))$, $s_1 = h \circ l_p(x_1) = (v(x_1), y(x_1), z(x_1))$ (see the illustration in Fig.34), and consider the half-planes $H_x = \{(v(x_1), y, z) | y \leq -z, y \geq -\frac{v(x_1)}{a}\}$, $H_y = \{(x, -\frac{v(x_1)}{a}, z) | x \geq \frac{v(x_1)}{a}\}$ - see the illustration in Fig.36. Now, let Q_3 denote the subset of $Q_2 = \{\dot{x} < 0\} \cap \{\dot{y} > 0\}$ (see the illustration in Fig.41) trapped between $\{\dot{x} = 0\}$, H_x and H_y (see the illustration in Fig.36). In particular, it follows $h \circ l_p(0, x_1)$ includes a curve γ , s.t. both $s_1, s_0 \in \gamma$ and γ begins and terminates at $H_x \cap \{\dot{x} = 0\}$.

Now, recall that given **any** initial condition $s \in l$, by $s \subseteq \overline{D_\alpha}$ it follows from Cor.3.0.1 that $f_p(s)$ is well-defined - i.e., its trajectory eventually returns to $\overline{D_\alpha} \subseteq \overline{U_p}$ in some finite time. However, since by definition $s' = h(s) \in l'$ lies on the flow line connecting $s, f_p(s)$ - which implies the forward trajectory of s' **also** eventually hits $\overline{D_\alpha}$. Consequentially, since H_y, H_x separate γ from $\overline{D_\alpha}$ in $\{\dot{x} \leq 0\}$ (see the illustration in Fig.5) it follows the forward trajectory of s' must hit $H_x \cup H_y$ transversely **before** hitting D_α . In other words, for every $s \in \gamma$ there exists some $t(s)$ s.t. $\gamma_s(t(s)) \in H_x \cup H_y$. In particular, it follows $C = \cup_{s \in \gamma} \gamma_s(t(s))$ forms a Jordan arc on $H_x \cup H_y$ whose endpoints are precisely $\gamma \cap H_x$ (see the illustration in Fig.36).

Now, let Ψ denote the surface made of flow lines connecting γ and C , and write $\dot{y}(s_0) = v_0$ (by the discussion above, $v_0 > 0$). Now, for $\epsilon \geq 1, \delta \in \mathbf{R}$ consider the half-plane $H_{\epsilon, \delta} = \{(x, -\frac{\epsilon x}{a} + \frac{v_0}{a} + \delta, z) | x, z \in \mathbf{R}\} \cap \{\dot{y} > 0\}$ (for $\epsilon = 1, \delta = 0$, we have $H_{1,0} = \{\dot{y} = v_0\} \cap \{\dot{y} > 0\}$). By the discussion above it follows that provided $\epsilon - 1, |\delta|$ are **both** sufficiently small, there exists a three-dimensional body B trapped between $\Psi, H_{\epsilon, \delta}$ and A_3 - in particular, $\overline{B} \subseteq \{\dot{x} \leq 0\} \cap \{\dot{y} \geq 0\}$, and lies away from both P_{In}, P_{Out} (see the illustration in Fig.37 and 38). Now, since by definition s_0 lies in the strip $S_{v_0} \subset H_{1,0}$ (see the discussion above) it follows that provided $\epsilon - 1, \delta$ are sufficiently small, F_p points inside B on $\partial B \cap H_{\epsilon, \delta}$. Similarly, since on A_3 the vector field F_p points into $\{\dot{x} < 0\}$, which implies that on $\partial B \cap A_3$ F_p points into B . Additionally, since F_p is tangent to Ψ it follows that all in all, no trajectory

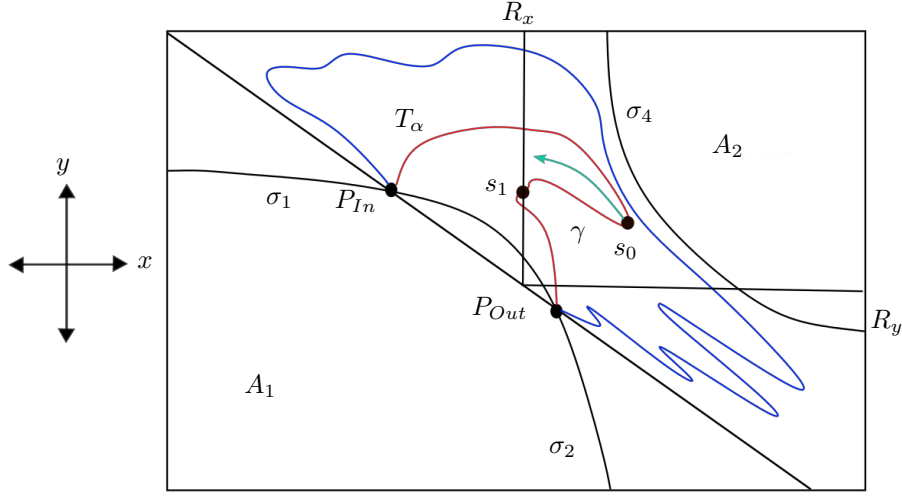


FIGURE 36. The curve γ , trapped between $R_x = H_x \cap \{\dot{x} = 0\}$ and $R_y = H_y \cap \{\dot{x} = 0\}$. The green line denotes a projection of a forward trajectory on γ to the plane $\{\dot{x} = 0\}$ - as can be seen, the trajectory flows in the positive y and negative x direction. We prove this scenario is impossible.

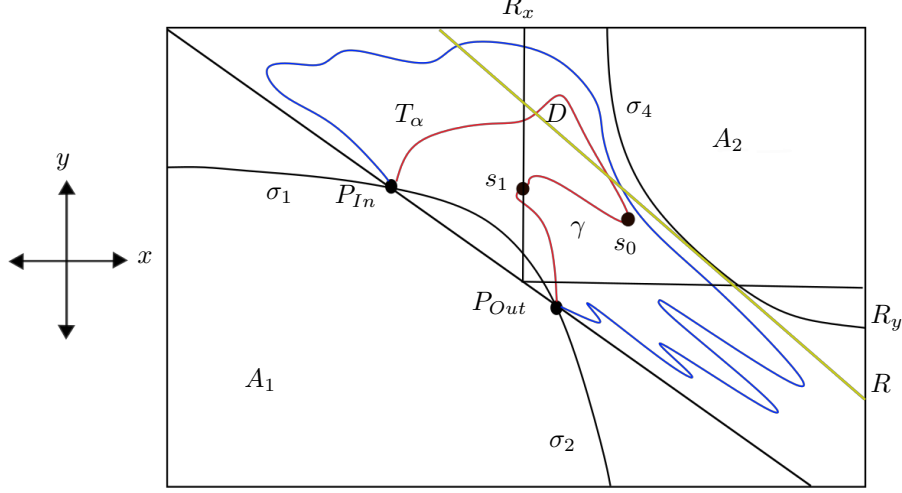


FIGURE 37. The yellow curve R denotes the intersection of $H_{\epsilon,\delta}$ with $\{\dot{x} = 0\}$ (for some ϵ, δ). As can be seen, provided ϵ, δ are suitably chosen, γ and R enclose a region, D . We prove this scenario generates a contradiction.

can escape \bar{B} under F_p (see the illustration in Fig.38).

From the discussion above we conclude \bar{B} must contain some F_p invariant set, A , s.t. A lies away from the fixed points. Moreover, $A \subseteq \{y \geq 0\}$. However, this implies that given any initial condition $s \in A$, its trajectory **cannot** intersect transversely with the cross-section U_p - which is a contradiction to Lemma 2.1. Consequentially, it follows x_0 is **not** strictly interior to $(0, c - ab]$ - i.e., $x_0 = c - ab$ and Lemma 3.1.2 now follows. \square

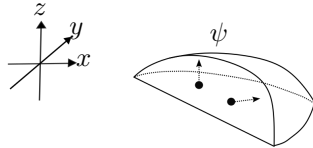


FIGURE 38. The body B , trapped between Ψ , A_3 and $H_{\epsilon,\delta}$ (for some sufficient ϵ, δ). As can be seen, F_p points into B on $\partial B \setminus \Psi$, thus implying a contradiction.

Having proven Lemma 3.1.2, we are now ready to prove the curve δ given by Prop.3.2 is inseparable from the fixed point P_{In} . To this end, given $s \in l$, define $t_2(s) < 0$ as the maximal time s.t. $\gamma_s(t_2(s)) \in \bar{T}_\alpha$. By Cor.3.1.1 and Lemma 3.8 we conclude that in order to analyze the topology of $f_p^{-1}(l)$ it would suffice to analyze the topology of the set $\Xi = \cup_{s \in l} \gamma_s(t_2(s))$ - this is so because by Lemma 3.8 $f_p^{-1}(l)$ is simply a homeomorphic copy of μ in \bar{D}_α

(i.e. $f_p^{-1}(l) = h^{-1}(\mu)$). As stated earlier, the analysis of $f_p^{-1}(l)$ using this method will take up most of the proof of Th.3.1 - we begin with the following fact:

Proposition 3.3. *Let $p \in P$ be a trefoil parameter, and let δ be as in Prop.3.2. Then, P_{In} and δ are in the boundary of the **same** component H_p of $D_\alpha \setminus f_p^{-1}(l)$ - and moreover, H_p is a topological disc (see the illustration in Fig.44).*

Proof. We prove Cor.3.3 by contradiction. That is, assume Cor.3.3 is mistaken, i.e., assume the fixed-point P_{In} and the curve δ lie in **different** components of $D_\alpha \setminus (f_p^{-1}(l) \setminus \delta)$, as illustrated in Fig.39. In order to generate a contradiction, we will apply Lemma 3.8 and Cor.3.1.2. To this end, recall the set $T_\alpha = h(D_\alpha)$ from Lemma 3.8 satisfies $\partial T_\alpha \cap \sigma_3 = \emptyset$ (see the illustration in Fig.40).

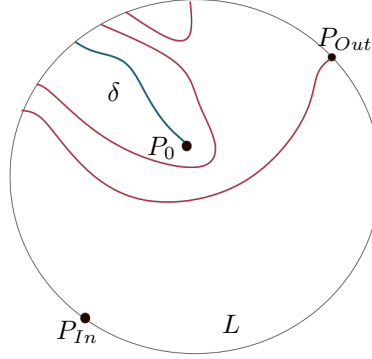


FIGURE 39. The red curves correspond to $f_p^{-1}(l) \setminus \delta$ - and in this scenario they separate P_{In} from δ . We will prove this is impossible. .

Now, set $\Delta = h(\delta)$. Since $p \in P$ is a trefoil parameter and because h from Lemma 3.8 is a homeomorphism, it follows Δ is a curve in T_α which connects $P_1 = h(P_0)$, a point on $\Theta \cap A_3$ and $\delta_1 = h(\delta_0)$, a point in l' (recall Θ denotes the bounded heteroclinic trajectory as in Def.2.4 - see the illustration in Fig.40). In particular, since P_0 is interior to D_α by Lemma 3.2, P_1 is interior to T_α . Now, denote by $(P_{In}, f_p(\delta_0)]$ the half-closed sub-arc on l connecting $P_{In}, f_p(\delta_0)$ - by Cor.3.1.1 and Prop.3.5, because $f_p(\delta) = (P_{In}, f_p(\delta_0)] \subset [P_{In}, \delta_0]$ it follows that given $s \in (P_{In}, f_p(\delta_0)]$, $\gamma_s(t_2(s)) \in \Delta$ (with t_2 as defined above). In particular, we have $\Delta = \cup_{s \in f_p(\delta)} \gamma_s(t_2(s))$.

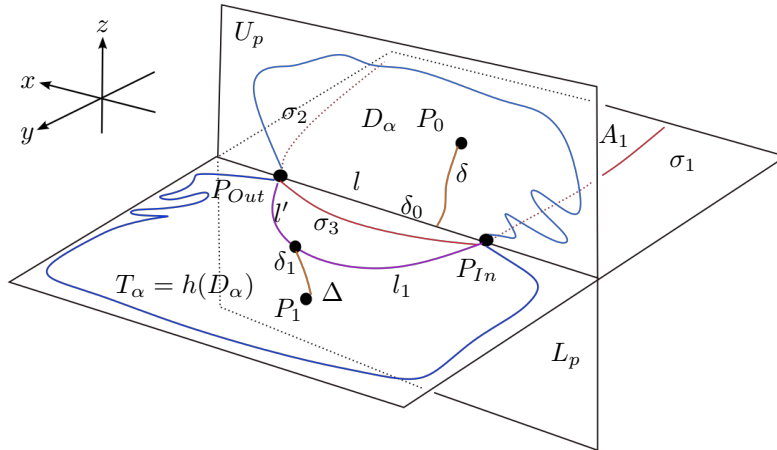


FIGURE 40. The sets $\Delta = h(\delta)$ and the points $\delta_1 = h(\delta_0)$, $P_1 = h(P_0)$.

Additionally, recall we assume δ, P_{In} are in different components of $\overline{D_\alpha} \setminus (f_p^{-1}(l) \setminus \delta)$. Therefore, set $\Xi = \cup_{s \in l} \gamma_s(t_2(s))$, and note $h^{-1}(\Xi) = f_p^{-1}(l)$. As such, by our assumption that P_{In} is separated from δ in D_α by $f_p^{-1}(l) \setminus \delta$, by Lemma 3.8 it follows Δ and P_{In} lie in different components of $\overline{T_\alpha} \setminus (\Xi \setminus \Delta)$ - see the illustration in Fig.41. That is, there exists a sub-arc $\gamma \subseteq \Xi$, $\gamma \cap \Delta = \emptyset$, separating P_{In}, Δ in T_α . Moreover, by definition, the flow lines connecting $l, \gamma \cup \Delta$ lie in the quadrant $Q_2 = \{\dot{x} \leq 0\} \cap \{\dot{y} > 0\}$ - see the illustration in Fig.41.

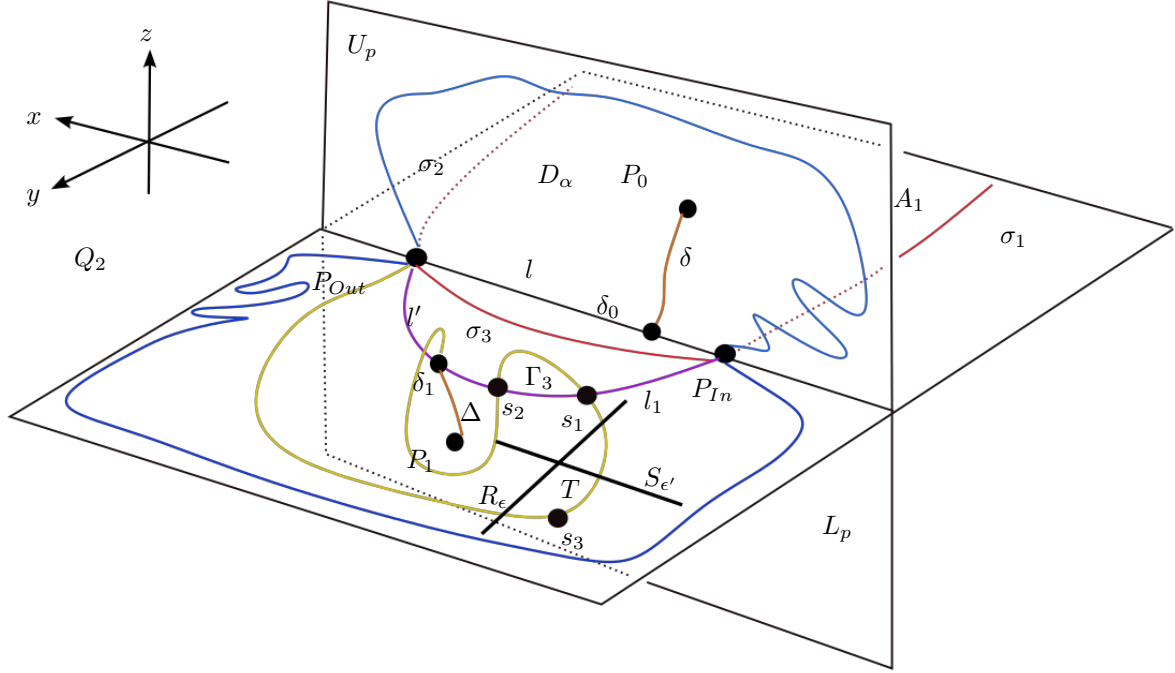


FIGURE 41. The first case - Γ is a connected arc in A_3 , with R_ϵ denoting $H_\epsilon \cap A_3$, $S_{\epsilon'} = S_{R-\epsilon'} \cap A_3$ and the yellow curve denotes Ξ (in this scenario, γ is the sub-curve connecting P_{Out}, s_1). We will prove this is impossible.

Now, let l_1 denote the sub arc on l' which connects $\delta_1 = h(\delta_0)$, P_{In} (see the illustration in Fig.40) consider the set $\eta = \cup_{s \in I} \gamma_s(t_2(s))$. By the discussion above, η includes at least two curves in $\overline{T_\alpha}$ - namely, γ, Δ (see the illustrations in Fig.41 and Fig.42) - moreover, both γ, Δ connect l_1 with interior points in T_α . In addition, γ connects **both** components of $l' \setminus \{\delta_1\}$ (see the illustration in Fig.41), and satisfies $P_{In} \notin \gamma$. Now, let I_1 denote the interval on $I \subseteq l$ s.t. $\gamma = \cup_{s \in I_1} \gamma_s(t_2(s))$, and let us denote by $L_1 = f_p(\delta)$. Now, set $J = l \setminus (I_1 \cup L_1)$, the arc separating I_1, L_1 in l , and write $\Gamma_3 = \cup_{s \in J} \gamma_s(t_2(s))$, $\Gamma = \cup_{s \in I} \gamma_s(t_2(s))$ (see the illustrations in Fig.41 and 42). There are now two possibilities to consider - namely, either Γ is a connected curve in $\overline{A_3}$ or not. We will show both are impossible - which would yield a contradiction to the existence of γ from which Prop.3.3 will follow.

We first rule out the possibility Γ is a connected curve in $\overline{A_3}$ (see the illustration in Fig.41) - and we do so by contradiction. We will generate a contradiction by constructing a bounded, three dimensional body $B \subseteq \{y \geq 0\}$ s.t. on ∂B , F_p is either tangent or points into B . Then, by using a similar argument to the one used to prove Lemma 3.1.2 we will derive a contradiction. Again, recall that for every $r < 0$, the set $\{x = r\}$ is given by the plane $\{(x, -y, y - r) | x, y \in \mathbf{R}\}$ (in particular, $\{x = r\}$ lies **above** $\{x = 0\}$). Conversely, for $R > 0$, the set $\{y = R\}$ is given by the plane $\{(x, -\frac{x}{a} + \frac{R}{a}, z) | x, z \in \mathbf{R}\}$ (see the discussion in the proof of Lemma 3.1.2). Additionally, recall that since the normal vector to $\{y = R\}$ is $N = (1, a, 0)$ it follows that given $v \in \{y = R\}$, $F_p(v) \bullet N \geq 0$ precisely on the half-plane curve $\{y = R\} \cap \{x \geq -R\}$ - and moreover, $F_p(v) \bullet N = 0$ precisely on the straight line $l_R = \{y = R\} \cap \{x = -R\}$. In particular, recall that for $a > 0$ we have $l_R \subseteq Q_2$, i.e., it lies **above** the plane $\{x = 0\}$ and **below** the plane $\{y = 0\}$ - again, see the discussion in the proof of Lemma 3.1.2 and the illustrations in Fig.41 and Fig.35.

Now, recall we denote by $\Gamma_3 = \cup_{s \in I_3} \gamma_s(t_2(s))$ and let $s_3 \in \Gamma_3$, $s_3 = (x_3, y_3, z_3)$ denote the point on Γ_3 which minimizes the x coordinate (recall $\Gamma = \Delta \cup \gamma \cup \Gamma_3$). As must be remarked, since γ separates P_{In} from Δ and since both intersect l' at points s_1, s_2 (respectively), setting $s_i = (x_i, y_i, z_i)$, $i = 1, 2$ by Lemma 3.1.2 it follows $x_2 \geq x_1$ and (see the illustration in Fig.41), hence, $x_2 \geq x_3$. Now, given $\epsilon > 0$ set $H_\epsilon = \{(x_3 - \epsilon, y, z) | y \geq y_3, z > -y_3\}$, and set $Y_R = \{y = R\}$. Since x_3 maximizes the x coordinate along Γ_3 , it follows that provided ϵ is chosen suitably, H_ϵ intersects transversely with $\gamma \cup \Gamma_3$ at some $s_4 = (x_4, y_4, z_4)$ (see the illustration in Fig.41). Now, since $s_4 \in \Gamma \cup \gamma$ it follows $s_4 \in \{y > 0\} \cap \{x = 0\}$, and in particular there exists some $R > 0$ s.t. $s_4 \in Y_R$. By the discussion above, there exists some strip on Y_R , $S_R = Y_R \cap \{0 \leq x \leq -R\}$ s.t. $s_4 \in S_R$ - and moreover, on that strip F_p points into $\{y > R\}$ (see the illustration in Fig.35).

by the boundedness and invariance of B_α under F_p it follows t_3 is always finite). Similar arguments to those used to prove Lemma 3.8 now imply the flow-lines which connect σ_3 to $\cup_{s \in \sigma_3} \gamma_s(t_3(s))$, denoted by Σ , lie strictly in the quadrant $Q_2 = \{\dot{x} \leq 0\} \cap \{\dot{y} > 0\}$ (that is, they all lie **above** the cross-section $\{\dot{x} = 0\}$). Now, similarly to the previous paragraph, we conclude there exists a bounded, three-dimensional body $B \subseteq \{\dot{y} \geq 0\}$ trapped between $\Phi, \Sigma, A_3, S_{R-\epsilon'}$ and H_ϵ (again, provided $\epsilon, \epsilon' > 0$ are suitably chosen - see the illustrations in Fig.42). Again, F_p is either tangent or points inside B throughout ∂B - therefore, similarly to the argument in the previous paragraph we again have a contradiction.

All in all, we have proven that the assumption δ is separated from P_{In}, P_{Out} by $f_p^{-1}(l) \setminus \delta$ implies the existence of a curve $\gamma \subseteq A_3 \cap \{\dot{y} > 0\}$, which separates Δ, P_{In} in T_α - and following that, we have shown that whatever the case, the existence of γ always yields a contradiction. As such, it follows δ, P_{In} are not separated in D_α by $f_p^{-1}(l) \setminus \delta$ - i.e., P_{In}, P_{Out}, δ are all subsets of ∂H_p , with H_p denoting some component of $D_\alpha \setminus f_p^{-1}(l)$. Finally, since no component of $f_p^{-1}(l)$ is strictly interior to $\overline{D_\alpha}$ (see the proof of Prop.3.2) we conclude H_p is simply connected - therefore, H_p is a topological disc and Prop.3.3 follows (see the illustration in Fig.48). \square

Remark 3.4. *An immediate consequence of Prop.3.3 and Prop.3.2 is that the function $f_p : \overline{H_p} \setminus \delta \rightarrow \overline{D_\alpha}$ is continuous.*

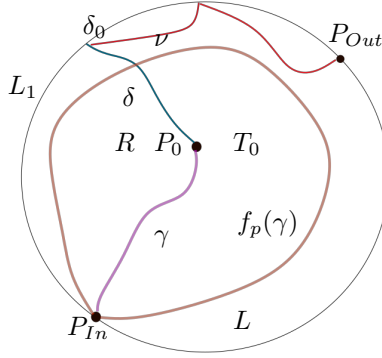


FIGURE 44. The regions R, T_0 and the topological disc H_p , bounded by δ , the red arc $\nu \subseteq f_p^{-1}(l)$ and $L_1 = [P_{In}, \delta_0]$. Additionally, γ and $f_p(\gamma)$ are also sketched. Again, the arc L denotes $\partial B_\alpha \cap U_p$.

Using Prop.3.3, we now conclude Stage I of the proof of Th.3.1 with a justification of the heuristic presented in page 31. To do so, note that by Prop.3.3, because H_p is a topological disc we can choose a curve $\gamma \subseteq H_p$ s.t. $\overline{\gamma} \cap \partial H_p = \{P_{In}, P_0\}$ - i.e., we have:

- γ connects the fixed point P_{In} and the point P_0 through H_p .
- $\gamma \cap f_p^{-1}(l) = \emptyset$.

Therefore, by Prop.3.2 f_p is **continuous** on γ . As previously remarked, since P_0 lies on the heteroclinic connection, f_p^{-1} is undefined at P_0 - and in particular, given any $s \in \overline{D_\alpha}$, $f_p(s) \neq P_0$. Additionally, since the trajectory of P_0 tends to the fixed-point P_{In} (in infinite time), we conclude $f_p(\gamma)$ is a closed loop in D_α which begins and terminates at P_{In} and separates $P_0, \partial D_\alpha$ - or, put simply, the heuristic given before the proof of Th.3.1 holds. In particular, we can impose $f_p(\gamma)$ on D_α as in Fig.27, Fig.28 and Fig.44. Namely, we have just proven:

Corollary 3.1.3. *Let $p \in P$ be a trefoil parameter and let $H_p \subseteq D_\alpha$ be as in Prop.3.3. Then, there exists a curve $\gamma \subseteq H_p$ satisfying:*

- $\overline{\gamma} \cap \partial H_p = \{P_{In}, P_0\}$.
- $\overline{f_p(\gamma)}$ is a closed loop in D_α , s.t. $\overline{f_p(\gamma)} \cap \partial D_\alpha = \{P_{In}\}$.
- $\overline{f_p(\gamma)}$ separates P_0 from $\partial D_\alpha \setminus \{P_{In}\}$ (see the illustration in Fig.44).

3.2. Stage II - analyzing the map $f_p : \overline{H_p} \rightarrow \overline{D_\alpha}$. Having proven Cor.3.1.3 we can almost begin proving the existence of chaotic dynamics for the first-return map f_p . However, before doing so we must first establish several technical results - which we will do now. To begin doing so, recall we denote by δ_0 the endpoint of the curve δ in the arc l (see the proof of Prop.3.2). From now on, let us denote by $[P_{In}, \delta_0)$ the component of $\delta \setminus \{\delta_0\}$ connecting P_{In}, δ_0 (see the illustration in Fig.44). Similarly, we often denote by $(P_{In}, \delta_0), [P_{In}, \delta_0]$ (and so on) the interior and closure of this arc, and given $s_1 \in (P_{In}, \delta_0)$ we denote by $[s_1, \delta_0)$ the sub-arc of $[P_{In}, \delta_0)$ connecting s_1, δ_0 . Let us further recall $\delta_0 \in \delta \cap l$ (see Prop.3.2). Therefore, by the definition of δ in Prop.3.2, by Lemma 2.5 and the definition of D_α as a subset of $\{\dot{y} = 0\}$ we conclude:

- $f_p(\delta_0) \in l$.
- The forward trajectory connecting $\delta_0, f_p(\delta_0)$ lies in $\{\dot{y} \geq 0\}$. In particular, \dot{y} vanishes alongside that flow-line **precisely** at $\delta_0, f_p(\delta_0)$

As a consequence, it follows the y -coordinate for $f_p(\delta_0)$ is strictly greater than that of δ_0 hence $\delta_0 \neq f_p(\delta_0)$ - as such, by $\{\delta_0\} = \delta \cap l$ (see Prop.3.2) it follows $f_p(\delta_0) \notin \delta$. As an immediate consequence of Prop.3.2 and this discussion, we have $f_p(\delta) = (P_{In}, f_p(\delta_0)) \subseteq [P_{In}, \delta_0]$. Using these ideas we first prove:

Lemma 3.9. *Let $p \in P$ be a trefoil parameter. Then, with previous notations, the following holds:*

- f_p is continuous on $[P_{In}, \delta_0]$ - that is, $f_p([P_{In}, \delta_0]) \cap \partial D_\alpha = \{P_{In}\}$. As a consequence, $[P_{In}, \delta_0] \subseteq \partial H_p$.
- $f_p([P_{In}, \delta_0])$ is a loop s.t. for $s \in [P_{In}, \delta_0]$, $s \rightarrow \delta_0$ we have $f_p(s) \rightarrow f_p^2(\delta_0)$ (see the illustration in Fig.68).
- $f_p([f_p(\delta_0), \delta_0])$ is a loop, winding once around P_0 - as a consequence, $P_0 \notin \overline{f_p(H_p)}$.

Proof. Let γ denote the curve from Cor.3.1.3. By Cor.3.1.3 $\overline{\gamma} \cap [P_{In}, \delta_0] = \{P_{In}\}$, and $\overline{f_p(\gamma)}$ is a closed loop in $\overline{H_p}$ satisfying $\overline{f_p(\gamma)} \cap \partial D_\alpha = \{P_{In}\}$ (that is, f_p is both continuous and injective on γ - see Cor.3.1.3 and the illustration in Fig.44). Now, as shown in the proof of Prop.3.2 f_p is continuous on some neighborhood of the saddle-focus P_{In} in $\overline{D_\alpha}$ - i.e., points on (P_{In}, δ_0) sufficiently close to P_{In} are mapped inside D_α . Motivated by this discussion, let us denote by T_0 the component of $D_\alpha \setminus f_p(\gamma)$ s.t. $P_0 \in T_0$ (see the illustration in Fig.44) - by this discussion and by the orientation-preserving properties of the flow, it follows that given $s \in [P_{In}, \delta_0]$, $s \neq P_{In}$ sufficiently close to P_{In} , $f_p(s) \in T_0$.

However, since by Cor.3.1.3 we have $f_p(\gamma) \cap f_p([P_{In}, \delta_0]) = \{P_{In}\}$ we conclude $f_p(P_{In}, \delta_0) \subseteq T_0$ - and since $\overline{T_0} \cap \partial D_\alpha = \{P_{In}\}$, by $P_0 \notin [P_{In}, \delta_0]$ (see Lemma 3.2) we conclude $\partial T_0 \cap f_p(P_{In}, \delta_0) = \emptyset$ which implies $f_p(P_{In}, \delta_0)$ is strictly interior to D_α , as illustrated in Fig.68. Or, put simply, because T_0 separates $l, f_p([P_{In}, \delta_0])$ we have $f_p([P_{In}, \delta_0])$ lies away from l - which implies f_p is continuous on $[P_{In}, \delta_0]$ (see Prop.3.2). By the continuity of ∂H_p , by $P_{In} \in \partial H_p$ and by Prop.4.0.1 it follows $[P_{In}, \delta_0] \subseteq \partial H_p$ (see the illustration in Fig.44). Therefore, all that remains to conclude the proof of Lemma 3.9 is to show two things:

- For $x \in [P_{In}, \delta_0]$, $x \rightarrow \delta_0$, we have $f_p(x) \rightarrow f_p^2(\delta_0)$.
- $P_0 \notin \overline{f_p(H_p)}$, and $f_p(f_p(\delta_0), \delta_0)$ winds once around P_0 .

We first prove that for $x \in [P_{In}, \delta_0]$, $x \rightarrow \delta_0$, we have $f_p(x) \rightarrow f_p^2(\delta_0)$. To do so, recall we denote by $[P_{In}, f_p(\delta_0)]$ the closed arc on l connecting $P_{In}, f_p(\delta_0)$ (see the illustration in Fig.68) - moreover, by the discussion above, $[P_{In}, f_p(\delta_0)] \subset [P_{In}, \delta_0]$, which implies f_p is continuous on $[P_{In}, f_p(\delta_0)]$. Moreover, by Prop.3.2, $(P_{In}, f_p(\delta_0)) = f_p(\delta \setminus \{P_0\})$ - therefore, since by Lemma 2.5 the forwards-trajectory of $f_p(\delta_0)$ enters $\{\dot{y} > 0\}$ immediately upon leaving $f_p(\delta_0)$, similar arguments to those used in the discussion preceding Lemma 3.9 again imply the y -coordinate of $f_p^2(\delta_0)$ must be strictly greater than that of $f_p(\delta_0)$. Since $f_p(\delta_0) \notin \delta$, we conclude $f_p^2(\delta_0) \notin f_p(\delta \setminus \{P_0\})$, i.e., $f_p^2(\delta_0) \notin (P_{In}, f_p(\delta_0))$. Recalling we parameterize l by $(x, -\frac{x}{a}, \frac{x}{a})$, $x \in (0, c - ab)$, because the y -coordinate increases along l when $x \rightarrow P_{In}$, $x \in l$, it follows that since $f_p^2(\delta_0)$ **cannot** hit $(P_{In}, f_p(\delta_0))$ it **must** hit D_α transversely - as such, with previous notations we conclude $f_p^2(\delta_0) \in T_0$ (with T_0 denoting the component of $D_\alpha \setminus f_p(\gamma)$ s.t. $P_0 \in T_0$).

As consequence, because $f_p^2(\delta_0)$ is the first transverse intersection point between the forward-trajectory of δ_0 and D_α , by the continuity of the flow $f_p^2(\delta_0)$ must lie on $f_p([P_{In}, \delta_0])$ - therefore, we conclude that given $x \in [P_{In}, \delta_0]$, $x \rightarrow \delta_0$ we have $f_p(x) \rightarrow f_p^2(\delta_0)$. In particular, $\overline{f_p([P_{In}, \delta_0])}$ includes a closed loop, corresponding to $\overline{f_p([f_p(\delta_0), \delta_0])}$ - in particular, this closed loop winds around P_0 (see the illustration in Fig.68).

All in all, to conclude the proof of Lemma 3.9 it remains to show $P_0 \notin \overline{f_p(H_p)}$, and that $\overline{f_p([f_p(\delta_0), \delta_0])}$ winds around P_0 once. To do so, consider the open region R in H_p bounded by δ, γ and $[P_{In}, \delta_0]$ (see the illustration in Fig.44) - since P_0 has no preimages in $\overline{D_\alpha}$, it immediately follows $P_0 \notin \overline{f_p(R)}$. As such, $f_p(R)$ is trapped between $f_p([P_{In}, \delta_0])$ and $f_p(\gamma)$ - hence, by the continuity of f_p on R , $f_p(P_{In}, \delta_0)$ must wind around P_0 precisely once. Therefore, by the orientation-preserving properties of the flow we conclude that in addition $f_p(\overline{H_p} \setminus R)$ and P_0 lie in different components of $\overline{D_\alpha} \setminus f_p(\gamma)$ (see Fig.68) - which, by $\overline{H_p} = R \cup (\overline{H_p} \setminus R)$ implies that all in all $P_0 \notin \overline{f_p(H_p)}$, and Lemma 3.9 now follows. \square

To continue, let us recall that P_0 is the **unique** intersection point of the bounded heteroclinic trajectory with $\overline{D_\alpha}$ (see Def.2.4 and Prop.3.2) - additionally, as proven in Lemma 3.0.1, given $x \in \overline{D_\alpha}$ we have $f_p(x) \neq P_0$. To continue, let D_0 denote the component of $\overline{D_\alpha} \setminus f_p([P_{In}, \delta_0])$ s.t. $P_0 \in D_0$ (see the illustration in Fig.68). By Lemma 3.9, D_0 is a Jordan domain and P_0 is strictly interior to it. Using this observation, we now prove:

Corollary 3.1.4. *Let $p \in P$ be a trefoil parameter, and let l be as above. Then, the set $f_p^{-1}(l)$ is connected - in particular, it is a connected curve in $\overline{D_\alpha}$ (see the illustration in Fig.48).*

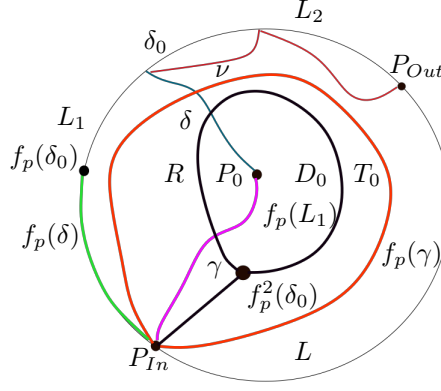


FIGURE 45. The image of $L_2 = [P_{In}, \delta_0]$ under f_p inside the topological disc H_p - in particular, it encloses an open Jordan domain D_0 s.t. $P_0 \in D_0$. Moreover, $f_p(L_2)$ lies inside H_p , the topological disc on D_α bounded by L_1, L_2, δ and ν (with L_1, L_2, ν as in Fig.44). L_2 denotes $[\delta_0, P_{Out}]$, the arc connecting δ_0, P_{Out} on l .

Proof. Before proving Cor.3.1.4, we first study the behavior of F_p on the set $l \subseteq \partial D_\alpha$. To do so, recall that given $s \in \mathbf{R}^3$, we parameterize its trajectory by $\gamma_s, \gamma_s(0) = s$. Additionally, recall we denote by (P_{In}, δ_0) the component of $l \setminus \{\delta_0\}$ connecting P_{In}, δ_0 . Now, for every $s \in l$, define $t_4(s) > 0$ to be the minimal positive time s.t. $\gamma_s(t_4(s))$ is a **transverse** intersection point between $\gamma_s, \overline{D_\alpha}$ (by Lemma 2.1 and Cor.3.0.1, $t_4(s)$ is well-defined for every $s \in l$). Using a similar reasoning to the one used in the proof of Lemma 3.8, given an initial condition $s \in l$ by Lemma 2.5 we conclude its forward-trajectory leaves s and flows through the half-space $\{\dot{y} \geq 0\}$ until hitting D_α at some interior point $\gamma_s(t_4(s))$. As must be stated, $\gamma_s(t_4(s))$ need not coincide with $f_p(s)$, as the flow-line γ_s **can** hit $\overline{D_\alpha}$ tangently more than once before hitting $\overline{D_\alpha}$ transversely at $\gamma_s(t_4(s))$. For example, as shown in the proof of Lemma 3.9, on the one hand $f_p(\delta_0) \in l$, while on the other $f_p^2(\delta_0)$ is strictly interior to $\overline{D_\alpha}$ (see the illustration in Fig.68). Therefore, we conclude, $\gamma_{\delta_0}(t_4(\delta_0)) = f_p^2(\delta_0) \neq f_p(\delta_0)$.

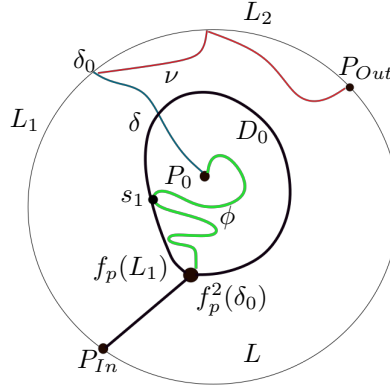


FIGURE 46. In this image, the set Ψ is the union $\phi \cup f_p(L_1)$, with $L_1 = [P_{In}, \delta_0]$. As can be seen, ϕ is tangent to $f_p(L_1)$ at both $s_1, f_p^2(\delta_0)$. L_2 denotes $[\delta_0, P_{Out}]$, the arc connecting δ_0, P_{Out} on l , while $\nu = f_p^{-1}(l) \setminus \delta$.

Let us now consider the set $\Psi = \cup_{s \in l} \gamma_s(t_4(s))$. The set Ψ is composed of curves in $\overline{D_\alpha}$ whose **closures** connect interior points of D_α to l (by definition, $\Psi \cap l = \emptyset$). As must be stated, any given component ψ of Ψ , ψ is a curve which is possibly self-intersecting - however, all such self-intersections of ψ are points at which the curve ψ is tangent to itself (see the illustration in Fig.46). Additionally, for every component ψ in Ψ there exists some connected sub-arc $I \subseteq l$ s.t. $\forall s \in I, \gamma_s(0, t_4(s))$ connects $s, \gamma_s(t_4(s))$ through $\{\dot{y} \geq 0\}$. Conversely, given $\nu \in \psi$, there exists **at least** one $s \in I$ s.t. γ_s connects s, ν through $\{\dot{y} \geq 0\}$. In particular, by the Existence and Uniqueness Theorem it follows that points at which ψ is tangent to itself corresponds to points $s \in I$ at which $\gamma_s(t_4(s)) \neq f_p(s)$, i.e., $\gamma_s(t_4(s)) = f_p^k(s)$ for some $k > 1$, and moreover, for every $0 < j < k, f_p^j(s) \in l$ (that is, γ_s is tangent to $\overline{D_\alpha}$ at $f_p^j(s)$). Hence, it is immediate that t_4 is continuous on the interval I corresponding to ψ .

Now, recall $p \in P$ is a trefoil parameter, and that P_0 lies on the bounded heteroclinic connection Θ (see Def.2.4) - therefore, a similar argument to the one used to prove Prop.3.2 implies there exists a component ψ of Ψ , which is

a curve beginning at P_0 , s.t. for every $s \in l$ sufficiently close to P_{Out} , $\gamma_s(t_4(s)) \in \psi$ (see the illustration in Fig.46). In particular, $\bar{\psi}$ is a curve which connects P_0 and some unique point P_1 on l . We now claim $P_1 = P_{In}$ - to see why this is so, recall that as mentioned earlier, with previous notations $D_\alpha \setminus f_p(P_{In}, \delta_0)$ includes a Jordan domain D_0 s.t. P_0 is interior to D_0 (see the illustration in Fig.68). By Lemma 3.9 we therefore conclude ∂D_0 separates P_0 and l .

By Lemma 3.9 it now follows that given $s \in (P_{In}, \delta_0)$, $f_p(s)$ is strictly interior to D_α , which implies $f_p(s)$ is a transverse point of intersection between γ_s and the cross-section \bar{D}_α . As such, given $s \in (P_{In}, \delta_0)$ it follows $f_p(s) = \gamma_s(t_4(s))$ - and as remarked earlier, $f_p^2(\delta_0) = \gamma_{\delta_0}(t_4(\delta_0))$. Therefore, since ψ connects P_0 and l , because ∂D_0 separates P_0 and l and since $\partial D_0 \subseteq f_p(P_{In}, \delta_0) = \cup_{s \in (P_{In}, \delta_0)} \gamma_s(t_4(s))$, it follows $f_p(P_{In}, \delta_0) \subseteq \psi$ - moreover, by the discussion above, $\psi \setminus f_p(P_{In}, \delta_0)$ cannot intersect transversely with $f_p(P_{In}, \delta_0)$. Therefore, by the uniqueness of P_1 , it therefore follows $P_1 = P_{In}$. Now, recall that by the discussion above it follows there exists a maximal arc $I \subseteq l$ s.t. every $s \in I$ has a forward-trajectory γ_s connecting $s, \gamma_s(t_4(s))$. Since both $P_0, P_{In} \in \bar{\psi}$, it follows $I = l$, and that t_4 is continuous on l - in particular, $\Psi = \psi$.

Having proven $\Psi = \psi$, we can finally prove Cor.3.1.4. To do so, let us first recall that per Lemma 3.3, the topological disc H_p is the component of $\bar{D}_\alpha \setminus f_p^{-1}(l)$ s.t. P_{In}, P_{Out} and δ are all subsets of ∂H_p (see Prop.3.3 and the illustration in Fig.44). Additionally, with the notations of Prop.3.9 recall we denote by R the subdomain of H_p bounded by $\delta, [P_{In}, \delta_0]$ and the curve γ , given by Cor.3.1.3 (see the illustration in Fig.44). Finally, recalling we denote by T_0 the component of $\bar{D}_\alpha \setminus f_p(\gamma)$ s.t. $P_0 \in T_0$ (see the proof of Lemma 3.9 and the illustrations in Fig.44 and Fig.68). As shown in the proof of Lemma 3.9, we have $f_p(P_{In}, \delta_0) \subseteq T_0$ (see the illustration in Fig.44) - therefore, it follows $\psi \subseteq T_0$ (see the illustration in Fig.47).

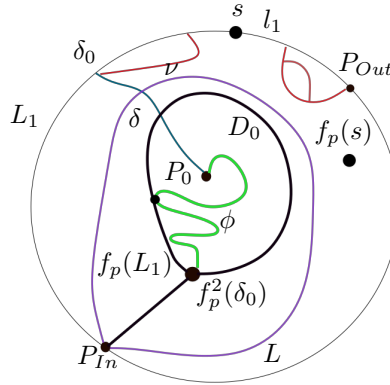


FIGURE 47. The red arcs correspond to $\nu = f_p^{-1}(l) \setminus \delta$ - as can be seen, ν is disconnected, thus there exists an arc $l_1 \subseteq l \cap \partial H_p$. Moreover, $\bar{\Psi} = \phi \cup f_p(L_1) \subseteq T_0$, with T_0 denoting the area trapped inside the purple loop, corresponding to $f_p(\gamma)$ (see Cor.3.1.3). In particular, there exists a point $s \in l_1$ s.t. $f_p(s) \notin \bar{T}_0$ - which generates a contradiction.

Having made these remarks, we are now ready to conclude the proof of Cor.3.1.4. Namely, we now use the facts above to prove $f_p^{-1}(l)$ is connected in \bar{D}_α - to do so, assume this is not the case, i.e., that $f_p^{-1}(l)$ includes at least two components (one of which has to include the curve δ_0 - see the illustration in Fig.47). Since l is a curve, every component of $f_p^{-1}(l)$ in \bar{D}_α is also a curve (which is possibly a singleton) - by Prop.3.2 and the continuity of the flow, if γ is a component of $f_p^{-1}(l)$ which **does not** include the curve δ , the curve γ does not have an end-point strictly interior to D_α . Additionally, since we assume $f_p^{-1}(l)$ is disconnected in \bar{D}_α , $f_p^{-1}(l)$ **cannot** separate the arc $l_1 = l \setminus [P_{In}, \delta_0]$ from the interior of H_p - i.e. there exists a point $s \in l_1 \cap \partial H_p$ (see the illustration in Fig.47).

Now, recall we denote by R the region in H_p bounded by $[P_{In}, \delta_0]$, δ , and the curve γ from Cor.3.1.3. Since $s \in l_1 \cap \partial H_p$, by $\bar{R} \cap l = [P_{In}, \delta_0]$ we conclude $\bar{R} \cap l_1 = \emptyset$, hence $s \notin \bar{R}$ - therefore, by the arguments found at the end of the proof Lemma 3.9 it follows $\bar{f}_p(R)$, $f_p(s)$ lie in different components of $D_\alpha \setminus f_p(\gamma)$ - T_0 and T_1 , respectively (see the illustration in Fig.47). In particular, $\bar{D}_0 \subseteq T_0$ (see the illustration in Fig.47). By the discussion above and with previous notations, we must have $s \in \Psi$, and as proven earlier, $\Psi \subseteq \bar{D}_0$ - by $\bar{D}_0 \cap T_1 = \emptyset$, we have a contradiction - as a consequence, $f_p^{-1}(l)$ is connected, hence, since l is a curve so is $f_p^{-1}(l)$ and Cor.3.1.4 now follows (see the illustration in Fig.48). \square

We now use both Cor.3.1.4 and ideas from the proof of Prop.3.3 to prove the following technical (yet useful) fact. To do so, denote by $[\delta_0, P_{Out}]$ the closed arc on l connecting P_{Out}, δ_0 - conversely, recall we denote by $[P_{In}, \delta_0]$ the

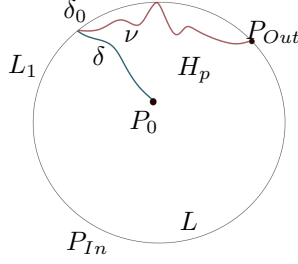


FIGURE 48. The cross-section H_p , homeomorphic to a slit disc, bounded by $L_1 = [P_{In}, \delta_0]$, $f_p^{-1}(l) = \delta \cup \nu$ and $L = \partial B_\alpha \cap U_p$. By Prop.3.3, $f_p^{-1}(l)$ is a curve connecting P_{Out}, δ_0 .

semi-open arc on l connecting P_{In}, δ_0 (see the illustration in Fig.68). We now prove the following list of properties of $f_p^{-n}(l)$, $n \geq 2$, which generalize Cor.3.1.4 and Prop.3.3. As we will see in Stage III, Prop.3.4 (and its corollaries) would form a major tool in proving the existence of symbolic dynamics for the first-return map in H_p .

Proposition 3.4. *Let $p \in P$ be a trefoil parameter and let H_p be as in Prop.3.3. Furthermore, denote by $\Delta_0 = f_p^{-1}(l)$ - then, the following holds:*

- For $n \geq 2$, $f_p^{-n}(l) \cap \overline{H_p}$ includes a component $\Delta_{n-1} \subseteq \overline{H_p}$ s.t. Δ_{n-1} is a curve connecting $P_{Out}, f_p^{-n+1}(\delta_0)$ and some point $\delta_{n-1} \in [P_{In}, \delta_0]$ (see the illustration in Fig.52).
- For every $n > 0$, Δ_n includes a curve $\Gamma_n \subseteq \Delta_n$ s.t. $f_p^{n+1}(\Gamma_n) = [\delta_0, P_{Out}]$.
- For $n \geq 1$, $\Delta_n \cap \delta = \emptyset$ (see the illustration in Fig.52).
- With the same notations, for every $n, k \geq 0$, $\Gamma_n \subseteq f_p^k(\overline{H_p})$ - and in particular, $f_p^{-n}(\delta_0) \in f_p^k(\overline{H_p})$.
- For every $n \geq 1$, $f_p^{-n+1}(\delta_0) \in \Delta_n \cap \Delta_{n-1}$.
- Write $\mu_n = \Delta_n \cap f_p^{-n}(\delta)$ - then, given $n \neq k$, we have $\mu_n \cap \mu_k = \emptyset$.

Proof. Before proving Cor.3.4, let us first make some general remarks. To begin, note that since the saddle-focus P_{Out} is a fixed-point, for every $n > 0$ we have $f_p^{-n}(P_{Out}) = P_{Out}$. Additionally, recalling P_{Out} is a saddle-focus with two-dimensional stable manifold W_{Out}^s transverse to the cross-section $U_p = \{\dot{y} = 0\} \cap \{\dot{x} = 0\}$ at P_{Out} , by the definition of $D_\alpha \subseteq U_p$ in Section 2.2 we conclude that a similar argument to the proof of Cor.3.0.2 implies that for every $n > 0$, $f_p^{-n-1}([\delta_0, P_{Out}]) \cap \overline{D_\alpha}$ includes a component Δ_n s.t. $P_{Out} \in \Delta_n$ (see the illustration in Fig.49). Moreover, by the definition of H_p in Cor.3.3 it follows that for every n , at least locally around P_{Out} the curve Δ_n lies in $\overline{H_p}$. With these remarks, we can now begin proving Cor.3.4 - and we do so by induction on n . Namely, we first prove that given $n \geq 1$ the curve Δ_n satisfies the following:

- For $n \geq 1$, $\Delta_n \cap \delta = \emptyset$.
- Δ_n is a curve in $\overline{H_p}$ connecting $P_{Out}, f_p^{-n}(\delta_0)$.
- For every $n > 0$, Δ_n includes a curve $\Gamma_n \subseteq \Delta_n$ s.t. $f_p^{n+1}(\Gamma_n) = [\delta_0, P_{Out}]$.
- Δ_n connects P_{Out} with some $\delta_n \in [P_{In}, \delta_0]$.

As we will see, these four facts will imply the entire list of properties in Prop.3.4. For the base of the induction, consider $n = 1$ - namely, we will now prove:

- $\Delta_1 \subseteq f_p^{-2}(l) \cap \overline{H_p}$.
- Δ_1 connects $P_{Out}, f_p^{-1}(\delta_0)$ and some $\delta_1 \in [P_{In}, \delta_0]$.
- Δ_1 contains a curve Γ_1 s.t. $f_p^2(\Gamma_1) = [\delta_0, P_{Out}]$.
- $\Delta_1 \cap \delta = \emptyset$.

We begin with $\Delta_1 \cap \delta = \emptyset$. To do so, let us first remark that by its definition in Prop.3.2, we have $\delta_0 \in l \cap f_p^{-1}(l)$ from which it follows $f_p^{-1}(\delta_0) \in f_p^{-1}(l) \cap f_p^{-2}(l)$. With previous notations, since by Prop.3.2 we have $f_p(\delta) \subseteq [P_{In}, \delta_0]$, by Cor.3.9 it follows $f_p^2(\delta)$ is interior to D_α - i.e., $f_p^2(\delta) \cap l = \emptyset$. Hence, $\delta \cap f_p^{-2}(l) = \emptyset$ - which, by $\Delta_1 \subseteq f_p^{-2}(l)$, implies both $f_p^{-1}(\delta_0) \notin \delta$ and $\delta \cap \Delta_1 = \emptyset$.

For the other properties of Δ_1 we need to work a little harder. To do so, first, recall the homeomorphism $h : \overline{D_\alpha} \rightarrow \overline{T_\alpha} \subseteq A_3 \cap \{\dot{y} \geq 0\}$ from Lemma 3.8, and define $\nu_1 = h(\Delta_1)$ - by the definitions for both h and ρ_1 it follows there exists a connected sub-arc on $f_p^{-1}(l) \subseteq \overline{D_\alpha}$, I_1 , s.t. $P_{Out} \in \overline{I_1}$ and the **backwards** trajectory of every $s \in I_1$ connects with some $x \in \Delta_1$ (see the illustration in Fig.49) - moreover, the flow-line connecting $s \in f_p^{-1}(l)$, $x \in \Delta_1$ lies strictly inside the quadrant $Q_2 = \{\dot{x} < 0\} \cap \{\dot{y} > 0\}$ (that is, above the cross-section $\{\dot{x} = 0\}$ - see the illustration in Fig.30). Writing $L' = h(f_p^{-1}(l))$, a similar argument proves that given any initial condition $s \in l$, its backwards trajectory is connected to some $x \in L'$ by its backwards trajectory - and again, the flow-line connecting s, x lies strictly inside Q_2 (see the illustration in Fig.49).

As such, the collection of flow-lines connecting l, L' form a surface S , which stretches from l to L' through Q_2 - and conversely, the flow-lines connecting I_1 to ν_1 also form a surface, β_1 . By Prop.3.4 $f_p^{-1}(l)$ is a connected arc in $\overline{D_\alpha}$, which is (at most) tangent to l at $f_p^{-1}(l) \cap l$ - therefore, it follows the surface β_1 **cannot** intersect S transversely. That is, β_1 slides over S , thus implying ν_1 is **at most** tangent to L' . As a consequence, because $\Delta_1 = h^{-1}(\nu_1)$, we conclude Δ_1 never intersects $f_p^{-1}(l)$ transversely as well. Therefore, since ∂H_p is composed of $f_p^{-1}(l)$, the arc $L = \partial B_\alpha \cap U_p$ and the arc $[P_{I_n}, \delta_0)$ (see Cor.4.0.1 and Cor.3.1.4), we conclude $\Delta_1 \subseteq \overline{H_p}$ (see the illustration in Fig.49).

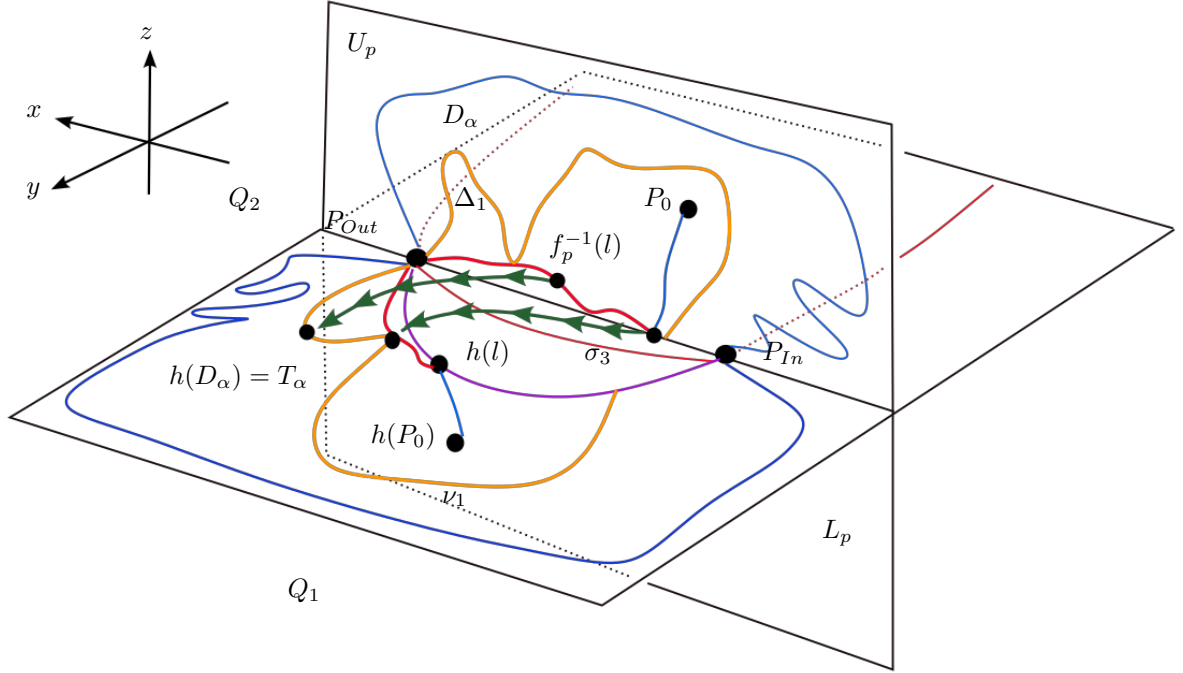


FIGURE 49. The **backward** trajectories connecting points in l with points in $h(f_p^{-1}(l))$ and points from $f_p^{-1}(l)$ with $h(\Delta_1) = \nu_1$. Both flow lines lie strictly in the quadrant $Q_2 = \{\dot{x} < 0\} \cap \{\dot{y} > 0\}$. L' is the union of the blue and red arcs on T_α .

We now claim Δ_1 is a curve connecting $P_{Out}, f_p^{-1}(\delta_0)$ in $\overline{H_p}$ (thus almost completing the base of the induction). To this end, assume this is not the case, i.e., assume that the curve Δ_1 **does not** connect $P_{Out}, f_p^{-1}(\delta_0)$ in $\overline{H_p}$ - as such, ν_1 **does not** connect $P_{Out}, h(f_p^{-1}(\delta_0))$ in $h(\overline{H_p})$. Now, recall the curve δ from Prop.3.2 - by $\Delta_1 \cap \delta = \emptyset$ we have $h(\delta) \cap \nu_1 = \emptyset$. Since $f_p^{-1}(l)$ separates the arc $[\delta_0, P_{Out}] \subseteq l$ from Δ_1 (and since $\Delta_1, f_p^{-1}(l)$ are **at most** tangent) it follows the curve ν_1 cannot intersect $h([\delta_0, P_{Out}])$ transversely - which implies ν_1 must terminate at $l' \setminus h(\delta_0, P_{Out})$, i.e., ν_1 connects P_{Out} with $l' = h(l)$ through $h(\overline{H_p})$, and it does so without **ever** touching $h(f_p^{-1}(\delta_0))$ (see the illustration in Fig.50).

To continue, since $f_p^{-1}(\delta_0) \in f_p^{-1}(l) \cap f_p^{-2}(l)$, because we assume $f_p^{-1}(\delta_0) \notin \Delta_1$ a similar argument to the one above proves there exists an arc $\rho_2 \subseteq f_p^{-2}(l)$ connecting $f_p^{-1}(\delta_0), l$ s.t. $\rho_2 \subseteq f_p^{-2}(l)$ - by $\delta \cap f_p^{-2}(l) = \emptyset$ we have $\rho_2 \cap \delta = \emptyset$. Now, setting $\nu_2 = h(\rho_2)$, a similar argument to the one used in the proof of Prop.3.3 (with ν_1, ν_2 taking the respective roles of γ, Δ) implies there exists a compact, three-dimensional body B , s.t. $P_{In}, P_{Out} \notin \overline{B}$ that no forward trajectory can escape. This is a contradiction to Lemma 2.1, therefore we conclude Δ_1 is a curve in $\overline{H_p} \cap f_p^{-2}(l)$ connecting $P_{Out}, f_p^{-1}(\delta_0)$. As such, by the continuity of the flow it immediately follows there exists a curve $\Gamma_1 \subseteq \Delta_1$, connecting $P_{Out}, f_p^{-1}(\delta_0)$ s.t. $f_p^2(\Gamma_1) = [\delta_0, P_{Out}]$.

As such, all in all, to complete the proof for the base of the induction it remains to prove Δ_1 connects P_{Out} and some $\delta_1 \in [P_{In}, \delta_0)$. To do so, recall we already proved $\Gamma_1 \subseteq \Delta_1 \subseteq H_p$ - which implies the sub-arc of $f_p^{-1}(l)$, $\Gamma_0 = f_p^{-1}([\delta_0, P_{Out}])$ lies in $f_p(H_p)$ (see the illustration in Fig.51). As a consequence, since by Cor.3.1.3, Prop.4.0.1 and Cor.3.1.4 $f_p(H_p)$ is the banana-shaped figure seen in Fig.51, by $P_0 \notin \overline{H_p}$ it follows $f_p(H_p)$ includes a sub-arc Ψ , s.t. both $\Gamma_0 \subset \Psi$ and $\Phi = \Psi \setminus \Gamma_0$ is an arc on δ , connecting $f_p([P_{In}, \delta_0))$ and δ_0 (see the illustration in Fig.51) - in particular, we conclude $\Psi \subseteq f_p(\Delta_1) \subseteq f_p^{-1}(l)$. Therefore, it trivially follows $f_p^{-1}(\Psi) \subseteq \Delta_1$ - hence, since $\Psi \cap f_p([P_{In}, \delta_0)) \neq \emptyset$ it follows $\Delta_1 \cap [P_{In}, \delta_0) \neq \emptyset$, i.e., there exists some δ_1 , the first point of intersection between

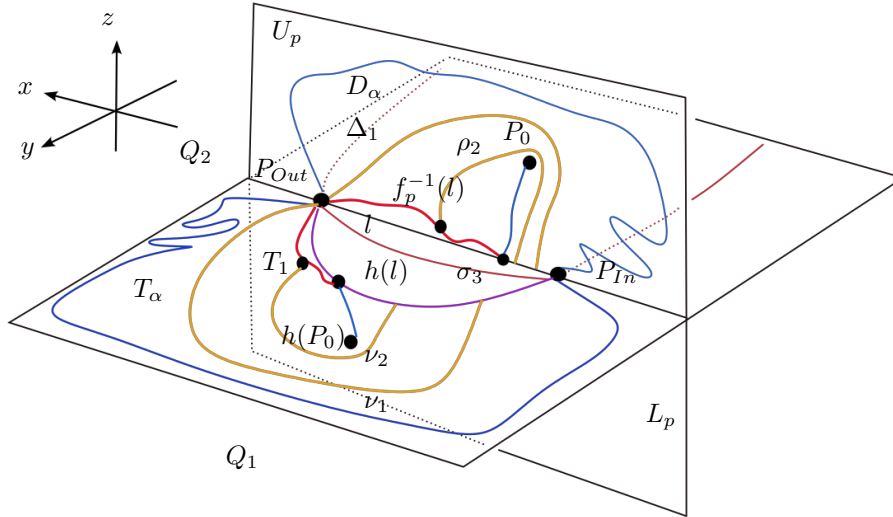


FIGURE 50. The curves Δ_1, ρ_2 and ν_1, ν_2 . The existence of ν_2 generates a contradiction. The point T_1 denotes $h(f_p^{-1}(\delta_0))$.

Δ_1 and $[P_{In}, \delta_0)$ (see the illustration in Fig.51). Therefore, the base of the induction now follows.

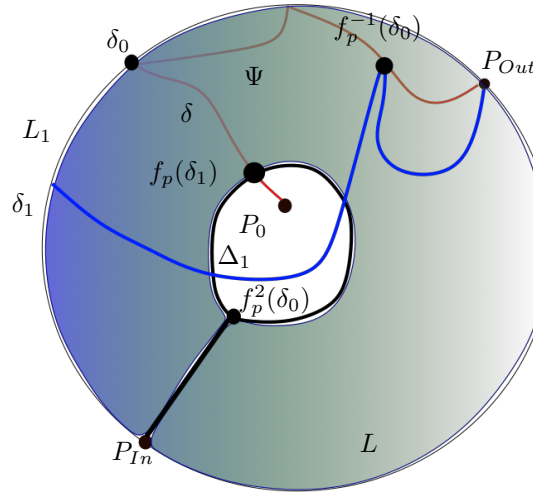


FIGURE 51. $f_p(H_p)$, denoted by the shaded region inside the cross-section D_α . As can be seen, the red curve inside $f_p(H_p)$, $\Psi = f_p(\Delta_1)$, connects P_{Out} and some $f_p(\delta_1) \in f_p([P_{In}, \delta_0])$ (in particular, $\Psi \cap \delta \neq \emptyset$) - as a consequence, Δ_1 connects P_{Out} and some $\delta_1 \in [P_{In}, \delta_0]$.

Having proven the base, for the step of the induction, assume that for all $0 < k \leq n$, $n \geq 1$ Δ_k is a curve in $f_p^{-k-1}(l) \cap \overline{H_p}$ s.t. the following is satisfied:

- Δ_k connects $f_p^{-k}(\delta_0)$, P_{Out} and some $\delta_k \in [P_{In}, \delta_0)$. Analogously δ_k would be defined as the first point of intersection as described above.
- $\Delta_k \cap \delta = \emptyset$.
- Δ_k includes a sub-arc Γ_k s.t. $f_p^{k+1}(\Gamma_k) = [\delta_0, P_{Out}]$.

We will now prove the same is true for Δ_{n+1} as well. To do so, note that similarly to the proof in the base of the induction, the backward-trajectories connecting $\Delta_{n-1} \subseteq \overline{D_\alpha}$ to $h(\Delta_n) \subseteq \overline{T_\alpha}$ generate a surface S_n (recall that when $n = 1$, we take $\Delta_0 = f_p^{-1}(l)$). As such, there exists an arc $I_1 \subseteq \Delta_n$ whose backwards trajectories all glide over S_n and hit $\nu_{n+1} = h(\Delta_{n+1})$. Again, similarly to the previous arguments, the collection of flow lines connecting ν_{n+1}, Δ_n , denoted by β_n , **cannot** intersect S_n transversely - hence again it follows $\nu_{n+1} \subseteq h(\overline{H_p})$, i.e., $\Delta_{n+1} \subseteq \overline{H_p}$. Again, a similar argument to the one used in the base of the induction proves Δ_{n+1} must connect $P_{Out}, f_p^{-n}(\delta_0)$ - which, again, implies there exists some $\Gamma_{n+1} \subseteq \Delta_{n+1}$ s.t. $f_p^{n+2}(\Gamma_{n+1}) = [\delta_0, P_{Out}]$. Additionally, since Δ_{n-1} connects P_{Out} and δ_n , because S_n, β_n cannot intersect transversely it follows S_n is a surface which

separates β_n from $h(\delta)$ in $\overline{T_\alpha}$ - therefore, $h(\delta) \cap \nu_{n+1} = \emptyset$ which implies $\delta \cap \Delta_{n+1} = \emptyset$. Finally, by replacing f_p with f_p^{n+1} , similarly to the argument in the base of the induction, again we conclude Δ_{n+1} must connect P_{Out} and some $\delta_{n+1} \in [P_{In}, \delta_0)$, the **first** point of intersection between Δ_{n+1} and $[P_{In}, \delta_0)$ (see the illustration in Fig.51).

All in all, we have proven that given $n \geq 1$ there exists a component $\Delta_n \subseteq f_p^{-n-1}(l) \cap \overline{H_p}$ s.t. the following holds:

- Δ_n is a curve in H_p connecting $P_{Out}, f_p^{-n+1}(\delta_0)$.
- Δ_n connects P_{Out} and some point $\delta_n \in [P_{In}, \delta_0)$.
- For every $n > 0$, Δ_n includes a curve $\Gamma_n \subseteq \Delta_n$ s.t. $f_p^{n+1}(\Gamma_n) = [\delta_0, P_{Out}]$.
- For $n \geq 1$, $\Delta_n \cap \delta = \emptyset$.

We now conclude the proof of Prop.3.4 by proving the last three assertions in Prop.3.4. First, by their definition, it immediately follows $f_p(\Delta_n) \subseteq \Delta_{n-1}$ - and since for every n , $f_p^{-n}([\delta_0, P_{Out}]) \subseteq \Delta_{n-1}$, it also follows that for every $n, k > 0$ we have both $f_p^{-n}([\delta_0, P_{Out}]) = \Gamma_n \subseteq f_p^k(\overline{H_p})$ and $f_p^{-n+1}(\delta_0) \in \Delta_n \cap \Delta_{n-1}$. In particular, for every $n, k > 0$ we have $f_p^{-n}(\delta_0) \in f_p^k(\overline{H_p})$. Finally, recalling we denote by $\mu_n = f_p^{-n}(\delta) \cap \Delta_n$, to conclude the proof of Cor.3.4 all that remains to proven is that given $n \neq k$, $\mu_n \cap \mu_k = \emptyset$. To do so, recall we have already proven $f_p^{-1}(\delta) \cap \delta = \emptyset$ - therefore, applying f_p^{-1} we see $\mu_2 \cap \mu_1 = \emptyset$, and in general, for $n \geq 1$, $\mu_{n+1} \cap \mu_n = \emptyset$. However, since by construction μ_n is separated from μ_{n+2} in $\overline{H_p} \setminus \cup_{n \geq 1} \Gamma_n$ by μ_{n+1} it follows $\mu_n \cap \mu_{n+2} = \emptyset$ - and by iterating this argument, Prop.3.4 follows (see the illustration in Fig.52). \square

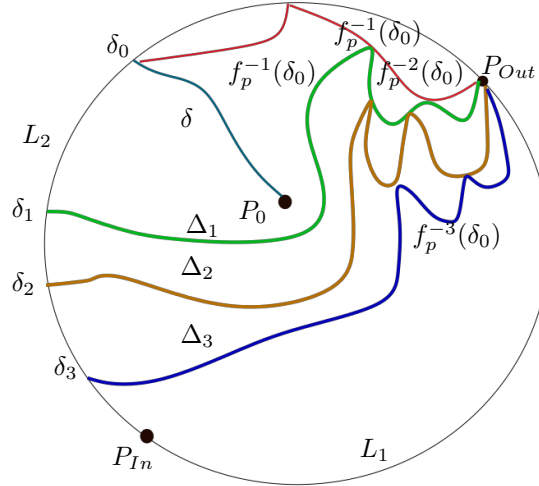


FIGURE 52. The cross-section H_p , with Δ_1, Δ_2 and Δ_3 imposed on it.

Now, recall the curve δ from Prop.3.2. As proven earlier, $f_p(\delta) = (P_{In}, f_p(\delta_0))$ (i.e., the semi-open arc connecting $P_{In}, f_p(\delta_0)$ on l) - while $f_p^2(\delta)$ is strictly interior to the cross-section D_α (see the illustration in Fig.51). Additionally, for every $n \geq 1$, set γ_n as the first point of intersection between $\Delta_n, f_p(P_{In}, \delta_0)$ - let us remark that since δ_{n+1} is the first point of intersection between $\Delta_{n+1} \cap [P_{In}, \delta_0)$, by $f_p(\Delta_{n+1}) \subseteq \Delta_n$, we have $\gamma_n = f_p(\delta_{n+1})$ (see the illustration in Fig.54). Having proven Prop.3.4, we conclude Stage II with a proof of the following Lemma, which follows immediately from Prop.3.4:

Lemma 3.10. *Let $p \in P$ be a trefoil parameter and let H_p be the cross-section from Prop.3.3 - then, with the notations of Cor.3.4, for every $n \geq 1$, $\delta_n \notin f_p(\delta)$. As a consequence, for every n we have the following:*

- For every $n \geq 1$, $\delta_n \notin f_p(\delta)$.
- For every $n \geq 1$, $\gamma_n \notin f_p^2(\delta)$.

As an immediate consequence, $f_p^2(\delta)$ is disjoint from $f_p^{-1}(l)$, hence $f_p^2(\delta) \subseteq H_p$.

Proof. We first prove that as a consequence from $\gamma_n \notin f_p^2(\delta)$, $n \geq 1$, it follows both $f_p^2(\delta) \cap f_p^{-1}(l) = \emptyset$ and $f_p^2(\delta) \subseteq H_p$. To do so, observe that by $\gamma_1 \notin f_p^2(\delta)$ it immediately follows $\Delta_1 \cap f_p^2(\delta) = \emptyset$ - for if that was **not** the case, $\Delta_1 \cap f_p^2(\delta) \neq \emptyset$ would force $\gamma_2 \in f_p^2(\delta)$, which is impossible. Therefore, all in all, we conclude $\Delta_1 \cap f_p^2(\delta) = \emptyset$. Now, recall that in the proof of Prop.3.4 we proved the intersection $\Delta_1 \cap f_p^{-1}(l)$ is at most tangent - therefore, by $\Delta_1 \cap f_p^2(\delta) = \emptyset$ and because Δ_1 connects $P_{Out}, \delta_1 \in [P_{In}, \delta_0)$ (see the illustration in Fig.51), it follows $f_p^2(\delta)$ is separated from $f_p^{-1}(l)$ by Δ_1 - as a consequence, $f_p^2(\delta) \cap f_p^{-1}(l) = \emptyset$. Therefore, to prove Lemma 3.10 it would

suffice to prove both $\gamma_n \notin f_p^2(\delta)$, $\delta_n \notin f_p(\delta)$ - we will begin by proving $\delta_n \notin f_p(\delta)$, and as we will see this would imply $\gamma_n \notin f_p^2(\delta)$.

To begin, using the notations used in the proof of Prop.3.4, recall we denote by $\nu_n = h(\Delta_n)$ (with h as in Lemma 3.8), and recall the surface $A_3 \subseteq \{\dot{x} = 0\}$. We can now prove $\delta_n \notin f_p(\delta)$. We do so by contradiction - that is, assume there exists some $n \geq 1$ s.t. $\delta_n \in (P_{In}, f_p(\delta_0)] = f_p(\delta)$. In that case, by $\Delta_n \subseteq f_p^{-n-1}(l)$ it follows $f_p^{-n-2}(l)$ intersects δ - therefore, by considering $f_p^{-1}(\Delta_n) \subseteq f_p^{-n-2}(l)$ we conclude $h(f_p^{-1}(\Delta_n))$ includes two sub-curves - $\nu_{n+1} = h(\Delta_{n+1})$, connecting $P_{Out}, \delta_{n+1} \in l'$ and another, ψ_{n+1} , which begins at $f_p^{-1}(\delta_n) \in \delta$ and connects to some $\rho_{n+1} \in l'$ - see the illustration in Fig.53. In particular, writing $\delta_{n+1} = (x_1, y_1, z_1)$, $\rho_{n+1} = (x_2, y_2, z_2)$ it follows by Lemma 3.1.2 that $x_1 \leq x_2$, $y_1 \geq y_2$ (see the illustration in Fig.53). Therefore, by considering the surface made of flow lines connecting Δ_n to $f_p^{-1}(\Delta_n)$, a similar argument to the proof of Prop.4.0.1 and Prop.3.4 implies there exists a compact, three-dimensional body B , s.t. $P_{In}, P_{Out} \notin \bar{B}$ that no forward trajectory can escape - this is a contradiction to Lemma 2.1 hence we conclude $\delta_n \notin f_p(\delta)$.

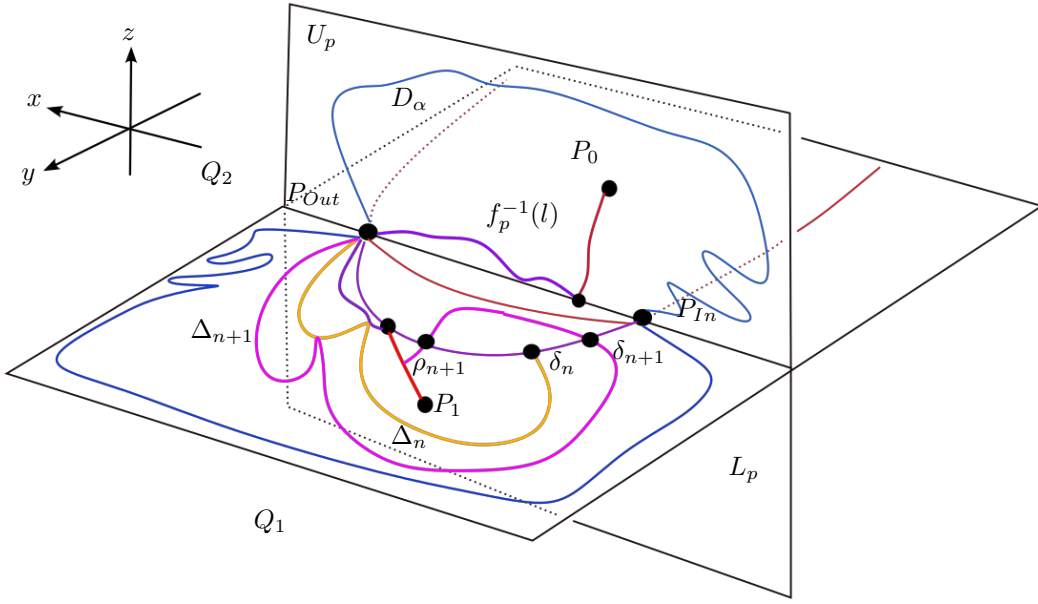


FIGURE 53. The scenario where $\delta_n \in f_p(\delta)$. We prove this scenario cannot occur.

Having proven that for $n \geq 1$, $\delta_n \notin f_p(\delta)$, to conclude the proof of Lemma 3.4 we must show that for every $n \geq 1$ we have $\gamma_n \notin f_p^2(\delta)$, $\gamma_n = f_p(\delta_{n+1})$. However, that is immediate - to see why, recall $f_p(\delta) \subseteq [P_{In}, \delta_0)$, and that by definition $f_p(\Delta_{n+1}) \subseteq \Delta_n$. Therefore, since δ_{n+1} is the first intersection point between Δ_{n+1} , $[P_{In}, \delta_0)$, it follows that $f_p(\delta_{n+1}) = \gamma_n$ is the **first** intersection point of Δ_n with $f_p([P_{In}, \delta_0))$. Since by previous paragraph $\delta_{n+1} \notin f_p(\delta)$, it follows $\gamma_n \notin f_p^2(\delta)$ (see the illustration in Fig.54). Therefore, given $n \geq 1$, $\gamma_n \notin f_p^2(\delta)$ and Lemma 3.10 now follows. \square

3.3. Stage III - concluding the proof of Th.3.1. Having analyzed the topology of $f_p^{-1}(l)$, we are now finally ready to prove f_p is chaotic on some invariant subset $Q \subseteq \bar{D}_\alpha$ - thus concluding the proof of Th.3.1. We will do so by analyzing the invariant set of f_p in the cross-section $H_p \subseteq D_\alpha$ introduced in the proof of Cor.3.3. To begin, recall Cor.3.1.3 and Lemma 3.9 - by both these assertions, it follows $f_p(H_p)$ is the banana-shaped region which intersects H_p as in Fig.55. By Lemma 3.10, we can sketch that image s.t. $f_p^2(\delta) \cap \delta = \emptyset$.

Therefore, using Cor.3.4, we now prove:

Proposition 3.5. *Let $p \in P$ be a trefoil parameter. Then, there exists an invariant $Q \subseteq \bar{H}_p$ and a continuous $\pi : Q \rightarrow \{1, 2\}^{\mathbb{N}}$ s.t. the following holds:*

- $\pi(Q)$ includes every sequence in $\{1, 2\}^{\mathbb{N}}$ which is **not** strictly pre-periodic to the constant $\{1, 1, 1, \dots\}$.
- f_p is continuous on Q and satisfies $\pi \circ f_p = \sigma \circ \pi$.
- Given any $s \in \pi(Q)$, $\pi^{-1}(s) = D_s$ is compact, connected, and homeomorphic to a convex set.
- With the same notations, provided $s \in \{1, 2\}^{\mathbb{N}}$ is not the constant $\{1, 1, 1, \dots\}$ nor pre-periodic to it, $P_{Out}, P_{In} \notin D_s$.

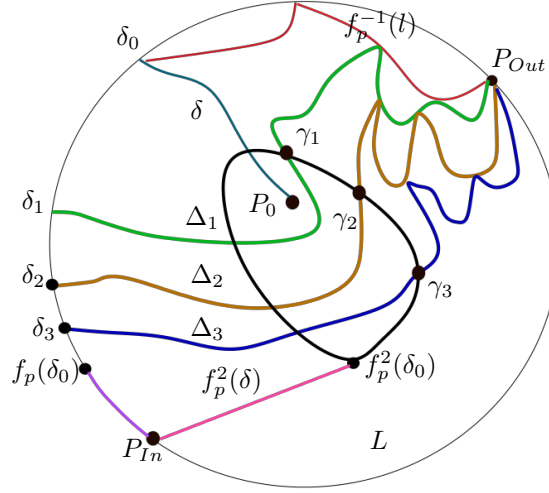


FIGURE 54. The arc $f_p(\delta)$ on l , imposed on the cross-section D_α . Again, $L = \partial B_\alpha \cap U_p$.

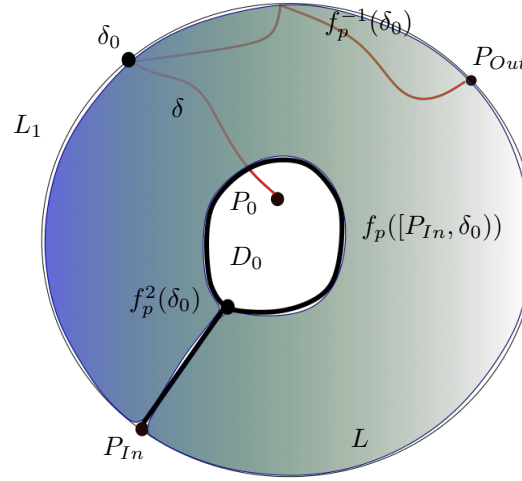


FIGURE 55. $f_p(H_p)$ imposed on the disc $\overline{D_\alpha}$ as the blue-green region, bounded by ∂D_α and the curve $f_p([P_{In}, \delta_0])$. In particular, $f_p(H_p) \cap \delta$ includes a sub-arc of δ connecting both components of ∂H_p . $\overline{D_\alpha} \setminus f_p(H_p)$ is the Jordan region D_0 .

Proof. We prove Prop.3.5 constructively. To do so, recall the curve $\delta \subseteq f_p^{-1}(l)$ introduced in Prop.3.2. Moreover, recall the component H_p of $\overline{D_\alpha} \setminus f_p^{-1}(l)$ introduced in the proof of Cor.3.3 has a boundary which is composed of three sets - $f_p^{-1}(l)$, $[P_{In}, \delta_0] = L_1$, and the arc $L = \partial B_\alpha \cap U_p$. By Prop.3.4 and Lemma 3.10, $\Delta_1 \subseteq \overline{H_p}$ is a sub-arc of $f_p^{-2}(l)$ which connects $P_{Out}, f_p^{-1}(\delta_0)$ and some $\delta_1 \in [P_{In}, \delta_0] \setminus f_p(\delta)$ - see the illustration in Fig.56. Therefore, $\overline{H_p} \setminus f_p^{-2}(l)$ is composed of three sets - T_1, T_2, T_3 s.t. the following conditions are satisfied (see the illustration in Fig.56):

- $P_{In}, P_{Out} \in \partial T_1$ and P_0 in ∂T_2 .
- T_1 is separated from T_2 by $\Delta_1 \subseteq f_p^{-2}(l)$.
- For $i = 1, 2$, $f_p(T_i) \subseteq \overline{H_p} \setminus f_p^{-1}(l)$, while $f_p(T_3) \cap H_p = \emptyset$ - i.e., T_3 is mapped outside of the cross-section $\overline{H_p}$ by f_p , while **both** T_1, T_2 are mapped inside $\overline{H_p}$.
- T_1, T_2 include (respective) Jordan domains D_1, D_2 s.t. $f_p(D_i) \cap D_j \neq \emptyset$, $i, j \in \{1, 2\}$.
- $\{P_{In}, P_{Out}\} \subseteq \partial D_1 \setminus \partial D_2$, while $P_0 \in \partial D_2 \setminus \partial D_1$. Moreover, $f_p(D_i) \cap H_p, i = 1, 2$ both connect P_{In}, δ .
- $\Delta_1 \subseteq \partial D_i, i = 1, 2$,

Now, denote by $I = [\delta_0, P_{Out}]$ the sub-arc of l connecting δ_0, P_{Out} - by Cor.3.4 we have $\cup_{n \geq 1} f_p^{-n}(I) \subseteq f_p(\overline{H_p}) \cap \overline{H_p}$ - and since for every n we have $\Delta_n \subseteq \overline{H_p}$, by their construction in the proof of Cor.3.4 it follows $\cup_{n \geq 1} \Delta_n \subseteq (\overline{D_1} \setminus (f_p(\delta)) \cup f_p^2(\delta))$. Now, choose some $i \in \{1, 2\}$ - because Cor.3.4 implies $f_p^{-1}(\delta_0) \in f_p(\overline{H_p})$, it follows $f_p(\overline{H_p}) \setminus \Delta_1$ has at least two components (see the illustration in Fig.57). Therefore, $D_i \setminus f_p^{-3}(l)$ consists of

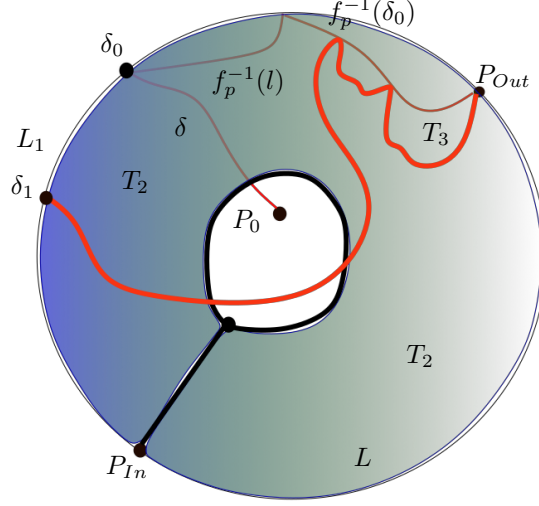


FIGURE 56. The red curve is a component of $f_p^{-2}(l) \cap H_p$, which intersects l at some point δ_1 - or, in the notation of Prop.3.4, the red curve is Δ_1 . The sets T_1, T_2, T_3 are imposed on $\overline{H_p}$ - while $\partial H_p = L_1 \cup L \cup f_p^{-1}(l)$.

the sets $T_{i,1}, T_{i,2}, T_{i,3}$ s.t. $f_p(T_{i,j}) \subseteq T_j$, with $j \in \{1, 2, 3\}$ (with previous notations, recall $\Delta_2 \subseteq f_p^{-3}(l)$). Again, this implies there exists a Jordan domain $D_{i,j}$, $j = 1, 2$ s.t. $f_p(D_{i,j}) \subseteq D_j$ - see the illustration in Fig.57. In particular, $f_p^2(D_{i,j}) \cap H_p$, $i, j \in \{1, 2\}$ connects δ, P_{In} .

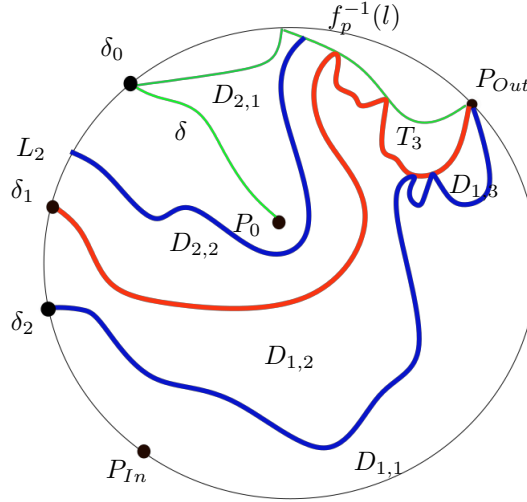


FIGURE 57. The green curve denotes $f_p^{-1}(l)$, the red denotes Δ_1 while the blue curves are the components of $f_p^{-3}(l) \cap H_p$, i.e., θ_1 and θ_2 . For simplicity, in this scenario we have $D_1 = T_1$, $T_2 = D_2$, and $D_1 = D_{1,1} \cup D_{1,2} \cup D_{1,3}$, $D_2 = D_{2,1} \cup D_{2,2}$.

Repeating this process, given $k \in \{1, 2\}$, because $f_p^{-2}(\delta_0) \in \overline{f_p^2(H_p)} \cap \overline{D_1}$ it again follows that given $i, j \in \{1, 2\}$ by considering $D_{i,j} \setminus f_p^{-4}(l)$ we can find a Jordan subdomain $D_{i,j,k} \subseteq D_{i,j}$ s.t. $f_p^2(D_{i,j,k}) \subseteq D_k$, and $f_p^3(D_{i,j,k}) \cap H_p$ connects P_{In}, δ . We may, of course, proceed in this fashion and conclude the following - let $s \in \{1, 2\}^{\mathbb{N}}$, $s = \{i_0, i_1, i_2, \dots\}$ be a symbol **not** strictly pre-periodic to the constant $\{1, 1, 1, \dots\}$. Define $D_s = \bigcap_{n \geq 0} \overline{D_{i_0, \dots, i_n}}$ - being the intersection of nested, compact sets, D_s is compact and non-empty. Additionally, since for every $n \geq 0$ D_{i_0, \dots, i_n} is a Jordan domain it follows D_s is homeomorphic to the intersection of a sequence of nested discs - hence, D_s is also homeomorphic to a convex set.

Moreover, by construction, for every $n \geq 0$, $f_p^n(D_s) \subseteq D_{i_n}$ - from which it follows that provided s is **not** the constant $\{1, 1, 1, \dots\}$, there exists some n s.t. $f_p^n(D_s) \subseteq D_2$ - hence, since by the discussion above $P_{In}, P_{Out} \in D_1$, $f_p(P_j) = P_j$, $j \in \{In, Out\}$, it immediately follows $P_{In}, P_{Out} \notin D_s$. Additionally, since we constructed D_s s.t. it lies **away** from $\bigcup_{n \geq 0} f_p^{-n}(l)$, by Prop.3.2 it follows that for every $k > 0$, f_p^k is continuous on D_s . Now, set

Q as the collection of such D_s (i.e., the collection of D_s s.t. $s \in \{1, 2\}^{\mathbb{N}}$ is **not** pre-periodic to the constant $\{1, 1, 1, \dots\}$). Denoting by $\sigma : \{1, 2\}^{\mathbb{N}} \rightarrow \{1, 2\}^{\mathbb{N}}$ the one-sided shift, by this discussion it follows there exists a function $\pi : Q \rightarrow \{1, 2\}^{\mathbb{N}}$ s.t. the following holds:

- $\pi \circ f_p = \sigma \circ \pi$.
- Since f_p is continuous on Q , π is also continuous on Q .

And moreover, given any $s \in \{1, 2\}^{\mathbb{N}}$ which is **not** strictly pre-periodic to the constant $\{1, 1, 1, \dots\}$ the following is also satisfied:

- $s \in \pi(Q)$.
- $\pi^{-1}(s) = D_s$ is a connected, compact set homeomorphic to a convex set.
- If s is not the constant $\{1, 1, 1, \dots\}$, then $P_{In}, P_{Out} \notin D_s = \pi^{-1}(s)$.

And with that, the proof of Prop.3.5 is complete. \square

Remark 3.5. Let $s \in \{1, 2\}^{\mathbb{N}}$ which is strictly pre-periodic to $\{1, 1, 1, \dots\}$. As must be remarked, there exists a **unique** point $x \in \overline{H_p}$ whose trajectories tends to $P_{In} - P_0$. Because P_0 has no preimages in $\{\dot{y} = 0\}$ (let alone H_p) any attempt to define D_s for such symbols is probably futile.

Remark 3.6. Consider some $s \in \{1, 2\}^{\mathbb{N}}$, $s = \{i_0, i_1, i_2, \dots\}$, and let J denote the boundary arc of $\partial D_2 \cap \partial H_p$ s.t. $\delta_0 \in J$. It is immediate there exists a component θ_2 of $f_p^{-1}(\Delta_1) \subseteq f_p^{-3}(I)$ which connects the two components of $J \setminus \{\delta_0\}$ - in fact, for every $j > 2$, $n > 0$, $f_p^{-j}(\Delta_n) \cap D_2$ includes an arc connecting the two components of $J \setminus \{\delta_0\}$. As such, it follows that when $i_0 = 2$, for every n the domain D_{i_0, \dots, i_n} also connects the two components of $J \setminus \{\delta_0\}$ - and as a consequence, so does D_s .

Remark 3.7. As must be remarked, the dynamics of the first-return map observed numerically at trefoil parameters in [29] were associated with bimodal rather than unimodal dynamics - i.e., the first-return map appeared to correspond to some subshift of finite type on three symbols rather than two. This suggests the dynamics of f_p on $\overline{D_\alpha}$ are more complex than those of f_p on $\overline{H_p}$ - or, in other words, the set T_3 from the proof of Prop.3.5 possibly plays a larger part in the dynamics than what initially appears.

As an immediate consequence from Prop.3.5 we obtain:

Corollary 3.1.5. Let $p \in P$ be a trefoil parameter, and let $s \in \{1, 2\}^{\mathbb{N}}$ be periodic of minimal period $k > 0$ - then, $\pi^{-1}(s) = D_s$ includes a periodic point x for f_p of minimal period k .

Proof. With the notations of the proof of Prop.3.5, by the construction of $D_s = \pi^{-1}(s)$ in the proof of Prop.3.5, D_s is homeomorphic to a compact convex set. Therefore, because Prop.3.5 proves $f_p^k : D_s \rightarrow D_s$ is continuous, by the Brouwer Fixed Point Theorem there exists a point $x \in D_s$ s.t. $f_p^k(x) = x$. Therefore, to conclude the proof it remains to show the minimal period of x is also k . To do so, recall we denote by $\sigma : \{1, 2\}^{\mathbb{N}} \rightarrow \{1, 2\}^{\mathbb{N}}$ the one-sided shift. Since the minimal period of s under σ is k , given $i, j \in \{0, \dots, k-1\}$, $i \neq j$, $\sigma^j(s) \neq \sigma^i(s)$ - which, by Prop.3.5 implies $\pi^{-1}(\sigma^i(s)) \cap \pi^{-1}(\sigma^j(s)) = \emptyset$. Therefore, since for $0 \leq i \leq k-1$ we have $f_p^i(D_s) \subseteq D_{\sigma^i(s)}$ we conclude $f_p^i(D_s) \cap D_s \neq \emptyset$ only when $i = k$, and the conclusion follows. \square

Remark 3.8. When s is the constant $\{1, 1, 1, \dots\}$, Cor.3.1.5 remains true - in that case, the argument used to prove Prop.3.5 shows $P_{In} \in D_{\{1, 1, 1, \dots\}}$, and by $f_p(P_{In}) = P_{In}$ the assertion follows.

Additionally, there is yet one more corollary to Prop.3.5 - namely, we have:

Corollary 3.1.6. The periodic trajectories in the set Q , given by Prop.3.5, all lie away from the fixed points P_{In}, P_{Out} .

Proof. Let us recall $D_\alpha \setminus f_p(H_p)$ includes an open Jordan domain D_0 s.t. $P_0 \in D_0$ (see Def.2.4 and Cor.3.1.3). Or, in other words, by $f_p(Q) \subseteq f_p(H_p)$, it follows $f_p(Q) \cap D_0 = \emptyset$ (see the illustration in Fig.55) - which implies the periodic trajectories in Q must be uniformly bounded away from P_0 . As a consequence, since P_0 lies on the bounded heteroclinic trajectory Θ (see Def.2.4), it follows there exists some neighborhood N of P_{In}, P_{Out} (in \mathbf{R}^3) s.t. given any periodic trajectory T (w.r.t. some initial condition in Q), we have $T \cap N = \emptyset$. In other words, the forward trajectories of periodic orbits in Q must lie uniformly away from some neighborhoods of both P_{In}, P_{Out} , and the conclusion follows. \square

We can now conclude the proof of Th.3.1. Let Q be the set given by Prop.3.5. As proven in Lemma 3.3, H_p is a topological disc, and so is $\overline{H_p}$ - and by Prop.3.5 there exists an f_p -invariant $Q \subseteq \overline{H_p}$ s.t.:

- f_p is continuous on Q .
- There exists a continuous $\pi : Q \rightarrow \{1, 2\}^{\mathbb{N}}$ s.t. $\pi \circ f_p = \sigma \circ \pi$.
- $\pi(Q)$ includes every $s \in \{1, 2\}^{\mathbb{N}}$ **not** pre-periodic to the constant $\{1, 1, 1, \dots\}$.

- Let $s \in \{1, 2\}^{\mathbb{N}}$ be periodic of minimal period k . Then, by Cor.3.1.5 and Remark 3.8, $\pi^{-1}(s)$ contains a periodic point x_s for f_p of minimal period k .
- The periodic trajectories in Q all lie away from some neighborhoods of P_{In}, P_{Out} .

As a consequence, f_p is chaotic on Q (w.r.t. Def.1.1). In addition, Q includes infinitely many periodic points for f_p - of all minimal periods, which lie away from the fixed points for the vector field F_p . Th.3.1 is now proven. \square

At this point, let us remark that the proof of Th.3.1 can probably be generalized to other heteroclinic parameters for the Rössler system, which generate knots more complex than a trefoil (see Def.2.3). **However**, it should also be stressed that the proof of any such generalization would greatly depend on the topology of the heteroclinic knot involved.

Before we conclude this section, let us also remark that Th.3.1 can be reformulated in a somewhat simpler way (the proof, however, remains the same). To begin, recall the cross-section U_p (see the discussion before Lemma 2.1), the curve Δ_1 from Cor.3.4 and the regions D_1, D_2 from Prop.3.5 (in particular, recall the chain of inclusions $\overline{H_p} \subseteq \overline{D_\alpha} \subseteq \overline{U_p}$). As proven in Cor.3.4, Δ_1 connects P_{Out} and some point $\delta_1 \in l$. Let ρ denote the component of $\Delta_1 \setminus l$ s.t. $\delta_1 \in \rho$ (by Cor.3.10 $\delta_1 \neq P_{In}$). As a consequence, ρ is a curve connecting δ_1 and l , s.t. $\overline{U_p} \setminus \rho$ is composed of **precisely** two components, U_1, U_2 - indexed by $D_i \subseteq U_i, i = 1, 2$ (see the illustration in Fig.58). Now, set I as the maximal invariant set of f_p in $\overline{U_p} \setminus \rho$ - that is, I is the collection of initial conditions in the cross-section U_p whose trajectories both never hit ρ **and** never escape to ∞ . With these ideas in mind, let us restate Th.3.1 as follows:

Corollary 3.1.7. *Let $p \in P$ be a trefoil parameter, and let $f_p : \overline{U_p} \rightarrow \overline{U_p}$ denote the first-return map for the corresponding Rössler system (wherever defined). Moreover, let I be as above and recall we denote by $\sigma : \{1, 2\}^{\mathbb{N}} \rightarrow \{1, 2\}^{\mathbb{N}}$ the one-sided shift - then, there exists an f_p -invariant $Q \subseteq I$, s.t. the following holds:*

- f_p is continuous on Q .
- There exists a continuous $\pi : Q \rightarrow \{1, 2\}^{\mathbb{N}}$ s.t. $\pi \circ f_p = \sigma \circ \pi$.
- $\pi(I)$ includes every $s \in \{1, 2\}^{\mathbb{N}}$ which is **not** strictly pre-periodic to $\{1, 1, 1, \dots\}$.
- If $s \in \{1, 2\}^{\mathbb{N}}$ is periodic of minimal period $k > 0$, then $\pi^{-1}(s)$ includes **at least** one periodic point for f_p of the same minimal period.

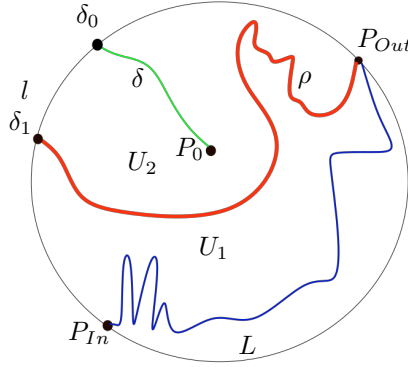


FIGURE 58. The cross-section U_p , sketched as a disc instead of a half-plane. The curve ρ bisects U_p to U_1, U_2 , with L denoting the curve $\partial B_\alpha \cap U_p$ (see Cor.3.1).

4. THE IMPLICATIONS:

Th.3.1 teaches us that at trefoil parameters, the dynamics of the Rössler system are complex essentially like those of a Smale Horseshoe, suspended around a heteroclinic trefoil knot - or, more precisely, it teaches us that the dynamics are complex **at least** like those of a suspended Smale Horseshoe map. Motivated by the theory of homoclinic bifurcations (and in particular, Shilnikov's Theorem - see [3]), in this section we use Th.3.1 to prove several results about the dynamical complexity of the Rössler system and its bifurcations around trefoil parameters.

To begin, recall P always denote the parameter space introduced in page 3, and let $p \in P$ **always** denote a trefoil parameter. Recall we denote by F_p the vector field corresponding to $p = (a, b, c)$ (see Eq.2). This section is organized as follows - first we study the question of hyperbolicity of the dynamics at trefoil parameter: namely, in Prop.4.1 we prove the flow at trefoil parameters $p \in P$ does not satisfy any dominated splitting condition, a weaker form of hyperbolicity. Following that, we prove that in the space of C^∞ vector fields (on \mathbf{R}^3), trefoil parameters are

inseparable from period-doubling and saddle-node bifurcation sets (for a more precise formulation, see Prop.4.2). Finally, we conclude this Section with the following result: given a trefoil parameter $p \in P$, a positive $n > 0$ and $v \in P$, provided v is sufficiently close to p the vector field F_v generates **at least** n distinct periodic trajectories (see Th.4.1).

To begin, let us first recall the cross-section $\overline{D_\alpha} \subseteq \overline{U_p}$ introduced in Section 2.2 (see Cor.3.0.1 and Prop.3.1) - by Cor.3.0.1, the first-return map $f_p : \overline{D_\alpha} \rightarrow \overline{D_\alpha}$ is well-defined. As proven in Section 3, the first-return map is continuous on each of the components of $\overline{D_\alpha} \setminus f_p^{-1}(l)$ (with l denoting the arc $\{(x, -\frac{x}{a}, \frac{x}{a}) | x \in (0, c - ab)\}$ - see the discussion at the beginning of Section 3 - and in particular, Prop.3.2). This motivates us to define $R = \cap_{n \geq 0} (\overline{D_\alpha} \setminus f_p^{-n}(l))$, the maximal invariant set of f_p in $\overline{D_\alpha} \setminus l$. Since we have the inclusion $\overline{H_p} \subseteq \overline{D_\alpha}$, by the construction of Q in Th.3.1 we conclude $Q \subseteq R$, hence $R \neq \emptyset$. By this definition, using a similar argument to the proof of Prop.3.5 it immediately follows:

Corollary 4.0.1. *Let C be a component of R . Then, for every $n > 0$, f_p^n is continuous on C - and moreover, R is dense in $\overline{D_\alpha}$.*

Proof. By definition, given C as above, f_p^n is continuous on C - for every n . Therefore, it remains to show R is dense in $\overline{D_\alpha}$. To do so, recall that since f_p is a first-return map, iterating the arguments used to prove Prop.3.2 we conclude that given $n \in \mathbf{N}$, $f_p^{-n}(l)$ is a collection of curves (possibly singletons) (see the illustration in Fig.59). As such, for every $n \geq 0$, $R_n = \overline{D_\alpha} \setminus (\cup_{0 \leq k \leq n} f_p^{-k}(l))$ is dense in $\overline{D_\alpha}$. $\overline{D_\alpha}$ is both a complete and separable metric space, hence, by the Baire Category Theorem it follows $R = \cap_{n \geq 1} R_n$ is dense in $\overline{D_\alpha}$ and Cor.4.0.1 follows. \square

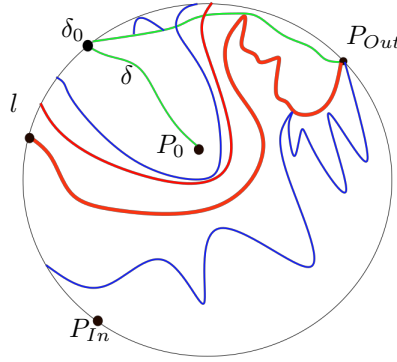


FIGURE 59. The set R_3 - the green curves correspond to $f_p^{-1}(l)$, the red to $f_p^{-2}(l)$, and the blue to $f_p^{-3}(l)$.

Using Cor.4.0.1, we now conclude the following result about the **non-hyperbolic** nature of the Rössler system:

Proposition 4.1. *Let $p \in P$ be a trefoil parameter - then, with previous notations, F_p does not satisfy any dominated splitting condition on the trajectories of initial conditions in R .*

Proof. Let us first recall the notion of **Dominated Splitting** - let M be a Riemannian manifold, and $\phi_t : M \rightarrow M, t \in \mathbf{R}$ be a smooth flow. Also, given a hyperbolic point $x \in M$ (w.r.t. ϕ_t) let us denote the components of the decomposition of the tangent space by $T_x M = E(x) \oplus F(x)$ - with $E(x), F(x)$ denoting the respective stable and unstable parts of the decomposition. A compact, ϕ_t -invariant set Λ is said to satisfy a **dominated splitting** condition if the following conditions are satisfied:

- The tangent bundle satisfies $T\Lambda = E \oplus F$, s.t. $E = \cup_{x \in \Lambda} E(x) \times \{x\}$, $F = \cup_{x \in \Lambda} F(x) \times \{x\}$.
- $\exists c > 0, 0 < \lambda < 1$, s.t. $\forall t > 0, x \in \Lambda$, $(\|D\phi_t|_{E(x)}\|)(\|D\phi_{-t}|_{F(\phi_t(x))}\|) < c\lambda^t$.
- $\forall x \in \Lambda, t > 0$, $E(x), F(x)$ vary continuously to $E(\phi_t(x)), F(\phi_t(x))$.

Now, let p be a trefoil parameter and let Λ be the **closure** in \mathbf{R}^3 of trajectories for initial conditions in R - by definition, Λ is also F_p -invariant. By Lemma 4.0.1, Λ is inseparable from P_{In} - as such, since $p \in P$ is a trefoil parameter the two dimensional manifolds W_{In}^u, W_{Out}^s coincide (see Def.17) hence Λ is also inseparable from P_{Out} . Now, recall P_{In}, P_{Out} are hyperbolic saddle-foci of opposing indices (see the discussion at page 3), connected by a bounded heteroclinic connection Θ (see Def.2.4) - with Θ being a component of **both** one-dimensional invariant manifolds W_{In}^s, W_{Out}^u . As such, by previous discussion and the compactness of Λ , we conclude $\Theta, P_{In}, P_{Out} \subseteq \Lambda$. Now, assume we can decompose $T\Lambda$ to $T\Lambda = E \oplus F$ as in the definition above - with previous notations, this implies $F(P_{Out})$ is one-dimensional, while $F(P_{In})$ is two dimensional. Hence, for $x \in \Theta$, $F(x)$ cannot vary continuously, and we have a contradiction. This contradiction proves F_p cannot satisfy any Dominated Splitting condition on Λ , and Lemma 4.1 follows. \square

Now, let $p \in P$ be a trefoil parameter, and recall we denote the saddle-indices for the saddle-foci P_{In}, P_{Out} by ν_{In}, ν_{Out} - respectively (see the definition at page 3). Additionally, recall that we assume that given $v \in P$, the saddle-indices corresponding to v always satisfy either $\nu_{In} < 1$ or $\nu_{Out} < 1$, i.e. $(\nu_{In} < 1) \vee (\nu_{Out} < 1)$. As must be remarked, the proof of Th.3.1 and Th.2.1 (and later on, Th.4.1) are independent of the assumption that $\nu_{Out} < 1 \vee \nu_{In} < 1$ - that is, Th.3.1 and Th.4.1 are both independent of the assumption that at least one of the fixed points for F_p satisfies the Shilnikov condition. Plugging in this assumption, we derive the following result:

Proposition 4.2. *Let $p \in P$ be a trefoil parameter. Then, p is an accumulation point in the space of vector fields for infinitely many period-doubling and saddle-node bifurcation sets in the space of C^∞ vector fields on \mathbf{R}^3 .*

Proof. For completeness, let us recall sections 2,3 of [11]. In that paper, the setting is that of a smooth, two-parameter family of smooth vector fields $\{X_{(a_1, a_2)}\}_{(a_1, a_2) \in O}$, with (a_1, a_2) varying smoothly in some open set $O \subseteq \mathbf{R}^2$. Assume there exists a curve $\gamma \subseteq O$ corresponding to the existence of homoclinic trajectories. Also assume the saddle indices along γ are all strictly lesser than 1 - that is, by Shilnikov's Theorem the dynamics around these homoclinic trajectories all generate infinitely many suspended Smale horseshoes.

As proven in [11], under these assumptions one can construct a function B from the phase space to O . The analysis of B allows one to find a family of spirals, $\{\delta_o\}_{o \in \gamma}$, s.t. δ_o is a curve in O , spiralling towards o . Each δ_o corresponds to the existence of a periodic trajectory, which undergoes a cascade of period-doubling and saddle-node bifurcations as δ_o accumulates on o . Moreover, this family of spirals varies continuously when $o \in \gamma$ varies - and provided the saddle index along γ is bounded, there exists some $c > 0$ s.t. $\forall o \in \gamma, \text{diam}(\delta_o) > c$ (with that diameter taken w.r.t. the Euclidean metric in O). When the function B was analyzed, its critical values corresponded to curves of period-doubling and saddle-node bifurcations - and these critical values accumulated around every point in γ (see Sections 2,3 in [11] for more details). That is, for any $\epsilon < 0$ and any $o \in \gamma$ there exist Γ_1, Γ_2 , a saddle node bifurcation curve and a period doubling bifurcation curve (respectively) s.t. $d(\Gamma_i, o) < \epsilon, i = 1, 2$.

Now, back to the Rössler System. Without any loss of generality, assume that w.r.t. the vector field F_p we have $\nu_{In} < 1$ (by our assumptions on the parameter space P , we have $\nu_{In} < 1 \vee \nu_{Out} < 1$ - see the discussion at page 3). Since $p \in P$ is a trefoil parameter, by Def.2.4 it follows the two dimensional manifolds W_{Out}^s, W_{In}^u coincide - therefore, we can perturb F_p at some small neighborhood of P_{Out} and combine Θ (the bounded heteroclinic connection) and some flow line in $W_{In}^u = W_{Out}^s$ to create a homoclinic trajectory to P_{In} . Or, in other words, there exists an arbitrarily small C^∞ approximation of F_p , V s.t. V generates a heteroclinic trajectory to the fixed point P_{In} - consequentially, there exists a smooth curve γ_{In} in the space of C^∞ vector fields on \mathbf{R}^3 , s.t. $\forall \omega \in \gamma_{In}$, the vector field corresponding to ω generates a homoclinic curve to P_{In} . Moreover, by the description of these approximations above, we can choose γ_{In} s.t. for every $\omega \in \gamma_{In}$, ω, F_p coincide around the fixed point P_{In} - consequentially, the saddle index ν_{In} is constant along γ_{In} .

Finally, as $\nu_{In} < 1$ the discussion above implies the period-doubling and saddle node bifurcations sets are dense around γ_{In} (in the space of C^∞ vector fields on \mathbf{R}^3). Since $F_p \in \bar{\gamma}_{In}$, it follows these sets are also dense around F_p . The argument for the case $\nu_{Out} < 1$ is symmetric, and Prop.4.2 now follows. \square

Remark 4.1. Assume **both** $\nu_{In}, \nu_{Out} < 1$. In that case, the proof of Prop.4.2 essentially proves the bifurcations around trefoil parameters in the space of C^∞ vector fields on \mathbf{R}^3 are **doubly as complicated** when compared to homoclinic bifurcations. This should be contrasted with the results of [15], where it was proven a two-dimensional parameter space **cannot** be used to completely describe the bifurcations around heteroclinic parameters.

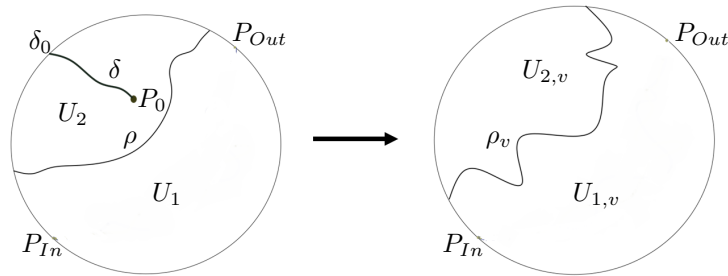


FIGURE 60. the deformation of U_p (on the left) to U_v (on the right). The curve ρ is deformed to ρ_v .

We are now ready to state and prove Th.4.1, with which we conclude this section - namely, we will now prove that given a trefoil parameter $p \in P$ and given any $n > 0$, provided $v \in P$ is sufficiently close to p the vector

field F_v generates **at least** n periodic trajectories. Or, in other words, Theorem 4.1 has the following meaning - the closer a parameter $v \in P$ is to a trefoil parameter p , the more complex its dynamics become. The idea behind the proof is based on the following intuition - if $p \in P$ is a trefoil parameter, by Th.3.1 the dynamics of f_p on the invariant set Q are complex at least like those of a Smale Horseshoe. As such, we would expect the periodic orbits of the first-return map f_p to be hyperbolic, thus they should persist under perturbations of the first-return map in P . In practice however, due to Prop.4.1 this line of reasoning simply cannot hold - or, put simply, there is no reason whatsoever to assume any hyperbolicity condition on the invariant set Q given by Th.3.1.

Therefore, to bypass this difficulty and prove the persistence of periodic dynamics we will take a different route, and apply the notion of the Fixed-Point Index (see [5]). As we will see, to prove the persistence of periodic dynamics it would be enough to construct a homotopy between the first-return map $f_p : \overline{H_p} \rightarrow \overline{H_p}$ to a Smale-Horseshoe. To begin, let us first recall several facts which would motivate our result and make its statement more precise. First, recall that given a trefoil parameter $p \in P$, $f_p : \overline{U_p} \rightarrow \overline{U_p}$ denotes the first-return map for F_p for the cross-section $U_p \subseteq \{\dot{y} = 0\}$ (wherever defined - see Lemma 2.1), and that we have the inclusion $Q \subseteq \overline{H_p} \subseteq \overline{D_\alpha} \subseteq \overline{U_p}$ - where Q denotes the set given by Cor.3.1.7. By Cor.3.1.7 (and Th.3.1) there exists a continuous $\pi : Q \rightarrow \{1, 2\}^{\mathbb{N}}$ s.t. the one-sided shift $\sigma : \{1, 2\}^{\mathbb{N}} \rightarrow \{1, 2\}^{\mathbb{N}}$ satisfies $\pi \circ f_p = \sigma \circ \pi$, and σ is chaotic on $\pi(Q)$ (w.r.t. Def.2.4). Secondly, we have also proven that given **any** periodic $s \in \{1, 2\}^{\mathbb{N}}$ which is both periodic of minimal period $k > 0$ **and** distinct from the constant $\{1, 1, 1, \dots\}$, $\pi^{-1}(s)$ contains a periodic point for f_p of minimal period k . Now, further recall that by Cor.3.1.7 we have $Q \subseteq I$, with I denoting the maximal invariant set of f_p in $\overline{U_p} \setminus \rho$ (with the curve ρ defined as in the discussion preceding Cor.3.1.7). As shown earlier, $\overline{U_p} \setminus \rho$ is composed of two subsets, U_1, U_2 , with which we defined the symbolic coding given by π (see the illustration in Fig.60 or Fig.58).

Now, given any $v \in P, v \neq p$, let $f_v : \overline{U_v} \rightarrow \overline{U_v}$ denote the first-return map for the vector field F_v (wherever defined) - with U_v as in Lemma 2.1. Since the cross-sections U_v vary smoothly when we vary $v \in P$ (see the discussion preceding Lemma 2.1), when F_p is continuously deformed to F_v the curve $\rho \subseteq \overline{U_p}$ is continuously deformed to $\rho_v \subseteq \overline{U_v}$. Hence, since ρ divides $\overline{U_p}$ to U_1, U_2 , we conclude ρ_v divides $\overline{U_v}$ to $U_{1,v}, U_{2,v}$ (see the illustration in Fig.60). This motivates us to define a symbolic coding on I_v , the invariant set of f_v in $\overline{U_v} \setminus \rho_v$ - provided I_v is non-empty, there exists a function $\pi_v : I_v \rightarrow \{1, 2\}^{\mathbb{N}}$ (not necessarily continuous, or surjective) s.t. $\pi_v \circ f_v = \sigma \circ \pi_v$ (again, with $\sigma : \{1, 2\}^{\mathbb{N}} \rightarrow \{1, 2\}^{\mathbb{N}}$ denoting the one-sided shift). We now prove:

Theorem 4.1. *With the notations above, let $p \in P$ be a trefoil parameter, and let $s \in \{1, 2\}^{\mathbb{N}}$ be periodic of minimal period k that is **not** the constant $\{1, 1, 1, \dots\}$. Then, for $v \in P$ sufficiently close to p we have:*

- $s \in \pi_v(I_v)$.
- $\pi_v^{-1}(s)$ contains at least one periodic point $x_s \in I_v$ for f_v , of minimal period k .
- The functions f_v, f_v^2, \dots, f_v^k are all continuous at x_s .
- π_v is continuous at $x_s, f_v(x_s), \dots, f_v^{k-1}(x_s)$.

Proof. As remarked earlier, we prove Th.4.1 with the aid of the Fixed-Point Index (see [5]). Therefore, in order to give a sketch of the proof, let us first recall its definition - let $V \subseteq \mathbb{R}^2$ be an **open** set, and let $f : V \rightarrow \mathbb{R}^2$ be continuous s.t. the set $\{x \in V | f(x) = x\}$ is compact. The **Fixed-Point Index** of f would be defined as the degree of $f(x) - x$ on V - in particular, when f has no fixed points in V its Fixed-Point Index is 0 (see Ch.VII.5.5 in [5]). Now, let $f_t : V \rightarrow \mathbb{R}^2, t \in [0, 1]$ be a homotopy of continuous maps, and for every $t \in [0, 1]$ set $F_t = \{x \in V | f_t(x) = x\}$. As proven in Ch.VII.5.8 in [5], provided $\cup_{t \in [0, 1]} F_t \times \{t\}$ is compact in $V \times [0, 1]$, the fixed point index is invariant under the homotopy. Or in other words, given homotopies as described above, if the Fixed-Point Index for f_0 is non-zero, the same is true for f_1 , i.e. f_1 has at least one fixed-point in V .

With these ideas in mind, let us sketch the proof of Th.4.1 - let $s \in \{1, 2\}^{\mathbb{N}}$ be periodic of minimal period $k \geq 1$, which is **not** the constant $\{1, 1, 1, \dots\}$, and let $\overline{H_p}$ and $Q \subseteq \overline{H_p}$ be as in Th.3.1 - as proven in Th.3.1, there exists a continuous $\pi : Q \rightarrow \{1, 2\}^{\mathbb{N}}$ s.t. $s \in \pi(Q)$ and $D_s = \pi^{-1}(s)$ is connected, and homeomorphic to a convex set (see Prop.3.5). Now, let $F = \{x \in D_s | f_p^k(x) = x\}$ - we will prove Th.4.1 in three consecutive stages organized as follows:

- First, we prove certain topological preliminaries about the dynamics of f_p in $\overline{D_\alpha}$ - with which we define a topological disc B s.t. $D_s \subseteq \overline{B}$ (see Lemma 4.2).
- Second, we prove the fixed-point index of f_p^k on B is positive - the proof of this fact will be the bulk of the proof. The reason this is so is because in order to compute the fixed-point index of f_p^k on B we will have to carefully construct a homotopy between f_p and a Smale Horseshoe map s.t. no periodic points escape to ∂B throughout the homotopy.
- Finally, we prove that given any $v \in P$ sufficiently close to p , $f_v^k : B \rightarrow U_v$ is well-defined and homotopic to $f_p^k : B \rightarrow U_p$, from which Th.4.1 would follow.

4.1. **Stage I - some topological preliminaries.** To begin, recall the cross-section $D_\alpha \subseteq U_p$ defined at the beginning of Section 3- by Cor.3.0.1 and Prop.3.1, the first-return map $f_p : \overline{D_\alpha} \rightarrow \overline{D_\alpha}$ is well-defined and satisfies $f_p(\overline{D_\alpha}) \subseteq \overline{D_\alpha}$. Now, recall W_{In}^u denotes the unstable, two dimensional manifold for the saddle-focus P_{In} , while W_{Out}^s denotes the stable, two dimensional invariant manifold of the saddle-focus P_{Out} (since $p \in P$ is a trefoil parameter, $W_{In}^u = W_{Out}^s = W$ - see Def.2.4). By Prop.3.1, D_α is a topological disc in the cross-section U_p , satisfying $\partial D_\alpha = \tilde{l} \cup L$ - with L denoting $\partial B_\alpha \cap U_p$ (with B_α denoting the topological ball bounded by P_{In}, P_{Out} and W - see the discussion following Def.2.4).

Additionally, recall l denotes the arc $\{(x, -\frac{x}{a}, \frac{x}{a}) | x \in (0, c - ab)\}$ (see the illustration in Fig.29) - and that we denote by $[P_{In}, \delta_0]$ the half open (and conversely, by $(P_{In}, \delta_0]$ the half-open) arc on l connecting P_{In} and the point δ_0 (see Prop.3.5). Similarly, let $[\delta_0, P_{Out}]$ denote the closed arc on l connecting δ_0, P_{Out} , and $[f_p(\delta_0), \delta_0]$ the closed arc connecting the points $\delta_0, f_p(\delta_0)$ on l (see the illustrations in Fig.54). Moreover, recall the set $\Delta_1 \subseteq f_p^{-2}(l)$ (see Cor.3.4). Finally, recall the cross-section $H_p \subseteq D_\alpha$ (see Prop.3.3), and that $\partial H_p = f_p^{-1}(l) \cup [P_{In}, \delta_0] \cup L$ (see the illustration in Fig.48). Finally, recall the point $\delta_1 \in [P_{In}, \delta_0]$ given by Cor.3.4, and the point $\delta_0 = \delta \cap l$ (see Prop.3.2) - since $\delta \subseteq f_p^{-1}(l)$ it follows $\delta_0 \in l \cap f_p^{-1}(l)$ hence $f_p^{-1}(\delta_0) \in f_p^{-1}(l) \cap f_p^{-2}(l)$.

Now, denote by J the arc on ∂H_p which connects δ_1 with δ_0 through l , and then connects δ_0 with $f_p^{-1}(\delta_0)$ through $f_p^{-1}(l)$ (by the connectedness of $f_p^{-1}(l)$, the arc J exists - see Prop.3.1.4 and the illustration in Fig.61). With the aid of the notions above and the ideas introduced in the proof of Prop.3.4 and Lemma 3.10, we first prove the following technical result:

Lemma 4.1. *Let $p \in P$ be a trefoil parameter. Then, if T is a periodic trajectory for the vector field F_p which is not a fixed-point, then $T \cap J = \emptyset$ - or, equivalently, the first-return map $f_p : \overline{D_\alpha} \rightarrow \overline{D_\alpha}$ has no periodic orbits intersecting J .*

Proof. Recall the set $\mu_1 = f_p^{-2}(\delta) \cap \Delta_1$ introduced in the proof of Cor.3.4, with δ, δ_0 as in Prop.3.2. We first prove μ_1 is an arc, s.t. $\mu_1 \setminus l$ includes a curve in H_p connecting $f_p^{-1}(\delta_0)$ and δ_1 (with δ_1 as in Cor.3.4 - see the illustration in Fig.61). To this end, recall that by Cor.3.4 μ_1 is the arc on Δ_1 connecting $\Gamma_1 = f_p^{-2}([\delta_0, P_{Out}])$ with $\delta_1 \in [P_{In}, \delta_0]$ (see the illustration in Fig.61). Since $f_p^{-1}(l) \subseteq \partial H_p$ (see Prop.3.3), because $\delta \cap l = \{\delta_0\}$ it follows $f_p^{-1}(\delta) \cap f_p^{-1}(l) = \{\delta_0\}$. Therefore, because $f_p(\mu_1) \subseteq \delta$, $\delta_0 \in f_p(\mu_1)$ we conclude that once μ_1 leaves $f_p^{-1}(\delta_0)$ it enters the interior of H_p and **does not** hit ∂H_p before hitting $\overline{H_p} \setminus f_p^{-1}(l)$. Therefore, since $\mu_1 \subseteq \Delta_1 \subseteq f_p^{-2}(l)$, by Cor.3.4 it follows that once μ_1 leaves $f_p^{-1}(\delta_0)$ it never hits ∂H_p before hitting δ_1 . Therefore, there exists a component $\gamma_1 \subseteq (\mu_1 \setminus \partial H_p)$ s.t. $\gamma_1 \cap \partial H_p = \{\delta_1, f_p^{-1}(\delta_0)\}$.

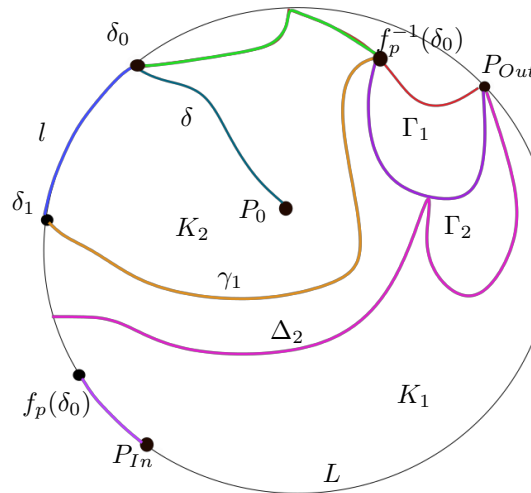


FIGURE 61. With previous notations, $J = \rho \cup \beta$, with β being the blue arc and ρ the green. Similarly, while $\Delta_1 = \gamma_1 \cup \Gamma_1$ (for simplicity, in this scenario $\gamma_1 = \mu_1$). The curves Γ_1, Γ_2 both lie strictly inside K_1 .

Now, consider K_1, K_2 the components of $\overline{H_p} \setminus \mu_1$, and recall the regions T_1, T_2 from the proof of Prop.3.5, defined by $\overline{H_p} \setminus \Delta_1$ - by definition, $D_1 \subseteq K_1$, $J \subseteq \partial K_2$ (see the illustration in Fig.61). In particular, $\partial H_p \cap \partial K_2 \cap l = [\delta_1, \delta_0]$, i.e., the sub-arc of $J \cap l$ connecting δ_1, δ_0 . Conversely, $\partial K_2 \cap \partial H_p \setminus l$ is the arc ρ on J connecting $\delta_0, f_p^{-1}(\delta_0)$ (see the illustration in Fig.61). Now, using a similar argument to the one used to prove Cor.3.4, it follows that **for**

every $n \geq 1$, we have $f_p^{-n}(\rho) \subseteq \Gamma_n$, $\Gamma_n \subseteq D_1$. Now, by $\rho \subseteq f_p^n(\Gamma_n)$, $\rho \subseteq \partial K_2$ and by $\Gamma_n \subseteq D_1 \subseteq K_1$, since $K_1 \cap K_2 = \emptyset$ it follows there can be no periodic orbits in ρ - as a consequence there are no periodic orbits for f_p in $f_p(\rho)$. And since ρ is the arc on $f_p^{-1}(l)$ connecting $\delta_0, f_p^{-1}(\delta_0)$ it follows $f_p(\rho) = [f_p(\delta_0), \delta_0]$, i.e., the arc on l connecting $f_p(\delta_0), \delta_0$ (see Fig.61).

Now, recall that by Lemma 3.10, δ_1 lies in $[P_{I_n}, \delta_0] \setminus f_p(\delta)$ - by definition, $f_p(\delta) = (P_{I_n}, f_p(\delta_0))$ (see Prop.3.2). Further recall that P_{I_n} is a saddle-focus with an unstable two-dimensional manifold transverse to $\{\dot{y} = 0\}$ at P_{I_n} - which implies that given $x \in \overline{H_p}$, $x \neq P_{I_n}$, $f_p^{-1}(x) \neq P_{I_n}$. Therefore, because $\delta_1 \in f_p^{-1}(\delta)$, as $P_{I_n} \notin \delta$ (see Prop.3.2) it follows $\delta_1 \neq P_{I_n}$ - which, by the discussion above, implies $\delta_1 \in (f_p(\delta_0), \delta_0)$. Or, in other words, the arc $[\delta_1, \delta_0] \subseteq l$ connecting δ_1, δ_0 satisfies $[\delta_1, \delta_0] \subseteq f_p(\rho)$. By definition, $J = [\delta_1, \delta_0] \cup \rho$, therefore, since there are no periodic orbits for f_p in ρ it follows there are no periodic orbits for f_p in J either, and Lemma 4.1 follows. \square

Having proven Lemma 4.1, we can now begin studying the periodic dynamics of f_p in the set Q in more depth. To begin, choose some $s \in \{1, 2\}^{\mathbb{N}}$, $s = \{i_0, \dots, i_k, i_0, \dots\}$ periodic of minimal period k , s.t. $i_0 = 2$. Let us now recall that per the notations in Prop.3.5 (and in more generality, Th.3.1), there exists a component D_s of Q s.t. $\pi(D_s) = s$, $\pi^{-1}(s) = D_s$ - and since we chose s to be periodic of minimal period k , by Cor.3.1.5 we know there exists at least one point $x_s \in D_s$ of minimal period k for f_p . As described earlier, in order to compute the Fixed Point Index of f_p^k on x_s we must first locate a neighborhood $B \subseteq H_p$ of x_s s.t. f_p^k has no fixed points in ∂B . We do so now -

Lemma 4.2. *Let $p \in P$ be a trefoil parameter, and let $s \in \{1, 2\}^{\mathbb{N}}$, $s = \{2, i_1, i_2, i_3, \dots\}$ be periodic of minimal period $k > 1$. Then, there exists an open set $B \subseteq H_p$ s.t. the following holds:*

- B is a topological disc.
- For every $j \in \{1, \dots, k\}$, f_p^j is continuous on \overline{B} .
- For every $i \neq j$, $i \in \{1, \dots, k-1\}$, $f_p^j(\overline{B}) \cap f_p^i(\overline{B}) = \emptyset$.
- $D_s \subseteq \overline{B}$.
- f_p^k has no fixed points in ∂B .
- Given any $\omega \in \{1, 2\}^{\mathbb{N}}$ of minimal period $j \leq k$, if $D_\omega \cap B \neq \emptyset$, then $s = \omega$ - i.e., D_s is the only component of Q corresponding to a periodic symbol of minimal period k which lies in B .

Proof. Recall that by its definition in Prop.3.5, for every $n \geq 1$ we have $f_p^n(D_s) \cap l = \emptyset$. Therefore, by the compactness of D_s , for every $n \geq 1$, the Euclidean Distance (in $\overline{D_\alpha}$) between D_s , and $I_n = \overline{f_p^{-n}(l)}$ must be positive. Now, recall the closed domains D_{i_0, \dots, i_n} introduced in the proof of Prop.3.5, with which we approximated D_s - by their construction in the proof of Prop.3.5, it follows immediately that $\partial D_{i_0, \dots, i_n}$ is a (finite) collection of arcs in $\cup_{n \geq 0} I_n$ (see the illustration in Fig.62). Therefore, it follows that provided n is sufficiently large, we have $\partial D_{i_0, \dots, i_n} \cap (\cup_{1 \leq j \leq 5k} f_p^{-j}(l) I_j) = \emptyset$ (with k denoting the minimal period of s) - that is, given any point $x \in \cup_{n \geq 0} I_n$, we in fact have $x \in I_j$, $j > 5k$. Now, recall that by the periodicity of s and the construction of D_s in Prop.3.5 it follows $f_p^r(D_s) \cap D_s \neq \emptyset$ only when $r = jk$ (for some $j \geq 1$). Therefore, provided we choose $n > 0$ to be sufficiently large, for every $i, j \in \{1, \dots, k-1\}$, $i \neq j$ we have $f_p^i(D_{i_0, \dots, i_n}) \cap f_p^j(D_{i_0, \dots, i_n}) = \emptyset$ - and moreover, for every $0 \leq i \leq k$ the function f_p^i is continuous on D_{i_0, \dots, i_n} .

Additionally, it should also be noted that because we chose $s = \{2, i_1, i_2, \dots\}$, in the notations introduced in the proof of Prop.3.5 it follows $D_s \subseteq D_2$ (see the proof of Prop.3.5) - as such, the domain D_{i_0, \dots, i_n} connects the two components of $J \setminus \{\delta_0\}$ (with J as in Lemma 4.1 - see Remark 3.6). As such, since D_{i_0, \dots, i_n} is trapped in D_2 by its construction, it follows $D_{i_0, \dots, i_n} \cap l \subseteq J$. Moreover, per the construction of D_{i_0, \dots, i_n} in the proof of Prop.3.5, D_{i_0, \dots, i_n} is the result of a finite number of intersections of Jordan domains - as such, by Kerekjarto's Theorem it is also a Jordan Domain - hence a topological disc (see [1], and the illustration in Fig.62).

To continue, choose two periodic symbols s_1, s_2 of minimal periods strictly greater than k s.t. $D_{s_1}, D_{s_2} \subseteq D_{i_0, \dots, i_n}$, and let B denote the **interior** of the component of $D_{i_0, \dots, i_n} \setminus (D_{s_1} \cup D_{s_2})$ s.t. $D_s \subseteq B$ (by the definition of D_{i_0, \dots, i_n} in the proof of Prop.3.5, there must exist such $s_1, s_2 \in \{1, 2\}^{\mathbb{N}}$). By the discussion above, since $B \subseteq D_{i_0, \dots, i_n}$, it must satisfy the following properties:

- For every $i \neq j$, $i \in \{1, \dots, k-1\}$, $f_p^j(\overline{B}) \cap f_p^i(\overline{B}) = \emptyset$.
- B is a topological disc.
- For every $1 \leq i \leq k$, f_p^i is continuous on \overline{B} .
- $D_s \subseteq \overline{B}$.
- $\partial B \cap (\cup_{1 \leq j \leq 5k} I_j) = \emptyset$.
- Every point in ∂B lies either in D_{s_1}, D_{s_2} , the arc J from Lemma 4.1, or $\cup_{j > 5k} I_j$. In particular, $\overline{B} \cap \delta = \emptyset$ (see the illustration in Fig.62).

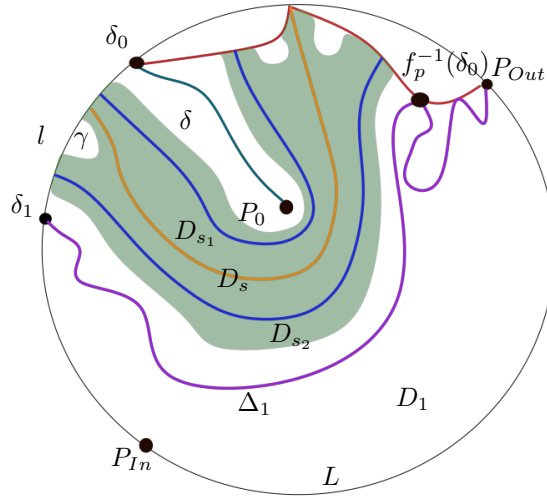


FIGURE 62. The set D_{i_0, \dots, i_n} is denoted by the green colored region, while B is the subset of D_{i_0, \dots, i_n} trapped between D_{s_1}, D_{s_2} and containing D_s .

Now, let $\omega \in \{1, 2\}^{\mathbb{N}}$ be periodic of minimal period **at most** k . For every such ω , by the compactness of both D_s, D_ω , the Euclidean distance between D_s, D_ω must be non-zero - and additionally, there is at most a finite number of such ω . Therefore, we choose D_{i_0, \dots, i_n} with n sufficiently large s.t. in addition to satisfying all the requirements above, if $D_\omega \subseteq Q \cap D_{i_0, \dots, i_n}$ then $\omega = s$. Therefore, this fact combined with the properties of B listed above implies that in order to conclude the proof of Lemma 4.2 it would suffice to prove ∂B has no fixed points for f_p^k .

To do so, recall we chose s_1, s_2 to be periodic of minimal period **greater** than k - additionally, by the invariance of Q under f_p it follows that $f_p^j(D_{s_i}) \subseteq D_{\sigma^j(s_i)}, i = 1, 2$, where $\sigma : \{1, 2\}^{\mathbb{N}} \rightarrow \{1, 2\}^{\mathbb{N}}$ denotes the one-sided shift (see Th.3.1 and in particular the proof of Prop.3.5). As such, since the minimal period of both s_1, s_2 is greater than k it follows that for $j, i \in \{0, \dots, k\}, r \in \{1, 2\}$ we have $f_p^i(D_{s_r}) \cap f_p^j(D_{s_r}) = \emptyset$. As such, f_p^k has no fixed points in $\partial B \cap (D_{s_1} \cup D_{s_2}) = A_1$. Additionally, since we chose D_{i_0, \dots, i_n} s.t. $\partial D_{i_0, \dots, i_n} \cap (\cup_{1 \leq j \leq 5k} I_j) = \emptyset$, it follows that if $x \in \partial B$ lies in I_n , for some n , n has to be greater than $5k$ - and in particular, $f_p^k(x) \neq x$, which implies f_p^k has no periodic points in $\partial B \cap (\cup_{j \geq 0} I_j) = A_2$ as well. Finally, by Lemma 4.1, f_p^k has no periodic points in $\partial B \cap J = A_3$. Therefore, since by construction $\partial B = A_1 \cup A_2 \cup A_3$ we conclude f_p^k has no periodic points in ∂B and Lemma 4.2 now follows. \square

Remark 4.2. In fact, we can say more - let us first recall the regions K_1, K_2 introduced in the proof of Lemma 4.1. By the arguments above, it follows $B \subseteq K_2$ - and since $\Gamma_n = f_p^{-n}([P_{Out}, \delta_0]) \subseteq K_1$ for every $n > 1$, it immediately follows that for every $n > 1$ we have $\partial B \cap \Gamma_n = \emptyset$. Or, in other words, since $f_p^{-1}(l) = \delta \cup \Gamma_1$ and because $f_p^{-n}(\Gamma_1) = \Gamma_{n+1} \subseteq K_1$ it follows that any arc $\gamma \subseteq \partial B$ which **does not** lie on either J, D_{s_1}, D_{s_2} lies in some pre-image of δ .

Having proven Lemma 4.2 we conclude Stage I of the proof of Th.4.1 with the following result:

Corollary 4.1.1. Let $p \in P$ be a trefoil parameter - then, with the assumptions and notations of Lemma 4.2, the set $F = \{x \in B | f_p^k(x) = x\}$ is non-empty and compact.

Proof. By the continuity of f_p^k on B , F is closed in \overline{B} . Since by Lemma 4.2 there are no fixed points for f_p^k in ∂B , it is also compact in B . Moreover, because $D_s \subseteq B$, by Cor.3.1.5 $F \neq \emptyset$ and the assertion follows. \square

4.2. Stage II - computing the fixed-point index of f_p^k on B . As stated in the beginning of the proof, we will prove Th.4.1 by applying the Fixed-Point Index - and to this end, we need an effective way of computing it. We do so now - namely, in this stage of the proof we prove the fixed point index of f_p^k on the set B defined in Stage I is positive, and we do so using Lemmas 4.1 and 4.2. We will do so by proving the dynamics of f_p on $\overline{H_p}$ can be continuously deformed to those of a Smale Horseshoe map $H : ABCD \rightarrow \mathbf{R}^2$ (acting on some rectangle $ABCD$) - therefore, by the hyperbolicity of periodic orbits for the Smale Horseshoe map and the invariance of the Fixed Point Index under homotopies the assertion will follow. However, as we will discover, for this argument to work we will need to construct the homotopy described above very carefully. Therefore, Stage II is entirely devoted to proving the following fact:

Proposition 4.3. *With previous notations and definitions, let $p \in P$ be a trefoil parameter, let $s \in \{1, 2\}^{\mathbb{N}}$ be periodic of minimal period k , $s = \{2, i_1, i_2, \dots\}$, and let D_s denote the corresponding component in Q . Finally, let B denote the topological disc constructed in Lemma 4.2 s.t. $D_s \subseteq \overline{B}$ - then, the Fixed-Point Index of f_p^k on B is non-zero.*

Proof. Recall the imposition of $f_p(H_p)$ on H_p in Fig.55, let $s \in \{1, 2\}^{\mathbb{N}}$, D_s be as above, and let B be as in Lemma 4.2 (in particular, recall D_s includes x_s , a periodic point for f_p of minimal period k - see Cor.3.1.5). Before diving into the technical details of the proof, let us first give a rough sketch of it - as stated, the proof is based upon constructing a very specific continuous deformation of the dynamics of $f_p : \overline{H_p} \rightarrow \overline{D_\alpha}$ to those of a Smale Horseshoe map $H : ABCD \rightarrow \mathbf{R}^2$ (with $ABCD$ denoting some topological rectangle, which can be continuously deformed to the slit disc H_p). As we will see, this deformation will induce a homotopy $g_t : B \rightarrow \mathbf{R}^2$, $t \in [0, 1]$ s.t. $g_0 = f_p$, $g_1 = H$ - and by the hyperbolicity of H on its non-wandering set, it will then follow the Fixed-Point Index of $g_1^k = H^k$ on B is positive. In more detail, denote by $F_t = \{x \in B | g_t^k(x) = x\}$ (by definition, $F_0 = F$ from Cor.4.1) - it will be clear from our construction of the homotopy $\{g_t\}_{t \in [0, 1]}$ that $\cup_{t \in [0, 1]} F_t \times \{t\}$ is compact in $B \times [0, 1]$. Therefore, since the Fixed-Point Index of $H^k = g_1^k$ on B is positive, by the invariance of the Fixed-Point Index under homotopies it would then follow the Fixed-Point Index of $f_p^k = g_0^k$ on B is also positive (see the discussion at the beginning of the proof of Th.4.1).

Per the sketch of proof above, let us begin with homotoping f_p to a Smale Horseshoe map. Let us first recall the cross-sections $\overline{H_p}$, $\overline{D_\alpha}$ introduced in Prop.3.3 and Prop.3.1, and recall $\overline{H_p} \subseteq \overline{D_\alpha}$, and that $f_p : \overline{H_p} \setminus \delta \rightarrow \overline{D_\alpha}$ is continuous (with δ as in Prop.3.2) - see Remark 3.4. We will construct the said homotopy in three consecutive steps, s.t. at each step we carefully construct another part of the homotopy. We begin with the following:

4.2.1. *Step I - constructing the homotopy $\{g_t\}_{t \in [0, \frac{1}{8}]}$.* Before constructing the deformation, we first study the set ∂B - as we will see, this will give us a clear motivation how to construct the deformation $\{g_t\}_{t \in [0, \frac{1}{8}]}$. As stated earlier, by its construction in Lemma 4.2 and Remark 4.2, ∂B is made out of arcs on the curve J , arcs on D_{s_1}, D_{s_2} and arcs γ on $\cup_{j>k} f_p^{-j}(\delta)$ (see Lemma 4.2 and Remark 4.2) - see the illustration in Fig.62. As such, $\partial B \setminus (D_{s_1} \cup D_{s_2})$ is composed from a collection of arcs in $M = J \cup (\cup_{j>k} f_p^{-j}(\delta))$ - moreover, any component of $M \setminus J$ is an arc γ in $\cup_{j>k} f_p^{-j}(\delta)$, s.t. γ is an arc with endpoints on J (see the illustration in Fig.62). As such, since the components of ∂B are strongly dependent on the dynamics of f_p , it follows that when we continuously deform the map $f_p : \overline{H_p} \rightarrow \overline{D_\alpha}$ to some $g : \overline{H_p} \rightarrow \overline{D_\alpha}$, the deformation induces a continuous deformation of B to another domain, B' .

To make things more precise, consider a homotopy $\{g_t\}_{t \in [0, \frac{1}{8}]}$, $g_t : \overline{H_p} \setminus \delta \rightarrow \overline{D_\alpha}$ s.t. $g_0 = f_p$, and write $B = B_0$. Since the deformation is continuous, because B_0 is generated by the dynamical properties of f_p (see the proof of Lemma 4.2) it will follow B_0 is continuously deformed under the homotopy to a topological disc B_t , $t \in (0, \frac{1}{8}]$ (at least provided the homotopy is sufficiently well-behaved). As we will prove, recalling the set J (see the discussion before Lemma 4.1), we can choose such a deformation s.t. for every $t \in [0, \frac{1}{8}]$ B_t is defined and g_t^k has no fixed-points in ∂B_t - and moreover, for $t = \frac{1}{8}$ we have $\partial B_{\frac{1}{8}} \subseteq D_{s_1, \frac{1}{8}} \cup D_{s_2, \frac{1}{8}} \cup J$. In other words, we prove there exists a deformation of f_p s.t. B is continuously deformed to $B_{\frac{1}{8}}$ s.t. no new fixed points for g_t^k are added, and moreover, the boundary arcs of $(\partial B \cap (\cup_{j>k} f_p^{-j}(\delta))) \setminus J$ are all removed (see the illustration in Fig.63 and 64). By construction, it will be evident the maps $g_t^k : \overline{B_t} \rightarrow \overline{D_\alpha}$ are also homotopic.

To begin, consider an arc $\gamma \subseteq \partial B \cap (\cup_{j>k} f_p^{-j}(\delta))$ as above (see the illustration in Fig.63). By the discussion above, γ lies in a component of $f_p^{-j}(\delta)$ for some $j > k$ - i.e., there exists some $j > 0$ s.t. $f_p^j(B) \cap \delta \neq \emptyset$. Moreover, $J \cup \gamma$ trap between them a Jordan domain, D_γ (see the illustration in Fig.63). Now, recall we have the inclusion $\overline{H_p} \setminus \overline{D_\alpha}$ and that $f_p(\overline{H_p}) \subseteq \overline{D_\alpha}$.

Now, define the homotopy $\{g_t\}_{t \in [0, \frac{1}{8}]}$, $g_t : \overline{H_p} \setminus \delta \rightarrow \overline{D_\alpha}$ s.t. the following conditions hold:

- For every $t \in [0, \frac{1}{8}]$, g_t is conjugate on $\overline{H_p} \setminus \delta$ to $f_p = g_0$.
- For every $\gamma \subseteq \partial B$ as described above, the homotopy contracts D_γ to a singleton on J . That is, when t goes from 0 to $\frac{1}{8}$, D_γ is contracted to a singleton $T_\gamma \in J$ for $g_{\frac{1}{8}}$ (see the illustration in Fig.64).
- For every $t \in [0, \frac{1}{8}]$, g_t is injective on $\overline{H_p} \setminus \delta$, and $P_0 \notin g_t(\overline{H_p} \setminus \delta)$ (see the illustration in Fig.64).

Now, recall the construction of the set Q from the proof of Th.3.1 (see Prop.3.5). Since g_t , $t \in (0, \frac{1}{8})$ is conjugate to f_p on $\overline{H_p} \setminus \delta$ the arguments used to prove Prop.3.5 and Cor.3.1.5 also apply for g_t , $t \in [0, \frac{1}{8}]$ - from which it follows that since g_t varies continuously in t , **so does the set Q** . Or, in other words, given any $t \in [0, \frac{1}{8}]$, there exists a g_t -invariant set $Q_t \subseteq \overline{H_p} \setminus \delta$, and a continuous map $\pi_t : Q_t \rightarrow \{1, 2\}^{\mathbb{N}}$ s.t. the following holds:

- $\pi_t \circ g_t = \sigma \circ \pi_t$, with $\sigma : \{1, 2\}^{\mathbb{N}} \rightarrow \{1, 2\}^{\mathbb{N}}$ denoting the one-sided shift.

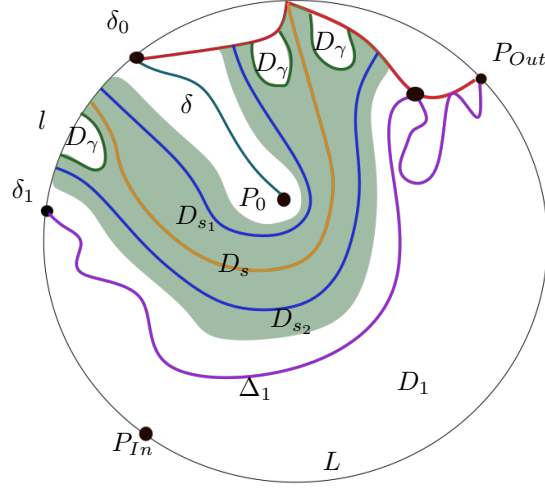


FIGURE 63. The set B is the subset of the green region, trapped between D_{s_1}, D_{s_2} and containing D_s (the orange curve). The dark green curves correspond to curves $\gamma \subseteq \cup_{j>k} f_p^{-j}(\delta) \setminus J$, while D_{γ} are the regions trapped between γ and J .

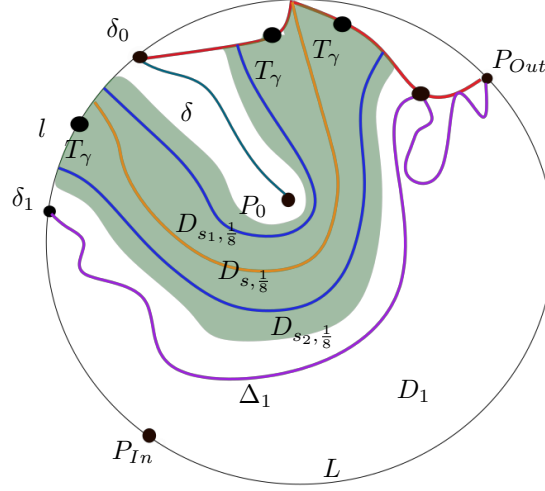


FIGURE 64. The set $B_{\frac{1}{8}}$ is the subset of the green region, trapped between $D_{s_1, \frac{1}{8}}, D_{s_2, \frac{1}{8}}$ and containing $D_{s, \frac{1}{8}}$ (the orange curve). The domains D_{γ} were contracted to the points T_{γ} .

- Given any periodic $\omega \in \{1, 2\}^{\mathbb{N}}$, $\omega \in \pi_t(Q_t)$.
- For any periodic $\omega = \{2, i_1, i_2, \dots\}$, $\pi_t^{-1}(\omega) = D_{\omega, t}$ is compact, and connects the two components of $\partial H_p \setminus \{P_0, P_{In}\}$.
- $\pi_0 = \pi$ and $Q_0 = Q$, with Q, π as in Th.3.1.
- Given any periodic $\omega \in \{1, 2\}^{\mathbb{N}}$, when we vary g_t to g_r , $D_{\omega, t}$ is continuously deformed to $D_{\omega, r}$ (see the illustration in Fig.64).

In fact, we can say more. Since $\{g_t\}_{t \in [0, \frac{1}{8}]}$ is a homotopy, it follows the set $\cup_{n \geq 0} g_t^{-n}(\partial H_p)$ varies continuously. Now, because the set B is bounded by arcs on $J, \cup_{n > 5k} f_p^{-n}(\partial H_p)$ and D_{s_1}, D_{s_2} (see the proof of Lemma 4.2), by $D_{s_i, 0} = D_{s_i}$, $i = 1, 2$ and $g_0 = f_p$, it follows the set B **also** varies continuously. That is, writing $B = B_0$, the homotopy $g_t, t \in [0, \frac{1}{8}]$ induces a continuous deformation of $B_t, t \in [0, \frac{1}{8}]$. As such, since $B = B_0$ is a topological disc, for every $t \in [0, \frac{1}{8}]$ B_t would be simply connected, and homeomorphic to a topological disc - and in particular, for every $t \in [0, \frac{1}{8}]$ $D_{s_1, t}, D_{s_2, t}$ intersect ∂B_t (see the illustration in Fig.64). Now, recall Lemma 4.2 proves that for every $j \in \{1, \dots, k\}$, f_p^j is defined and continuous on \bar{B} - and that for every $i, j \in \{0, \dots, k-1\}$ we have $f_p^i(\bar{B}) \cap f_p^j(\bar{B}) = \emptyset$. Additionally, recall the curve γ defined above, $\gamma \subseteq \partial B_0 = \partial B$ - by this discussion it follows that we can deform $f_p = g_0$ to $g_{\frac{1}{8}}$ s.t. the following extra conditions are **also** satisfied by the homotopy $\{g_t\}_{t \in [0, \frac{1}{8}]}$:

- For every γ as defined above, $T_{\gamma} \in \partial B_{\frac{1}{8}}$ (see the illustration in Fig.64).
- For every $j \in \{1, \dots, k\}$, g_t^j is defined and continuous on \bar{B}_t .

- For every $i, j \in \{0, \dots, k-1\}$ we have $g_t^i(\overline{B_t}) \cap g_t^j(\overline{B_t}) = \emptyset$.
- Recall the definition of $\Gamma_n = f_p^{-n}([\delta_0, P_{Out}])$ - because $B \cap \Gamma_n = \emptyset$ for every $n > 1$ (see Remark 4.2), we choose the continuous deformation $\{g_t\}_{t \in [0, \frac{1}{8}]}$ s.t. for every $n > 1$, $g_t^{-n}([\delta_0, P_{Out}]) \cap \overline{B_t} = \emptyset$ (that is, $g_t^{-n}(J) \cap \overline{B_t} = \emptyset$ for every $t \in -[0, \frac{1}{8}]$ - see the illustration in Fig.64).

As a consequence, $g_t^k : \overline{B_t} \rightarrow \overline{D_\alpha}$ defines a homotopy of continuous maps. Additionally, because B_t vary continuously in $t \in [0, \frac{1}{8}]$ and because $T_\gamma \in J$ for every γ it follows $\partial B_{\frac{1}{8}} \subseteq J \cup D_{s_1, \frac{1}{8}} \cup D_{s_2, \frac{1}{8}}$. In particular, it follows the arguments of Lemma 4.2 and Lemma 4.1 **both** apply to $B_{\frac{1}{8}}$. Or, in other words, writing $F_{\frac{1}{8}} = \{x \in B_{\frac{1}{8}} | g_{\frac{1}{8}}^k(x) = x\}$ it follows $F_{\frac{1}{8}}$ is compact in the (open) topological disc $B_{\frac{1}{8}}$ - that is, $g_{\frac{1}{8}}^k$ has no fixed points in $\partial B_{\frac{1}{8}}$.

Analogously, for every $t \in [0, \frac{1}{8}]$ define $F_t = \{x \in B_t | g_t^k(x) = x\}$ - since for every $t \in [0, \frac{1}{8}]$ the function g_t is conjugate to $f_p = g_0$ on $\overline{H_p} \setminus \delta$, it follows that because $F = F_0$ is compact in $B = B_0$, the same is true for F_t in B_t , $t \in [0, \frac{1}{8}]$ (i.e., F_t lies in a positive distance from ∂B_t). We now claim the set $Fix(\frac{1}{8}) = \cup_{t \in [0, \frac{1}{8}]} F_t \times \{t\}$ is compact in $B(\frac{1}{8}) = \cup_{t \in [0, \frac{1}{8}]} B_t \times \{t\}$. Since the set $Fix(\frac{1}{8}) = \cup_{t \in [0, \frac{1}{8}]} F_t \times \{t\}$ is already closed in $\overline{H_p} \times [0, \frac{1}{8}]$, it would suffice to prove there are no sequences $\{(x_n, t_n)\}_n \subseteq Fix(\frac{1}{8})$ accumulating in $\cup_{t \in [0, \frac{1}{8}]} \partial B_t \times \{t\}$. We do so by contradiction - assume there exists such a sequence, and let (x, t) be its partial limit in $\cup_{t \in [0, \frac{1}{8}]} \partial B_t \times \{t\}$. Now, recall $f_p = g_0$ is deformed continuously to $g_{\frac{1}{8}}$. Moreover, recall that by our construction of the homotopy $\{g_t\}_{t \in [0, \frac{1}{8}]}$, g_t^j is continuous on $\overline{B_t}$ for every $t \in [0, \frac{1}{8}]$. Therefore, since for every $n > 1$ we have $g_{t_n}^k(x_n) = x$, by the continuous deformation of $f_p = g_0$ to g_t it follows $g_t^k(x) = x$, i.e., g_t^k has a fixed point in ∂B_t . As we already proved this cannot occur, we have a contradiction and we conclude $Fix(\frac{1}{8})$ is compact in $B(\frac{1}{8}) = \cup_{t \in [0, \frac{1}{8}]} B_t \times \{t\}$.

Therefore, all in all, we may summarize our results as follows:

Corollary 4.1.2. *There exists a homotopy $\{g_t\}_{t \in [0, \frac{1}{8}]}$, $g_t : \overline{H_p} \setminus \delta \rightarrow \overline{D_\alpha}$ s.t. the following holds:*

- Every component γ in $\partial B \setminus (J \cup D_{s_1} \cup D_{s_2})$ is removed by the homotopy.
- The homotopy varies $B = B_0$ to B_t - and in particular, for every $t \in [0, \frac{1}{8}]$, B_t is a topological disc.
- The fixed-points of g_t^k , $t \in [0, \frac{1}{8}]$ remain away from ∂B_t - namely, the set $Fix(\frac{1}{8})$ is compact in $B(\frac{1}{8}) = \cup_{t \in [0, \frac{1}{8}]} B_t \times \{t\}$.

As must be remarked at this stage, by the discussion at the beginning of the proof of Th.4.1, it follows the Fixed-Point Indices of $f_p^k = g_0^k$ on $B = B_0$ and that of $g_{\frac{1}{8}}^k$ on $B_{\frac{1}{8}}$ **are the same** (however, we still need to compute them).

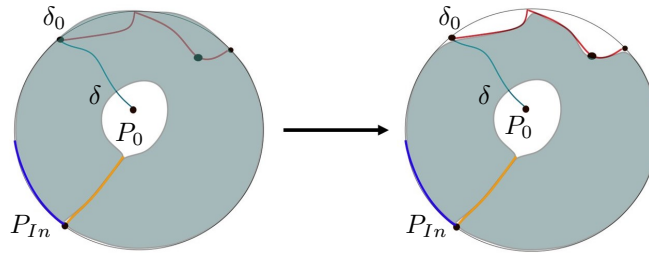


FIGURE 65. The homotopy deforming $g_{\frac{1}{8}}(\overline{H_p} \setminus \delta)$ (the grey area) on the left to $g_{\frac{1}{4}}(\overline{H_p} \setminus \delta)$ on the right, with the blue and orange curves corresponding to the double-sided limits at δ . As can be seen, $g_{\frac{1}{4}}(\overline{H_p} \setminus \delta) \subseteq \overline{H_p}$.

4.2.2. Step II - constructing $\{g_t\}_{t \in [\frac{1}{8}, \frac{3}{4}]}$. Having constructed the homotopy $\{g_t\}_{t \in [0, \frac{1}{8}]}$ we now extend the homotopy to the interval $[\frac{1}{8}, \frac{3}{4}]$ - and we do so in two steps: first we extend $\{g_t\}_t \in [0, \frac{1}{8}]$ to $[\frac{1}{8}, \frac{1}{2}]$, and then to $[\frac{1}{2}, \frac{3}{4}]$. After that, we prove that B_t in fact also extends and varies for $t \in [0, \frac{3}{4}]$ - and most importantly, that throughout the homotopy, no new fixed-points are generated in ∂B_t . In particular, we will conclude this section by showing the set of fixed points for $\{g_t^k\}_{t \in [0, \frac{3}{4}]}$ is compact in $\cup_{t \in [0, \frac{3}{4}]} B_t \times \{t\}$ - thus extending the conclusions of Cor.4.1.2 to the interval $[0, \frac{3}{4}]$.

To begin, first continuously deform $g_{\frac{1}{8}}$ to $g_{\frac{1}{4}}$ by pushing $g_{\frac{1}{8}}(\partial H_p \setminus \delta)$ inside $\overline{H_p}$, as depicted in Fig.65 - that is, the homotopy $g_t : \overline{H_p} \setminus \delta \rightarrow \overline{D_\alpha}$, $t \in [\frac{1}{8}, \frac{1}{4}]$ is a continuous deformation which ends in a way s.t. $g_{\frac{1}{4}}(\overline{H_p} \setminus \delta) \subseteq \overline{H_p}$ (see the illustration in Fig.65). Like we did for $t \in [0, \frac{1}{8}]$, we extend the homotopy to $t \in [\frac{1}{8}, \frac{1}{4}]$ the homotopy s.t. the following two conditions are satisfied for every $t \in [0, \frac{1}{4}]$:

- $P_0 \notin g_t(\overline{H_p} \setminus \delta)$.
- g_t is injective on $\overline{H_p} \setminus \delta$.

Now, having constructed the homotopy $\{g_t\}_{t \in [0, \frac{1}{4}]}$, extend it to $[\frac{1}{4}, \frac{1}{2}]$ as follows - blow up δ to an open set as described in Fig.66, thus blowing up all the components of $\cup_{j>0} g_t^{-j}(\delta)$, $\frac{1}{2} > t > \frac{1}{4}$ to open sets (see the illustration in Fig.66). This also has the effect of continuously extending g_t , $\frac{1}{2} > t > \frac{1}{4}$ to δ , as illustrated in Fig.66, which turns $g_t(\overline{H_p})$ into the Banana-shaped figure in Fig.66 (i.e., we blow up δ to a Jordan arc CD with two endpoints, C, D on ∂H_p - see the illustration in Fig.66). Moreover, choose the homotopy $g_t : \overline{H_p} \setminus \delta \rightarrow \overline{D_\alpha}$ s.t. $P_0 \notin g_t(\overline{H_p})$, $t \in [\frac{1}{4}, \frac{1}{2}]$ - therefore, again, using similar arguments to those in Stage I we conclude the set $Q = Q_0$ is continuously deformed to Q_t , $t \in [0, \frac{1}{2}]$. That is, given $\omega \in \{1, 2\}^{\mathbb{N}}$, the components D_ω are continuously deformed to $D_{\omega, t}$. In particular, there exists a continuous map $\pi_t : Q_t \rightarrow \{1, 2\}^{\mathbb{N}}$ s.t. for $t \in [0, \frac{1}{4}]$:

- $\pi_t \circ g_t = \sigma \circ \pi_t$, with $\sigma : \{1, 2\}^{\mathbb{N}} \rightarrow \{1, 2\}^{\mathbb{N}}$ denoting the one-sided shift.
- Given any periodic $\omega \in \{1, 2\}^{\mathbb{N}}$, $\omega \in \pi_t(Q_t)$.
- For any periodic ω , $\pi_t^{-1}(\omega) = D_{\omega, t}$ is compact, and connects the two components of $\partial H_p \setminus \{P_0, P_{I_n}\}$.
- $\pi_0 = \pi$ and $Q_0 = Q$, with Q, π as in Th.3.1.
- Given any periodic $\omega \in \{1, 2\}^{\mathbb{N}}$, when we vary g_t to g_r , $D_{\omega, t}$ is continuously deformed to $D_{\omega, r}$.
- Since by definition $\cup_{n>0} f_p^{-n}(\delta)$ varies continuously to $\cup_{n>0} g_{\frac{1}{2}}^{-n}(CD)$, similar arguments to those used in

Step I now imply the set $B = B_0$ is continuously deformed to B_t when we vary t from 0 to $t \in (0, \frac{1}{2}]$. Moreover, for every $t \in [0, \frac{1}{2}]$, B_t remains a topological disc.

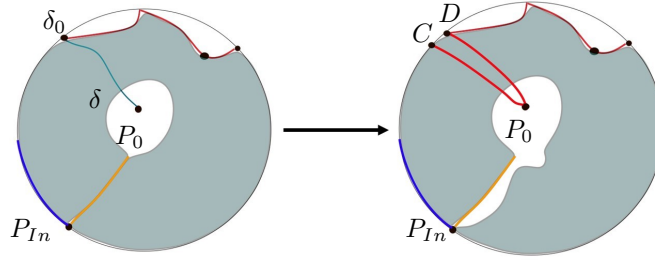


FIGURE 66. The homotopy deforming $g_{\frac{1}{4}}(\overline{H_p} \setminus \delta)$ (the grey area) on the left to $g_{\frac{1}{2}}(\overline{H_p} \setminus \delta)$ on the right, with the blue and orange curves corresponding to the double-sided limits at δ for $g_{\frac{1}{4}}$. As can be seen, the homotopy splits the curve δ to the arc $[C, D]$, s.t. the **union** blue and orange line now denote $g_{\frac{1}{2}}(CD)$ (with $P_{I_n} = g_{\frac{1}{2}}(P_0)$).

Having constructed the homotopy $\{g_t\}_{t \in [0, \frac{1}{2}]}$, we now extend it to $[\frac{1}{2}, \frac{3}{4}]$, by deforming $g_{\frac{1}{2}}$ to a (topological) rectangle map as described below. To do so, open up the fixed point P_{I_n} to an interval $AB = I_{I_n}$ s.t. $g_t : \overline{H_p} \rightarrow \overline{D_\alpha}$, $t \in [\frac{1}{2}, \frac{3}{4}]$ is an isotopy **and** $g_{\frac{3}{4}}$ satisfies both $g_{\frac{3}{4}}(I_{I_n}) \subseteq I_{I_n}$ and $g_{\frac{3}{4}}(CD) \subseteq I_{I_n}$ (see the illustration in Fig.67). Moreover, choose the isotopy s.t. for every $t \in [\frac{1}{2}, \frac{3}{4}]$, we have $g_t(P_0) \notin g_t(\overline{H_p})$. Now, after choosing an AB and CD sides, we can now re-draw $g_{\frac{3}{4}}$ as a rectangle map, as illustrated in Fig.68.

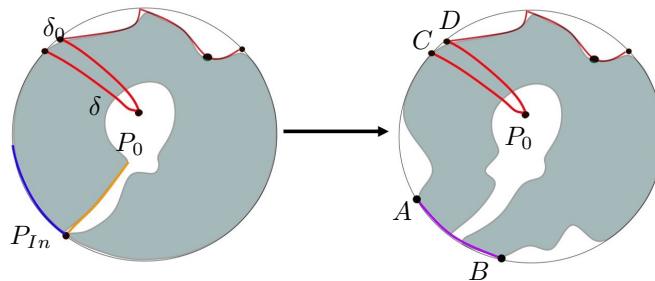


FIGURE 67. The homotopy deforming $g_{\frac{1}{2}}(\overline{H_p} \setminus \delta)$ (the grey area) on the left to $g_{\frac{3}{4}}(\overline{H_p} \setminus \delta)$ on the right. As can be seen, the homotopy stretches the fixed point P_{I_n} on the boundary to an interval $I_{I_n} = [A, B]$ s.t. $g_{\frac{3}{4}}(C, D) \subseteq I_{I_n}$.

Now, let us recall that by the construction of $Q = Q_0$ in Prop.3.5, its components lie away from both P_{I_n}, δ - therefore, because by our construction $P_0 \notin g_t(\overline{H_p} \setminus \delta)$, $t \in [0, \frac{3}{4}]$, we conclude again that $Q = Q_0$ is continuously deformed to Q_t , $t \in [0, \frac{3}{4}]$. As a consequence, again it follows the set B is deformed to B_t , $t \in [0, \frac{3}{4}]$ - in particular,

because $\overline{B_0} = \overline{B}$ lies away from P_{In}, δ for $f_p = g_0$ (see the proof of Lemma 4.2), it follows that when we vary $f_p = g_0$ to $g_{\frac{3}{4}}$, the set $B = B_0$ is continuously deformed to $B_{\frac{3}{4}}$. And because we constructed the homotopy in Stage I s.t. $\partial B_{\frac{1}{8}} \subseteq J \cap D_{s_1, \frac{1}{8}} \cup D_{s_2, \frac{1}{8}}$, on top of the properties listed above, we can further choose the homotopy $\{g_t\}_{t \in [0, \frac{3}{4}]}$ s.t. the following conditions are satisfied:

- $g_t : \overline{B_t} \rightarrow \overline{D_\alpha}$, $t \in [0, \frac{3}{4}]$ is a homotopy of continuous maps.
- Since $g_{\frac{1}{8}}^j$ is continuous and defined on $\overline{B_{\frac{1}{8}}}$ for every $j \in \{1, \dots, k\}$, we choose the homotopy s.t. for $\frac{3}{4} \geq t > \frac{1}{8}$ g_t^j is also defined and continuous on $\overline{B_t}$ (i.e., for $j \in 1, \dots, k$, $g_t^j(\overline{B_t}) \subseteq \overline{H_p}$).
- Since for every $i, j \in \{0, \dots, k-1\}$, $i \neq j$ we have $g_{\frac{1}{8}}^i(\overline{B_{\frac{1}{8}}}) \cap g_{\frac{1}{8}}^j(\overline{B_{\frac{1}{8}}}) = \emptyset$, we construct the homotopy s.t. for $\frac{3}{4} \geq t > \frac{1}{8}$ we also have $g_t^i(\overline{B_t}) \cap g_t^j(\overline{B_t}) = \emptyset$.
- For $\frac{3}{4} \geq t > \frac{1}{8}$, the action of g_t^k on $\overline{B_t}$ is conjugate to that of $g_{\frac{1}{8}}^k$ on $\overline{B_{\frac{1}{8}}}$. **Consequently**, by Cor.4.1.2 it follows that setting $Fix(t) = \{x \in B_t | g_t^k(x) = x\}$ is compact in B_t , $t \in [0, \frac{3}{4}]$.
- For every $t \in [0, \frac{3}{4}]$, the map g_t is injective on $\overline{H_p} \setminus \delta$ (with $\delta = CD$ for $t \geq \frac{1}{2}$).

To conclude Step II in the proof of Prop.4.3, let us remark that again, similar arguments to those used in Step I now imply the set $Fix(\frac{3}{4}) = \cup_{t \in [0, \frac{1}{2}]} F_t \times \{t\}$ is compact in $\cup_{t \in [0, \frac{3}{4}]} B_t \times \{t\}$. Therefore, combined with Cor.4.1.2 we can summarize our results as follows:

Corollary 4.1.3. *There exists a homotopy $\{g_t\}_{t \in [0, \frac{3}{4}]}$, $g_t : \overline{H_p} \setminus \delta \rightarrow \overline{D_\alpha}$ s.t. $B = B_0$ is continuously varied to B_t - moreover, for every t , B_t is a topological disc. Additionally, the fixed-points of g_t^k , $t \in [0, \frac{3}{4}]$ in B_t remain away from ∂B_t - namely, the set $Fix(\frac{3}{4})$ defined above is compact in $\cup_{t \in [0, \frac{3}{4}]} B_t \times \{t\}$.*

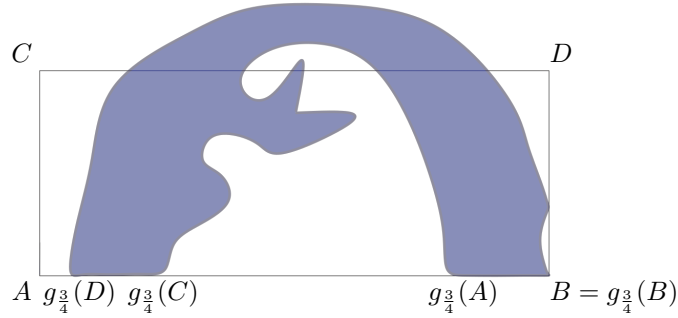


FIGURE 68. $g_{\frac{3}{4}}(\overline{H_p} \setminus \delta)$ sketched as a rectangle map.

4.2.3. Step III - constructing $\{g_t\}_{t \in [\frac{3}{4}, 1]}$ and concluding the proof. Having constructed the homotopy $\{g_t\}_{t \in [\frac{3}{4}, 1]}$, we now extend it to $[\frac{3}{4}, 1]$ and conclude the proof of Prop.4.3. To this end, let us consider the components of $Q_{\frac{3}{4}}$ - similarly to the argument in the proof of Prop.3.5, every component $D_{\omega, \frac{3}{4}}$, $\omega \in \{1, 2\}^{\mathbb{N}}$ in $Q_{\frac{3}{4}}$ is homeomorphic to a convex set, thus contractible. Because $g_{\frac{3}{4}}$ is a rectangle map of the rectangle $ABCD$ (see Fig.68), the argument used to prove Prop.3.5 now implies the following fact - for every $t \in [0, \frac{3}{4}]$ there exists a g_t -invariant $Q_t \subseteq \overline{H_p}$ and a continuous map $\pi_t : Q_t \rightarrow \{1, 2\}^{\mathbb{N}}$ s.t. the following conditions are satisfied (with $Q_0 = Q$, $\pi_0 = \pi$ from Th.3.1):

- $\pi_t \circ g_t = \sigma \circ \pi_t$, with $\sigma : \{1, 2\}^{\mathbb{N}} \rightarrow \{1, 2\}^{\mathbb{N}}$ denoting the one-sided shift.
- Given any periodic $\omega \in \{1, 2\}^{\mathbb{N}}$, $\omega \in \pi_t(Q_t)$.
- For any periodic ω , $\pi_t^{-1}(\omega) = D_{\omega, t}$ is compact, and connects the two components of $\partial H_p \setminus \{P_0, P_{In}\}$ (with P_0, P_{In} replaced by the arcs CD, AB for $t > \frac{1}{4}$ - see Fig.66).
- $\pi_0 = \pi$ and $Q_0 = Q$, with Q, π as in Th.3.1.
- Given **any** periodic $\omega \in \{1, 2\}^{\mathbb{N}}$ (which is not the constant $\{1, 1, 1, \dots\}$), when we vary g_t to g_r , $D_{\omega, t}$ is continuously deformed to $D_{\omega, r}$.

However, unlike Prop.3.5, this time we can say a little more about $Q_{\frac{3}{4}}$ the invariant set of $g_{\frac{3}{4}}$ inside the rectangle $ABCD$. Since $g_{\frac{3}{4}}$ is a rectangle map as in Fig.68, using similar arguments to the proof of Prop.3.5 and Cor.3.1.5, we conclude there exists an invariant set $I \subseteq ABCD$ and a continuous, surjective map $\xi : I \rightarrow \{1, 2\}^{\mathbb{Z}}$ s.t. the following holds:

- $\xi \circ g_{\frac{3}{4}} = \zeta \circ \xi$, with $\zeta : \{1, 2\}^{\mathbb{N}} \rightarrow \{1, 2\}^{\mathbb{Z}}$ denoting the double-sided shift.
- Given $s \in \{1, 2\}^{\mathbb{Z}}$, $\xi^{-1}(s)$ is convex - hence, contractible.
- If $s \in \{1, 2\}^{\mathbb{Z}}$ is periodic of minimal period k (which is not the constant $\{\dots, 1, 1, 1, \dots\}$), $\xi^{-1}(s)$ contains a periodic point x_s of minimal period k - and moreover, for the said periodic point we **also** have $x_s \in D_{s, \frac{3}{4}}$, i.e., $x_s \in Q_{\frac{3}{4}}$.

- Conversely, given a periodic $s \in \{1, 2\}^{\mathbb{N}}$ of minimal period k , $s = \{i_0, i_1, \dots\}$ (which is not the constant $\{1, 1, 1, \dots\}$) all the periodic points in $D_{s, \frac{3}{4}}$ lie in $\xi^{-1}(s')$, $s' = \{\dots, i_k, i_0, i_1, \dots\}$.

Armed with this information, we now homotope $g_{\frac{3}{4}} : ABCD \rightarrow \overline{D_\alpha}$ to a Smale Horseshoe map $g_1 = H : ABCD \rightarrow \overline{D_\alpha}$. To do so, let R denote the maximal invariant set of $g_{\frac{3}{4}}$ in the rectangle $ABCD$ - first, homotope $g_{\frac{3}{4}}$ to $g_{\frac{7}{8}}$ by removing every component of $R \setminus I$, and then, homotope $g_{\frac{7}{8}}$ to $g_1 = H$ by crushing every component of I to a singleton. In particular, if $C \subseteq I$ a component of I which contains a periodic point x_C , crush C to x_C - as such, it now follows $g_1 = H$ is a Smale Horseshoe map, hence hyperbolic on its invariant set in $ABCD$ (see the illustration in Fig.69).

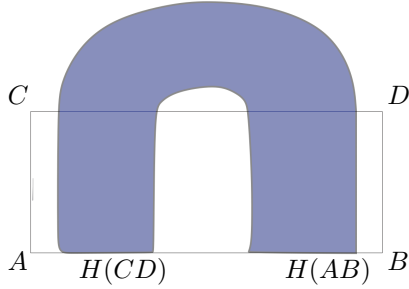


FIGURE 69. The map $g_1 = H$, a Smale Horseshoe map.

Now, let $\{g_t\}_{t \in [0,1]}$ denote the homotopy $g_t : \overline{H_p} \setminus \delta \rightarrow \overline{D_\alpha}$ (for $t > \frac{1}{2}$, δ is simply the CD side of the rectangle $ABCD$) - again, similar arguments to those used in Steps *I* and *II* imply we can choose the homotopy s.t. that the following conditions are satisfied:

- Recalling $D_s = D_{s,0}$ (see the discussion at the beginning of the proof), we always have $D_{s,t} \subseteq \overline{B_t}$. In particular, D_s is deformed continuously to $D_{s,1}$.
- Every component $D_{\omega,t}$ of Q_t is continuously deformed to a unique component $D_{\omega,1}$ of Q_t , $t \in [0,1]$. In particular, the deformation **does not** generate any new periodic points in Q_t , for $t > \frac{3}{4}$.
- Given two symbols in $\{1, 2\}^{\mathbb{N}}$, $\omega_1 \neq \omega_2$, we have $D_{\omega_1,1} \cap D_{\omega_2,1} = \emptyset$.
- Recall we denote by $\sigma : \{1, 2\}^{\mathbb{N}} \rightarrow \{1, 2\}^{\mathbb{N}}$ the one-sided shift. Therefore, for $t \in [0,1]$ it follows $g_t(D_{\omega,t}) \subseteq g(D_{\sigma(\omega),t})$. As a consequence, if the minimal period of $\omega \in \{1, 2\}^{\mathbb{N}}$ is d , then for every $0 \leq i, j < d$, if $i \neq j$ then $g_t^i(D_{\omega,t}) \cap g_t^j(D_{\omega,t}) = \emptyset$.
- All the periodic points in Q_t , $t \in [0,1]$ lie away from ∂H_p .
- The set $B_0 = B$ is continuously deformed to B_t , $t \in [0,1]$. Moreover, B_t is an open topological disc.

Now, recall the component D_s , the compact component of $Q = Q_0$ s.t. $\pi_0(D_s) = s \in \{1, 2\}^{\mathbb{N}}$, a periodic symbol of minimal period $k > 0$ s.t. $s = \{2, i_1, i_2, \dots\}$. In particular, because $s = \{2, i_1, i_2, \dots\}$ is periodic of minimal period k , a similar argument to that of Cor.3.1.5 implies that given $t \in [0,1]$, there exists a fixed point for g_t^k in $D_{s,t}$ - and since for every $t \in [0,1]$ we have $D_{s,t} \setminus \partial H_{p,t} \subseteq B_t$ it follows the set $F_t = \{x \in B_t | g_t^k(x) = x\}$ is not empty for all $t \in [0,1]$. As a consequence from the discussion above, similar arguments to those used in Steps *I* and *II* imply the homotopy $\{g_t\}_{t \in [0,1]}$ also induces a homotopy B_1 s.t. $g_t^k : \overline{B_t} \rightarrow \overline{D_\alpha}$, $t \in [0,1]$. Moreover, again we can choose the homotopy s.t. $\{g_t\}_{t \in [0,1]}$:

- For every $t \in [0,1]$ and every $j \in \{0, \dots, k\}$, g_t^j is defined and continuous on $\overline{B_t}$.
- For every $t \in [0,1]$ and every $i, j \in \{1, \dots, k-1\}$, $i \neq j$, we have $g_t^j(\overline{B_t}) \cap g_t^i(\overline{B_t}) = \emptyset$.
- Given $j \in \{1, \dots, k\}$, $1 \geq t > \frac{3}{4}$ we always have $g_t^j(\partial B_t) \subseteq H_p$, i.e., $g_{\frac{3}{4}}^j(\overline{B_t})$ is **strictly interior** to the rectangle $ABCD$. Consequentially, g_t^k has no fixed points on $\partial B_t \cap (AC \cup BD)$.

By the results of Steps *I* and *II*, we already know the set $Fix(\frac{3}{4}) = \cup_{t \in [0, \frac{3}{4}]} F_t \times \{t\}$ is compact in $B(\frac{3}{4}) = \cup_{t \in [0, \frac{3}{4}]} B_t \times \{t\}$ (with $F_t = \{x \in B_t | g_t^k(x) = x\}$). We now prove that for every $t \in [\frac{3}{4}, 1]$, g_t^k has no fixed points in ∂B_t . To see why it is so, first consider $B_{\frac{3}{4}}$ - by its construction in Step *II*, $\partial B_{\frac{3}{4}}$ is made out of two disjoint sub-arcs in the union $(AC \cup BD)$, along with subsets of $D_{s_1, \frac{3}{4}}, D_{s_2, \frac{3}{4}}$ (see the illustration in Fig.69). Therefore, when we homotope $g_{\frac{3}{4}}$ to g_1 it follows, again, that we can choose the homotopy s.t. for every $t \in [\frac{3}{4}, 1]$, ∂B_t is composed of precisely two arcs on $AC \cup BD$, along with subsets of $D_{s_1, t}, D_{s_2, t}$ - that is, for every $t \in [0,1]$, $\partial B_t \subseteq D_{s_1, t} \cup D_{s_2, t} \cup AC \cup BD$.

Now, let us recall that by the construction of $B = B_0$ in Lemma 4.2, s_1, s_2 are **both** periodic of minimal period **strictly greater** than k - therefore, for every $t \in [0,1]$, $D_{s_1, t}, D_{s_2, t}$ have no periodic points for g_t of minimal period $j \leq k$. Now, recall we constructed the homotopy $g_t : B_t \rightarrow \overline{D_\alpha}$ s.t. for $t \in (\frac{3}{4}, 1]$ g_t^k has no fixed points in

$\partial B_t \cap (AC \cup BD)$. Hence, all in all it follows $g_t^k, t \in (\frac{3}{4}, 1]$ has no fixed points in ∂B_t . Consequentially, the set $F_t = \{x \in B_t | g_t^k(x) = x\}$ is compact in the topological disc B_t for $t \in (\frac{3}{4}, 1]$.

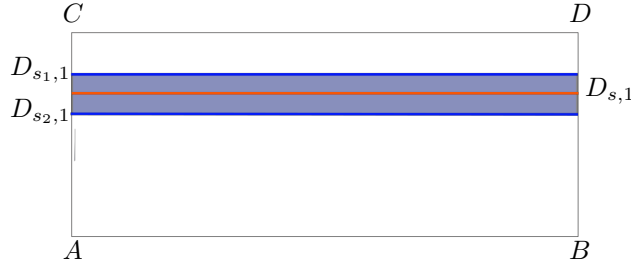


FIGURE 70. The set B_1 inside $ABCD$. The blue lines correspond to $D_{s1,1}$ and $D_{s2,1}$ while the orange line corresponds to $D_{s,1}$.

However, by the discussions preceding Cor.4.1.2 and 4.1.3 we already know that given $t \in [0, \frac{3}{4}]$, F_t is compact in B_t (with $B = B_0$) - by the discussion above we now conclude that given **any** $t \in [0, 1]$, F_t is compact in B_t . Therefore, using similar arguments to those used to prove both Cor.4.1.2 and 4.1.3 it follows the set $Fix(1) = \cup_{t \in [0,1]} F_t \times \{t\}$ has no accumulation points in $\cup_{t \in [0,1]} \partial B_t$ - that is, $Fix(1)$ is compact in $B(1) = \cup_{t \in [0,1]} B_t \times \{t\}$. Therefore, because $g_t^k : \overline{B_t} \rightarrow \overline{D_\alpha}$, $t \in [0, 1]$ is a homotopy by Ch.VII.5.8 in [5], it follows the Fixed-Point Index is constant along $g_t^k : B_t \rightarrow \overline{D_\alpha}$, $t \in [0, 1]$ - or, put simply, the fixed-point index of $f_p^k = g_0^k$ on $B = B_0$ is the same as that of g_1^k on B_1 . Let us denote the said index by $Ind(B, s)$ - all that remains to conclude the proof of Prop.4.3 is therefore to prove $Ind(B, s) \neq 0$.

To do so, we first prove $F_1 = \{x_1\}$, i.e., that F_1 is a singleton - to begin, recall we proved the sets B_t, Q_t all vary continuously with the homotopy $\{g_t\}_{t \in [0,1]}$. In particular, let us recall we constructed $B_0 = B$ s.t. if $\omega \in \{1, 2\}^{\mathbb{N}}$ is periodic of minimal period $j \leq k$ satisfying $D_\omega \cap B \neq \emptyset$, then $\omega = s$ - or, put simply, D_s is the **only** component of $Q = Q_0$ corresponding to a periodic symbol in $\{1, 2\}^{\mathbb{N}}$ of minimal period $j \leq k$ which intersects B . Therefore, because Q, B are varied continuously to $B_t, Q_t, t > 0$ as described above, given a periodic $\omega \in \{1, 2\}^{\mathbb{N}}$ of minimal period $j \leq k$ s.t. $D_{\omega,t} \cap B_t \neq \emptyset$, we have $s = \omega$. In other words, for every $t \in [0, 1]$, $F_t \subseteq D_{s,t} \cap B_t$. Consequentially, $F_1 \subseteq D_{s,1} \cap B_1$ - and since g_1 is a Smale horseshoe map, it follows $D_{s,1}$ contains **precisely** one fixed point, x_1 - hence $F_1 = \{x_1\}$.

Now, to conclude, since $g_1 : ABCD \rightarrow \overline{D_\alpha}$ is a Smale Horseshoe map by definition it is hyperbolic on its invariant set (see [4]). In particular, since g_1 is a \cap -Horseshoe map (see Fig.69), given a point $x \in ABCD$ in the invariant set of g_1 , the differential $D_x g_1$ has one eigenvalue $\lambda_1 > 1$ and another $\lambda_2 \in (0, 1)$ - therefore, if x is an isolated periodic point for g_1 of minimal period j , the degree of $g_1^j - Id$ is non-zero. Therefore, since $F_1 = \{x_1\} = \{x \in B_1 | g_1^k(x) = x\}$, it follows the degree of $g_1^k - Id$ on F_1 is non-zero. However, by definition, the Fixed-Point Index is simply the degree of $g_1^j - Id$ on the topological disc B_1 - therefore we conclude $Ind(B, s) \neq 0$ and Prop.4.3 follows. \square

Remark 4.3. As must be remarked, the rectangle map $g_{\frac{3}{4}} : ABCD \rightarrow \overline{D_\alpha}$ is a Topological Horseshoe (as defined in [17]). Topological Horseshoes were proven to exist in the Rössler System with the aid of rigorous numerics (albeit in non-heteroclinic parameters) - see [19])

4.3. Stage III - concluding the proof of Th.4.1. Having proven Prop.4.3, we now use it to conclude the proof of Th.4.1. To do so, recall we assume $p \in P$ is a trefoil parameter (see Def.2.4), and recall the cross-sections U_p and D_α (see the discussion before Lemma 2.1 and Lemma 3.1, respectively). Additionally, let us recall we originally chose a periodic $s \in \{1, 2\}^{\mathbb{N}}$, $s = \{2, i_1, i_2, \dots\}$ of minimal period k . Moreover, we constructed an open set B s.t. $f_p^j, j \in \{1, \dots, k\}$ is **continuous** on \overline{B} , s.t. $D_s \subseteq \overline{D_s}$ (see Lemma 4.2) - by Prop.4.3, the Fixed-Point Index of f_p^k on B is non-zero. Additionally, since $\overline{B} \subseteq \overline{H_p}$, by $\overline{H_p} \subseteq \overline{D_\alpha}$ (see Prop.3.3) and by Prop.3.2 it follows that given any $x \in \overline{B}$, $f_p^j(x)$ is strictly interior to the cross-section $\overline{D_\alpha} \subseteq \overline{U_p}$. That is, the flow line connecting $x, f_p(x), \dots, f_p^k(x)$ **always** intersects the cross-section transversely.

Now, recall that given any $v \in P$, the cross-section $\overline{U_p}$ is smoothly deformed to $\overline{U_v}$ (see the discussion before Lemma 2.1) - therefore, since $\overline{B} \subseteq \overline{U_p}$ it follows that when the vector field F_p is perturbed to F_v , the set B is continuously deformed to $\overline{B_v}$, $v \in P$. As a consequence, by previous paragraph we conclude that given $v \in P$ sufficiently close to p , the trefoil parameter, when we perturb the vector field F_p to F_v , $v \in P$, for every $s \in B_v$, $j \in \{1, \dots, k\}$ $f_p^j(s)$ is **transverse** to U_v - which, by the compactness of \overline{B} implies f_p^k is homotopic to f_v^k on $\overline{B_v}$. We now claim:

Lemma 4.3. *Let $p \in P$ be a trefoil parameter. Then, there exists a neighborhood $p \in O \subseteq P$, s.t. $\forall v \in O$, f_p^k has no fixed points in ∂B_v .*

Proof. Assume the assumption is incorrect - that is, assume there exists a sequence $\{(x_n, v_n)\}_n \subseteq \cup_{v \in P} B_v \times \{v\}$ s.t. the following holds:

- $(x_n, v_n) \in \overline{\cup_{v \in P} B_v \times \{v\}}$ for every n .
- $v_n \rightarrow p$.
- $f_{v_n}^k(x_n) = x_n$.
- $x_n \rightarrow \partial B$ (in \mathbf{R}^3).

Let $x \in \partial B$ be the limit (or partial limit) of x_n . Since by construction $\overline{B} \subseteq \overline{H_p}$, from $\overline{H_p} \subseteq \overline{D_\alpha}$ and by both Prop.3.1 and Lemma 3.0.1 it follows the trajectory of x is bounded. Since the vector fields $\{F_{v_n}\}_n$ converge to F_p in the C^∞ metric and because every x_n lies on a periodic trajectory for F_{v_n} , it follows x must lie on T , a periodic trajectory for F_p , and satisfy $f_p^k(x) = x$ - however, since $x \in \partial B \cap T$ this contradicts Lemma 4.2, hence there is no such sequence. That is, there exists a neighborhood $O \subseteq P$ of p s.t. for every $v \in O$, f_v^k has no fixed points in ∂B_v . \square

As a consequence of Lemma 4.3 and Prop.4.3, for $v \in P$ sufficiently close to a trefoil parameter $p \in P$, we immediately conclude:

Corollary 4.1.4. *Let $p \in P$ be a trefoil parameter, and let O be as in Lemma 4.3 - then, for every $v \in O$ the Fixed Point Indices of $f_p^k : \overline{B} \rightarrow \overline{U_p}$, $f_v^k : \overline{B_v} \rightarrow \overline{U_v}$ coincide. In particular, it is always non-zero. Consequentially, f_v^k has a fixed-point x_v in B_v , which lies on some periodic trajectory T_v for F_v .*

However, we can say more. Since the flow lines connecting $x \in B_v$ with $f_v(x), \dots, f_v^k(x)$ always intersect $\overline{U_v}$ transversely it follows that provided the neighborhood O defined above is sufficiently small, f_v, \dots, f_v^k are all continuous - hence, because $x_v \in B_v$ it follows all the intersection points of T_v with $\overline{U_v}$ are **transverse** intersection points. Additionally, since we constructed B s.t. $f_p^i(\overline{B}) \cap f_p^j(\overline{B}) = \emptyset$ for every $i \neq j$, $i, j \in \{0, \dots, k-1\}$ it follows that provided v is sufficiently close to B_v , we also have $f_v^i(\overline{B_v}) \cap f_v^j(\overline{B_v}) = \emptyset$ - hence, all in all, we conclude that provided $v \in P$ is sufficiently close to the trefoil parameter p , the minimal period of x_v w.r.t. f_v is k . That is, we have just proven:

Corollary 4.1.5. *Let $p \in P$ be a trefoil parameter, let O be as in Lemma 4.3, and let x_v be as in Cor.4.1.4. Then, provided O is a sufficiently small neighborhood of P , the minimal period of x_v w.r.t. f_v is k .*

We can now conclude the proof of Th.4.1. To do so, first recall we originally chose $s \in \{1, 2\}^{\mathbf{N}}$ s.t. it is periodic of minimal period k , $s = \{2, i_1, i_2, \dots\}$ and **not** the constant $\{1, 1, 1, \dots\}$. Additionally, recall the curve $\rho \subseteq U_p$ and the curve ρ_v which divides the cross-section U_v to $U_{1,v}, U_{2,v}$ - and additionally, recall the invariant set I_v , and the map $\pi_v : I_v \rightarrow \{1, 2\}^{\mathbf{N}}$ (see the discussion before Th.4.1). Finally, recall we constructed B in Lemma 4.2 s.t. $B \subseteq D_{i_0, \dots, i_n}$, $n > k$, which immediately implies that given $i \in \{0, \dots, n\}$, $f_p^i(\overline{B}) \cap \rho = \emptyset$ (with ρ as in Cor.3.1.7). In particular, given any $x \in \overline{B}$, $f_p^i(x)$ is a point of transverse intersection between the trajectory of x and the cross-section U_p .

Now, by Lemma 4.2, $D_s \subseteq \overline{B}$ - and by Cor.3.1.5, there exists a periodic point $x_s \in D_s$ of minimal period k for f_p , satisfying $\pi(x_s) = s$ (with π as in Th.3.1 and Cor.3.1.7). As a consequence, since ρ is continuously deformed to ρ_v when the vector field F_p is deformed to F_v , it follows that provided $v \in P$ is sufficiently close to a trefoil parameter p , we have $f_v^i(\overline{B_v}) \cap \rho_v = \emptyset$, $i \in \{0, \dots, n\}$. To continue, let $x_v \in B_v$ be the periodic point for f_v given by Cor.4.1.4. Because $n > k$ and because $x_v \in B_v$ is periodic of minimal period k for f_v , by the definition of π_v in page 55 and the discussion above it follows $\pi_v(x_v) = s$. Now, let T_v denote the periodic trajectory s.t. $x_v \in T_v$ - by previous paragraph it follows that provided $v \in O$ is sufficiently close to p , because all the intersection points of T_v with $\overline{U_v}$ are transverse we conclude f_v, \dots, f_v^k are continuous at x_v . Consequentially, π_v is also continuous at x_s .

To summarize our results so far, we have proven that given any periodic $s \in \{1, 2\}^{\mathbf{N}}$ of minimal period k , $s = \{2, i_1, i_2, \dots\}$ and given any $v \in P$ sufficiently close to a trefoil parameter $p \in P$, the following holds:

- There exists a periodic point of minimal period k , $x_v \in \overline{U_v} \setminus \rho_v$ s.t. $\pi_v(x_v) = s$.
- f_v, \dots, f_v^k are continuous at x_v .
- π_v is continuous at $x_v, f_v(x_v), \dots, f_v^{k-1}(x_v)$.

Now, by the definition of π_v in page 55, we already know $\pi_v \circ f_v = \sigma \circ \pi_v$ (where $\sigma : \{1, 2\}^{\mathbf{N}} \rightarrow \{1, 2\}^{\mathbf{N}}$ denoting the one-sided shift). Additionally, recall that up to this point we always assume $s \in \{1, 2\}^{\mathbf{N}}$ is periodic of minimal period k and satisfies $s = \{2, i_1, i_2, \dots\}$. As a consequence, recalling we denote by I_v the invariant set of f_v in $\overline{U_v} \setminus \rho_v$, given s as above it follows that provided $v \in P$ is sufficiently close to a trefoil parameter we have $x_v, f_v(x_v), \dots, f_v^k(x_v) \in I_v$ - which yields that $s, \sigma(s), \dots, \sigma^k(s)$ are **also** all in $\pi_v(I_v)$. However, this implies that

given **any** periodic $s \in \{1, 2\}^{\mathbb{N}}$ of minimal period k that is **not** the constant $\{1, 1, 1, \dots\}$, and given **any** $v \in P$ sufficiently close to p , we have:

- There exists a periodic point $y_v \in \overline{U_v} \setminus \rho_v$ of minimal period k s.t. $\pi_v(y_v) = s$.
- f_v, \dots, f_v^k are all continuous at y_v .
- π_v is continuous at $y_v, f_v(y_v), \dots, f_v^{k-1}(y_v)$.

Therefore, all in all, the proof of Th.4.1 is now complete. \square

Remark 4.4. As must be stated, given $v \in P$, the set $\pi_v(I_v)$ is **never** empty. As remarked in the discussion before Cor.3.1.7, the curve ρ **does not** include the fixed point P_{In} . As such, the same is true for ρ_v - or in other words, for every $v \in P$, $P_{In} \in U_{1,v}$. Since P_{In} is a fixed-point, it follows $P_{In} \in I_v$ **and** consequentially that the constant $\{1, 1, 1, \dots\}$ is in $\pi_v(I_v)$.

Remark 4.5. In [14], the fixed-point index was applied to prove the existence of infinitely many periodic trajectories in the Rössler System (albeit in a non-heteroclinic setting).

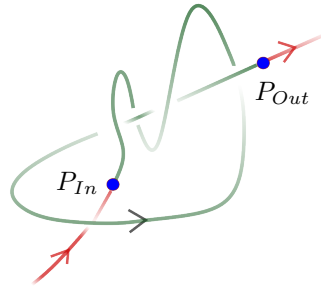


FIGURE 71. A heteroclinic knot more complex than a trefoil.

5. DISCUSSION:

Before we conclude this paper, there are two remarks about Th.4.1 (and Th.3.1) which must be made. The first is that the proof of Th.4.1 gives us a heuristic how the periodic dynamics in Q are created (and destroyed) in the Rössler System - namely, when we perturb the dynamics of a trefoil parameter $p \in P$ to those of some other $v \in P$, the periodic dynamics of Q are destroyed by collision with the curve ρ_v . This heuristic, as must be stated, is very similar to the well-known one dimensional saddle-node bifurcations in discrete-time dynamics. A second remark is that even though Th.4.1 guarantees the persistence of periodic dynamics for perturbations of trefoil parameters, it **does not** guarantee the persistence of periodic trajectories in the set Q . In other words, even though the periodic, symbolic dynamics for the first-return map $f_p : \overline{U_p} \rightarrow \overline{U_p}$ (wherever defined) persist under sufficiently small perturbations in the parameter space P , we do not know if the periodic trajectories in Q **also** survive such perturbations.

These two remarks (and the questions they raise) can and will be studied rigorously. In a series of future papers it will be proven that by applying ideas from [10],[7] and [8], it is possible to both classify the knot-types of periodic trajectories in the set Q - and prove their persistence under perturbations in the parameter space P . Moreover, it will also be proven that the seemingly one-dimensional heuristic above about the creation (and destruction) of periodic orbits for the first-return map can be justified - namely, by using Kneading Theory it will be shown that the discrete-time dynamics of the Rössler System around trefoil parameters in P can be described by those of the Logistic map. Meanwhile, we conclude this paper with the following conjecture:

Conjecture 1. Let $p \in P$ be a heteroclinic parameter for the Rössler System (not necessarily a trefoil parameter - see Def.2.3). Then, provided the heteroclinic knot it generates is complex **at least** like a trefoil knot, its first-return map $f_p : \overline{U_p} \rightarrow \overline{U_p}$ is chaotic w.r.t. Def.1.1.

REFERENCES

- [1] M.H.A. Newman. *Elements Of The Topology Of Plane Sets Of Points*. Cambridge, at the University Press, 1954.
- [2] E.N Lorenz. "Deterministic Nonperiodic Flow". In: *Journal of the Atmospheric Sciences* 20 (1963), pp. 130–141.

- [3] L. Shilnikov. “A case of the existence of a denumerable set of periodic motions”. In: *Sov. Math. Dok.* 6 (1967), pp. 163–166.
- [4] S. Smale. “Differentiable dynamical systems”. In: *Bull. Amer. Math. Soc.* 73 (1967), pp. 747–817.
- [5] A. Dold. *Lectures on Algebraic Topology*. Springer, 1972.
- [6] O.E. Rössler. “An equation for continuous chaos”. In: *Physics Letters A* 57 (1976), pp. 397–398.
- [7] K.T. Alligood, J.M. Paret, and J.A. Yorke. “Geometric Dynamics”. In: Springer Verlag, 1983. Chap. 1 - *An index for the continuation of relatively isolated sets of periodic orbits*.
- [8] J.S. Birman and R.F. Williams. “Knotted periodic orbits in dynamical systems II: Knot holders for fibered knots”. In: *Contemporary Mathematics* 20 (1983), pp. 1–60.
- [9] O.E. Rössler. “The Chaotic Hierarchy”. In: *Zeitschrift für Naturforschung A* 38 (1983), pp. 788–801.
- [10] K.T. Alligood and J.A. Yorke. “Families of periodic orbits: Virtual periods and global continuability”. In: *Journal of Differential Equations* 55 (1984), pp. 59–71.
- [11] P. Gaspard, R. Kapral, and G. Nicolis. “Bifurcation Phenomena near Homoclinic Systems: A Two-Parameter Analysis”. In: *Journal of Statistical Physics* 35 (5/6) (1984), pp. 597–727.
- [12] J. Banks et al. “On Devaney’s Definition of Chaos”. In: *The American Mathematical Monthly* 99 (1992), pp. 332–334.
- [13] C. Letellier, P. Dutertre, and B. Maheu. “Unstable periodic orbits and templates of the Rössler system: Toward a systematic topological characterization”. In: *Chaos* 5, 271 (1995).
- [14] P. Zgliczynski. “Computer assisted proof of chaos in the Rössler equations and in the Hénon map”. In: *Nonlinearity* 10(1) (1997), pp. 243–252.
- [15] V.V. Bykov. “On systems with separatrix contour containing two saddle-foci”. In: *Journal of Mathematical Sciences* 95 (1999), pp. 2513–2522.
- [16] M.T. Teryokhin and T.L. Paniflova. “Periodic Solutions of the Rössler System”. In: *Russian Mathematics* 43 (8) (1999), pp. 66–69.
- [17] J. Kennedy and J.A. Yorke. “Topological Horseshoes”. In: *Transactions of the American Mathematical Society* 353 (2001), pp. 2513–2530.
- [18] John W. Milnor. *Topology from the Differentiable viewpoint*. New Jersey: World Scientific, 2001.
- [19] X.S. Yang, Yu Y., and Zhang S. “A new proof for existence of horseshoe in the Rössler system”. In: *Chaos, Solitons, and Fractals* 18 (2003), pp. 223–227.
- [20] V. Araujo and M. Jose Pacifico. *Three-Dimensional Flows*. Springer, 2010.
- [21] J.C. Gallas. “The Structure of Infinite Periodic and Chaotic Hub Cascades in Phase Diagrams of Simple Autonomous Flows”. In: *International Journal of Bifurcation and Chaos* 20(2) (2010), pp. 197–211.
- [22] M.F.S. Lima and J. Llibre. “Global dynamics of the Rössler system with conserved quantities”. In: *J. Phys. A: Math. Theor.* 44 (2011).
- [23] R. Barrio, F. Blesa, and S. Serrano. “Topological Changes in Periodicity Hubs of Dissipative Systems”. In: *Phys. Rev. Lett.* 108, 214102 (2012).
- [24] R. Barrio, A. Shilnikov, and L.P. Shilnikov. “Chaos, CNN, Memristors and beyond – a festschrift for Leon Chua”. In: World Scientific, 2013. Chap. 33 - *Symbolic Dynamics and Spiral Structures due to the Saddle Focus Bifurcations*.
- [25] R. Barrio, F. Blesa, and S. Serrano. “Unbounded dynamics in dissipative flows: Rössler model”. In: *Chaos* 242 (2014).
- [26] R. Barrio and S. Serrano. “Unbounded dynamics in dissipative flows: Rössler model”. In: *Chaos* 24 (2014).
- [27] M. Rosalie. “Templates and subtemplates of Rössler attractors from a bifurcation diagram”. In: *Journal of Physics A: Mathematical and Theoretical, IOP Publishing* 49(31) (2016).
- [28] M.R. Cândido, D. D. Novaes, and C. Valls. “Periodic solutions and invariant torus in the Rössler system”. In: *Nonlinearity* 33 4512 (2020), pp. 66–69.
- [29] S. Malykh et al. “Homoclinic chaos in the Rössler model”. In: *Chaos* 30 (2020).
- [30] T. Pinsky. “Analytical study of the Lorenz system: Existence of infinitely many periodic orbits and their topological characterization”. In: *Proceedings of the National Academy of Sciences* 120 (2023).